Mapping MERS-CoV Immune Responses

A Blueprint for Rational Vaccine Design

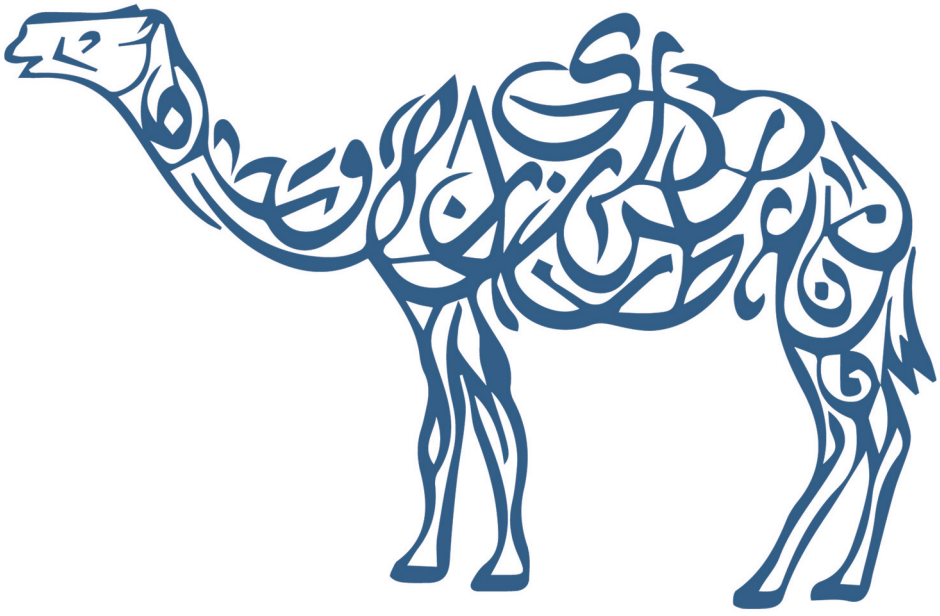

Nisreen Mamdouh Ahmed Okba

Mapping MERS-CoV Immune Responses: A blueprint for rational vaccine design

Nisreen Mamdouh Ahmed Okba

The research described in this thesis was mainly conducted at the Department of Viroscience, Erasmus MC, Rotterdam, The Netherlands within the framework of the Erasmus Molecular Medicine Post Graduate School. The research presented in this thesis was financially supported by the Zoonotic Anticipation and Preparedness Initiative (ZAPI project) [Innovative Medicines initiative (IMI) grant 115760], with assistance and financial support from IMI and the European Commission and contributions from European Federation of Pharmaceutical Industries and Associations (EFPIA) partners.

Cover	Nisreen Okba & Brigitta Laksono Arabic MERS-CoV Calligraphy: Hosam Mostafa & Ehab Elhamzawy
Layout	Renate Siebes | Proefschrift.nu
Printed by	Proefschriftmaken.nl
ISBN	978-94-6380-826-2

Mapping MERS-CoV Immune Responses: A blueprint for rational vaccine design

MERS-CoV-immuunreacties in kaart brengen:
een blauwdruk voor rationeel vaccinontwerp

Thesis

to obtain the degree of Doctor from the
Erasmus University Rotterdam
by command of the
rector magnificus
Prof.dr. R.C.M.E. Engels
and in accordance with the decision of the Doctorate Board.
The public defence shall be held on
Thursday, 28 May 2020 at 9.30

by

Nisreen Mamdouh Ahmed Okba

born in Cairo, Egypt

Erasmus University Rotterdam

Doctoral Committee

Promotor:	Prof.dr. M.P.G. Koopmans
Other members:	Prof.dr. C.A.B. Boucher Prof.dr. A. Verbon Prof.dr. M. Beer
Copromotor:	Dr. B.L. Haagmans

To my parents Soad and Mamdouh,
and my siblings, Doaa and Ahmed
For whom I'll be forever grateful and deeply indebted…
Thank you for all the love and support

Content

Chapter 1

Introduction

Based on: Current Opinion in Virology, 23, 2017

Emerging and re-emerging infectious diseases (EID) pose a serious global threat. In this century, more often do we encounter epidemics caused by infectious diseases spreading wider and quicker than ever before. Ecological changes (environmental, agricultural, behavioral, etc.), urbanization and population growth have contributed to their significant increase over time (1, 2). Because of the ease and speed of modern global travel and trade, EIDs, once confined to a geographical area, now have the potential to spread globally in a matter of days, risking the health and lives of millions of people and causing devastating outcomes on global health and economy. With over 70% of the newly discovered human pathogens found to originate from animals or animal products, EIDs are dominated by zoonoses; the majority of which originate from wildlife (3-5). HIV, avian influenza, Ebola, Lassa virus (LASV), Rift Valley fever virus (RVFV), severe acute respiratory syndrome coronavirus (SARS-CoV) and Middle East respiratory syndrome coronavirus (MERS-CoV), are just a few examples of wildlife-introduced zoonoses. Among EIDs, zoonotic viruses have and will continue to cause the most devastating epidemics in history. And since we are and will continue to be insulted by attacks of emerging and re-emerging viruses, it is a matter of when and where, not if, the next epidemic will take place with potential devastating outcomes. The potentially fatal outcomes and devastating economic impacts of (re-)emerging infections demands crucial and urgent global responses to be prepared for prevention and control of epidemics to limit their ruinous influence. These include surveillance as well as countermeasure development. A major challenge in combating such diseases is that for many of them, there are no effective treatment or vaccines available. This underlines an urgent need for the development of vaccines and therapeutics against these diseases.

With no licensed CoV therapy or vaccines, zoonotic coronaviruses (CoVs) pose a serious public health risk. Coronaviruses are the largest positive sense single stranded RNA viruses. To date, there are six coronaviruses known to infect humans including four endemic human CoVs (HCoVs), HCoV-229E, HCoV-OC43, HCoV-NL63, and HCoV-HKU1 which are mainly known to cause mild respiratory infections. Over the past two decades, two previously unknown zoonotic coronaviruses, severe acute respiratory syndrome coronavirus (SARS-CoV) and Middle East respiratory syndrome coronavirus (MERS-CoV), have emerged to cause severe respiratory infections and fatalities in the human population. The SARS-CoV epidemic in 2002-2003 resulted in a 10% fatality among ~8000 infected cases in 26 countries with a heavy economic impact of over $50 billion (6, 7). This has thrusted efforts to develop SARS-CoV vaccines. Nonetheless, patient isolation, contact tracing, and implementation of infection control measures managed to put an end to the SARS outbreak (8). As the SARS-CoV outbreak waned off, so did interest and funding for the development of therapeutics and vaccines. Later in 2012, another zoonotic CoV- MERS-CoV – emerged in the human population (9) causing over 2400 infections in 27 countries to date, 35 % of which were

fatal (10). Accumulating serological and molecular evidence pointed to dromedary camels as the reservoir for MERS-CoV (11-13). This poses a continuous risk of virus spill-over to people in contact with camels, such as those working in slaughter houses and animal farms, evidenced by the presence of MERS-CoV antibodies in sera of those individuals (14, 15). Human-to-human transmission accounted for about 48% of the cases, mainly as outbreaks in healthcare settings, while 52% were community-acquired through sporadic camel-to-human transmission (16-24) although a substantial part of infections that occur result in unrecognized asymptomatic or mild illnesses (25-29). Thus, in addition to camel contacts, other highly-at-risk groups are healthcare workers and patient household contacts (21, 22, 26, 28, 30-32). Despite the ability of infection control to reduce MERS cases (16), unlike SARS-CoV, it did not put an end to MERS-CoV. With cases still reported 7 years after its first discovery, MERS-CoV continues to pose a threat to human health due to continuous zoonotic introductions (10, 19). To limit these spillovers events, continuous vigilance and surveillance of dromedaries and in-contact humans, rapid development of vaccines for both humans and dromedaries is crucial (19, 33). Due to its potential to cause future epidemics, by adapting to the human host and becoming more transmissible, and the lack of effective countermeasures, MERS-CoV is listed as in the WHO R&D blueprint for high-priority pathogens for which countermeasures are urgently needed (34). This aims at accelerating research by setting an R&D roadmap for the development of diagnostics, therapeutics, and vaccines for early detection and responses (33).

Immune correlates of protection

Considering the ongoing MERS-CoV outbreaks, it is crucial to develop intervention measures among which vaccines play an important role. Despite the fact that the emergence of MERS-CoV and SARS-CoV has dramatically changed the way we view CoVs, there is no licensed CoV vaccine or therapeutic drug available to date (35, 36). A cornerstone for rational vaccine design is defining the determinants of immune protection. Accumulating data from studies done so far on MERS-CoV and other coronaviruses revealed that a combination of both virus-specific humoral and cellular immune responses is required for full protection against coronaviruses. Especially neutralizing antibodies are considered key players in the protective immunity against CoVs. Neutralizing monoclonal antibodies (Mabs) reduced viral loads in MERS-CoV receptor-transduced mice, rabbits and macaques. (37-40) Similarly, convalescent camel sera increased virus clearance and decreased lung pathological outcomes in mice with an efficacy directly proportional to anti-MERS-CoV-neutralizing antibody (Nab) titers (41). Also polyclonal sera produced in transchromosomic bovines protected mice against MERS-CoV challenge (42).

Evidence for the protective role of antibodies also comes from recent studies analyzing immune responses in patients that survived or succumbed to MERS-CoV. Although neutralizing antibodies were only weakly inversely correlated to viral loads, serum antibody responses were higher in survivors compared to fatal cases but viral RNA was not eliminated from the lungs (43, 44). Administration of convalescent sera, however, did not lead to significant reduction in viral loads (43, 45). The presence of mucosal IgA Abs, on the other hand, was found to influence infectious virus isolation (46).

Besides humoral immunity, cellular immune responses are also considered to play a crucial role in protection against coronaviruses. While B-cell deficient mice were able to clear MERS-CoV, those lacking T-cells failed to eliminate the virus, pointing out the crucial role of T-cells in viral clearance (47). This is further supported by the observation that T-cells were able to protect aged mice against (48) SARS-CoV infection and the fact that a reduced T-cell count was associated with enhanced disease severity in SARS patients (49). Along with other studies, these data highlight the importance of T-cells for virus clearance and protection against MERS-CoV (47, 48) and SARS-CoV (50, 51). It is also noteworthy to mention that while neither antibodies nor memory B cells were detectable 6-years post-infection (52), SARS-CoV-specific memory T-cells, despite being low in frequency, persisted up to 11 years post-recovery (53). Nonetheless, the protective capacity of such memory response is not known. Hence, taking into account the waning of virus-specific humoral responses, generating a long-lived memory T cell response through vaccination could be favorable, but as proper B- and T-cell immune responses are required for efficient protection, vaccination should target the induction of both. At the moment we have limited information concerning the longevity of anamnestic immune responses following MERS-CoV infection. While longevity of cellular responses have not been evaluated, longevity of antibody responses following MERS-CoV infection varied according to disease severity (54-56). While being undetectable a year following mild infections (54), antibodies persisted up to 34 months, the longest time-point tested thus far, post-severe infection (55). The role of immune responses in protection is also in line with the observed increased fatality among the aged population following MERS-CoV infection. Retrospective studies on MERS-CoV patients have found that older age and associated co-morbidities, significantly correlated with disease severity and mortality (22, 30, 57-59);. a pattern that has been also reported for other respiratory viruses such as SARS-CoV (6), respiratory syncytial virus (RSV) (60) and influenza virus (61). This is most likely caused by a dysregulated immune response which could be induced by underlying co-morbidities such as diabetes (62) or by immunosenescence; a failure to produce protective immune response to new pathogens in elderly due to impaired antigen presentation , altered function of TLRs, and a reduced naïve B and T cell repertoire (63, 64). This age-related increase in mortality was also reported in SARS-CoV laboratory-infected

animals, that is, mice and nonhuman primates (NHPs) (65, 66), and was associated with low neutralizing antibodies and poor T-cell responses (67-69). Several factors that play a role in T-cell activation were also found to be dysregulated in an age-related manner. Age-related increase in phospholipase A2 group IID (PLA2G2D), and prostaglandinD2 in the lungs contributed to a diminished T-cell response and severe lung damage through diminishing respiratory dendritic cell (DC) migration (70, 71). Likewise, adoptive transfer of T-cells to mice enhanced viral clearance and survival (50), highlighting the contribution of a reduced T-cell response in severe disease outcome. These observations also highlight the need for more effective preventive measures for the elderly. In this sense, induction of a potent airway T-cell response may be crucial to protect against CoVs (48). Thus, a promising approach to protect against MERS-CoV-induced fatality is to enhance virus-specific tissue (airway) resident memory T-cell responses through intranasal vaccination. These observations also highlight the need for more effective preventive measures for the elderly.

Current MERS-CoV vaccine candidates

Although the MERS-CoV genome encodes for 16 non-structural proteins (nsp1-16) and four structural proteins, the spike (S), envelope (E), membrane (M), and nucleocapsid (N) (72) (Figure 1), the viral structural proteins, S and N, show the highest immunogenicity (73). While both S and N proteins can induce T-cell responses, neutralizing antibodies are almost solely directed against the S protein, with the receptor binding domain (RBD) being the major immunodominant region (74). Thus, current MERS-CoV vaccine candidates mainly employ the spike protein or (parts of) the gene coding for this glycoprotein (Figure 1C).

These MERS-CoV vaccine candidates were developed using a wide variety of platforms, including whole virus vaccines, vectored-virus vaccines, DNA vaccines, (Table 1) and protein-based vaccines (Table 2). Although live attenuated vaccines produce the most robust immune responses, they pose a risk from reversion to virulence. Inactivated whole virus-based vaccines may cause harm due to incomplete inactivation or the risk to induce lung immunopathology (75). The latter was associated with a Th2-biased immune responses and eosinophilic infiltrations (75, 76). Some studies have shown that optimizing the inactivation method and adjuvants used could help avert such effects (77, 78), however, further research is warranted to confirm their safety. Viral-vector-based vaccines, on the other hand, provide a safer alternative and have been developed using modified vaccinia virus Ankara (MVA) (79-81), adenovirus (AdV) (82, 83), measles virus (MeV) (84), rabies virus (RABV) (85), and Venezuelan equine encephalitis replicons (VRP) (47, 86), all expressing MERS-S/S1 proteins (48). A major hurdle facing these viral-vector-based platforms is preexisting immunity in the host which potentially can impair the vaccine efficacy. However, this can be prevented

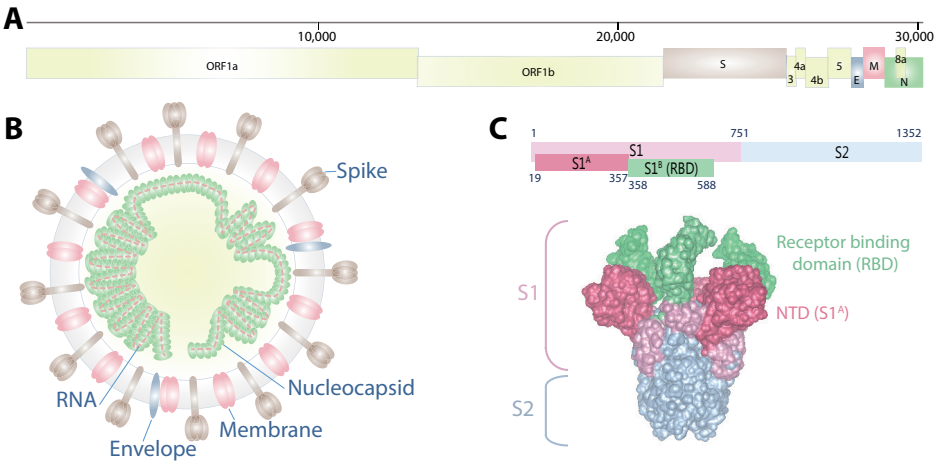

Figure 1. Schematic representation of the MERS-CoV genome, virion structure and spike protein. **A)** MERS-CoV genome (~ 31,000 nucleotides) showing open reading frames 1-8 and the genes encoding the four structural proteins: Spike (S), Membrane (M), Envelope (E) and Nucleocapsid (N). **B)** MERS-CoV virion structure showing the four structural proteins. **C)** the MERS-CoV spike protein showing the N-terminal spike S1 subunit and the c-terminal S2 subunit along with the two functional S1 domains: Domain A ($S1^A$) or the N-terminal domain (NTD) and Domain B ($S1^B$) or the receptor binding domain (RBD).

by using virus strains not circulating in the targeted population or immunization strategies involving heterologous prime-boost immunization, for example, MVA and AdV. Although plasmid DNA vaccines are considered to be of low immunogenicty in humans, current versions developed seem to induce potent immune responses. DNA-based vaccines directed at inducing anti S responses were also shown to exert protection in NHPs (87, 88). Noteworthy to mention is that a combination of DNA (S) and recombinant protein (S1) in a heterologous prime-boost immunization strategy induced higher immune response (Nab) compared to each component alone (88). Additionally, protein-based vaccines were developed in various platforms as virus-like particles (VLPs) (89), nanoparticles (90), peptide-based (91), and subunit vaccines directed against various regions of the spike protein S1 (88), the N-terminal domain (92), and the RBD (74, 93-99). Those recombinant protein-based vaccines have the highest safety profile among vaccine platforms but confer variable degrees of immunogenicity which need adjustment for the dose, adjuvants, and site of administration to get optimal protective responses. Adjuvants influence the type and magnitude of immune response produced by vaccines, and thus the doses used (90, 94, 97). Additionally, the route of administration is a determining factor for the type of vaccine-induced immune response produced in the host. While intranasal (i.n.) vaccination with SARS-N produced a protective airway T-cell response against SARS-CoV in mice, subcutaneous (s.c.) vaccination, inducing systemic T-cell responses, did not (48). Likewise,

Table 1. Virus and DNA-based MERS-CoV vaccine candidates

Vaccine Platform		Vaccine Candidate	Target Antigen	Animal model	Route; adjuvant	Immunological Response		Efficacy	Reference
						Nab	T-cell		
Live attenuated vaccine		rMERS-CoV-ΔE	MERS-CoV	ND	--	ND	ND	ND	(100)
Inactivated whole virus		Whole inactivated virus (WIV)	MERS-CoV	hDPP4 Tg-mice	i.m.; alum/ MF59	+	ND	Protective [b]	(75)
Recombinant Viral vectors	MVA	MVA-S	S	Ad/hDPP4-mice	2x i.m. /s.c.[c]	+	+	Protective	(80)
				camel	2x i.n. + i.m.	+; Mucosal	+	Protective	(81)
	Adenovirus	Ad5-S /S1	S/S1	mice	1:i.m.; 2: i.n.	+	+	ND	(82)
		Ad5-S / Ad41-S	S	mice	intragastric	+	-	ND	(83)
					i.m.	+	+	ND	(83)
	Measles	MVvac2-MERS-S / solS	S / solS	Ad/hDPP4-mice[a]	2x i.p.	+	+	Protective	(84)
	Venezuelan equine encephalitis virus	VRP-N	N	Ad/hDPP4-mice	2x i.n.	-	Airway	Protective	(48)
		VRP-S	S	Ad/hDPP4-mice	2x footpad	+	+	Protective	(47)
		VRP-S	S	288/330$^{+/+}$mice	2x footpad	+	ND	Protective	(86)
	Rabies virus	BNSP333-S1	S1	Ad/hDPP4-mice	3x i.m.	+	ND	Protective	(85)

Table 1. *Continued*

Vaccine Platform	Vaccine Candidate	Target Antigen	Animal model	Route; adjuvant	Immunological Response		Efficacy	Reference
					Nab	T-cell		
DNA Vaccines	VRC8400-S	S	NHP	3x i.m. + EP	+	ND	Protective	(88)
			mice	3x i.m. + EP	+	ND	ND	(88)
	pVax1-S	S	NHP	3x i.m.+ EP	+	+	Protective	(87)
			camel	3x i.m.+ EP	+	ND	ND	(87)
			mice	3x i.m.+ EP	+	+	ND	(87)
DNA + rProtein	S DNA (VRC8400-S) / S1 protein	S/S1	NHPs	2x S-DNA: i.m + e.p.; 1x S1 Protein: i.m.	+	ND	Protective	(88)

[a] Ad/hDPP4-IFNAR -/- -CD46Ge mice.

[b] Neutralizing antibody and protection against viral infection was found in WIV preparation with and without adjuvant but hypersensitivity-type lung reaction was produced post-challenge.

[c] S.c. vaccination was less immunogenic at lower virus doses.

Ad, adenovirus; Ad/hDPP4-mice, mice transduced with hDPP4 in an adenoviral vector; alum, aluminum hydroxide; E, envelope protein; EP, electroporation; hDPP4, human dipeptidyl peptidase 4; i.m., intramuscular; i.n., intranasal; i.p., intraperitoneal; MERS-CoV, Middle East respiratory syndrome coronavirus; MVA, modified vaccinia virus Ankara; N, nucleocapsid protein; Nab, neutralizing antibodies; ND, not done; NHP, non-human primate; rMERS-CoV, recombinant Middle East respiratory syndrome coronavirus; S, spike protein; S1, S1 domain of spike protein; solS, spike protein lacking transmembrane domain; Tg-mice, transgenic mice; VRP, virus replicon particle.

Table 2. MERS-CoV protein-based vaccine candidates

Vaccine Platform	Vaccine Candidate	Target Antigen	Animal model	Route ; adjuvant	Immunological Response		Efficacy	Reference
					Nab	T-cell		
Virus-like particles	MERS-CoV VLPs	S,M,E	NHP	4x i.m. ;alum	+	+	ND	(89)
Nanoparticle vaccine	S	S	mice	2x i.m.;alum / Matrix M1	+	ND	ND	(90)
Recombinant S1 proteins	S1	S1	mice	2x i.m.	+	ND	ND	(88)
			NHP	2x i.m.	+	ND	protective	(88)
			Alpaca	2x i.m.; Advax HCXL / Sigma Adjuvant	+	ND	protective	(101)
			camel	2x i.m.; Advax HCXL / Sigma Adjuvant	+/-	ND	Non-protective	(101)

Table 2. *Continued*

Vaccine Platform		Vaccine Candidate	Target Antigen	Animal model	Route ; adjuvant	Immunological Response		Efficacy	Reference
						Nab	T-cell		
	RBD Subunit Vaccines	RBD-Fc	S358-588	Rabbit	i.m.; incomplete Freund's	+	ND	ND	(74)
		rRBD	S367-606	NHP	3x i.m.; alum	+	+	Protective	(93)
		rRBD	S367–606	mice	3x i.m. ;alum / CpG ODN[a]	++	+	ND	(94)
		RBD-Fc	S377-588[b]	Ad/hDPP4-mice	3x s.c. +MF59[c]	+	+	protective	(95-97)
		Trimer RBD-Fc	S377-588	Ad/hDPP4-mice	2x i.m. + alum	+	ND	Protective	(98)
		RBD-Fc	S377-662	mice	5x i.n. ; Poly(I:C)[d]	+	+	ND	(99)
	Extra-RBD targets	rNTD	S18-353	Ad/hDPP4-mice	3x i.m. ;alum + CpG	+	+	Protective	(92)
		SP3	S736–761-KLH	Rabbit	Prime: CFA ; 3x boost: incomplete Freund's	+		ND	(91)

[a] i.m.; alum / CpG ODN produced higher neutralizing antibody responses than s.c. ; IFA / CpG ODN.
[b] S350-588-Fc, S358-588-Fc, S367-588-Fc, S367-606-Fc, and S377-588-Fc were tested and S377-588-Fc had the highest Nab titers although some produced equal S1 IgG response (95).
[c] MF59 produced the highest immunogenicity at low doses of antigen compared to S377-588-Fc only, or with Freund's/ Alum/ mPLA-SM/ ISA51/ MF59. (96) 1 mg of antigen with MF59 was sufficient to produce humoral and cellular immune responses similar to higher doses (5 mg or 20 mg) (97).
[d] i.n.+poly(I:C) vaccination induced stronger systemic cellular responses and higher local immune responses in mice lungs (IgA and neutralizing antibody titers) than s.c.+ Montanide ISA51 vaccination.
Ad/hDPP4-mice, mice transduced with hDPP4 in an adenoviral vector; alum, aluminum hydroxide; E, envelope protein; hDPP4, human dipeptidyl peptidase 4; i.m., intramuscular; i.n., intranasal; M, matrix protein; MERS-CoV, Middle East respiratory syndrome coronavirus; Nab, neutralizing antibodies; ND, not done; NHP, non-human primate; rNTD, recombinant N-terminal domain; RBD, receptor-binding domain; rRBD, recombinant RBD; RBD-Fc, RBD fused to the antibody crystallizable fragment of human IgG; S, spike protein; S1, S1 domain of spike protein; S367–606, amino acid residues 367–606 of the S protein; S736–761-KLH, peptide S736–761coupled to keyhole limpet haemocyanin; s.c., subcutaneous; VLPs, Virus-like particles.

i.n. vaccination with MERS-RBD induced a significantly higher neutralizing and IgA antibody responses in the mice airways compared to s.c. vaccination (99). This is important because mucosal immunity and airway memory T-cell responses are crucial players in protection against respiratory viruses, since these areas are the first to encounter the virus. Therefore, along with selecting antigens for a vaccine, the route of vaccination and adjuvants are key players that cannot be neglected in vaccine design.

Novel approaches for CoV vaccines

Immune focusing can be beneficial for the generation of a robust vaccine-induced immune response. During vaccine preparation, some epitopes which are normally hidden in the full length protein structure get exposed. Some epitopes could be immunodominant and have a negative contribution on the overall neutralization capacity produced by the vaccine (102). This also holds true for some non-neutralizing immunodominant epitopes, as S1-based vaccines induced slightly higher neutralization than whole S ectodomain-based ones (82, 88). Additionally, the RBD induced higher neutralizing antibodies compared to an S1 subunit vaccine (74), and shorter regions of RBD induced even higher neutralization responses (95), indicating that additional regions inducing non-neutralizing antibodies may contribute negatively to the overall neutralization response produced. Antibody-dependent enhancement of the viral infection by non-neutralizing antibodies (103-105) despite not being reported so far for MERS-CoV, needs also to be taken into consideration when developing a coronavirus vaccine. One approach to enhance the efficacy of subunit vaccines is to mask those negatively-contributing epitopes through glycosylation (102). Other approaches are immunefocusing and epitope-based vaccines, all aiming at narrowing the immune response to target only critical or beneficial epitopes to produce a stronger protective response. A prerequisite to reach that goal is to map epitopes targeted by the immune system and identify their biological role as being neutralizing, non-neutralizing, infection enhancing, containing a T-cell epitope, and so on. This can be achieved by analyzing the activity and fine specificity of convalescent patient sera, infected animal polyclonal sera, monoclonal antibodies, animal and human PBMCs. Subsequently the predicted epitopes can also provide a basis for potential vaccine candidates when produced as nanoparticles or VLPs. Further characterization of the immune responses induced by these vaccine candidates when evaluated in an animal model may be utilized to optimize the vaccines for efficacy (Figure 2). This epitope-focused vaccine approach may allow for targeting less immunodominant B- and T-cell epitopes having broader protection, avoid eliciting immune responses against epitopes playing no role in protection or having a negative or harmful role. In addition to better targeting of protective immunodominant

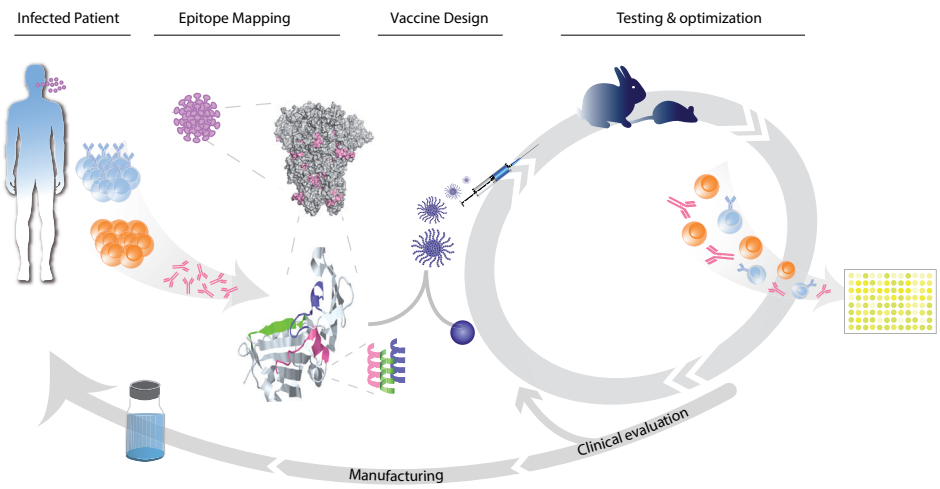

Figure 2. Epitope-based vaccine design. Following a virus infection, potential protective B- and T-cell epitopes are mapped. Peptides or proteins containing promising epitopes are produced and formulated using a suitable platform, for example, nanoparticles and tested for immunogenicity and efficacy in animals. Following several cycles of testing and optimization, a final vaccine suitable for human use may be produced.

epitopes, a combination of those B- and T-cell epitopes targeting different viral proteins, could be used to produce a broader and stronger protective immune response for both strain-specific and universal CoV vaccines.

Target populations for MERS-CoV vaccines

Next to the choice of the MERS-CoV vaccine candidate, it is also important to take into account the target population that needs to be protected through vaccination. Populations at risk of MERS-CoV infection include camel contacts, healthcare workers and patient contacts (Figure 3). The latter two groups could benefit from the rapid onset of immunity though passive immunization using Mabs or convalescent sera, provided that it is given in time. Another alternative strategy for short-term protection is the use of vaccines capable of rapidly inducing high titers of neutralizing antibodies. This will provide a short-term immunity beneficial to protect those highly-at-risk groups when a new case is identified, to prevent outbreaks. To prevent virus infection of primary cases, vaccination of the dromedary camels may also be considered. So far, among the available vaccine candidates, three have been tested in dromedary camels, pVax1-S, rS1, and MVA-S. pVax1-S, a DNA-based vaccine, induced neutralizing antibodies in two of three camels tested so far, but has not been tested for efficacy (87).The recombinant S1 (rS1) protein-based vaccine, induced low

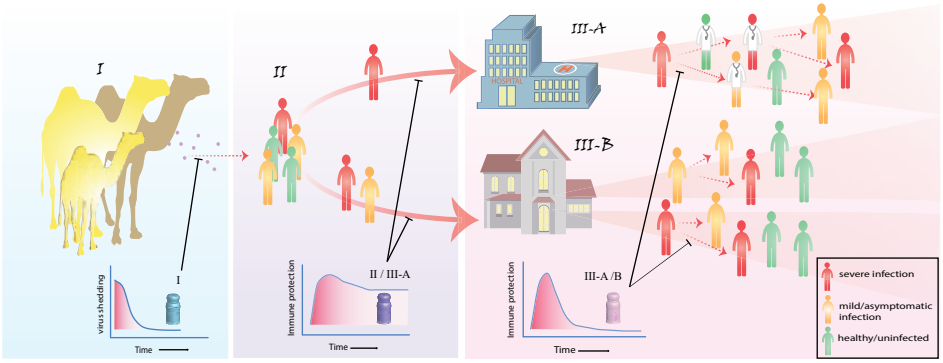

Figure 3. MERS-CoV vaccine target groups and the desired vaccine-induced immunological response for each. I: camels; II: camel contacts; III-A: healthcare workers and patients; III-B: house-hold contacts and MERS cases.

levels of neutralizing antibodies in two of the three vaccinated camels and was not able to reduce nasal virus shedding and rhinitis upon MERS-CoV challenge (101). The third candidate MVA-S, a viral-vector-based vaccine, induced systemic neutralizing antibodies and mucosal immunity which conferred protection against MERS-CoV challenge and reduced virus shedding in vaccinated camels (81) Therefore, this vaccine candidate may provide a means to prevent zoonotic transmission of the virus to the human population. For camel contacts and healthcare workers in endemic areas, being at a continuous risk of MERS-CoV infection either from infected camels or patients, respectively, it would be beneficial to induce a longer-term (mucosal) protection. While these could be rewarding approaches to stop MERS-CoV outbreaks, it is still worthwhile to develop platforms and vaccines that aim to induce more broad protection against different related CoVs, that could potentially cause future outbreaks.

Thesis outline

With the lack of licensed CoV vaccines, emerging zoonotic CoVs will continue to have devastating impacts. Seven years after its first discovery in 2012, MERS-CoV continues to cause outbreaks. With the lack of therapeutics and vaccines, MERS-CoV can potentially adapt and become more transmissible among humans with the potential to cause future epidemics. Learning from previous epidemics, the WHO issued a list of priority pathogens posing a high-risk to the human population and requiring urgent development of countermeasures, among which MERS-CoV and highly pathogenic CoVs are of high priority. This was followed by publishing an R&D roadmap to guide the rapid development of MERS-CoV diagnostics, therapeutics and vaccines (33, 34). This thesis focuses on understanding

MERS-CoV immune responses following infection and vaccination to help guide vaccine development, we used an immune-correlate-guided approach to rationally design MERS-CoV vaccines (Figure 2), aiming at the development of platforms which could be used for the rapid development of countermeasures for emerging viruses. The studies presented in this thesis aimed at using an immune-correlate-guided approach to allow for the rapid and rational design of vaccines for MERS-CoV and the development of platforms which could be applied for the rapid development of countermeasures to other emerging CoVs. In chapter 2, we developed and validated protein-based assays and used these to map immunogenic domains following natural infection, highlighting the potential use of such assays for MERS-CoV diagnostic and seroepidemiological studies. In chapter 3, we mapped the immune responses following vaccination through generating single domain antibodies which we used to further characterize protective antigenic sites, emphasizing their potential role in protection against MERS-CoV infections. By identifying immunogenic domains which are targets for protective antibodies, in chapter 4, we designed and tested the efficacy of recombinant protein-based vaccine candidates produced using two different platforms which could be implemented for the rapid development of vaccines against MERS-CoV and other emerging viruses. Finally, chapter 5, summarizes and discusses the key findings of this thesis.

References

1. Hui EK. Reasons for the increase in emerging and re-emerging viral infectious diseases. Microbes and infection. 2006 Mar;8(3):905-16.
2. Farag E, Sikkema RS, Vinks T, Islam MM, Nour M, Al-Romaihi H, et al. Drivers of MERS-CoV Emergence in Qatar. Viruses. 2018 Dec 31;11(1).
3. Allen T, Murray KA, Zambrana-Torrelio C, Morse SS, Rondinini C, Di Marco M, et al. Global hotspots and correlates of emerging zoonotic diseases. Nature communications. 2017 Oct 24;8(1):1124.
4. Jones KE, Patel NG, Levy MA, Storeygard A, Balk D, Gittleman JL, et al. Global trends in emerging infectious diseases. Nature. 2008 Feb 21;451(7181):990-3.
5. Belay ED, Kile JC, Hall AJ, Barton-Behravesh C, Parsons MB, Salyer S, et al. Zoonotic Disease Programs for Enhancing Global Health Security. Emerg Infect Dis. 2017 Dec;23(13):S65-S70.
6. Chen J, Subbarao K. The Immunobiology of SARS*. Annual review of immunology. 2007;25:443-72.
7. World Health Organization. SARS (Severe Acute Respiratory Syndrome). [cited 10 Oct 2019]; Available from: https://www.who.int/ith/diseases/sars/en/
8. Cheng VC, Chan JF, To KK, Yuen KY. Clinical management and infection control of SARS: lessons learned. Antiviral Res. 2013 Nov;100(2):407-19.
9. Zaki AM, van Boheemen S, Bestebroer TM, Osterhaus AD, Fouchier RA. Isolation of a novel coronavirus from a man with pneumonia in Saudi Arabia. The New England journal of medicine. 2012 Nov 8;367(19):1814-20.
10. World Health Organization. Middle East respiratory syndrome coronavirus (MERS-CoV) [cited 01-11-2019]; Available from: http://www.who.int/emergencies/mers-cov/en/

11. Haagmans BL, Al Dhahiry SH, Reusken CB, Raj VS, Galiano M, Myers R, et al. Middle East respiratory syndrome coronavirus in dromedary camels: an outbreak investigation. The Lancet Infectious diseases. 2014 Feb;14(2):140-5.
12. Alagaili AN, Briese T, Mishra N, Kapoor V, Sameroff SC, Burbelo PD, et al. Middle East respiratory syndrome coronavirus infection in dromedary camels in Saudi Arabia. mBio. 2014 Feb 25;5(2):e00884-14.
13. Reusken CB, Haagmans BL, Muller MA, Gutierrez C, Godeke GJ, Meyer B, et al. Middle East respiratory syndrome coronavirus neutralising serum antibodies in dromedary camels: a comparative serological study. The Lancet Infectious diseases. 2013 Oct;13(10):859-66.
14. Reusken CB, Farag EA, Haagmans BL, Mohran KA, Godeke GJt, Raj S, et al. Occupational Exposure to Dromedaries and Risk for MERS-CoV Infection, Qatar, 2013-2014. Emerg Infect Dis. 2015 Aug;21(8):1422-5.
15. Muller MA, Meyer B, Corman VM, Al-Masri M, Turkestani A, Ritz D, et al. Presence of Middle East respiratory syndrome coronavirus antibodies in Saudi Arabia: a nationwide, cross-sectional, serological study. The Lancet Infectious diseases. 2015 May;15(5):559-64.
16. Donnelly CA, Malik MR, Elkholy A, Cauchemez S, Van Kerkhove MD. Worldwide Reduction in MERS Cases and Deaths since 2016. Emerg Infect Dis. 2019 Sep;25(9):1758-60.
17. Alanazi KH, Killerby ME, Biggs HM, Abedi GR, Jokhdar H, Alsharef AA, et al. Scope and extent of healthcare-associated Middle East respiratory syndrome coronavirus transmission during two contemporaneous outbreaks in Riyadh, Saudi Arabia, 2017. Infection control and hospital epidemiology. 2019 Jan;40(1):79-88.
18. Conzade R, Grant R, Malik MR, Elkholy A, Elhakim M, Samhouri D, et al. Reported Direct and Indirect Contact with Dromedary Camels among Laboratory-Confirmed MERS-CoV Cases. Viruses. 2018 Aug 13;10(8).
19. World Health Organization. WHO MERS Global Summary and Assessment of Risk. 2019.
20. Bernard-Stoecklin S, Nikolay B, Assiri A, Bin Saeed AA, Ben Embarek PK, El Bushra H, et al. Comparative Analysis of Eleven Healthcare-Associated Outbreaks of Middle East Respiratory Syndrome Coronavirus (Mers-Cov) from 2015 to 2017. Scientific Reports. 2019 May 14;9(1):7385.
21. Assiri A, McGeer A, Perl TM, Price CS, Al Rabeeah AA, Cummings DA, et al. Hospital outbreak of Middle East respiratory syndrome coronavirus. The New England journal of medicine. 2013 Aug 1;369(5):407-16.
22. Korea Centers for Disease Control and Prevention. Middle East Respiratory Syndrome Coronavirus Outbreak in the Republic of Korea, 2015. Osong Public Health Res Perspect. 2015 Aug;6(4):269-78.
23. Chowell G, Abdirizak F, Lee S, Lee J, Jung E, Nishiura H, et al. Transmission characteristics of MERS and SARS in the healthcare setting: a comparative study. BMC Med. 2015 Sep 3;13:210.
24. Cauchemez S, Nouvellet P, Cori A, Jombart T, Garske T, Clapham H, et al. Unraveling the drivers of MERS-CoV transmission. Proceedings of the National Academy of Sciences of the United States of America. 2016 Aug 9;113(32):9081-6.
25. Alraddadi BM, Al-Salmi HS, Jacobs-Slifka K, Slayton RB, Estivariz CF, Geller AI, et al. Risk Factors for Middle East Respiratory Syndrome Coronavirus Infection among Healthcare Personnel. Emerg Infect Dis. 2016 Nov;22(11):1915-20.
26. Omrani AS, Matin MA, Haddad Q, Al-Nakhli D, Memish ZA, Albarrak AM. A family cluster of Middle East Respiratory Syndrome Coronavirus infections related to a likely unrecognized asymptomatic or mild case. Int J Infect Dis. 2013 Sep;17(9):e668-72.
27. Alshukairi AN, Khalid I, Ahmed WA, Dada AM, Bayumi DT, Malic LS, et al. Antibody Response and Disease Severity in Healthcare Worker MERS Survivors. Emerg Infect Dis. 2016 Jun;22(6).

28. Drosten C, Meyer B, Muller MA, Corman VM, Al-Masri M, Hossain R, et al. Transmission of MERS-coronavirus in household contacts. The New England journal of medicine. 2014 Aug 28;371(9):828-35.
29. Ko JH, Muller MA, Seok H, Park GE, Lee JY, Cho SY, et al. Serologic responses of 42 MERS-coronavirus-infected patients according to the disease severity. Diagnostic microbiology and infectious disease. 2017 Oct;89(2):106-11.
30. Saad M, Omrani AS, Baig K, Bahloul A, Elzein F, Matin MA, et al. Clinical aspects and outcomes of 70 patients with Middle East respiratory syndrome coronavirus infection: a single-center experience in Saudi Arabia. Int J Infect Dis. 2014 Dec;29:301-6.
31. Ki HK, Han SK, Son JS, Park SO. Risk of transmission via medical employees and importance of routine infection-prevention policy in a nosocomial outbreak of Middle East respiratory syndrome (MERS): a descriptive analysis from a tertiary care hospital in South Korea. BMC pulmonary medicine. 2019 Oct 30;19(1):190.
32. Memish ZA, Cotten M, Watson SJ, Kellam P, Zumla A, Alhakeem RF, et al. Community case clusters of Middle East respiratory syndrome coronavirus in Hafr Al-Batin, Kingdom of Saudi Arabia: a descriptive genomic study. Int J Infect Dis. 2014 Jun;23:63-8.
33. Modjarrad K, Moorthy VS, Ben Embarek P, Van Kerkhove M, Kim J, Kieny MP. A roadmap for MERS-CoV research and product development: report from a World Health Organization consultation. Nat Med. 2016 Jul 7;22(7):701-5.
34. World Health Organization. R&D Blueprint: List of Blueprint priority diseases. [cited 20/05/2019]; Available from: https://www.who.int/blueprint/priority-diseases/en/
35. van Doremalen N, Munster VJ. Animal models of Middle East respiratory syndrome coronavirus infection. Antiviral Res. 2015 Oct;122:28-38.
36. Baseler L, de Wit E, Feldmann H. A Comparative Review of Animal Models of Middle East Respiratory Syndrome Coronavirus Infection. Vet Pathol. 2016 May;53(3):521-31.
37. Johnson RF, Bagci U, Keith L, Tang X, Mollura DJ, Zeitlin L, et al. 3B11-N, a monoclonal antibody against MERS-CoV, reduces lung pathology in rhesus monkeys following intratracheal inoculation of MERS-CoV Jordan-n3/2012. Virology. 2016 Mar;490:49-58.
38. Agrawal AS, Ying T, Tao X, Garron T, Algaissi A, Wang Y, et al. Passive Transfer of A Germline-like Neutralizing Human Monoclonal Antibody Protects Transgenic Mice Against Lethal Middle East Respiratory Syndrome Coronavirus Infection. Scientific Reports. 2016 Aug 19;6:31629.
39. Houser KV, Gretebeck L, Ying T, Wang Y, Vogel L, Lamirande EW, et al. Prophylaxis With a Middle East Respiratory Syndrome Coronavirus (MERS-CoV)-Specific Human Monoclonal Antibody Protects Rabbits From MERS-CoV Infection. The Journal of Infectious Diseases. 2016 May 15;213(10):1557-61.
40. Pascal KE, Coleman CM, Mujica AO, Kamat V, Badithe A, Fairhurst J, et al. Pre- and postexposure efficacy of fully human antibodies against Spike protein in a novel humanized mouse model of MERS-CoV infection. Proceedings of the National Academy of Sciences of the United States of America. 2015 Jul 14;112(28):8738-43.
41. Zhao J, Perera RA, Kayali G, Meyerholz D, Perlman S, Peiris M. Passive immunotherapy with dromedary immune serum in an experimental animal model for Middle East respiratory syndrome coronavirus infection. Journal of Virology. 2015 Jun;89(11):6117-20.
42. Luke T, Wu H, Zhao J, Channappanavar R, Coleman CM, Jiao JA, et al. Human polyclonal immunoglobulin G from transchromosomic bovines inhibits MERS-CoV in vivo. Sci Transl Med. 2016 Feb 17;8(326):326ra21.
43. Min CK, Cheon S, Ha NY, Sohn KM, Kim Y, Aigerim A, et al. Comparative and kinetic analysis of viral shedding and immunological responses in MERS patients representing a broad spectrum of disease severity. Scientific Reports. 2016 May 5;6:25359.

44. Corman VM, Albarrak AM, Omrani AS, Albarrak MM, Farah ME, Almasri M, et al. Viral Shedding and Antibody Response in 37 Patients With Middle East Respiratory Syndrome Coronavirus Infection. Clin Infect Dis. 2016 Feb 15;62(4):477-83.
45. Park WB, Perera RA, Choe PG, Lau EH, Choi SJ, Chun JY, et al. Kinetics of Serologic Responses to MERS Coronavirus Infection in Humans, South Korea. Emerg Infect Dis. 2015 Dec;21(12):2186-9.
46. Muth D, Corman VM, Meyer B, Assiri A, Al-Masri M, Farah M, et al. Infectious Middle East Respiratory Syndrome Coronavirus Excretion and Serotype Variability Based on Live Virus Isolates from Patients in Saudi Arabia. J Clin Microbiol. 2015 Sep;53(9):2951-5.
47. Zhao J, Li K, Wohlford-Lenane C, Agnihothram SS, Fett C, Zhao J, et al. Rapid generation of a mouse model for Middle East respiratory syndrome. Proceedings of the National Academy of Sciences of the United States of America. 2014 Apr 1;111(13):4970-5.
48. Zhao J, Zhao J, Mangalam AK, Channappanavar R, Fett C, Meyerholz DK, et al. Airway Memory CD4(+) T Cells Mediate Protective Immunity against Emerging Respiratory Coronaviruses. Immunity. 2016 Jun 21;44(6):1379-91.
49. Wong RS, Wu A, To KF, Lee N, Lam CW, Wong CK, et al. Haematological manifestations in patients with severe acute respiratory syndrome: retrospective analysis. Bmj. 2003 Jun 21;326(7403):1358-62.
50. Zhao J, Zhao J, Perlman S. T cell responses are required for protection from clinical disease and for virus clearance in severe acute respiratory syndrome coronavirus-infected mice. Journal of Virology. 2010 Sep;84(18):9318-25.
51. Channappanavar R, Fett C, Zhao J, Meyerholz DK, Perlman S. Virus-specific memory CD8 T cells provide substantial protection from lethal severe acute respiratory syndrome coronavirus infection. Journal of Virology. 2014 Oct;88(19):11034-44.
52. Tang F, Quan Y, Xin ZT, Wrammert J, Ma MJ, Lv H, et al. Lack of peripheral memory B cell responses in recovered patients with severe acute respiratory syndrome: a six-year follow-up study. J Immunol. 2011 Jun 15;186(12):7264-8.
53. Ng OW, Chia A, Tan AT, Jadi RS, Leong HN, Bertoletti A, et al. Memory T cell responses targeting the SARS coronavirus persist up to 11 years post-infection. Vaccine. 2016 Apr 12;34(17):2008-14.
54. Choe PG, Perera R, Park WB, Song KH, Bang JH, Kim ES, et al. MERS-CoV Antibody Responses 1 Year after Symptom Onset, South Korea, 2015. Emerg Infect Dis. 2017 Jul;23(7):1079-84.
55. Payne DC, Iblan I, Rha B, Alqasrawi S, Haddadin A, Al Nsour M, et al. Persistence of Antibodies against Middle East Respiratory Syndrome Coronavirus. Emerg Infect Dis. 2016 Oct;22(10):1824-6.
56. Al-Abdely HM, Midgley CM, Alkhamis AM, Abedi GR, Lu X, Binder AM, et al. Middle East Respiratory Syndrome Coronavirus Infection Dynamics and Antibody Responses among Clinically Diverse Patients, Saudi Arabia. Emerg Infect Dis. 2019 Apr;25(4):753-66.
57. Cauchemez S, Fraser C, Van Kerkhove MD, Donnelly CA, Riley S, Rambaut A, et al. Middle East respiratory syndrome coronavirus: quantification of the extent of the epidemic, surveillance biases, and transmissibility. The Lancet Infectious diseases. 2014 Jan;14(1):50-6.
58. Majumder MS, Kluberg SA, Mekaru SR, Brownstein JS. Mortality Risk Factors for Middle East Respiratory Syndrome Outbreak, South Korea, 2015. Emerg Infect Dis. 2015 Nov;21(11):2088-90.
59. Feikin DR, Alraddadi B, Qutub M, Shabouni O, Curns A, Oboho IK, et al. Association of Higher MERS-CoV Virus Load with Severe Disease and Death, Saudi Arabia, 2014. Emerg Infect Dis. 2015 Nov;21(11):2029-35.
60. Falsey AR, Hennessey PA, Formica MA, Cox C, Walsh EE. Respiratory syncytial virus infection in elderly and high-risk adults. The New England journal of medicine. 2005 Apr 28;352(17):1749-59.

61. Thompson WW, Shay DK, Weintraub E, Brammer L, Cox N, Anderson LJ, et al. Mortality associated with influenza and respiratory syncytial virus in the United States. Jama. 2003 Jan 8;289(2):179-86.
62. Kulcsar KA, Coleman CM, Beck SE, Frieman MB. Comorbid diabetes results in immune dysregulation and enhanced disease severity following MERS-CoV infection. JCI Insight. 2019;4(20):e131774.
63. Del Giudice G, Weinberger B, Grubeck-Loebenstein B. Vaccines for the elderly. Gerontology. 2015;61(3):203-10.
64. Crooke SN, Ovsyannikova IG, Poland GA, Kennedy RB. Immunosenescence and human vaccine immune responses. Immun Ageing. 2019;16:25.
65. Nagata N, Iwata N, Hasegawa H, Fukushi S, Harashima A, Sato Y, et al. Mouse-passaged severe acute respiratory syndrome-associated coronavirus leads to lethal pulmonary edema and diffuse alveolar damage in adult but not young mice. The American journal of pathology. 2008 Jun;172(6):1625-37.
66. Smits SL, de Lang A, van den Brand JM, Leijten LM, van IWF, Eijkemans MJ, et al. Exacerbated innate host response to SARS-CoV in aged non-human primates. PLoS pathogens. 2010 Feb 5;6(2):e1000756.
67. Zhao J, Zhao J, Van Rooijen N, Perlman S. Evasion by stealth: inefficient immune activation underlies poor T cell response and severe disease in SARS-CoV-infected mice. PLoS pathogens. 2009 Oct;5(10):e1000636.
68. Sheahan T, Whitmore A, Long K, Ferris M, Rockx B, Funkhouser W, et al. Successful vaccination strategies that protect aged mice from lethal challenge from influenza virus and heterologous severe acute respiratory syndrome coronavirus. Journal of Virology. 2011 Jan;85(1):217-30.
69. Channappanavar R, Zhao J, Perlman S. T cell-mediated immune response to respiratory coronaviruses. Immunol Res. 2014 Aug;59(1-3):118-28.
70. Zhao J, Zhao J, Legge K, Perlman S. Age-related increases in PGD(2) expression impair respiratory DC migration, resulting in diminished T cell responses upon respiratory virus infection in mice. The Journal of clinical investigation. 2011 Dec;121(12):4921-30.
71. Vijay R, Hua X, Meyerholz DK, Miki Y, Yamamoto K, Gelb M, et al. Critical role of phospholipase A2 group IID in age-related susceptibility to severe acute respiratory syndrome-CoV infection. The Journal of experimental medicine. 2015 Oct 19;212(11):1851-68.
72. van Boheemen S, de Graaf M, Lauber C, Bestebroer TM, Raj VS, Zaki AM, et al. Genomic characterization of a newly discovered coronavirus associated with acute respiratory distress syndrome in humans. mBio. 2012 Nov 20;3(6).
73. Agnihothram S, Gopal R, Yount BL, Jr., Donaldson EF, Menachery VD, Graham RL, et al. Evaluation of serologic and antigenic relationships between middle eastern respiratory syndrome coronavirus and other coronaviruses to develop vaccine platforms for the rapid response to emerging coronaviruses. The Journal of Infectious Diseases. 2014 Apr 1;209(7):995-1006.
74. Mou H, Raj VS, van Kuppeveld FJ, Rottier PJ, Haagmans BL, Bosch BJ. The receptor binding domain of the new Middle East respiratory syndrome coronavirus maps to a 231-residue region in the spike protein that efficiently elicits neutralizing antibodies. Journal of Virology. 2013 Aug;87(16):9379-83.
75. Agrawal AS, Tao X, Algaissi A, Garron T, Narayanan K, Peng BH, et al. Immunization with inactivated Middle East Respiratory Syndrome coronavirus vaccine leads to lung immunopathology on challenge with live virus. Hum Vaccin Immunother. 2016 Sep;12(9):2351-6.

76. Bolles M, Deming D, Long K, Agnihothram S, Whitmore A, Ferris M, et al. A double-inactivated severe acute respiratory syndrome coronavirus vaccine provides incomplete protection in mice and induces increased eosinophilic proinflammatory pulmonary response upon challenge. Journal of Virology. 2011 Dec;85(23):12201-15.
77. Iwata-Yoshikawa N, Uda A, Suzuki T, Tsunetsugu-Yokota Y, Sato Y, Morikawa S, et al. Effects of Toll-like receptor stimulation on eosinophilic infiltration in lungs of BALB/c mice immunized with UV-inactivated severe acute respiratory syndrome-related coronavirus vaccine. Journal of Virology. 2014 Aug;88(15):8597-614.
78. Deng Y, Lan J, Bao L, Huang B, Ye F, Chen Y, et al. Enhanced protection in mice induced by immunization with inactivated whole viruses compare to spike protein of middle east respiratory syndrome coronavirus. Emerging Microbes & Infections. 2018 Apr 4;7(1):60.
79. Song F, Fux R, Provacia LB, Volz A, Eickmann M, Becker S, et al. Middle East respiratory syndrome coronavirus spike protein delivered by modified vaccinia virus Ankara efficiently induces virus-neutralizing antibodies. Journal of Virology. 2013 Nov;87(21):11950-4.
80. Volz A, Kupke A, Song F, Jany S, Fux R, Shams-Eldin H, et al. Protective Efficacy of Recombinant Modified Vaccinia Virus Ankara Delivering Middle East Respiratory Syndrome Coronavirus Spike Glycoprotein. Journal of Virology. 2015 Aug;89(16):8651-6.
81. Haagmans BL, van den Brand JM, Raj VS, Volz A, Wohlsein P, Smits SL, et al. An orthopoxvirus-based vaccine reduces virus excretion after MERS-CoV infection in dromedary camels. Science. 2016 Jan 1;351(6268):77-81.
82. Kim E, Okada K, Kenniston T, Raj VS, AlHajri MM, Farag EA, et al. Immunogenicity of an adenoviral-based Middle East Respiratory Syndrome coronavirus vaccine in BALB/c mice. Vaccine. 2014 Oct 14;32(45):5975-82.
83. Guo X, Deng Y, Chen H, Lan J, Wang W, Zou X, et al. Systemic and mucosal immunity in mice elicited by a single immunization with human adenovirus type 5 or 41 vector-based vaccines carrying the spike protein of Middle East respiratory syndrome coronavirus. Immunology. 2015 Aug;145(4):476-84.
84. Malczyk AH, Kupke A, Prufer S, Scheuplein VA, Hutzler S, Kreuz D, et al. A Highly Immunogenic and Protective Middle East Respiratory Syndrome Coronavirus Vaccine Based on a Recombinant Measles Virus Vaccine Platform. Journal of Virology. 2015 Nov;89(22):11654-67.
85. Wirblich C, Coleman CM, Kurup D, Abraham TS, Bernbaum JG, Jahrling PB, et al. One-Health: a Safe, Efficient, Dual-Use Vaccine for Humans and Animals against Middle East Respiratory Syndrome Coronavirus and Rabies Virus. Journal of Virology. 2017 Jan 15;91(2).
86. Cockrell AS, Yount BL, Scobey T, Jensen K, Douglas M, Beall A, et al. A mouse model for MERS coronavirus-induced acute respiratory distress syndrome. Nature microbiology. 2016 Nov 28;2:16226.
87. Muthumani K, Falzarano D, Reuschel EL, Tingey C, Flingai S, Villarreal DO, et al. A synthetic consensus anti-spike protein DNA vaccine induces protective immunity against Middle East respiratory syndrome coronavirus in nonhuman primates. Sci Transl Med. 2015 Aug 19;7(301):301ra132.
88. Wang L, Shi W, Joyce MG, Modjarrad K, Zhang Y, Leung K, et al. Evaluation of candidate vaccine approaches for MERS-CoV. Nature communications. 2015 Jul 28;6(1):7712.
89. Wang C, Zheng X, Gai W, Zhao Y, Wang H, Wang H, et al. MERS-CoV virus-like particles produced in insect cells induce specific humoural and cellular imminity in rhesus macaques. Oncotarget. 2017 Feb 21;8(8):12686-94.
90. Coleman CM, Liu YV, Mu H, Taylor JK, Massare M, Flyer DC, et al. Purified coronavirus spike protein nanoparticles induce coronavirus neutralizing antibodies in mice. Vaccine. 2014 May 30;32(26):3169-74.

91. Yang Y, Deng Y, Wen B, Wang H, Meng X, Lan J, et al. The amino acids 736-761 of the MERS-CoV spike protein induce neutralizing antibodies: implications for the development of vaccines and antiviral agents. Viral immunology. 2014 Dec;27(10):543-50.
92. Jiaming L, Yanfeng Y, Yao D, Yawei H, Linlin B, Baoying H, et al. The recombinant N-terminal domain of spike proteins is a potential vaccine against Middle East respiratory syndrome coronavirus (MERS-CoV) infection. Vaccine. 2017 Jan 3;35(1):10-8.
93. Lan J, Yao Y, Deng Y, Chen H, Lu G, Wang W, et al. Recombinant Receptor Binding Domain Protein Induces Partial Protective Immunity in Rhesus Macaques Against Middle East Respiratory Syndrome Coronavirus Challenge. EBioMedicine. 2015 Oct;2(10):1438-46.
94. Lan J, Deng Y, Chen H, Lu G, Wang W, Guo X, et al. Tailoring subunit vaccine immunity with adjuvant combinations and delivery routes using the Middle East respiratory coronavirus (MERS-CoV) receptor-binding domain as an antigen. PloS one. 2014;9(11):e112602.
95. Ma C, Wang L, Tao X, Zhang N, Yang Y, Tseng CK, et al. Searching for an ideal vaccine candidate among different MERS coronavirus receptor-binding fragments--the importance of immunofocusing in subunit vaccine design. Vaccine. 2014 Oct 21;32(46):6170-6.
96. Zhang N, Channappanavar R, Ma C, Wang L, Tang J, Garron T, et al. Identification of an ideal adjuvant for receptor-binding domain-based subunit vaccines against Middle East respiratory syndrome coronavirus. Cellular & molecular immunology. 2016 Mar;13(2):180-90.
97. Tang J, Zhang N, Tao X, Zhao G, Guo Y, Tseng CT, et al. Optimization of antigen dose for a receptor-binding domain-based subunit vaccine against MERS coronavirus. Hum Vaccin Immunother. 2015;11(5):1244-50.
98. Tai W, Zhao G, Sun S, Guo Y, Wang Y, Tao X, et al. A recombinant receptor-binding domain of MERS-CoV in trimeric form protects human dipeptidyl peptidase 4 (hDPP4) transgenic mice from MERS-CoV infection. Virology. 2016 Dec;499:375-82.
99. Ma C, Li Y, Wang L, Zhao G, Tao X, Tseng CT, et al. Intranasal vaccination with recombinant receptor-binding domain of MERS-CoV spike protein induces much stronger local mucosal immune responses than subcutaneous immunization: Implication for designing novel mucosal MERS vaccines. Vaccine. 2014 Apr 11;32(18):2100-8.
100. Almazan F, DeDiego ML, Sola I, Zuniga S, Nieto-Torres JL, Marquez-Jurado S, et al. Engineering a replication-competent, propagation-defective Middle East respiratory syndrome coronavirus as a vaccine candidate. mBio. 2013 Sep 10;4(5):e00650-13.
101. Adney DR, Wang L, van Doremalen N, Shi W, Zhang Y, Kong WP, et al. Efficacy of an Adjuvanted Middle East Respiratory Syndrome Coronavirus Spike Protein Vaccine in Dromedary Camels and Alpacas. Viruses. 2019 Mar 2;11(3):212.
102. Du L, Tai W, Yang Y, Zhao G, Zhu Q, Sun S, et al. Introduction of neutralizing immunogenicity index to the rational design of MERS coronavirus subunit vaccines. Nature communications. 2016 Nov 22;7:13473.
103. Yip MS, Leung NH, Cheung CY, Li PH, Lee HH, Daeron M, et al. Antibody-dependent infection of human macrophages by severe acute respiratory syndrome coronavirus. Virol J. 2014 May 6;11:82.
104. Jaume M, Yip MS, Kam YW, Cheung CY, Kien F, Roberts A, et al. SARS CoV subunit vaccine: antibody-mediated neutralisation and enhancement. Hong Kong Med J. 2012 Feb;18 Suppl 2:31-6.
105. Wang SF, Tseng SP, Yen CH, Yang JY, Tsao CH, Shen CW, et al. Antibody-dependent SARS coronavirus infection is mediated by antibodies against spike proteins. Biochem Biophys Res Commun. 2014 Aug 22;451(2):208-14.

Chapter 2.1

Sensitive and specific detection of low-level antibody responses in mild MERS-CoV infections

Nisreen M.A. Okba | V. Stalin Raj | Ivy Widjaja | Corine H. GeurtsvanKessel | Erwin de Bruin | Felicity D. Chandler | Wan Beom Park | Nam-Joong Kim | Elmoubasher A. B. A. Farag | Mohammed Al-Hajri | Berend-Jan Bosch | Myoung-don Oh | Marion P.G. Koopmans | Chantal B.E.M. Reusken | Bart L. Haagmans

Emerging infectious diseases. 2019;25(10)

Abstract

Middle East respiratory syndrome coronavirus (MERS-CoV) infections in humans can cause asymptomatic to fatal lower respiratory lung disease. Despite posing a probable risk for virus transmission, asymptomatic to mild infections can go unnoticed; a lack of seroconversion among some PCR-confirmed cases has been reported. We found that a MERS-CoV spike S1 protein–based ELISA, routinely used in surveillance studies, showed low sensitivity in detecting infections among PCR-confirmed patients with mild clinical symptoms and cross-reactivity of human coronavirus OC43–positive serum samples. Using in-house S1 ELISA and protein microarray, we demonstrate that most PCR-confirmed MERS-CoV case-patients with mild infections seroconverted; nonetheless, some of these samples did not have detectable levels of virus-neutralizing antibodies. The use of a sensitive and specific serologic S1-based assay can be instrumental in the accurate estimation of MERS-CoV prevalence.

Introduction

Middle East respiratory syndrome coronavirus (MERS-CoV) poses a public health threat; ongoing outbreaks have been reported since its detection in 2012 (1). MERS-CoV infection may be asymptomatic or may cause illness ranging from mild to fatal; fatal infections account for 35% of reported cases (2-5). Dromedary camels are the virus reservoir (6, 7) and pose a high risk of infecting humans in contact with them (4, 7-9). These spillover events may seed outbreaks in the community (10), which occur mainly in healthcare settings (11, 12), and, to a lesser extent, among patient household contacts (13-15). Although not sustained, human-to-human transmission accounts for most reported cases (16), and may initiate outbreaks outside endemic areas, as seen in the 2015 South Korea outbreak (17). However, the rate of human-to-human transmission and total disease burden of MERS-CoV are not fully clear because we lack accurate data on the frequency of asymptomatic and mild infections.

Diagnostic assays with validated high sensitivity and specificity are crucial to estimate the prevalence of MERS-CoV. Molecular-based assays have been developed that enable sensitive and specific diagnosis of MERS-CoV infections (18, 19). Although the molecular detection of viral nucleic acid by reverse transcription PCR (RT-PCR) is the standard for MERS-CoV diagnosis, serologic detection remains necessary. Viral nucleic acid is detectable within a limited timeframe after infection, and samples from the lower respiratory tract are required for reliable results. Furthermore, whereas mutations in the viral regions where the PCR probes bind could lead to decreased sensitivity (20), genetically diverse MERS-CoV strains may retain antigenic similarity (21). Validated serologic assays are needed to ensure that the full spectrum of infections is identified; antibodies can be detected for longer periods after infection and even if viruses mutate. Several research groups and companies have developed serologic assays allowing for high-throughput surveillance for MERS-CoV infections among large populations (15, 19, 22-25).

Despite the number of serological assays developed, none is considered to be fully validated. There are 2 major challenges concerning specificity and sensitivity aspects of MERS-CoV serologic assays. The first challenge is that 90% of the human population have antibodies against common cold–causing human coronaviruses (HCoVs) that could cross-react, resulting in false positives in serologic assays, especially in persons infected with viruses belonging to the same genus of β-coronaviruses as human seasonal coronaviruses OC43 and HKU1 (26). The spike protein, specifically its N-terminal S1 domain, is highly immunogenic and divergent among HCoVs, so it is an ideal candidate for virus-specific serologic assays (27). The second challenge is the low antibody responses among mildly infected and asymptomatic cases. Severe MERS-CoV infections result in a robust immune

response allowing serologic detection in patients with positive or negative PCR outcomes (28), but PCR-diagnosed mild or asymptomatic infections may cause variable immune responses that can be undetectable by serologic assays (5, 15, 17). Therefore, a sensitive assay is necessary to avoid false-negative results that can cause failure in detection of subclinical infections and underestimation of prevalence in serosurveillance studies. We evaluated the antibody responses following severe and mild laboratory-confirmed MERS-CoV infections, validating and comparing different assay platforms for the specific and sensitive detection of MERS-CoV infections.

Materials and methods

Serum Samples

We used a total of 292 serum samples in this study (Table 1. Cohorts used in study of specificity and sensitivity of assays for MERS-CoV*; Appendix). The samples represented patients with serologically identified (8) and PCR-confirmed MERS-CoV infections (17, 29), a cohort of healthy blood donors as a control group, and patients confirmed by RT-PCR to have non–MERS-CoV respiratory virus infections to assess assay specificity. The use of serum samples from the Netherlands was approved by the Erasmus Medical Center local medical ethics committee (MEC approval 2014-414). The Institutional Ethics Review Board of Seoul National University Hospital approved the use of samples from patients in South Korea (approval no. 1506–093–681). The Ethics and Institutional Animal Care and Use Committees of the Medical Research Center, Hamad Medical Corporation, approved the use of samples from Qatar (permit 2014–01–001).

Serologic Assays

We tested all serum samples for MERS-CoV neutralizing antibodies using plaque reduction neutralization assay (PRNT). For S1 reactivity, we used a routine ELISA (rELISA; Euroimmun, https://www.euroimmun.com (15)), an in-house ELISA (iELISA), and protein microarray (8, 23). For nucleocapsid reactivity, we used luciferase immunoprecipitation assay (N-LIPS) (24). For S2 reactivity, we used ELISA (Appendix).

Statistical Analyses

We evaluated the specificity and sensitivity and predictive values of the assay platforms using serum samples from patients with PCR-diagnosed MERS-CoV infections, respiratory virus–infected patients, and healthy controls. We compared performance of assay platforms to PCR performance using Fisher exact test and used receiver operating characteristic (ROC)

curve to compare performance of different platforms. We performed all statistical analyses using GraphPad Prism version 7 (https://www.graphpad.com).

Results

Low Antibody Responses following Mild MERS-CoV Infection

Several studies have proposed that antibody levels and longevity following MERS-CoV infection are dependent on disease severity (5, 15, 17). Among PCR-confirmed MERS patients, mild infections may result in undetectable or lower, short-lived immune responses when compared with severe infections. We evaluated MERS-CoV–specific antibody responses in severe and mild MERS-CoV infections using serum samples collected 6, 9, and 12 months after disease onset from PCR-confirmed MERS-CoV patients from the 2015 South Korea outbreak, 6 with severe and 5 with mild infections (17). First, we tested serum samples for MERS-CoV S1 antibodies using different assay platforms (Figure 1; Appendix Table). Consistent with the earlier report (17), the routinely used rELISA detected only 2/6 mild infections (Figure 1, panel A). In contrast, iELISA detected 5/6 mild infections (Figure 1, panel B). Similar results were obtained using the S1 protein microarray to screen for MERS-CoV–specific antibodies (Figure 1, panel C). Although these serum samples lacked MERS-CoV neutralizing antibodies (17), the presence of nucleocapsid antibodies up to 1 year postinfection in 4/6 mildly infected patients' samples confirmed the results of the S1 ELISA with an assay targeting another MERS-CoV protein (Figure 1, panel D). All severe cases, on the other hand, were found positive in all tested platforms up to 1 year after disease onset, indicating a robust immune response of high antibody titers in severe cases (Figure 1; Appendix Table). Compared with milder infections, both S1 and neutralizing antibody responses were higher in severely infected cases, confirming that antibody responses are lower following nonsevere infection.

Specificity and Sensitivity of In-house S1 ELISA and Microarray

To confirm that the variation in the detection of mild cases is caused by the sensitivity of the different platforms used, we further validated the platforms for specificity and sensitivity using 292 serum samples (Table 1). Using MERS-CoV neutralization as the standard for MERS-CoV serology, we tested all serum samples using plaque reduction neutralization assay ($PRNT_{90}$) and for S1, S2, and nucleocapsid reactivities.

We assessed the specificity of the assays using serum samples from cohorts A–C: healthy blood donors (cohort A), patients with PCR-confirmed acute respiratory non-CoV infections (cohort B), and patients with acute to convalescent PCR-confirmed α- and β-HCoV infections (cohort C). None of the serum samples from specificity cohorts A–C were reactive by

Table 1. Cohorts used in study of specificity and sensitivity of assays for MERS-CoV*

Cohort	Country	Sample source	Infection	No. samples	Postdiagnosis range
A	The Netherlands	Healthy blood donors (negative cohort)	NA	50	NA
B	The Netherlands	Non-CoV respiratory infections†	Adenovirus	5	2–4 w
			Bocavirus	2	2–4 w
			Enterovirus	2	2–4 w
			HMPV	9	2–4 w
			Influenza A	13	2–4 w
			Influenza B	6	2–4 w
			Rhinovirus	9	2–4 w
			RSV	9	2–4 w
			PIV-1	4	2–4 w
			PIV-3	4	2–4 w
			Mycoplasma pneumoniae	1	2–4 w
			CMV	9	2–4 w
			EBV	12	2–4 w
C	The Netherlands	Persons with recent CoV infections†	α-CoV HCoV-229E	19	2 w–1 y
			α-CoV HCoV-NL63	18	2 w–1 y
			β-CoV HCoV-OC43	23	2 w–1 y

Table 1. *Continued*

Cohort	Country	Sample source	Infection	No. samples	Postdiagnosis range
D1	Qatar	S1-microarray positive persons with camel contact	NA	19	NA
D2		S1-microarray negative persons with camel contact	NA	18	NA
E	The Netherlands	RT-PCR confirmed MERS case-patients‡	Acute‡	21	1–14 d
F			Convalescent‡	7	15–228 d
G	South Korea	RT-PCR confirmed MERS case-patients	Mild infection§	17	6–12 mo
H			Severe infection¶	15	6–12 mo

* Cohorts A–C were established to test assay specificity; cohorts D–H were established to test assay sensitivity. CoV, coronavirus; CMV, Cytomegalovirus; EBV, Epstein-Barr virus; HCoV, human coronavirus; HMPV, human metapneumovirus; MERS, Middle East respiratory syndrome; mo, month; NA, not applicable; PIV, parainfluenza virus; RSV, respiratory syncytial virus.
† Cross-reactivity.
‡ Samples taken from 2 case-patients at different time points.
§ Samples taken from 6 case-patients at different time points.
¶ Samples taken from 5 case-patients at different time points.

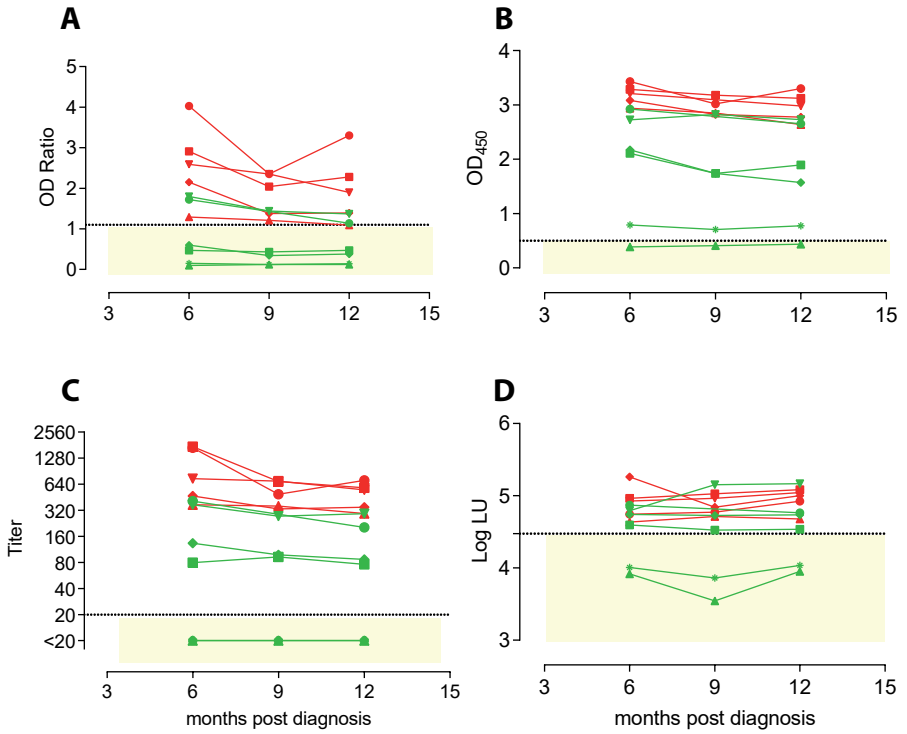

Figure 1. Detection of MERS-CoV–specific antibody responses 6–12 months following PCR-diagnosed mild and severe infections using different assays. Spike S1–specific antibody responses were tested with a routinely used S1 ELISA (rELISA) **(A)**, in-house S1 ELISA (iELISA) **(B)**, and S1 microarray **(C)**. Nucleocapsid-specific antibody responses were tested using a luciferase immunoprecipitation assay **(D)**. Severe infections (red, $n = 5$; cohort H) resulted in antibody responses detected for up to 1 year by all assays, while detection of mild infections (green, $n = 6$; cohort G) varied among assays. Horizontal dotted line indicates cutoff for each assay; yellow shaded area indicates serum undetected by each assay. CoV, coronavirus; LU, luminescence units; MERS, Middle East respiratory syndrome; OD, optical density.

iELISA at the set cutoff, indicating 100% specificity (Figure 2, panel A; Appendix). We also evaluated the sensitivity for detecting MERS-CoV infections; iELISA was able to detect MERS-CoV infections among persons with camel contact (cohort D1) who had low antibody levels as determined by protein microarray (8). Using samples from acute-phase PCR-diagnosed patients (cohort E), we detected seropositivity 6–8 days postdiagnosis (dpd). All convalescent-phase serum samples (cohort F) were positive up to the last time point tested: 228 dpd for patient 1 and 44 dpd for patient 2 (Appendix Figure 1).

These results reveal the high specificity and sensitivity of this ELISA platform, supporting our earlier findings and confirming the sensitivity of our platform in detecting low immune responses among cases of milder infection (cohort G) (Figure 1). Overall, iELISA was 100%

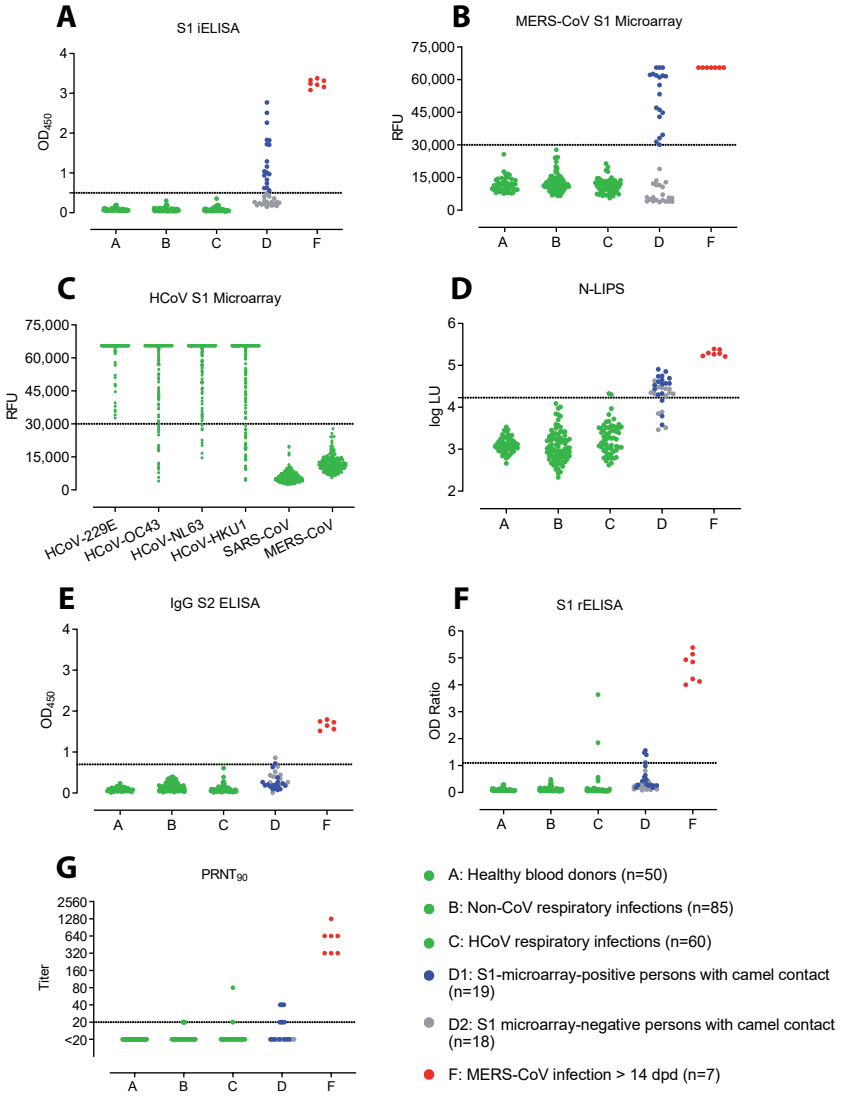

Figure 2. MERS-CoV–specific antibody responses detected by different assay platforms. **A)** In-house IgG of S1 ELISA (iELISA); **B)** MERS-CoV S1 protein microarray; **C)** HCoV S1 microarray reactivity of non-MERS-CoV–infected serum samples to the S1 proteins of 6 different HCoVs; **D)** nucleocapsid-luciferase immunoprecipitation assay; **E)** IgG S2 ELISA; **F)** routinely used IgG S1 ELISA expressed as the ratio of optical density of sample to kit calibrator; **G)** plaque reduction neutralization test (PRNT), expressed as endpoint titer for 90% plaque reduction. Serum samples tested were obtained from healthy blood donors ($n = 50$, cohort A); patients with PCR-diagnosed respiratory infections including human coronaviruses ($n = 145$, cohorts B and C); S1-microarray positive ($n = 18$, cohort D1) and negative ($n = 19$, cohort D2) camel contacts; and longitudinal serum samples from 2 PCR-confirmed MERS-CoV–infected patients taken 15–228 days after diagnosis ($n = 7$, cohort F). Cohort E is not included because patients in this cohort were in the acute phase of infection (<14 days postdiagnosis), in which seroconversion may not have occurred. Cohorts A, B, C, and F are from the Netherlands, cohort D from Qatar. Serum samples were tested at dilutions 1:101 for ELISA and N-LIPS, 1:20 for S1 microarray, and 1:20 to 1:2,560 for PRNT. Dotted lines indicate cutoff for each assay. CoV, coronavirus; LU, luminescence units; MERS, Middle East respiratory syndrome; OD, optical density; RFU, relative fluorescence units.

(95% CI 98.07%–100%) specific and 92.3% (11/13; 95% CI 66.7%–99.6%) sensitive for detection of PCR-confirmed cases (96.9% overall in the tested cohorts; 95% CI 84.3%–99.8%) (Table 2). Moreover, the iELISA performance was in accordance with that of the MERS-CoV S1 protein microarray (Figure 2, panel B). S1 microarray validation showed the same pattern of specificity with no false positives (100% specificity, 95% CI 98.07%–100%) in cohorts A–C and was 84.6% sensitive (95% CI 57.8%–97.3%) for PCR-confirmed cases and 93.8% overall (95% CI 79.9%–98.9%). Specificity of S1 as an antigen for MERS-CoV serology was further supported by the rates of seropositivity of all the serum samples from cohorts A–C: 87.4% for HCoV-HKU1, 91.3% for HCoV-OC43, 96.4% for HCoV-NL63, and 100% for HCoV-229E, as determined by microarray (Figure 2, panel C). All samples were seronegative for SARS-CoV, and no MERS-CoV false positives were detected in the iELISA and microarray. Overall, these results provided evidence for the use of S1 as a specific antigen for MERS-CoV serology.

Table 2. Specificity and sensitivity of assay platforms for the detection of MERS-CoV antibodies among PCR-confirmed cases*

Test characteristic	In-house S1 ELISA	S1 microarray	$PRNT_{90}$	Routinely used S1 ELISA
p value	<0.0001	<0.0001	<0.0001	<0.0001
Sensitivity, *N* = 13				
No. tested positive	12	11	9	9
n/N value (95% CI)	0.9231 (0.6669–0.9961)	0.8462 (0.5777–0.9727)	0.692 (0.4237–0.8732)	0.6923 (0.4237–0.8732)
Specificity, *N* = 195				
No. tested positive	0	0	1	2
n/N value (95% CI)	1 (0.9807–1)	1 (0.9807–1)	0.9949 (0.9715–0.9997)	0.9897 (0.9634–0.9982)
Positive predictive value				
Value (95% CI)	1 (0.7575–1)	1 (0.7412–1)	0.9 (0.5958 –0.9949)	0.8182 (0.523–0.9677)
Negative predictive value				
Value (95% CI)	0.9949 (0.9717–0.9997)	0.9898 (0.9637–0.9982)	0.9798 (0.9492–0.9921)	0.9797 (0.949–0.9921)
Positive likelihood ratio	NA	NA	135	67.5
Area under the ROC curve				
Area	1	0.9893	0.7348	0.9481
SE	0	0.005409	0.07513	0.01767
95% CI	1–1	0.9787–0.9999	0.5876–0.8821	0.9134–0.9827
p value	<0.0001	<0.0001	<0.0001	<0.0001

* p value calculated by Fisher exact test. CoV, coronavirus; MERS, Middle East respiratory syndrome; NA, not applicable; PRNT, plaque reduction neutralization test; $PRNT_{90}$, 90% endpoint PRNT; ROC, receiver operating characteristic.

We evaluated nucleocapsid and S2 antibody responses after MERS-CoV infections. At the set cutoff, none of the control serum samples tested positive for nucleocapsid antibodies (Figure 2, panel D). We detected seroconversion by nucleocapsid-luciferase immunoprecipitation assay among all severely infected, 4/6 (66.7%) mildly infected, and 5/18 (28%) asymptomatic S1-positive persons with camel contact. When testing for MERS-CoV S2–specific antibody responses, none of the control serum samples in cohorts A–C was cross-reactive (Figure 2, panel E), whereas 1/17 S1-negative samples and 1/18 S1-positive samples from persons with camel contact tested positive. These findings indicate low immune responsiveness in mild MERS cases. Thus, when comparing the use of S1, S2, and N proteins for the detection of MERS-CoV infections, S1 showed the highest specificity and sensitivity among the 3 tested proteins.

rELISA Validation

Strikingly, the routinely used ELISA showed the least sensitivity among the tested S1 platforms (Table 2; Figure 1; Figure 2, panel F). We saw this difference in the cohort of persons with camel contact from Qatar who had mild to asymptomatic infections and who were identified to be seropositive for MERS-CoV in an earlier study (8) (Figure 2, panel F, cohort D1). Although they tested seropositive by iELISA and the microarray platform, only 20% of those also tested positive using the rELISA platform. We tested different coating conditions and found that a reduction in antigen coating or a loss of some conformational epitopes could have contributed to the low sensitivity seen in the rELISA versus the iELISA, despite testing the same antigen (S1) (Figure 3). This low sensitivity confirms the likelihood of false-negative detection of some MERS-CoV cases using rELISA.

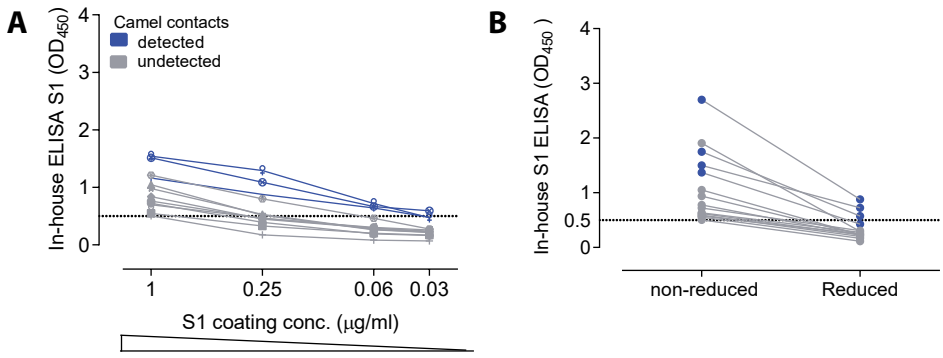

Figure 3. Low sensitivity of commercial S1 ELISA shown as the effect of lowering coating antigen concentration **(A)** or antigen denaturation **(B)** on the sensitivity of antibody detection among Middle East respiratory syndrome coronavirus–infected persons with camel contact. All samples were seropositive by in-house S1 ELISA and microarray. Dark blue indicates those that tested seropositive by commercial S1 ELISA.

We evaluated the specificity of the rELISA platform using cohorts A–C. Among these, serum samples from 2 patients with HCoV-OC43 (a β-CoV) infection tested positive (Figure 2, panel F) but tested negative for MERS-CoV neutralization by $PRNT_{90}$ and S1 antibodies by iELISA and microarray (Table 3). Thus, to confirm the cross-reactivity of the 2 serum samples with MERS-CoV S1 in rELISA, we tested serum samples taken from both patients at different time points, before and after OC43 infection. All preinfection serum samples were negative, but all postinfection serum samples were positive in the rELISA (Figure 4). On the contrary, none of the serum samples was positive when tested by PRNT, Western blot, immunofluorescence assay, iELISA, or S1 protein microarray (using commercial and in-house S1 proteins), indicating a false-positive reaction in the rELISA. Overall, the rELISA was 98.97% (95% CI 96.3%–99.8%) specific in the tested cohorts (Table 3. Sensitivity and specificity results of routinely used commercial S1 ELISA and $PRNT_{90}$ assays for MERS-CoV*). Using a lower cutoff (optical density ratio 0.4) to show 100% specificity and sensitivity as suggested in an earlier study (30), did increase the sensitivity, (from 69.2% to 84.6%), but doing so reduced specificity; numbers of false-positive results increased from 2 to 7 and specificity decreased from 98.97% to 96.4% (Appendix Figure 2).

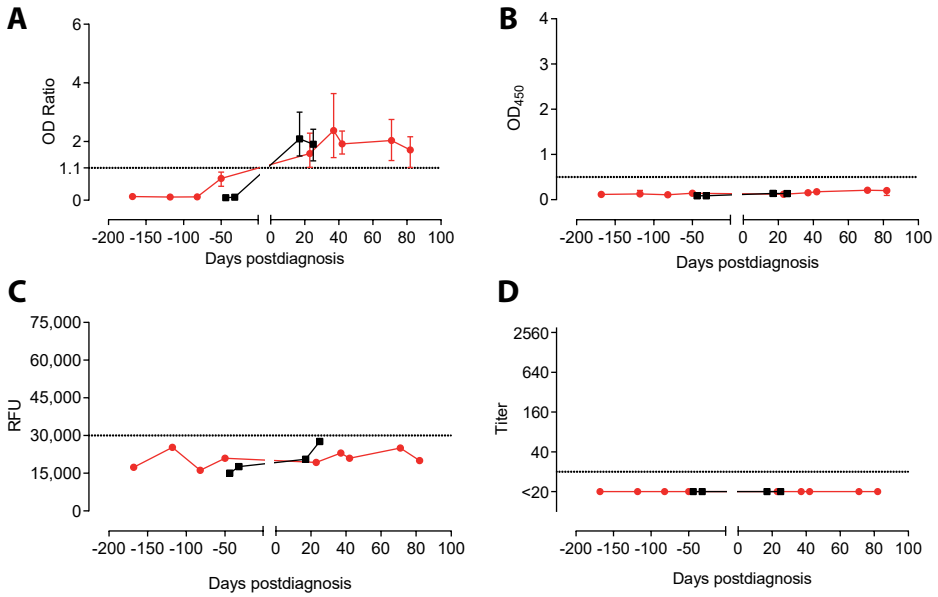

Figure 4. Reactivity to Middle East respiratory syndrome coronavirus of serum samples from 2 patients with human coronavirus OC43 in different assays. Longitudinal serum samples, collected before and after OC43 infection, from the 2 patients (red, patient 1; black, patient 2) were analyzed by commercial IgG S1 ELISA **(A)**; in-house IgG S1 ELISA **(B)**; S1 protein microarray **(C)**; and $PRNT_{90}$ **(D)**. Dotted line indicates the cutoff for each assay. Error bars indicate 95% CIs. OD, optical density; $PRNT_{90}$, 90% reduction in plaque reduction neutralization test; RFU, relative fluorescence units.

Mild MERS-CoV infections and Neutralizing Antibodies

To investigate the difference in the neutralization responses produced following severe and mild infections and the reliability of neutralization assays as confirmatory assays for mild infections, we validated $PRNT_{90}$ for specific and sensitive detection of MERS-CoV infections. Although none of the healthy blood donors (cohort A) were reactive, the respiratory patients (cohorts B and C) showed low levels of cross-neutralization (titer 20) in 12 serum samples. One sample with a titer of 80 (Figure 2, panel G) was from an HCoV-OC43 patient; none of the serum samples taken at 4 earlier time points from that patient showed any neutralization by PRNT (data not shown). All 13 serum samples tested negative for S1 antibodies in all tested platforms (Table 3); none of the serum samples was positive in 2 assays. For PCR-diagnosed MERS cases (cohorts E–H), $PRNT_{90}$ showed 100% sensitivity for detecting severe cases after the seroconversion period (>14 dpd; cohort F) and for up to 1 year (cohort H), indicating strong neutralizing antibody responses.

In contrast, results varied for mild cases (cohort G). Neutralizing antibodies were detected in 3/6 (50%) of mild infections (Appendix Table 1), highlighting lower, shorter-lived neutralizing responses among mild cases. This finding is consistent with the results of a cohort of mild to asymptomatic MERS-CoV–infected persons with camel contact from Qatar (8) (Figure 2, panel G, cohort D1). These persons had low to undetectable neutralizing antibodies while being reactive to S1 on the protein microarray platform and in our iELISA.

Nonneutralizing Antibodies after Mild MERS-CoV Infections

For the PCR-confirmed MERS-CoV patients (cohorts E–H) and serologically positive persons with camel contact (cohort D1), S1 antibody titers as determined by iELISA strongly correlated with neutralization titers (Figure 5, panel A), showing that S1 antibody response is a reliable predictor of neutralization activity. This finding indicates that a population of mildly infected patients with S1-reactive antibodies but no detectable neutralizing antibodies could easily be missed in attempts to confirm cases by neutralization assay.

Discussion

Serologic detection of MERS-CoV exposure is valuable for identifying asymptomatic cases and virus reservoirs in population screening and epidemiologic studies, as well as for contact investigations. Detection aids in understanding the host immune response to the virus, identifying key viral immunogens, and mapping key neutralizing antibodies, which all lead to implementing appropriate preventive and therapeutic measures. Antibody responses varied among PCR-confirmed MERS-CoV cases; case-patients with mild and asymptomatic

Table 3. Sensitivity and specificity results of routinely used commercial S1 ELISA and $PRNT_{90}$ assays for MERS-CoV*

Assay parameter and sample source	Infection	No. positive/no. tested			Specificity or sensitivity, %	
		S1 rELISA‡	$PRNT_{90}$ (titer)			
			S1-positive	S1-negative	S1 rELISA	$PRNT_{90}$
Specificity					98.97	93.33 (1:20); 99.5 (1:40)
Healthy blood donors	None	0/50	NA	0/50		
Non-CoV respiratory infections	Adenovirus	0/5	NA	1/5(20)		
	Bocavirus	0/2	NA	0/2		
	Enterovirus	0/2	NA	0/2		
	HMPV	0/9	NA	1/9 (20)		
	Influenza A	0/13	NA	4/13 (20, 20, 20, 20)		
	Influenza B	0/6	NA	0/6		
	Rhinovirus	0/9	NA	2/9 (20, 20)		
	RSV	0/9	NA	1/9 (20)		
	PIV-1	0/4	NA	0/4		
	PIV-3	0/4	NA	0/4		
	Mycoplasma	0/1	NA	0/1		
	CMV	0/9	NA	0/9		
	EBV	0/12	NA	0/12		
Recent CoV infections†	α-CoV HCoV-229E	0/19	NA	3/19 (20, 20, 20)		
	α-CoV HCoV-NL63	0/18	NA	0/18		
	β-CoV HCoV-OC43	2/23	0/2	1/21 (80)		

Table 3. *Continued*

Assay parameter and sample source	Infection	No. positive/no. tested			Specificity or sensitivity, %	
		S1 rELISA‡	$PRNT_{90}$ (titer)			
			S1-positive	S1-negative	S1 rELISA	$PRNT_{90}$
Sensitivity						
Persons with camel contact	S1-microarray positive§	4/19	4/4 (40, 40, 40, 20)	6/15 (40, 40, 20, 20, 20, 20)	21	52.6
	S1-microarray negative	0/18	NA	1/18 (20)	NA	NA
RT-PCR–confirmed MERS cases	≤14 d postdiagnosis	11/21	11/11	1/10 (80)	NA	NA
	>14 d postdiagnosis	7/7	7/7	NA	100	100
	6–12 mo postdiagnosis; mild infection	5/17	5/5	NA	35.3	35.3
	6–12 mo postdiagnosis; severe infection	15/15	15/15	NA	100	100

*CMV, Cytomegalovirus; CoV, coronavirus; EBV; Epstein-Barr virus; ELISA, enzyme-linked immunosorbent assay; HCoV, human coronavirus; HMPV; human metapneumovirus; MERS, Middle East respiratory syndrome; NA, not applicable; PIV, parainfluenza virus; PRNT, plaque reduction neutralization test; $PRNT_{90}$, 90% endpoint PRNT; rELISA routine ELISA; RSV, respiratory syncytial virus; RT-PCR, reverse transcription PCR.

† Cross-reactivity.

‡ None of the serum samples from specificity cohorts tested positive by in-house S1 ELISA or microarray.

§ All 19 serum samples (protein microarray positive) tested positive by in-house S1 ELISA.

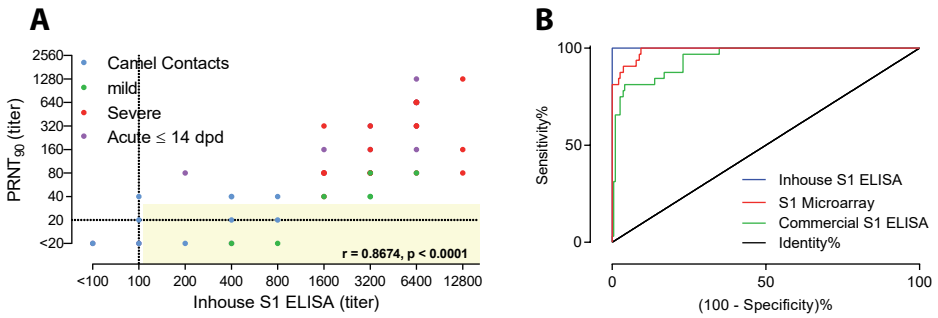

Figure 5. Correlation between neutralizing and S1 antibody responses and comparison of different S1 platforms. **A)** $PRNT_{90}$ neutralization titers and IgG titers obtained by in-house S1 ELISA among PCR-confirmed MERS-CoV patients and persons with camel contact. Spearman correlation r value and 2-tailed p-value are shown. Yellow shading indicates S1-reactive nonneutralizing antibodies. **B)** Receiver operator characteristic (ROC) curves comparing the specificity and sensitivity of different MERS-CoV S1–based platforms for the diagnosis of MERS-CoV infections among PCR-confirmed cases. AUC for iELISA (blue) is 1; for S1 microarray (red) is 0.9893; for rELISA (green) is 0.9481. Dotted lines show the cutoff for each assay. AUC, area under the curve; dpd, days postdiagnosis; $PRNT_{90}$, 90% reduction in plaque reduction neutralization test.

infections showed low or undetectable seroconversion, in contrast to severe infections that resulted in robust responses (5, 17, 31). The low-level antibody responses produced following nonsevere infections led to failure in detecting such responses in some patients by a routinely used ELISA and neutralization assays (5, 17, 32). This result may have impeded estimation of prevalence of virus infections in surveillance studies. We were able to detect nonneutralizing antibody responses among previously infected mild and asymptomatic cases that were previously unidentified; this finding indicates that MERS-CoV prevalence could be higher than current estimates and that using sensitive platforms could lead to more precise calculation of incidence rates.

Although an earlier study evaluating serologic responses among PCR-confirmed MERS patients reported seroconversion in only 2/6 (33%) mildly infected cases (17), we were able to detect 5/6 (83.5%) by our in-house S1 ELISA and 4/6 (67%) by microarray. S1 iELISA and microarray were highly sensitive for detecting MERS-CoV infections, showing 100% specificity in the tested cohorts. Although the rELISA platform detected severe infections with no false negatives, it did not detect seroconversion among some mildly infected PCR-confirmed and asymptomatic persons with camel contact who had low antibody responses. In addition, rELISA results showed cross-reactivity with some serum samples from HCoV-OC43–infected persons. The variation in the reactivity between the 2 ELISA platforms could be attributed to the difference in the coating protein preparations used in each or to the reduced stability of the protein during storage of the rELISA platform.

Overall, our results validate the use of S1 as a specific antigen for MERS-CoV serology if folding is correct, providing a highly specific 1-step diagnostic approach without false positives omitting the need for a confirmatory assay. In particular, neutralizing antibodies were undetectable after most asymptomatic and some mild infections. Using 50% instead of 90% reduction as a cutoff for PRNT can increase the sensitivity of the assay for confirming mild or asymptomatic infections (15, 21, 33), but it is crucial to precede PRNT with a sensitive screening assay to avoid false-negative results.

Prolonged viral shedding observed in severely infected patients but not in patients with mild infections (5, 17, 34) indicated that a short-lived infection in nonsevere cases may account for lower antibody responses, including functional neutralizing antibodies. A possible reason is that nonneutralizing antibodies comprise a substantial proportion of antibodies elicited after a viral infection; these antibodies can be elicited against viral proteins, including immature forms of surface proteins, released through lysis of infected cells following a short-lived abortive infection (35, 36). We found that spike antibody titers were produced at higher titers than nucleocapsid antibodies and neutralizing antibodies were undetectable following nonsevere infections. These findings indicate that anti-spike antibodies are more sensitive predictors for previous MERS-CoV infections, especially mild and asymptomatic infections, and that conducting neutralization assays to confirm serologic findings, as recommended by the World Health Organization (37), could result in potential underestimation of the true prevalence in epidemiologic studies.

Further studies testing patients with previously indeterminate infection could provide further clues on the epidemiology of MERS-CoV. A recent study reported the presence of MERS-CoV–specific CD8+ T-cell responses after MERS-CoV infection, irrespective of disease severity (38). Therefore, T-cell assays can be used to confirm serologic findings in epidemiologic studies (mainly asymptomatic cases) instead of neutralization assays that could yield underestimated results. However, further studies are needed to rule out possible T-cell cross-reactivity with other HCoV.

Despite the use of 90% reduction as endpoint for PRNT, we observed cross-neutralization in the respiratory panel samples (13/195). All but 1 sample had a titer of 20, and all 13 were S1-negative. We reported a similar finding in an earlier study, where 1 of 35 S1 negative serum samples had a neutralization titer of 20 (8). This finding was unexpected because neutralization assays, with their high specificity, are considered the standard for MERS-CoV serodiagnosis. Such seemingly false positives could be attributed to the presence of natural antibodies or cross-reactive HCoV antibodies (15, 32, 35, 39).

Cross-neutralization among human coronaviruses has rarely been reported. Chan et al. described cross-neutralization between SARS-CoV and MERS-CoV at low titers (<20) (32).

However, these serum samples also tested positive for HCoV-OC43 neutralization. This finding, along with ours, raises the probability that HCoV-OC43 antibodies caused cross-reactivity; antibodies in the serum sample could be recognizing an epitope outside S1 and thus not detected in ELISA. Of interest, we detected an HCoV-OC43 patient serum sample that could neutralize MERS-CoV at $PRNT_{90}$ titer <80, but we found that the patient received an oncolytic medication shown to have antiviral activity (40). This finding could also be a probable reason for the observed cross-neutralization. Overall, while serum samples from healthy blood donors showed no cross-neutralization or cross-reactivity to S2 or N proteins, we observed some cross-neutralization and comparably higher reactivity to S2 and N proteins in serum samples of patients with respiratory infections, which we did not detect by our in-house S1 platforms. Thus, we could not avoid cross-reactivity to S2 and N proteins, leading to false positives, without loss of sensitivity. The high specificity of the S1 protein enabled us to set a cutoff high enough to ensure specificity without losing sensitivity.

Using S1 in optimized platforms enabled us to detect seroconversion among otherwise unrecognized nonsevere MERS-CoV cases with very high sensitivity and 100% specificity. Our findings indicate that our iELISA and microarray for MERS-CoV diagnostics (Table 2; Figure 5, panel B) could be reliable diagnostic tools for identifying MERS-CoV infections. For further standardization of the assay, a calibrator (e.g., monoclonal antibody) can be included in each run to avoid intraassay variations.

Although further testing on a larger cohort may be required to rule out cross-reactivity, ensure sensitivity, and thereby validate general use as a 1-step diagnostic assay, the data obtained in this study indicate that cross-reactivity between HCoVs (at least when testing for MERS-CoV and SARS-CoV reactivity) is unlikely to occur when using optimized platforms with the divergent S1 protein. A more recent follow-up study revealed that, among 454 serum samples tested using our in-house S1 ELISA, including those from persons with camel contact, only 2 samples, both MERS-CoV–neutralization positive, tested positive whereas all other serum samples were found to be negative in the iELISA (R. Bassal et al., unpub. data). Thus, in principle, low-level antibody responses among nonsevere MERS-CoV cases may be revealed by a single ELISA test.

Because patients with mild or asymptomatic infections do not develop severe illness and thus go unrecognized, they might play a role in spreading the virus into the community, initiating outbreaks in which index case-patients report no history of camel or patient exposure. Therefore, defining the subclinical burden of infection will enable better understanding of the extent, severity, and public health threat posed by MERS-CoV, which, in turn, will guide the development and implementation of proper strategies to contain and prevent ongoing outbreaks of infection with this virus.

Appendix

Serum Samples

We collected serum samples from 50 healthy blood donors (Cohort A) as negative controls Sanquin Blood Bank (Rotterdam, the Netherlands) obtained written informed consent for research use. We assessed specificity using cohorts B and C, which consisted of 145 serum specimens from patients confirmed by RT-PCR to be positive for human respiratory infections. Those included samples from persons recently infected with 13 different respiratory viruses, or with acute IgM-positive CMV and EBV infection, which are known to be cross-reactive in serologic assays; as well as *Mycoplasma pneumoniae*. Because MERS has no pathognomonic signs distinguishing it from other respiratory infections, cohort B, including 85 samples from acute non-HCoV respiratory infections, was used to assess specificity in acute cases. To further evaluate specificity, cohort C included serum samples from acute to convalescent HCoV-NL63, 229E, and -OC43 patients. Furthermore, we assessed Cohorts D-G were used to evaluate sensitivity of the different platforms. Serologically identified MERS-CoV–infected mild and asymptomatic persons with camel contact (D1) and healthy donors (D2) from Qatar characterized in an earlier study (8) constituted cohort D. Serial serum samples from 2 RT-PCR–diagnosed MERS-CoV case-patients imported to the Netherlands (29) were used as positive controls and to evaluate antibody kinetics; these were 15 serum samples from patient 1, ranging 4–228 days postdiagnosis (dpd), and 13 from patient 2, ranging 1–44 dpd. These 28 samples were categorized into cohorts E (<14 dpd, acute phase) and F (>14 dpd, convalescent phase). Finally, samples from the PCR-diagnosed mild (cohort G) and severely (cohort H) infected MERS-CoV case-patients from South Korea, described earlier (34), formed the last 2 cohorts.

All samples were stored at -20°C until use. The use of serum samples from the Netherlands was approved by the local medical ethical committee (MEC approval: 2014–414). The Institutional Ethics Review Board of Seoul National University Hospital approved use of samples from South Korea (approval no. 1506–093–681). The Ethics and Institutional Animal Care and Use Committees of the Medical Research Center, Hamad Medical Corporation, approved the use of samples from Qatar (permit 2014–01–001).

Protein Expression

We expressed MERS S1 (amino acids 1–751) in HEK-293T cells as a C-terminal human IgG Fc (hFc) tagged protein. We purified S1-hFc protein using protein A sepharose beads (ThermoFisher Scientific, https://www.thermofisher.com) and cleaved off the hFc domain using Factor Xa (EMD Millipore, http://www.emdmillipore.com). We used X-arrest Agarose (EMD Millipore, http://www.emdmillipore.com) to obtain soluble S1 after removal of Factor Xa; S1 protein was used for coating our in-house S1 ELISA plates and microarray.

Spike S1 proteins of other HCoVs, –HKU1 (residues 1–750), –OC43 (residues 1–760), NL63 (residues 1–717), 229E (residues 1–537), and SARS-CoV (residues 1–676), were expressed as C-terminal murine IgG2a Fc tagged proteins as described earlier (41) and used for coating S1 protein microarray.

Recombinant MERS-CoV spike S2 subunit (amino acids 752–1262) was produced in the baculovirus expression system. Briefly, we cloned the codon-optimized MERS-CoV S2 encoding sequence into the pFastbac transfer vector (Invitrogen, https://www.thermofisher.com) in-frame between honeybee melittin (HBM) secretion signal peptide and a triple StrepTag purification tag. We produced acmid DNA and recombinant baculovirus according to protocols from the Bac-to-Bac system (Invitrogen). We expressed MERS-CoV S2 protein in Sf-9 cells after infection with the recombinant baculovirus. We harvested recombinant S2 from cell culture supernatants 3 days postinfection and purified it using StrepTactin sepharose affinity chromatography (IBA, https://www.iba-lifesciences.com). The protein was used to coat ELISA plates.

PRNT

PRNT was used as a reference for this study, because it is the standard for MERS-CoV serology. We tested serum samples for their neutralization capacity against MERS-CoV (Erasmus MC isolate) by plaque-reduction neutralization test (PRNT) using Huh-7 cells in a 96-well plate format. Heat-inactivated samples were 2-fold serially diluted (1:20 up to 1:2560) in RPMI1640 medium supplemented with penicillin, streptomycin, and 1% fetal bovine serum, starting at a dilution of 1:10 in 50 µL. We added 50 µL of the virus suspension to each well (500 TCID50) and incubated at 37°C for 1 h. Following incubation, we transferred the mixtures (virus and serum) on Huh-7 cells cultured in 96-well plates and incubated them at 37°C for 8 h. We then fixed the cells and stained them with immunofluorescent staining. The serum neutralization titer is the reciprocal of the highest dilution resulting in an infection reduction of >90% ($PRNT_{90}$). A titer of >20 was considered to be positive.

S1 ELISA

We performed MERS-CoV IgG S1 ELISA using a commercial kit (Euroimmun, https://www.euroimmun.com) and performed the assay according to manufacturer's protocol. The optical density (OD) was measured at 450 nm, and a ratio of the reading of each sample to the reading of the calibrator, included in the kit, was calculated for each sample (OD ratio). According to the manufacturer's guidelines, samples with an OD ratio <0.8 were considered negative, those with an OD ratio >1.1 were considered positive, whereas those in between were considered borderline.

We performed inhouse S1 ELISA by coating 96-well microtiter ELISA plates with MERS-CoV S1 protein (1 µg/mL) in PBS overnight at 4°C. Following blocking, diluted serum (1:100 or 2-fold serially diluted [1:100–1:12800] for titers) were added and incubated at 37°C for 1h. Bound antibodies were detected using peroxidase-labeled rabbit anti–human IgG (Dako, https://www.agilent.com) and TMB as a substrate. The absorbance of each sample was measured at 450 nm. We set a cutoff at 0.5, which is >6 standard deviations above the mean value of the negative respiratory cohort (0.46). Serum titers correspond to the reciprocal of the highest dilution giving a signal above the cutoff. We tested all samples twice in 2 independent assays.

S1 Protein Microarray

We diluted serum 4-fold (1:20 to 1:1280) and tested using an HCoV S1 protein microarray as previously described (23); including S1 domains of the 6 known HCoVs. We set a cutoff was set at 30,000 relative fluorescent units and determined serum titers as the reciprocal of the serum dilution corresponding to the EC_{50} of each serum sample interpolated from a concentration-response curve (42).

N-LIPS Assay

Anti-nucleocapsid antibody responses were tested using a luciferase immunoprecipitation assay (LIPS). The N protein was expressed in HEK-293T cells as an N terminal *Renilla* luciferase (Ruc)-tagged protein (Ruc-N) using pREN2 expression vector kindly provided by Dr. Peter D. Burbelo (43). The cells were harvested in lysis buffer (50 mM Tris [pH 7.5], 100 mM NaCl, 5 mM $MgCl_2$, 1% Triton X-100, 50% glycerol, protease inhibitors), and the luminescence units (LU) per µL was used as a measure of antigen concentration in cell lysates. We conducted LIPS assay according to Burbelo et al. (44) with minor modifications. Briefly, we diluted serum 1:10 in buffer A (50 mM Tris [pH 7.5], 100 mM NaCl, 5 mM $MgCl_2$, 1% Triton X-100). Then we incubated a mixture containing 10 µL of diluted serum and 1×10^7 RLU of Ruc-Ag in a total volume of 100 µL of buffer A per well at room temperature on a rotary shaker for 1 h. We transferred the mixture containing antigen-antibody complex (100 µL) into MultiScreenHTS BV Filter Plate (Merck Millipore, https://www.merckmillipore.com) containing 5 µL of a 30% suspension of UltraLink protein A/G beads and reincubated under the same conditions for 1 more hour. After that, the wells were washed 8 times with buffer A and twice with PBS and luminescence was measured for each well after adding 100 µL of 0.1 µM coelenterazine (Nanolight Technology, www.nanolight.com) in assay buffer (50 mM potassium phosphate, pH 7.4, 500 mM NaCl, 1 mM EDTA). We tested serum samples in duplicates in >2 independent assays and averaged the data to determine the LU value for each sample. A cutoff was set at 30,000 LU.

S2 ELISA

We conducted MERS-CoV IgG S2 ELISA following the same protocol used for the inhouse S1 ELISA. A cutoff was set at 0.72, which is equal to 6 standard deviations above the mean value of the negative cohorts.

Appendix Table 1. Serologic responses of Middle East respiratory syndrome coronavirus, South Korea, 2015

		Euroimmun S1 ELISA OD ratio			In-house S1 ELISA OD (titer)			S1 microarray titer			$PRNT_{90}$ titer			N-LIPS LU x 103		
Disease severity	Pt	6 mpi	9 mpi	12 mpi	6 mpi	9 mpi	12 mpi	6 mpi	9 mpi	12 mpi	6 mpi	9 mpi	12 mpi	6 mpi	9 mpi	12 mpi
Severe	C	3.30	2.35	4.03	3.24 (6400)	3.11 (3200)	3.44 (12800)	1685	490	707	640	ND	ND	55.4	59.3	84.2
	D	2.91	2.04	2.28	3.27 (12800)	3.18 (6400)	3.12 (3200)	1734	689	581	ND	ND	80	92.2	106.2	121.3
	F	1.29	1.21	1.09	2.99 (1600)	2.77 (1600)	2.65 (1600)	370	358	293	ND	ND	160	43.3	51.5	47.7
	G	2.59	2.35	1.90	3.21 (3200)	3.19 (3200)	3.01 (3200)	740	693	551	ND	ND	80	84.3	92.3	111.0
	H	2.15	1.38	1.39	3.09 (3200)	2.82 (1600)	2.76 (1600)	468	332	347	ND	ND	40	182.1	69.3	100.6
Mild	K	1.72	NA	1.14	3.06 (3200)	NA	2.64 (1600)	407	NA	203	ND	ND	40	74.2	NA	58.0
	L	0.47	0.43	0.47	2.1 (1600)	1.7 (800)	1.87 (800)	80	93	76	ND	ND	<20	39.4	33.5	27.8
	M	0.10	0.12	0.12	0.4 (<100)	0.41 (<100)	0.45 (<100)	<20	<20	<20	ND	ND	<20	8.3	3.5	9.0
	N	1.80	1.44	1.37	2.67 (6400)	2.84 (3200)	2.74 (3200)	371	274	292	ND	ND	80	61.9	142.4	147.0
	O	0.60	0.34	0.38	2.33 (800)	1.79 (400)	1.58 (400)	133	98	87	ND	ND	20	55.2	53.3	54.5
	P	0.15	0.12	0.14	0.78 (200)	0.67 (200)	0.73 (400)	<20	<20	<20	ND	ND	<20	10.2	7.3	10.8
Severe		5/5	5/5	5/5	5/5	5/5	5/5	5/5	5/5	5/5	5/5	ND	ND	5/5	5/5	5/5
Mild		2/6	2/6	2/6	2/6	5/6	4/5	5/6	4/6	3/5	4/6	ND	ND	3/6	4/6	3/5

* Red type indicates serum samples that tested negative in each assay. LU, luminescence units; mpi, months post-infection; N-LIPS, nucleocapsid luciferase immunoprecipitation assay; OD, optical density; $PRNT_{90}$, >90% plaque-reduction neutralization test; Pt., patient; S1, spike S1 protein.

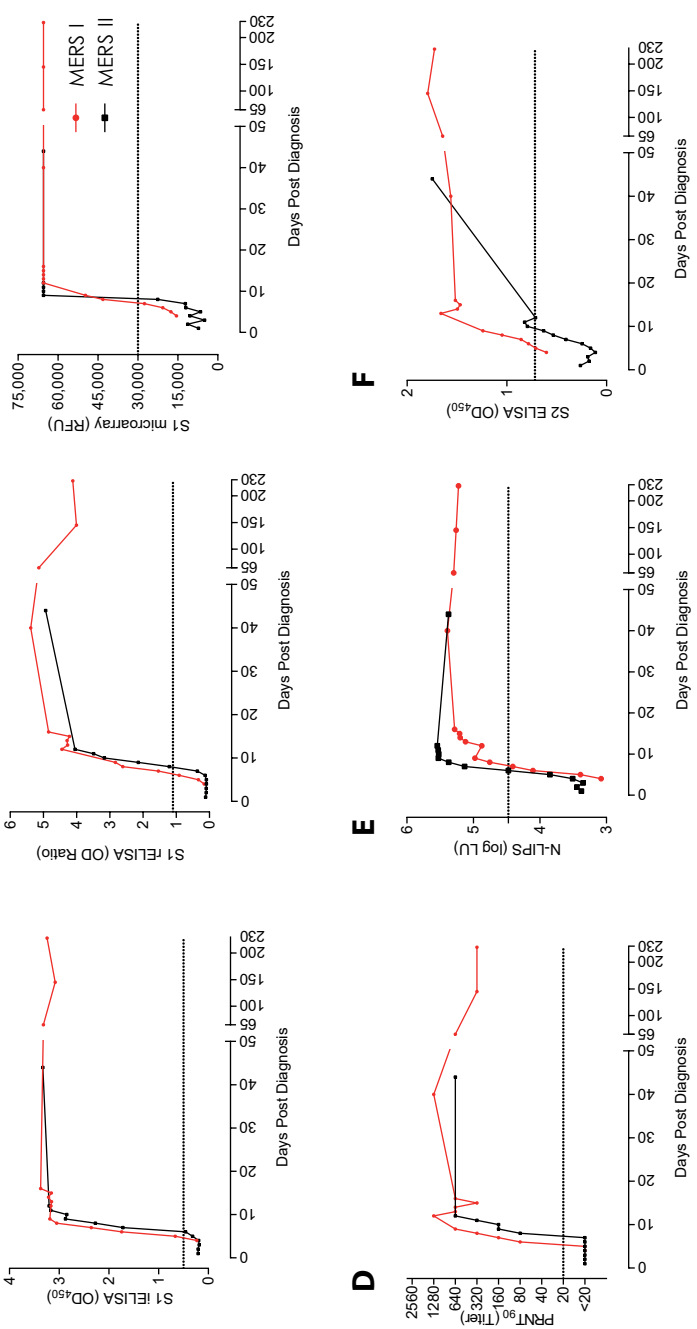

Appendix Figure 1. Kinetics of MERS-CoV specific S1, S2, N and neutralizing antibody responses in 2 patients with Middle East respiratory syndrome. We tested antibody responses in serum samples using **(A)** an inhouse S1 ELISA (iELISA); **(B)** a routinely used S1 ELISA (rELISA); **(C)** S1 microarray; **(D)** plaque reduction neutralization test (PRNT); **(E)** nucleocapsid luciferase immunoprecipitation assay (N-LIPS); **(F)** S2 ELISA. Shown are antibody responses in time for serum from 2 patients (red, patient 1; black, patient 2). The dotted lines show the cutoff for each assay. LU, luminescence units, N-LIPS, nucleocapsid luciferase immunoprecipitation assay; OD, optical density at 450 nm; $PRNT_{90}$, 90% reduction in plaque reduction neutralization test; and RFU, relative fluorescence units.

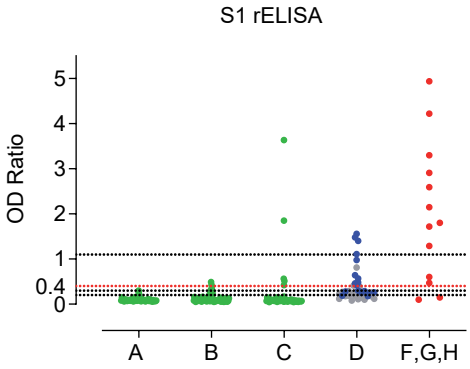

cut-off (OD ratio)		Specificity		Sensitivity	
Reference	value	n	%	n	%
assay kit	1.1	193/195	98.97	9/13	69.23
(10)	0.4	188/195	96.41	11/13	84.62
(11,12)	0.3	185/195	94.87	11/13	84.62
(10)	0.2	177/195	90.77	11/13	84.62

Appendix Figure 2. Effect of lowering the assay cutoff on the specificity and sensitivity of the rELISA for detection of MERS-CoV specific antibodies. The overall specificity and sensitivity of rELISA in the specificity cohorts A–C and sensitivity cohorts D–H. Graph shows the ratio of optical density of sample to kit calibrator for study cohorts. Dotted lines indicate different cutoffs (OD ratio 1.1, 0.4, 0.3, 0.2). The table shows the number and percentage specificity (cohorts A–C; *n* = 195) and sensitivity in PCR-confirmed cases (cohorts F, G, H; *n* = 13). Cohorts: A, healthy blood donors (*n* = 50); B, acute non-CoV respiratory infections (*n* = 85); C, acute to convalescent non-MERS-CoV respiratory infections (n = 60); D, S1-microarray positive persons with camel contact (*n* = 18; blue; D1) and S1-microarray negative persons with camel contacts (*n* = 19; gray; D2); F–H, PCR-confirmed MERS-CoV–infected patients (*n* = 13).

References

1. Zaki AM, van Boheemen S, Bestebroer TM, Osterhaus AD, Fouchier RA. Isolation of a novel coronavirus from a man with pneumonia in Saudi Arabia. The New England journal of medicine. 2012 Nov 8;367(19):1814-20.
2. World Health Organization. Middle East respiratory syndrome coronavirus (MERS-CoV) [cited 16-7-2017]; Available from: http://www.who.int/emergencies/mers-cov/en/
3. Puzelli S, Azzi A, Santini MG, Di Martino A, Facchini M, Castrucci MR, et al. Investigation of an imported case of Middle East Respiratory Syndrome Coronavirus (MERS-CoV) infection in Florence, Italy, May to June 2013. Euro surveillance : bulletin Europeen sur les maladies transmissibles = European communicable disease bulletin. 2013 Aug 22;18(34).
4. Al Hammadi ZM, Chu DK, Eltahir YM, Al Hosani F, Al Mulla M, Tarnini W, et al. Asymptomatic MERS-CoV Infection in Humans Possibly Linked to Infected Dromedaries Imported from Oman to United Arab Emirates, May 2015. Emerg Infect Dis. 2015 Dec;21(12):2197-200.
5. Alshukairi AN, Khalid I, Ahmed WA, Dada AM, Bayumi DT, Malic LS, et al. Antibody Response and Disease Severity in Healthcare Worker MERS Survivors. Emerg Infect Dis. 2016 Jun;22(6).
6. Reusken CB, Haagmans BL, Muller MA, Gutierrez C, Godeke GJ, Meyer B, et al. Middle East respiratory syndrome coronavirus neutralising serum antibodies in dromedary camels: a comparative serological study. The Lancet Infectious diseases. 2013 Oct;13(10):859-66.
7. Haagmans BL, Al Dhahiry SH, Reusken CB, Raj VS, Galiano M, Myers R, et al. Middle East respiratory syndrome coronavirus in dromedary camels: an outbreak investigation. The Lancet Infectious diseases. 2014 Feb;14(2):140-5.
8. Reusken CB, Farag EA, Haagmans BL, Mohran KA, Godeke GJt, Raj S, et al. Occupational Exposure to Dromedaries and Risk for MERS-CoV Infection, Qatar, 2013-2014. Emerg Infect Dis. 2015 Aug;21(8):1422-5.
9. Muller MA, Meyer B, Corman VM, Al-Masri M, Turkestani A, Ritz D, et al. Presence of Middle East respiratory syndrome coronavirus antibodies in Saudi Arabia: a nationwide, cross-sectional, serological study. The Lancet Infectious diseases. 2015 May;15(5):559-64.
10. Kayali G, Peiris M. A more detailed picture of the epidemiology of Middle East respiratory syndrome coronavirus. The Lancet Infectious diseases. 2015 May;15(5):495-7.
11. Assiri AM, Biggs HM, Abedi GR, Lu X, Bin Saeed A, Abdalla O, et al. Increase in Middle East Respiratory Syndrome-Coronavirus Cases in Saudi Arabia Linked to Hospital Outbreak With Continued Circulation of Recombinant Virus, July 1-August 31, 2015. Open Forum Infect Dis. 2016 Sep;3(3):ofw165.
12. Park JW, Lee KJ, Lee KH, Lee SH, Cho JR, Mo JW, et al. Hospital Outbreaks of Middle East Respiratory Syndrome, Daejeon, South Korea, 2015. Emerg Infect Dis. 2017 Jun;23(6):898-905.
13. Memish ZA, Zumla AI, Al-Hakeem RF, Al-Rabeeah AA, Stephens GM. Family cluster of Middle East respiratory syndrome coronavirus infections. The New England journal of medicine. 2013 Jun 27;368(26):2487-94.
14. Assiri A, McGeer A, Perl TM, Price CS, Al Rabeeah AA, Cummings DA, et al. Hospital outbreak of Middle East respiratory syndrome coronavirus. The New England journal of medicine. 2013 Aug 1;369(5):407-16.
15. Drosten C, Meyer B, Muller MA, Corman VM, Al-Masri M, Hossain R, et al. Transmission of MERS-coronavirus in household contacts. The New England journal of medicine. 2014 Aug 28;371(9):828-35.
16. Aleanizy FS, Mohmed N, Alqahtani FY, El Hadi Mohamed RA. Outbreak of Middle East respiratory syndrome coronavirus in Saudi Arabia: a retrospective study. BMC Infect Dis. 2017 Jan 5;17(1):23.
17. Choe PG, Perera R, Park WB, Song KH, Bang JH, Kim ES, et al. MERS-CoV Antibody Responses 1 Year after Symptom Onset, South Korea, 2015. Emerg Infect Dis. 2017 Jul;23(7):1079-84.

18. Corman VM, Eckerle I, Bleicker T, Zaki A, Landt O, Eschbach-Bludau M, et al. Detection of a novel human coronavirus by real-time reverse-transcription polymerase chain reaction. Euro surveillance : bulletin Europeen sur les maladies transmissibles = European communicable disease bulletin. 2012 Sep 27;17(39).
19. Corman VM, Muller MA, Costabel U, Timm J, Binger T, Meyer B, et al. Assays for laboratory confirmation of novel human coronavirus (hCoV-EMC) infections. Euro surveillance : bulletin Europeen sur les maladies transmissibles = European communicable disease bulletin. 2012 Dec 6;17(49).
20. Furuse Y, Okamoto M, Oshitani H. Conservation of nucleotide sequences for molecular diagnosis of Middle East respiratory syndrome coronavirus, 2015. Int J Infect Dis. 2015 Nov;40:25-7.
21. Park SW, Perera RA, Choe PG, Lau EH, Choi SJ, Chun JY, et al. Comparison of serological assays in human Middle East respiratory syndrome (MERS)-coronavirus infection. Euro surveillance : bulletin Europeen sur les maladies transmissibles = European communicable disease bulletin. 2015;20(41).
22. Al-Abdallat MM, Payne DC, Alqasrawi S, Rha B, Tohme RA, Abedi GR, et al. Hospital-associated outbreak of Middle East respiratory syndrome coronavirus: a serologic, epidemiologic, and clinical description. Clin Infect Dis. 2014 Nov 1;59(9):1225-33.
23. Reusken C, Mou H, Godeke GJ, van der Hoek L, Meyer B, Muller MA, et al. Specific serology for emerging human coronaviruses by protein microarray. Euro surveillance : bulletin Europeen sur les maladies transmissibles = European communicable disease bulletin. 2013 Apr 4;18(14):20441.
24. Alagaili AN, Briese T, Mishra N, Kapoor V, Sameroff SC, Burbelo PD, et al. Middle East respiratory syndrome coronavirus infection in dromedary camels in Saudi Arabia. mBio. 2014 Feb 25;5(2):e00884-14.
25. Perera RA, Wang P, Gomaa MR, El-Shesheny R, Kandeil A, Bagato O, et al. Seroepidemiology for MERS coronavirus using microneutralisation and pseudoparticle virus neutralisation assays reveal a high prevalence of antibody in dromedary camels in Egypt, June 2013. Euro surveillance : bulletin Europeen sur les maladies transmissibles = European communicable disease bulletin. 2013 Sep 5;18(36):pii=20574.
26. Meyer B, Muller MA, Corman VM, Reusken CB, Ritz D, Godeke GJ, et al. Antibodies against MERS coronavirus in dromedary camels, United Arab Emirates, 2003 and 2013. Emerg Infect Dis. 2014 Apr;20(4):552-9.
27. Meyer B, Drosten C, Muller MA. Serological assays for emerging coronaviruses: challenges and pitfalls. Virus Res. 2014 Dec 19;194:175-83.
28. Payne DC, Iblan I, Rha B, Alqasrawi S, Haddadin A, Al Nsour M, et al. Persistence of Antibodies against Middle East Respiratory Syndrome Coronavirus. Emerg Infect Dis. 2016 Oct;22(10):1824-6.
29. Fanoy EB, van der Sande MA, Kraaij-Dirkzwager M, Dirksen K, Jonges M, van der Hoek W, et al. Travel-related MERS-CoV cases: an assessment of exposures and risk factors in a group of Dutch travellers returning from the Kingdom of Saudi Arabia, May 2014. Emerg Themes Epidemiol. 2014;11:16.
30. Ko JH, Muller MA, Seok H, Park GE, Lee JY, Cho SY, et al. Suggested new breakpoints of anti-MERS-CoV antibody ELISA titers: performance analysis of serologic tests. European journal of clinical microbiology & infectious diseases : official publication of the European Society of Clinical Microbiology. 2017 Nov;36(11):2179-86.
31. Ko JH, Muller MA, Seok H, Park GE, Lee JY, Cho SY, et al. Serologic responses of 42 MERS-coronavirus-infected patients according to the disease severity. Diagnostic microbiology and infectious disease. 2017 Oct;89(2):106-11.

32. Chan KH, Chan JF, Tse H, Chen H, Lau CC, Cai JP, et al. Cross-reactive antibodies in convalescent SARS patients' sera against the emerging novel human coronavirus EMC (2012) by both immunofluorescent and neutralizing antibody tests. The Journal of infection. 2013 Aug;67(2):130-40.
33. Liljander A, Meyer B, Jores J, Muller MA, Lattwein E, Njeru I, et al. MERS-CoV Antibodies in Humans, Africa, 2013-2014. Emerg Infect Dis. 2016 Jun;22(6):1086-9.
34. Oh MD, Park WB, Choe PG, Choi SJ, Kim JI, Chae J, et al. Viral Load Kinetics of MERS Coronavirus Infection. The New England journal of medicine. 2016 Sep 29;375(13):1303-5.
35. Hangartner L, Zinkernagel RM, Hengartner H. Antiviral antibody responses: the two extremes of a wide spectrum. Nat Rev Immunol. 2006 Mar;6(3):231-43.
36. Sakurai H, Williamson RA, Crowe JE, Beeler JA, Poignard P, Bastidas RB, et al. Human antibody responses to mature and immature forms of viral envelope in respiratory syncytial virus infection: significance for subunit vaccines. Journal of Virology. 1999 Apr;73(4):2956-62.
37. World Health Organization. Laboratory Testing for Middle East Respiratory Syndrome Coronavirus, Interim Guidance. (WHO/MERS/LAB/15.1/Rev1/2018). Licence: CC BY-NC-SA 3.0 IGO. Geneva, Switzerland; 2018.
38. Zhao J, Alshukairi AN, Baharoon SA, Ahmed WA, Bokhari AA, Nehdi AM, et al. Recovery from the Middle East respiratory syndrome is associated with antibody and T-cell responses. Sci Immunol. 2017 Aug 4;2(14).
39. Buchholz U, Muller MA, Nitsche A, Sanewski A, Wevering N, Bauer-Balci T, et al. Contact investigation of a case of human novel coronavirus infection treated in a German hospital, October-November 2012. Euro surveillance : bulletin Europeen sur les maladies transmissibles = European communicable disease bulletin. 2013 Feb 21;18(8).
40. Patel DA, Patel AC, Nolan WC, Zhang Y, Holtzman MJ. High throughput screening for small molecule enhancers of the interferon signaling pathway to drive next-generation antiviral drug discovery. PloS one. 2012;7(5):e36594.
41. Li W, Hulswit RJG, Widjaja I, Raj VS, McBride R, Peng W, et al. Identification of sialic acid-binding function for the Middle East respiratory syndrome coronavirus spike glycoprotein. Proceedings of the National Academy of Sciences of the United States of America. 2017;114(40):E8508-E17.
42. Koopmans M, de Bruin E, Godeke GJ, Friesema I, van Gageldonk R, Schipper M, et al. Profiling of humoral immune responses to influenza viruses by using protein microarray. Clin Microbiol Infect. 2012 Aug;18(8):797-807.
43. Burbelo PD, Goldman R, Mattson TL. A simplified immunoprecipitation method for quantitatively measuring antibody responses in clinical sera samples by using mammalian-produced Renilla luciferase-antigen fusion proteins. BMC Biotechnol. 2005 Aug 18;5:22.
44. Burbelo PD, Ching KH, Klimavicz CM, Iadarola MJ. Antibody profiling by Luciferase Immunoprecipitation Systems (LIPS). Journal of visualized experiments : JoVE. 2009 Oct 7(32):e1549.

Chapter 2.2

Middle East respiratory syndrome coronavirus (MERS-CoV) seropositive camel handlers in Kenya

Alice Kiyong'a* | Elizabeth A.J. Cook* | Nisreen M.A. Okba* | Velma Kivali | Chantal Reusken | Bart L. Haagmans | Eric M. Fèvre

*Authors contributed equally

Viruses. 2020;12(4):396

Abstract

Middle East Respiratory Syndrome (MERS) is a respiratory disease caused by a zoonotic coronavirus (MERS-CoV). Camel handlers, including slaughterhouse workers and herders, are at risk of acquiring MERS-CoV infections. However, there is limited evidence of infections among camel handlers in Africa. The purpose of this study was to determine the presence of antibodies to MERS-CoV in high-risk groups in Kenya. Sera collected from 93 camel handlers, 58 slaughterhouse workers and 35 camel herders, were screened for MERS-CoV antibodies using ELISA and PRNT. We found four seropositive slaughterhouse workers by PRNT. Risk factors amongst the slaughterhouse workers included being the slaughterrman and drinking camel blood. Further research is required to understand the epidemiology of MERS-CoV in Africa in relation to occupational risk, with a need for additional studies on the transmission of MERS-CoV from dromedary camels to humans, seroprevalence and associated risk factors.

Introduction

Middle East respiratory syndrome (MERS) is caused by an emerging beta-coronavirus (MERS-CoV). It is a zoonotic respiratory disease that was first reported in the Kingdom of Saudi Arabia in 2012 (1). Dromedary camels are the reservoir of MERS-CoV (2) and contact with camels and their products is considered to be a risk factor for human MERS-CoV infection (3). Occupational exposure has been reported in camel handlers, including camel farm workers and camel slaughterhouse workers (4) in the Middle East. It is hypothesized that the disease is transmitted from camels to people and person-to-person via respiratory secretions (5).

Previous research in Kenya has demonstrated a high MERS-CoV seropositivity in camels (6). However, so far MERS-CoV neutralizing antibodies have only been detected in two non-camel-livestock keepers in Kenya (7). In a targeted surveillance, none of the camel herders exposed to seropositive camels had MERS-CoV neutralizing antibodies (8).

In Kenya, populations living in semi-arid to arid environments have adopted camel rearing for drought resilience. Livestock keepers have a close relationship with their animals and cultural, animal husbandry and consumption practices may expose them to zoonotic agents. Poor hygienic conditions at farms and slaughterhouses, a lack of adequate infrastructure, the slaughtering and consumption of sick animals and weak monitoring and surveillance systems may contribute to an increased risk of exposure to MERS-CoV. There are limited data on MERS-CoV human infections in relation to occupational risk in Africa, with a need for additional studies on the transmission of MERS-CoV from dromedary camels to humans, seroprevalence and associated risk factors. The aims of this study were to determine the presence of antibodies to MERS-CoV in people in contact with camels and identify the risk factors associated with seropositivity.

Materials and methods

The study was conducted in Isiolo, Laikipia and Machakos counties, Kenya, from October to November 2016 (Supplementary Figure S1). Slaughterhouse workers and camel herders were recruited in Isiolo and Laikipia and slaughterhouse workers only in Machakos. These areas represent rural arid and semi-arid regions in Kenya where camels are kept and/or where camel slaughterhouses are located. Isiolo and Laikipia counties are in the arid and semi-arid northern region of Kenya and are inhabited by pastoral communities who keep camels as part of their livelihoods. Camels are transported to slaughterhouses in Isiolo, Laikipia and Machakos counties.

The study was conducted in accordance with the Declaration of Helsinki, and the protocol was approved on August 17th 2016 by the Institutional Research Ethics Committee of the International Livestock Research Institute (IREC 2016-07), a committee approved by the Kenya National Commission for Science, Technology and Innovation. Permission to work in the slaughterhouses was granted by the Directorate of Veterinary Services for the Ministry of Agriculture, Livestock Development and Fisheries in Kenya. Written informed consent was sought from all the participants who agreed to take part in the study and anonymity and confidentiality were adhered to by using randomly assigned barcodes to label samples.

Data were collected from participants on their demographics and occupational and consumption practices using structured questionnaires from October to November 2016. Trained personnel collected clotted blood samples in 10 ml vacutainer tubes (Becton–Dickinson). The serum was separated by centrifugation at 1150× g for 20 minutes using a Beckman Coulter Avanti J-E centrifuge. The sera samples were stored in duplicate at −20°C until testing.

All the sera were tested for the presence of MERS-CoV specific antibodies using the commercial Euroimmun Anti-MERS-CoV ELISA at the International Livestock Research Institute (ILRI) laboratory in Nairobi. The positive and negative controls were human sera supplied by the manufacturer. The tests were carried out as per the manufacturers' instructions. The extinction value or optical density of each analyzed sample was divided by the extinction value of the calibrator (supplied by the manufacturer) to calculate an extinction ratio. Samples with an extinction ratio of 0.3 were considered positive.as previously described (7).

The sera were tested for the presence of MERS-CoV spike specific antibodies using an in-house S1 ELISA at the Erasmus MC Viroscience Laboratory in Rotterdam according to the previously validated protocol (9).

Twenty-one samples, including all Euroimmun and in-house S1 ELISA positive samples and a random selection of negative samples, were tested for the presence of MERS-CoV neutralizing antibodies using PRNT as described earlier with some modifications (9). The positive and negative controls were the same as those described previously (9). The testing was performed at the Erasmus MC Viroscience Laboratory in Rotterdam. Heat-inactivated sera were serially diluted in an RPMI1640 medium supplemented with penicillin, streptomycin and 1% fetal bovine serum (starting 1:10), mixed 1:1 with MERS-CoV (EMC/2012; 400 PFU) and incubated at 37°C for one hour. Following that, the mix was transferred to a monolayer of HuH-7 cells in 96-well plates and incubated at 37°C for one hour. The mix was then removed and the cells were further incubated at 37°C for eight hours. The cells were then fixed and stained using an anti-MERS-CoV N protein mouse

monoclonal antibody (1:5000, Sino Biological) and a secondary peroxidase-labelled goat anti-mouse IgG1 (1:2000, SouthernBiotech). The signal was developed using a precipitate forming TMB substrate (True Blue, KPL). The numbers of infected cells per well were counted using the ImmunoSpot® Image analyzer (CTL Europe GmbH). The neutralization titer of each serum sample was determined as the reciprocal of the highest dilution resulting in a ≥50% reduction in the number of infected cells ($PRNT_{50}$). A titer of ≥20 was considered to be positive.

The statistical analysis was performed in R (http://CRAN.R-project.org/). To identify the risk factors associated with MERS-CoV seropositivity, a univariable analysis was conducted using Pearson's chi-square with a Monte Carlo simulation of 10,000 repetitions to account for the small sample size. The results of the PRNT were used as a final determination of sero-reactivity. The statistical significance was set at $p = 0.05$ and confidence intervals were determined using a standard error of 1.96.

Results

A total of 58 slaughterhouse workers were sampled from three slaughterhouses; 5 were from Machakos, 16 from Laikipia and 37 from Isiolo (Supplementary Table S2). The majority of workers were male (n = 47) and the mean age was 37 years (range 17–73 years). In Machakos, 8–10 camels were slaughtered daily, in Laikipia 5 camels were slaughtered one day per week and in Isiolo 10–20 camels were slaughtered two days per week.

Thirty-five camel herders were sampled—33 in Isiolo and 2 in Laikipia. The majority of herders were male (n = 30) and the mean age was 45 years (range 2–82 years). The mean number of camels owned was 36 (range 0–149). The ratio of juvenile camels (less than 12 months) to adults in herds was 1:1.4.

The results of the three serological tests are presented in Table 1. Samples from five slaughterhouse workers (8.6%; 95% CI 3.8%–19.0%) and three camel herders (8.6%; 95% CI 8.6%–22.1%) were seropositive for MERS-CoV when tested using the Euroimmun ELISA. The samples were retested with the S1 ELISA and four slaughterhouse workers (6.9%; 95% CI 2.8%–16.3%) demonstrated antibodies to MERS-CoV compared to one camel herder (2.9%; 95% CI 0.7%–14.2%).

Four of the twenty-one samples tested using PRNT were positive. The agreement between the tests is shown in Supplementary Table S1 and Figure 1. All the PRNT positive samples originated from slaughterhouse workers in Isiolo, where the apparent prevalence was 10.8% (95% CI 4.4%–24.6%).

Table 1. The proportion of slaughterhouse workers and camel herders who were positive for MERS-CoV antibodies when tested by the Euroimmun ELISA, S1 ELISA and PRNT

Cohort	Number of Samples	Euroimmun S1 ELISA Positive Number (%)	In-house S1 ELISA Positive Number (%)	$PRNT_{50}$ Positive Number	
				Commercial S1 ELISA positive	In-House S1 ELISA positive
Slaughterhouse workers	58	5 (8.6)	4 (6.8)	2/5	4/4
Camel herders	35	3 (8.6)	1 (2.9)	0/3	0/1
Total	93	8 (8.6)	5 (5.4)	2/8	4/5

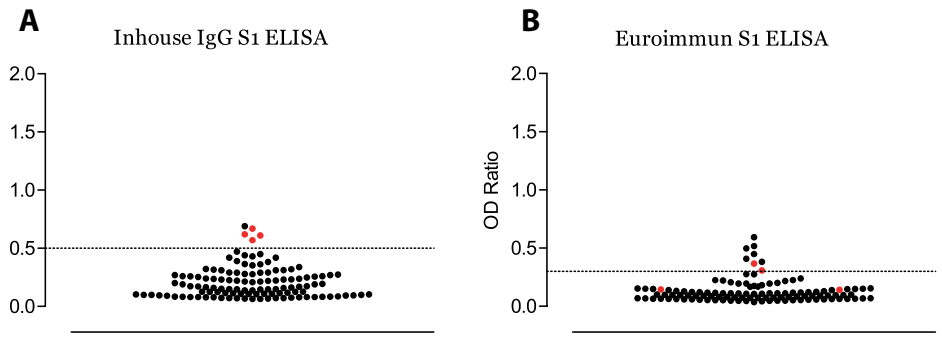

Figure 1. The testing of human serum samples for MERS-CoV antibodies, Kenya, (2016). The reactivities of individual serum samples to MERS-CoV S1—tested using in-house **(A)** and commercial **(B)** S1 ELISAs—are plotted. PRNT positive serum samples are shown in red. The dotted line indicates the cut-off of each assay (7, 9).

The proportion of PRNT positive samples at the Isiolo slaughterhouse is demonstrated in Supplementary Table S3. A risk factor analysis was conducted on samples from the Isiolo slaughterhouse only. Only PRNT positive samples were considered in the analysis. The proportion of positive male slaughterhouse workers (3/26) was not significantly different to the proportion of positive female workers (1/11) ($Chi^2 = 0.04$, $p = 1$). There was a higher but not significant proportion of positive workers aged 40 years and over (2/12) compared to those less than 40 years (2/25) ($Chi^2 = 0.49$, $p = 0.60$). The three positive men were slaughtermen, meaning they were responsible for the slaughtering event, and the positive female worker had another role in the slaughterhouse. The proportion of positive slaughtermen (3/8) was significantly different to that of other roles in the slaughterhouse (1/29) ($Chi^2 = 5.2$, $p = 0.05$). Drinking camel blood was also significantly associated with seropositivity (3/6) compared to those who did not drink camel blood (1/31) ($Chi^2 = 7.3$, $p = 0.03$). Other non-significant exposures included drinking camel milk (3/22) compared to not consuming the milk (1/15) ($Chi^2 = 0.37$, $p = 0.64$) and milking camels (3/14) compared to not milking camels (1/23) ($Chi^2 = 2.05$, $p = 0.28$).

Discussion

This is the first report of MERS-CoV neutralizing antibodies in camel handlers in Kenya. We detected an apparent prevalence of 10.8% MERS-CoV seropositivity by PRNT in slaughterhouse workers working in a camel-keeping area of the country. The detection of MERS-CoV in dromedary camels in Kenya in recent years (10) has highlighted the potential for transmission of the virus to people in close contact with camels as reported in the Middle East (4), but previous research investigating high-risk groups failed to detect individuals who were seropositive by virus neutralization (8). The clinical significance of detecting MERS-CoV seropositivity by PRNT in our population is unknown. This was a cross-sectional serosurvey of healthy workers; we highlight that these individuals did not show clinical signs of disease and we are unable to determine when the exposures took place. The low virus neutralizing antibody titers may suggest asymptomatic infections (4) and clinical infections, which most likely present as transient infections, may be misdiagnosed as other endemic diseases (11).

Studies investigating the potential for transmission of MERS-CoV from camels to high-risk groups in other regions have had variable findings. Despite virus detection in camels at slaughterhouses in Nigeria, neutralizing antibodies were not detected in slaughterhouse workers (12) Similarly, neutralizing antibodies have not been detected in slaughterhouse workers in the Kingdom of Saudi Arabia (13). In contrast, virus neutralizing antibodies were detected in slaughterhouse workers in Qatar, where active MERS-CoV shedding has been demonstrated in slaughter animals (4). A substantial pool of susceptible animals is necessary to support virus transmission and result in a risk to people (2). Susceptible animals brought together for slaughter from different regions may drive virus amplification and zoonotic transmission (14).

Our previous research in Kenya has demonstrated a high seroprevalence of MERS-CoV antibodies in camels (6). However, research in Kenya and elsewhere has demonstrated that juvenile camels have a higher rate of viral RNA positivity than adult animals (10, 15). In Kenya, the primary purpose of camel keeping is for milk production and therefore only mature animals (greater than three years) are presented for slaughter. This may limit the potential for transmission of the virus to slaughterhouse workers and explain the small number of positive samples in this study. Further studies targeting camel handlers who work with younger animals are required.

The currently available commercial ELISA is the Euroimmun Anti-MERS-CoV. This study demonstrates that even when using a low cut-off as recommended [7], the test is less specific and sensitive in detecting MERS-CoV seropositives compared to our in-house S1 ELISA, as previously observed (9). However, there was a good correlation between the

results of the in-house S1 ELISA and the PRNT. A sample reactive in both the S1 ELISA and PRNT was considered to be positive. Having a sensitive assay is crucial to avoid errors in the estimation of prevalence in seroepidemiological studies.

In this study, the small sample size makes it difficult to draw conclusions about risk factors for MERS-CoV seropositivity. The sample size is limited because the population of camel slaughterhouse workers is small. The statistical analysis accounted for the small sample size, but the results should be interpreted with caution. Potential risk factors that might be investigated in future studies include being a slaughterman (the person who cuts the animal's throat). This has been reported for other zoonotic viruses transmitted by the respiratory route, including Rift Valley fever (RVF) (16).

Other risk factors that should be investigated include drinking camel blood (3). This has not been significantly associated with MERS-CoV seropositivity but has been reported for RVF, another zoonotic RNA virus (16). The milking of camels has also been reported by other studies as a risk factor for MERS-CoV and this needs further evaluation (3). Further targeted studies investigating these and other risk factors in larger populations over longer periods of time are required.

Acknowledgments

We thank ILRI colleague Fredrick Amanya and Robert Rono, for their involvement in sampling of human serum.

Supplementary Data

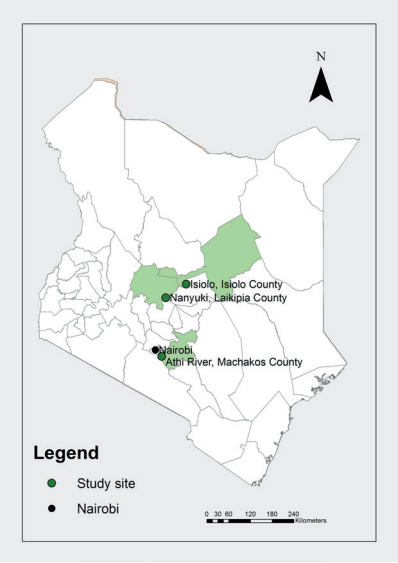

Supplementary Figure S1. Map of sites where camel handlers were sampled in Kenya in 2016. Counties are indicated in light green and the locations of the slaughterhouses in dark green.

Table S1. Results of testing selected sera from slaughterhouse workers and 268 camel herders for antibodies to MERS-CoV by Euroimmun ELISA, S1 ELISA and PRNT

ID	Classification	Euroimmun extinction ratio	S1 ELISA OD	$PRNT_{50}$
UZ035342	Herder	0.20	0.20	<20
UZ035755		0.50	0.44	<20
UZ035881		0.22	0.23	<20
UZ036131		0.41	0.43	<20
UZ036167		0.59	0.69	<20
UZ036168		0.06	0.29	<20
UZ036195		0.07	0.39	<20
UZ035771	Worker	0.38	0.29	<20
UZ035899		0.20	0.26	<20
UZ035901		0.15	0.42	<20
UZ035902		0.17	0.31	<20
UZ035903		0.14	0.67	40
UZ035906		0.52	0.42	<20
UZ035917		0.45	0.23	<20
UZ035924		0.37	0.61	20
UZ035926		0.11	0.31	<20
UZ035929		0.14	0.57	20
UZ035981		0.09	0.26	<20
UZ035988		0.28	0.27	<20
UZ035994		0.11	0.17	<20
UZ035998		0.31	0.62	40

Table S2. Demographics and practices of slaughterhouse workers in the three counties, Machakos, Laikipia and Isiolo, Kenya, in 2016

Variable	Machakos *n* = 5	Laikipia *n* = 16	Isiolo *n* = 37	Total *n* = 58
Gender				
Male	5	16	26	47
Female	0	0	11	11
Age				
<20	1	0	1	2
20-39	2	11	24	37
40-59	2	5	10	17
>60	0	0	2	2
Job				
Slaughterman	0	2	8	10
Flayer	1	5	7	13
Cleaner	1	5	5	11
Other	3	4	17	24
Camel Milk				
No	3	11	15	29
Boiled	0	3	5	8
Raw	2	2	17	21
Milk camel				
No	4	14	23	41
Yes	1	2	14	17
Drink blood				
No	5	16	31	52
Yes	0	0	6	6

Table S3. Univariable risk factor analysis for MERS-CoV seropositivity in slaughterhouse workers at Isiolo Camel Slaughterhouse, Kenya in 2016

Variable	Isiolo *n* = 37	Odds Ratio (95% CI)	p-value
Gender			
Male	3/26 (11.5)	1.26 (0.09-72.58)	1
Female	1/11 (9.1)	1	
Age			
<40	2/25 (8.0)	1	
40 and over	2/12 (16.7)	2.04 (0.13-31.43)	0.60
Job			
Slaughterman	3/8 (37.5)	10.09 (0.70-587.39)	0.50
Other	1/29 (3.4)	1	
Drink Camel Milk			
No	1/15 (6.7)	1	
Yes	3/22 (13.6)	2.01 (0.15-114.36)	0.64
Milk camel			
No	1/23 (4.3)	1	
Yes	3/14 (21.4)	4.74 (0.34-269.27)	0.29
Drink blood			
No	1/31 (3.2)	1	
Yes	3/6 (50.0)	14.02 (0.95-833.42)	0.03

References

1. Zaki AM, van Boheemen S, Bestebroer TM, Osterhaus AD, Fouchier RA. Isolation of a novel coronavirus from a man with pneumonia in Saudi Arabia. The New England journal of medicine. 2012 Nov 8;367(19):1814-20.
2. Dudas G, Carvalho LM, Rambaut A, Bedford T. MERS-CoV spillover at the camel-human interface. eLife. 2018 Jan 16;7:e31257.
3. Alraddadi BM, Watson JT, Almarashi A, Abedi GR, Turkistani A, Sadran M, et al. Risk Factors for Primary Middle East Respiratory Syndrome Coronavirus Illness in Humans, Saudi Arabia, 2014. Emerg Infect Dis. 2016 Jan;22(1):49-55.
4. Reusken CB, Farag EA, Haagmans BL, Mohran KA, Godeke GJt, Raj S, et al. Occupational Exposure to Dromedaries and Risk for MERS-CoV Infection, Qatar, 2013-2014. Emerg Infect Dis. 2015 Aug;21(8):1422-5.
5. Aly M, Elrobh M, Alzayer M, Aljuhani S, Balkhy H. Occurrence of the Middle East Respiratory Syndrome Coronavirus (MERS-CoV) across the Gulf Corporation Council countries: Four years update. PloS one. 2017;12(10):e0183850.
6. Deem SL, Fevre EM, Kinnaird M, Browne AS, Muloi D, Godeke GJ, et al. Serological Evidence of MERS-CoV Antibodies in Dromedary Camels (Camelus dromedaries) in Laikipia County, Kenya. PloS one. 2015;10(10):e0140125.
7. Liljander A, Meyer B, Jores J, Muller MA, Lattwein E, Njeru I, et al. MERS-CoV Antibodies in Humans, Africa, 2013-2014. Emerg Infect Dis. 2016 Jun;22(6):1086-9.
8. Munyua P, Corman VM, Bitek A, Osoro E, Meyer B, Muller MA, et al. No Serologic Evidence of Middle East Respiratory Syndrome Coronavirus Infection Among Camel Farmers Exposed to Highly Seropositive Camel Herds: A Household Linked Study, Kenya, 2013. The American journal of tropical medicine and hygiene. 2017 Jun;96(6):1318-24.
9. Okba NMA, Raj VS, Widjaja I, GeurtsvanKessel CH, de Bruin E, Chandler FD, et al. Sensitive and Specific Detection of Low-Level Antibody Responses in Mild Middle East Respiratory Syndrome Coronavirus Infections. Emerg Infect Dis. 2019 Oct;25(10):1868-77.
10. Kiambi S, Corman VM, Sitawa R, Githinji J, Ngoci J, Ozomata AS, et al. Detection of distinct MERS-Coronavirus strains in dromedary camels from Kenya, 2017. Emerging Microbes & Infections. 2018 Nov 28;7(1):195.
11. Roess A, Carruth L, Lahm S, Salman M. Camels, MERS-CoV, and other emerging infections in east Africa. The Lancet Infectious diseases. 2016 Jan;16(1):14-5.
12. So RT, Perera RA, Oladipo JO, Chu DK, Kuranga SA, Chan KH, et al. Lack of serological evidence of Middle East respiratory syndrome coronavirus infection in virus exposed camel abattoir workers in Nigeria, 2016. Euro surveillance : bulletin Europeen sur les maladies transmissibles = European communicable disease bulletin. 2018 Aug;23(32).
13. Aburizaiza AS, Mattes FM, Azhar EI, Hassan AM, Memish ZA, Muth D, et al. Investigation of anti-middle East respiratory syndrome antibodies in blood donors and slaughterhouse workers in Jeddah and Makkah, Saudi Arabia, fall 2012. The Journal of Infectious Diseases. 2014 Jan 15;209(2):243-6.
14. Hemida MG, Al-Naeem A, Perera RA, Chin AW, Poon LL, Peiris M. Lack of middle East respiratory syndrome coronavirus transmission from infected camels. Emerg Infect Dis. 2015 Apr;21(4):699-701.
15. Dighe A, Jombart T, Van Kerkhove MD, Ferguson N. A systematic review of MERS-CoV seroprevalence and RNA prevalence in dromedary camels: Implications for animal vaccination. Epidemics. 2019 Dec;29:100350.
16. Nicholas DE, Jacobsen KH, Waters NM. Risk factors associated with human Rift Valley fever infection: systematic review and meta-analysis. Trop Med Int Health. 2014 Dec;19(12):1420-9.

Chapter 2.3

Serologic detection of Middle East respiratory syndrome coronavirus functional antibodies

Nisreen M.A. Okba | Ivy Widjaja | Wentao Li | Corine H. GeurtsvanKessel | Elmoubasher A.B.A. Farag | Mohammed Al-Hajri | Wan Beom Park | Myoung-don Oh | Chantal B.E.M. Reusken | Marion P.G. Koopmans | Berend-Jan Bosch | Bart L. Haagmans

Emerging Infectious Diseases. 2020;26(5)

Abstract

We developed and validated 2 species-independent protein-based assays to detect Middle East respiratory syndrome coronavirus functional antibodies that can block virus receptor-binding or sialic acid-attachment. Antibody levels measured in both assays correlated strongly with virus-neutralizing antibody titers, proving their use for serologic confirmatory diagnosis of Middle East respiratory syndrome.

The study

The zoonotic introductions and ongoing outbreaks of Middle East respiratory syndrome (MERS) coronavirus (MERS-CoV) pose a global threat (1, 2) necessitating continuous serosurveillance to monitor virus spread alongside the development of vaccine and antibodies as countermeasures. Both approaches require validated assays to evaluate specific antibody responses. Although MERS-CoV serologic assays have been developed (2-6), those detecting functional antibodies cannot be applied in all laboratories and can require Biosafety Level 3 (BSL-3) containment. Recombinant protein-based immunoassays are easier to operate and standardize and do not require BSL-3 containment. However, MERS-CoV protein-based assays developed thus far can only detect antibody binding and give no information on antibody functionality. The MERS-CoV spike protein N terminal subunit (S1) contains 2 functional domains: the N-terminal domain ($S1^A$), which binds sialic acid, the viral attachment factor; and the receptor-binding domain (RBD) ($S1^B$), which binds dipeptidyl peptidase 4, the virus receptor (7, 8). Antibodies against those 2 domains can block MERS-CoV infection (9). Based on this fundamental knowledge, we developed 2 recombinant protein-based functional assays.

First, we developed an S1-based competitive ELISA, a receptor-binding inhibition assay (RBI), to test for antibodies that block the interaction with dipeptidyl peptidase 4, the viral receptor (Appendix Figure 1). We validated the specificity of the assay for human diagnostics using serum samples from healthy blood donors, PCR-confirmed non–coronavirus-infected patients and non–MERS-CoV–infected patients (cohorts H1–H3; Appendix Table 1). At a 1/20 dilution, none of the samples from non–MERS-CoV-infected humans showed a >50% reduction in signal (RBI_{50}) (Figure 1, panel A), indicating a high specificity of the assay. MERS-CoV–specific RBI antibodies were detected in all the 90% plaque reduction neutralization assay ($PRNT_{90}$)–positive serum samples of the PCR-confirmed MERS-CoV patients tested (Appendix Table 2, Figure 2). The percentage reduction in signal strongly correlated with neutralizing antibody titers (Figure 1, panel B). The RBI_{50} assay showed similar sensitivity to the $PRNT_{90}$.

Because the RBI assay is species-independent, we validated its ability to detect RBI antibodies in dromedaries. At a 1/20 dilution, none of the naive dromedary serum samples (10) reacted in the assay, whereas all samples from MERS-CoV–infected dromedaries (2) resulted in a >90% reduction in signal (Appendix Table 1, Figure 3, panel A). We detected RBI antibodies in the samples of vaccinated and experimentally infected dromedaries (Appendix Figure 3, panel B). Overall, the RBI_{50} was highly specific and showed comparable sensitivity to $PRNT_{90}$ for detection of MERS-CoV–specific RBI (neutralizing) antibodies after infection and vaccination (Appendix Figure 3, panel C).

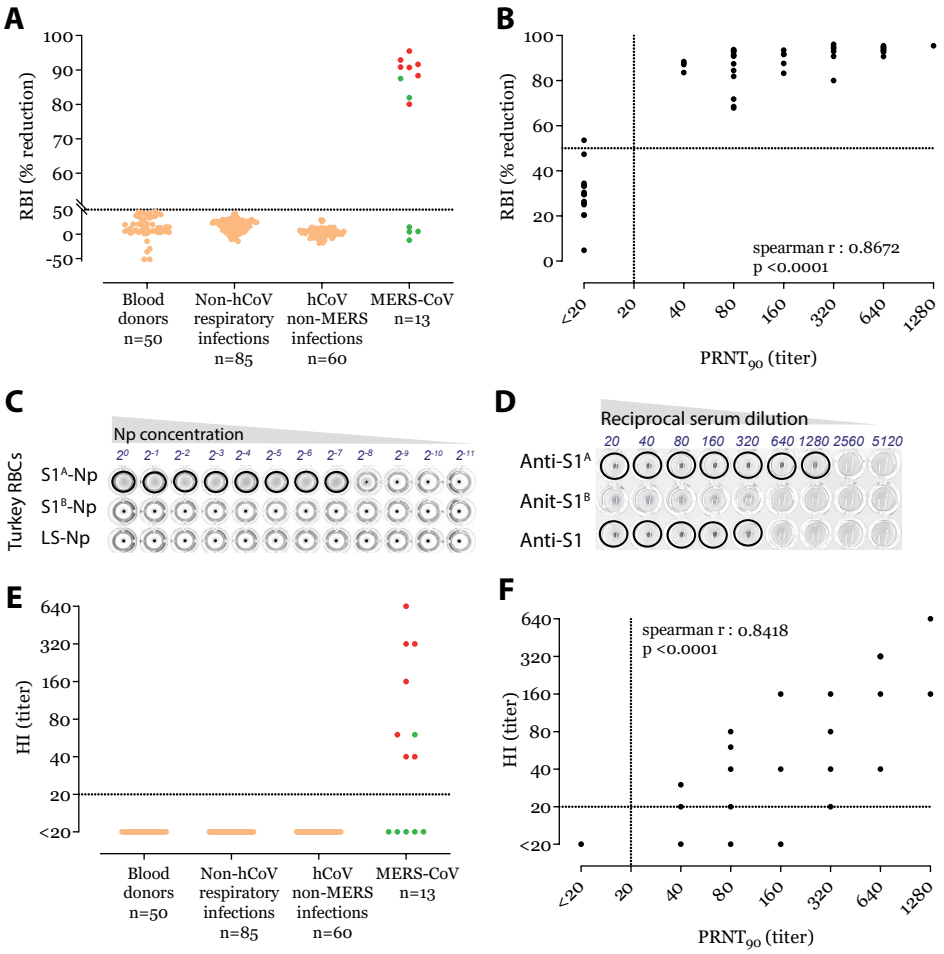

Figure 1. MERS-CoV–specific RBI and HI assays for MERS-CoV human diagnostics. **A)** Validation of the specificity of the RBI assay for the detection of MERS-CoV–specific antibodies in humans. Red dots indicate severe illness. Green dots indicate mild illness. **B)** Correlation between neutralizing and RBI antibody responses after MERS-CoV infection. **C)** Hemagglutination of turkey erythrocytes using $S1^A$-nanoparticles. $S1^A$-, $S1^B$-, or empty self-assembling lumazine synthase nanoparticles were serially diluted and tested for the ablity to agglutinate turkey RBCs. **D)** Specificity of the HI assay for the detection of MERS-CoV $S1^A$–directed antibodies. Rabbit anti-$S1^A$, anti $S1^B$, or anti-S1 serum samples were serially diluted and tested for the ability to block $S1^A$-nanoparticles–induced hemagglutination of turkey RBCs. **E)** Validation of HI assay for the detection of MERS-CoV–specific antibodies in humans. **F)** Scatter plot correlating $PRNT_{90}$ neutralization titers and HI titers after MERS-CoV infection. CoV, human coronavirus; HI, hemagglutination inhibition; MERS-CoV, Middle East respiratory syndrome coronavirus; PRNT90, 90% reduction in plaque reduction neutralization test; RBI, receptor-binding inhibition.

Apart from the RBD, the MERS-CoV S1 contains an α2,3 sialic acid–binding $S1^A$ domain (7). When this domain was multivalently presented on self-assembling lumazine synthase (LS) nanoparticles ($S1^A$-Np), it was able to hemagglutinate human erythrocytes. To generate

$S1^A$-Np, we genetically fused the $S1^A$ domain to LS and expressed the particles in HEK-293S cells (Appendix Figure 4, panel A). By using $S1^A$-Np, we developed a hemagglutination inhibition (HI) assay to detect antibodies capable of blocking virus interaction with sialic acids (Appendix Figure 4, panel B). To set up the assay using turkey RBCs, we tested the ability of $S1^A$-Np to agglutinate turkey erythrocytes by using empty (LS)-Np and $S1^B$-Np as negative controls. Although neither the lumazine synthase–Np nor the $S1^B$-Np showed any hemagglutination at any temperature tested, the $S1^A$-Np induced hemagglutination at 4°C; we also noted hemagglutination when using dromedary erythrocytes (Figure 1, panel C; Appendix Figure 4, panel C). Although antibodies against the S1 and $S1^A$ domain inhibited hemagglutination showing high HI titers, $S1^B$ antibodies were negative for HI (Figure 1, panel D).

Next, we used the same cohort of serum samples for validating the RBI assay. None of the samples from healthy blood donors, PCR-confirmed non–coronavirus-infected and non–MERS-CoV–infected patients (cohorts H1–H3) showed any HI at the 1/20 dilution (Figure 1, panel E). HI antibodies were detected in the samples of all severely infected MERS-CoV patients and that of 1 mildly infected MERS-CoV patient (Figure 1, panel E; Appendix Figure 5); only 2 of the mildly infected MERS-CoV patients were $PRNT_{90}$-positive (Appendix Table 2). Serum HI titers correlated strongly with neutralizing antibody titers detected by a whole virus neutralization assay ($PRNT_{90}$); nonetheless, the $PRNT_{90}$ assay was more sensitive (Figure 1, panel F). Similarly, only serum samples from MERS-CoV–infected dromedaries were HI-positive (10/13), whereas none of the naive dromedary camel serum samples showed any HI (Appendix Figure 6, panel A). HI antibodies were detected in serum samples of vaccinated dromedaries after booster immunization (Appendix Figure 6, panel B). Overall, although less sensitive, the antibody titers detected by the HI assay correlated strongly with the neutralizing antibody titers detected by $PRNT_{90}$ assay (Appendix Figure 6, panel C).

The RBI and HI assays we developed are easy to operate and standardize and can detect functional antibodies against 2 MERS-CoV S1 domains responsible for virus entry (RBD) and attachment ($S1^A$). Both assays are protein-based and can be carried out in a 96-well plate format, therefore providing BSL-1 high-throughput platforms. The assays can be used as confirmatory assays for human and dromedary MERS-CoV diagnostics and for therapeutic antibody and vaccine evaluation.

References

1. World Health Organization. Middle East respiratory syndrome coronavirus (MERS-CoV) [cited 10-5-2019]; Available from: http://www.who.int/emergencies/mers-cov/en/
2. Haagmans BL, Al Dhahiry SH, Reusken CB, Raj VS, Galiano M, Myers R, et al. Middle East respiratory syndrome coronavirus in dromedary camels: an outbreak investigation. The Lancet Infectious diseases. 2014 Feb;14(2):140-5.
3. Corman VM, Muller MA, Costabel U, Timm J, Binger T, Meyer B, et al. Assays for laboratory confirmation of novel human coronavirus (hCoV-EMC) infections. Euro surveillance : bulletin Europeen sur les maladies transmissibles = European communicable disease bulletin. 2012 Dec 6;17(49).
4. Reusken C, Mou H, Godeke GJ, van der Hoek L, Meyer B, Muller MA, et al. Specific serology for emerging human coronaviruses by protein microarray. Euro surveillance : bulletin Europeen sur les maladies transmissibles = European communicable disease bulletin. 2013 Apr 4;18(14):20441.
5. Perera RA, Wang P, Gomaa MR, El-Shesheny R, Kandeil A, Bagato O, et al. Seroepidemiology for MERS coronavirus using microneutralisation and pseudoparticle virus neutralisation assays reveal a high prevalence of antibody in dromedary camels in Egypt, June 2013. Euro surveillance : bulletin Europeen sur les maladies transmissibles = European communicable disease bulletin. 2013 Sep 5;18(36):pii=20574.
6. Trivedi S, Miao C, Al-Abdallat MM, Haddadin A, Alqasrawi S, Iblan I, et al. Inclusion of MERS-spike protein ELISA in algorithm to determine serologic evidence of MERS-CoV infection. Journal of medical virology. 2018 Feb;90(2):367-71.
7. Li W, Hulswit RJG, Widjaja I, Raj VS, McBride R, Peng W, et al. Identification of sialic acid-binding function for the Middle East respiratory syndrome coronavirus spike glycoprotein. Proceedings of the National Academy of Sciences of the United States of America. 2017 Oct 3;114(40):E8508-E17.
8. Mou H, Raj VS, van Kuppeveld FJ, Rottier PJ, Haagmans BL, Bosch BJ. The receptor binding domain of the new Middle East respiratory syndrome coronavirus maps to a 231-residue region in the spike protein that efficiently elicits neutralizing antibodies. Journal of Virology. 2013 Aug;87(16):9379-83.
9. Widjaja I, Wang C, van Haperen R, Gutierrez-Alvarez J, van Dieren B, Okba NMA, et al. Towards a solution to MERS: protective human monoclonal antibodies targeting different domains and functions of the MERS-coronavirus spike glycoprotein. Emerging Microbes & Infections. 2019 2019/01/01;8(1):516-30.
10. Haagmans BL, van den Brand JM, Raj VS, Volz A, Wohlsein P, Smits SL, et al. An orthopoxvirus-based vaccine reduces virus excretion after MERS-CoV infection in dromedary camels. Science. 2016 Jan 1;351(6268):77-81.

TECHNICAL APPENDIX

Materials and Methods

Serum Samples

To validate the specificity of the developed assays for the detection of MERS-CoV-specific antibodies in humans, we used a set of sera we previously described in an earlier study to validate a MERS-CoV specific S1 ELISA (1) (Appendix Table 1, cohorts H1-H5). We also included sera from MERS-CoV infected camels (2) as well as sera from MERS-CoV vaccinated camels (3) to validate the use of the assays for camel MERS-CoV diagnostics and evaluation of immune responses following vaccination (Appendix Table 1, sample sets D1-D3). The use of human sera from the Netherlands was approved by the local medical ethical committee (MEC approval: 2014–414) and from South Korea by the Institutional Ethics Review Board of Seoul National University Hospital (approval no. 1506–093–681). The use of camel sera was approved as previously described (2, 3).

Protein Production

For the receptor binding inhibition assay, both DPP4 and MERS-S1-mFc were produced in HEK-293T cells as previously described. The DPP4 ectodomain (39–766) was expressed as an N terminally strep-tagged protein and purified from cell culture supernatant using Strep-Tactin sepharose beads (IBA GmbH). MERS-CoV S1 (1–751) was C-terminally fused to a mouse IgG2a Fc in pCAGGS expression vector and purified from cell culture supernatant using protein A sepharose beads.

For the hemagglutination inhibition assay, empty lumazine synthase nanoparticles (LS-Np) were produced as previously described (4). $S1^A$ nanoparticles ($S1^A$-Np) were produced by genetically linking the $S1^A$ encoding region of the MERS-CoV spike (amino acids19–357; EMC strain GenBank Acc. no. JX869059.2) to the lumazine synthase encoding gene in pCAGGS vector encoding a CD5 signal peptide and strep tag. $S1^A$-Np were expressed in HEK-293S cells and purified using Strep-Tactin sepharose beads.

Receptor Binding Inhibition Assay

We developed a competitive ELISA to detect antibodies capable of blocking of the binding of MERS-CoV to its cellular receptor DPP4. ELISA plates were coated overnight at 4°C with 2 ug/ml recombinant DPP4 in PBS. The plates were washed with PBS and blocked with 3% BSA/PBS-0.5% tween-20 for 1 hr at room temp. In the meantime, 1/20 diluted sera (or further 2-fold serially diluted for titer determination) were mixed with 5 ng of S1-mFc in a total

volume of 100 ul blocking buffer per well and incubated for 1 hr at room temperature. Wells with no serum (only S1-mFc) were included in each run to calculate to maximum binding. Following 1 hr of incubation the mix was transferred to blocked plates and allowed to incubate for 1 hr further. The plates were washed 3 times with PBS/0.05% tween-20, and the amount of S1-mFc bound to the plate was determined by adding HRP-labeled anti-mouse IgG (1:2000, Dako) and incubating for 1 hr. Following washing, the signal was revealed by adding 100 ul of TMB and the reaction was stopped using sulfuric acid. Absorbance was measured using Tecan. Blocking was determined as percentage reduction of the sample signal from the blank signal (no serum). A 50% reduction in signal (RBI_{50}) in a ≥1/20 diluted sample was considered positive. Serum antibody titers were determined as the reciprocal of the highest serum dilution resulting in a ≥50% signal reduction.

Hemagglutination Assay

We tested the ability of $S1^A$ multivalently-expressed on lumazine synthase nanoparticles ($S1^A$-Np) to agglutinate turkey and dromedary RBCs.

For the HA assay, fifty µl of 2-fold serially diluted Nps were mixed with an equal volume of 0.5% RBCs in PBS and incubated for 1 hr at 4°C. Following incubation, the hemagglutination activity was assessed and the HA titer (HA units; HAU) of the Nps was recorded as the dilution of the last well showing hemagglutination.

Hemagglutination Inhibition Assay

To carry out the hemagglutination inhibition assay, sera were 2-fold serially diluted starting at a 1/10 dilution in a total volume of 50 ul PBS. $S1^A$-Nps corresponding to 4 HAU in 25 ul PBS were added to each well and the mix was incubated for 30 min at 37°C. Following incubation, 25 ul of 0.5% turkey RBCs in PBS were added and further incubated for 1 hr at 4°C after which the serum HI titer was scored. A serum titer ≥20 was considered positive.

Plaque Reduction Neutralization Assay (PRNT)

All sera included in this study were previously tested for MERS-CoV neutralization using the $PRNT_{90}$ assay (1-3). Owing to the specificity and sensitivity, neutralization assays are considered the gold standard for MERS-CoV serology. Thus, we compared the performance of the developed assays RBI and HI to $PRNT_{90}$ to assess their specificity and sensitivity.

References

1. Okba NMA, Raj VS, Widjaja I, GeurtsvanKessel CH, de Bruin E, Chandler FD, et al. Sensitive and Specific Detection of Low-Level Antibody Responses in Mild Middle East Respiratory Syndrome Coronavirus Infections. Emerg Infect Dis. 2019 Oct;25(10):1868-77.
2. Haagmans BL, Al Dhahiry SH, Reusken CB, Raj VS, Galiano M, Myers R, et al. Middle East respiratory syndrome coronavirus in dromedary camels: an outbreak investigation. The Lancet Infectious diseases. 2014 Feb;14(2):140-5.
3. Haagmans BL, van den Brand JM, Raj VS, Volz A, Wohlsein P, Smits SL, et al. An orthopoxvirus-based vaccine reduces virus excretion after MERS-CoV infection in dromedary camels. Science. 2016 Jan 1;351(6268):77-81.
4. Li W, Hulswit RJG, Widjaja I, Raj VS, McBride R, Peng W, et al. Identification of sialic acid-binding function for the Middle East respiratory syndrome coronavirus spike glycoprotein. Proceedings of the National Academy of Sciences of the United States of America. 2017 Oct 3;114(40):E8508-E17.

Appendix Table 1. Sample sets used in this study

Species	Country	Cohort	Sample source			No. Samples	Range (post diagnosis)	Reference
Human	The Netherlands	H1	Blood Donors (Negative cohort)			50	NA	(1)
		H2	Non-hCoV Respiratory Infections (*N* = 85)	Adenovirus		5	2- 4 w	
				Bocavirus		2		
				enterovirus		2		
				HMPV		9		
				Influenza A		13		
				Influenza B		6		
				Rhinovirus		9		
				RSV		9		
				PIV-1		4		
				PIV-3		4		
				M.pneumoniae		1		
				CMV		9		
				EBV		12		
		H3	Recent hCoV infections (*N* = 60)	α-CoV	HCoV-229E	19	>2w –1y	
					HCoV-NL63	18		
				β-CoV	HCoV-OC43	23		
		H4[†]	RT-PCR confirmed MERS cases (*n* = 60 longitudinal specimen from 13 patients)	Acute		21	1-14 d	
				Convalescent		7	15-228 d	
	South Korea	H5		Mild infection[‡]		17	6-12 mo	
				Severe infection[§]		15	6-12 mo	

Appendix Table 1. *Continued*

Species	Country	Cohort	Sample source		No. Samples	Range (post diagnosis)	Reference
Dromedary camels	Qatar	D1	MERS-CoV seropositive		13	NA	(2)
	Canary Islands	D2	MERS-CoV seronegative (longitudinal specimen)	Vaccinated¶	28	0-63 dpv	(3)
		D3	MERS-CoV infected (longitudinal specimen)	Infected*	28	0-14 dpi	

CoV, coronavirus; CMV, Cytomegalovirus; d, day; dpi, days post-infection; dpv, days post-vaccination; EBV, Epstein-Barr virus; HCoV, human coronavirus; HMPV, Human metapneumovirus; MERS, Middle East respiratory syndrome; mo, month; NA, not applicable; PIV, parainfluenza virus; RSV, respiratory syncytial virus; w, week; y, year.
† Samples taken from 2 case-patients at different time points.
‡ Samples taken from 6 case-patients at different time points.
§ Samples taken from 5 case-patients at different time points.
¶ Samples taken from 4 camels at different time points.
* Samples taken from 4 camels at different time points

Appendix Table 2. Comparative validation results of the RBI and HI assays versus the $PRNT_{90}$

						N positives / N tested				
						RBI_{50}		HI		
Species	Cohort	Sample source			No Samples	$PRNT_{90}$ Positive	$PRNT_{90}$ Negative	$PRNT_{90}$ Positive	$PRNT_{90}$ Negative	
Human	H1	Blood Donors			50	--	0/50	--	0/50	
	H2	Non-CoV Respiratory Infections (*N* = 85)	Adenovirus		5	--	0/5	--	0/5	
			Bocavirus		2	--	0/2	--	0/2	
			enterovirus		2	--	0/2	--	0/2	
			HMPV		9	--	0/9	--	0/9	
			Influenza A		13	--	0/13	--	0/13	
			Influenza B		6	--	0/6	--	0/6	
			Rhinovirus		9	--	0/9	--	0/9	Specificity
			RSV		9	--	0/9	--	0/9	
			PIV-1		4	--	0/4	--	0/4	
			PIV-3		4	--	0/4	--	0/4	
			M.pneumoniae		1	--	0/1	--	0/1	
			CMV		9	--	0/9	--	0/9	
			EBV		12	--	0/12	--	0/12	
	H3	Recent CoV infections (*N* = 60)	α-CoV	HCoV-229E	19	--	0/19	--	0/19	
				HCoV-NL63	18	--	0/18	--	0/18	
			β-CoV	HCoV-OC43	23	0/2	0/23	0/2	0/23	

Appendix Table 2. *Continued*

Species	Cohort	Sample source		No Samples	N positives / N tested				
					RBI_{50}		HI		
					$PRNT_{90}$ Positive	$PRNT_{90}$ Negative	$PRNT_{90}$ Positive	$PRNT_{90}$ Negative	
	H4[†]	RT-PCR confirmed MERS cases (n = 60 longitudinal specimen from 13 patients)	≤ 14 days post diagnosis	21	11/11	1/10	7/11	0/10	Sensitivity
			> 14 days post diagnosis	7	7/7	--	7/7	--	
	H5		Mild infection[‡]	17	5/5	0/12	2/5	0/12	
			Severe infection[§]	15	15/15	--	15/15	--	
Dromedary camels	D1	MERS-CoV seropositive		13	13/13	--	10/13	--	
	D2	MERS-CoV seronegative (longitudinal specimen)	Vaccinated[¶]	28	16/20	0/8	16/20	0/8	
	D3		Infected*	28	5/6	0/22	0/6	0/22	

CoV, coronavirus; CMV, Cytomegalovirus; EBV, Epstein-Barr virus; HCoV, human coronavirus; HMPV, Human metapneumovirus; MERS, Middle East respiratory syndrome; PIV, parainfluenza virus; RSV, respiratory syncytial virus.

[†] Samples taken from 2 case-patients at different time points.

[‡] Samples taken from 6 case-patients at different time points.

[§] Samples taken from 5 case-patients at different time points.

[¶] Samples taken from 4 camels at different time points.

* Samples taken from 4 camels at different time points

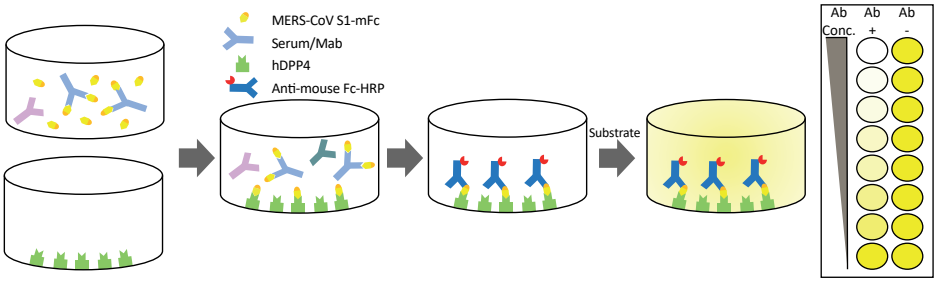

Appendix Figure 1. Schematic diagram showing the principle of the receptor binding inhibition (RBI) assay. S1-mFc, MERS-CoV S1 protein with a mouse Fc tag; hDPP4, human Dipeptidyl Peptidase-4 (MERS-CoV receptor); HRP, horse radish peroxidase.

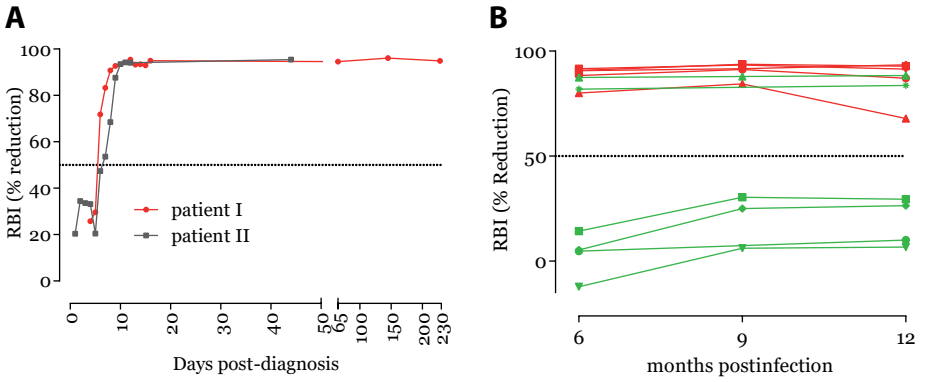

Appendix Figure 2. Kinetics of RBI antibody responses in PCR-confirmed MERS patients. RBI antibody responses in **(A)** two acute to convalescent phase patients and in **(B)** severe (red, *n* = 5) and mild (green, *n* = 6) MERS-CoV patients six to twelve months post-infection.

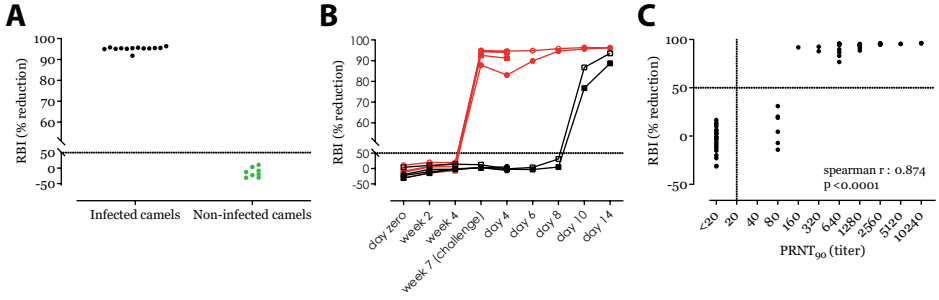

Appendix Figure 3. MERS-CoV specific receptor binding inhibition (RBI) assay for MERS-CoV dromedary camel diagnostics. **(A)** Validation of the specificity of the RBI assay for the detection of MERS-CoV specific antibodies in the sera of MERS-CoV-infected (black) and naïve (green) dromedary camels. **(B)** Kinetics of RBI antibody responses in dromedary camels following vaccination (red) and infection (black). **(C)** Correlation between neutralizing and RBI antibody responses following MERS-CoV infection or vaccination in dromedaries. $PRNT_{90}$, 90% reduction in plaque reduction neutralization test.

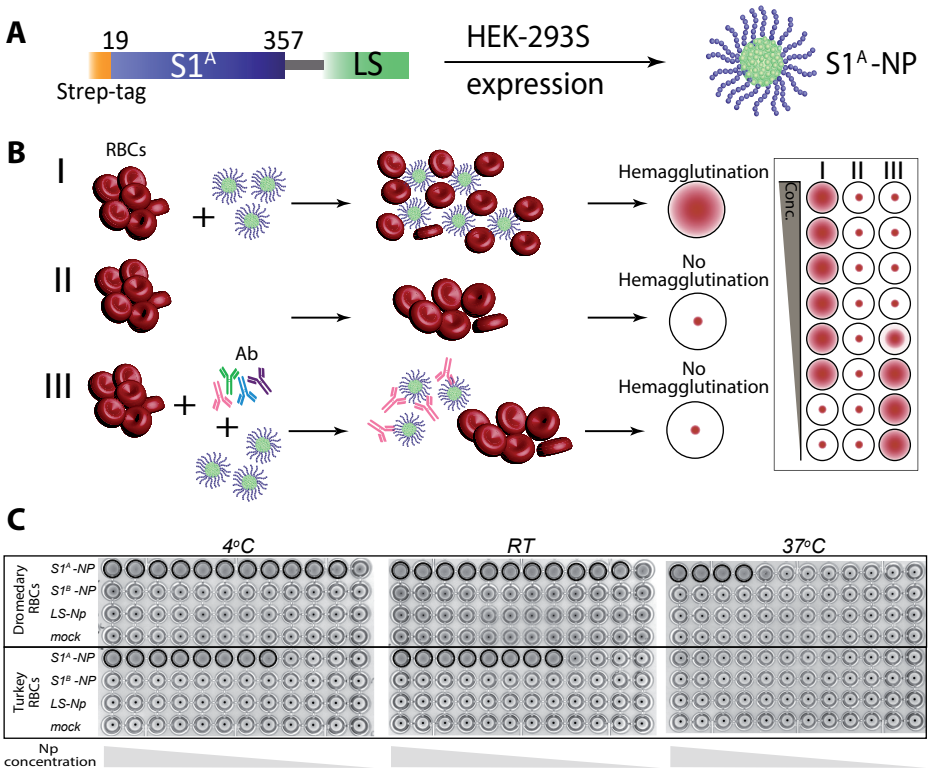

Appendix Figure 4. Development of MERS-CoV HI assay. **(A)** Schematic diagram of the production of $S1^A$ lumazine synthase (LS) nanoparticles (Np). **(B)** The principle of the HI assay showing the hemagglutination of red blood cells (RBCs) in the presence of $S1^A$-Np(I), no-hemagglutination in the absence of the particles (II) and the inhibition of hemagglutination (HI) by $S1^A$-directed antibodies (III). **(C)** $S1^A$-Np induced hemagglutination of dromedary and turkey RBCs at different temperatures.

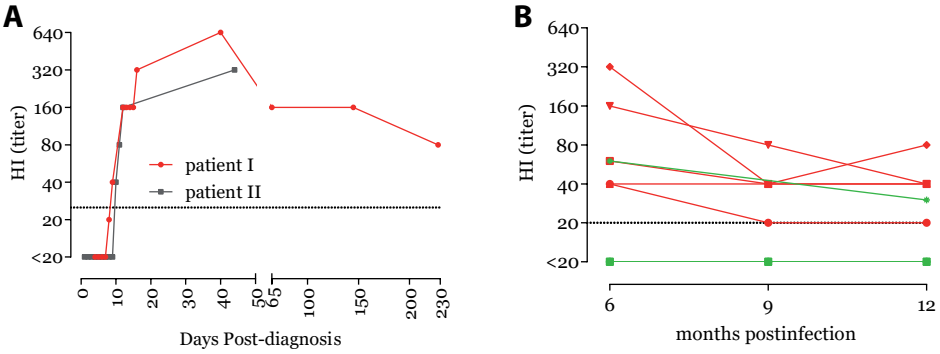

Appendix Figure 5. Kinetics of HI antibody responses in PCR-confirmed MERS patients. HI antibody titers in **(A)** two acute to convalescent phase patients and in **(B)** six severe (red) and five mild (green) MERS-CoV patients six to twelve months post-infection.

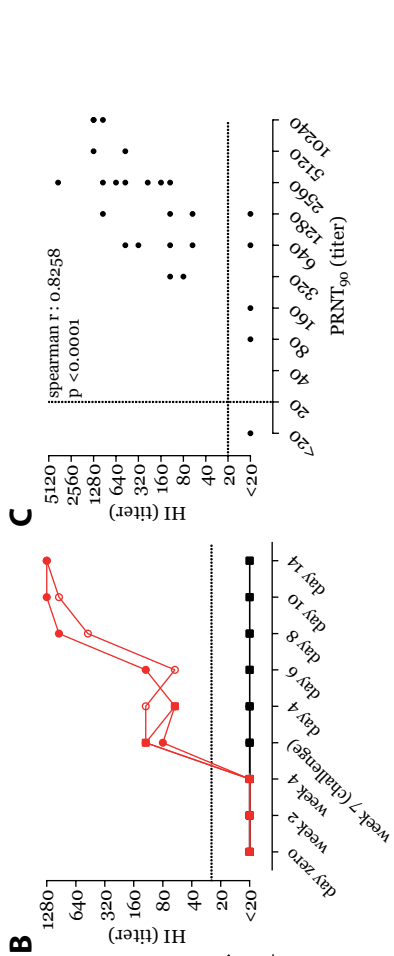

Appendix Figure 6. MERS-CoV hemagglutination inhibition (HI) assay for MERS-CoV dromedary camel diagnostics. **(A)** Validation of the specificity of the HI assay for the detection of MERS-CoV specific antibodies in the sera of MERS-CoV-infected (black) and naïve (green) dromedary camels. **(B)** Kinetics of HI antibody responses in dromedary camels following vaccination (red) and infection (black). **(C)** Correlation between neutralizing and HI antibody responses following MERS-CoV infection or vaccination in dromedaries. $PRNT_{90}$: 90% reduction in plaque reduction neutralization test.

Chapter 3.1

Chimeric camel/human heavy-chain antibodies protect against MERS-CoV infection

V. Stalin Raj* | Nisreen M.A. Okba* | Javier Gutierrez-Alvarez | Dubravka Drabek | Brenda van Dieren | W. Widagdo | Mart M. Lamers | Ivy Widjaja | Raul Fernandez-Delgado | Isabel Sola | Albert Bensaid | Marion P. Koopmans | Joaquim Segalés | Albert D.M.E. Osterhaus | Berend Jan Bosch | Luis Enjuanes | Bart L. Haagmans

*Authors contributed equally

Sci Adv. 2018;4(8)

Abstract

Middle East respiratory syndrome coronavirus (MERS-CoV) continues to cause outbreaks in humans as a result of spillover events from dromedaries. In contrast to humans, MERS-CoV–exposed dromedaries develop only very mild infections and exceptionally potent virus-neutralizing antibody responses. These strong antibody responses may be caused by affinity maturation as a result of repeated exposure to the virus or by the fact that dromedaries—apart from conventional antibodies—have relatively unique, heavy chain–only antibodies (HCAbs). These HCAbs are devoid of light chains and have long complementarity-determining regions with unique epitope binding properties, allowing them to recognize and bind with high affinity to epitopes not recognized by conventional antibodies. Through direct cloning and expression of the variable heavy chains (VHHs) of HCAbs from the bone marrow of MERS-CoV–infected dromedaries, we identified several MERS-CoV–specific VHHs or nanobodies. In vitro, these VHHs efficiently blocked virus entry at picomolar concentrations. The selected VHHs bind with exceptionally high affinity to the receptor binding domain of the viral spike protein. Furthermore, camel/human chimeric HCAbs—composed of the camel VHH linked to a human Fc domain lacking the CH1 exon—had an extended half-life in the serum and protected mice against a lethal MERS-CoV challenge. HCAbs represent a promising alternative strategy to develop novel interventions not only for MERS-CoV but also for other emerging pathogens

Introduction

In 2012, a novel virus, termed Middle East respiratory syndrome coronavirus (MERS-CoV), was identified in humans (1). Six years later, more than 2000 laboratory-confirmed MERS cases, including 36% with a fatal outcome, have been reported globally. Most cases thus far originated from the Arabian Peninsula, as a result of hospital outbreaks (2). There is convincing evidence that dromedary camels are the primary source of MERS-CoV infection in humans. The virus isolated from camels is similar to that isolated from humans and also replicates in human cells (3). In addition, epidemiological and phylogenetic analyses suggest multiple introductions of MERS-CoV into the human population (2, 4). This raises a great concern as MERS-CoV could continue to cause outbreaks in the near future. Effective prophylactic and therapeutic intervention strategies are therefore needed to combat this virus.

Monoclonal antibodies (mAbs) are promising candidates for the treatment and prevention of viral infections. Recently, MERS-CoV–neutralizing mAbs have been identified and characterized by several research groups, using various approaches. These antibodies have been isolated from human naïve B cells (5), memory B cells of MERS-CoV–infected individuals (6), or transgenic mice expressing human antibody variable heavy chains (VHHs) and κ light chains (7). All these mAbs target the receptor binding domain (RBD) of the MERS-CoV spike protein. The MERS-CoV spike protein is a structural viral component that contains the RBD, located in the S1 subunit of the protein, which binds to the MERS-CoV entry receptor dipeptidyl peptidase-4 (DPP4) (8). Antibodies raised against the S1 or RBD block MERS-CoV infection in vitro (9, 10) and the most potent mAbs identified against MERS-CoV thus far recognize the RBD (5, 7, 11-14). However, production of these mAbs at a large scale is costly and requires a long developmental process, and relative large quantities might be needed to protect humans against a viral infection (15). Alternatively, antibody engineering technologies allow the cloning of variable regions of mAbs for expression in *Escherichia coli* or yeast to produce large amounts of recombinant antibody fragments (16). To date, 68 therapeutic mAbs have been licensed, of which 7 are chimeric antibodies (17).

Heavy chain–only antibodies (HCAbs) are naturally produced in camelid species (18). These antibodies are dimeric and do not contain a light chain, and their antigen recognition region is solely formed by the VHH region termed single-domain antibody fragment. This fragment is about 14 kDa in size, is relatively stable, and can be produced with high yields in prokaryotic systems (18, 19). Camelid VHHs have long complementarity-determining region 3 (CDR3) loops, capable of binding to unique epitopes not accessible to conventional antibodies (20). Because of these beneficial properties, VHHs have been exploited for a range of biotechnological applications, including diagnostics, therapeutics, and fundamental research (21, 22). The recent preclinical success of a VHH that blocks von

Willebrand factor–mediated platelet aggregation (23) shows their therapeutic potential. VHHs may also efficiently prevent entry of viruses into host cells (24). Chimeric HCAbs, which have the camel VHH and the human Fc portion (lacking the CH1 exon as in camel HCAbs), allow them to interact with human effector cells and complement cascade factors (15).

Several studies have demonstrated the presence of high levels of MERS-CoV–specific neutralizing antibodies (mean virus neutralization titer ≈ 1000) in dromedary camels in the Middle East and Africa (25-27). Therefore, next to human mAbs, characterization of MERS-CoV–neutralizing VHHs from dromedary camels could serve as an alternative strategy to develop neutralizing antibodies. Here, we report the identification and characterization of neutralizing VHHs against MERS-CoV from immunized dromedary camels and demonstrate the prophylactic activity of camel/human chimeric HCAbs in a MERS-CoV transgenic mouse model.

Results

Identification of MERS-CoV–specific VHHs from a dromedary camel bone marrow complementary DNA library

First, we identified MERS-CoV–neutralizing VHHs by direct cloning and screening of VHH complementary DNA (cDNA) libraries derived from bone marrow cells (given the high frequency of specific plasma cells) rather than using B cells from peripheral blood of immunized animals (Figure 1). Bone marrow was obtained from two dromedary camels immunized with modified vaccinia virus encoding the MERS-CoV spike protein and subsequently challenged with live MERS- CoV (28). At the time of sampling, MERS-CoV–neutralizing antibodies were detected at very high levels (titer > 10,000) in the sera of these dromedaries (Figure 2A). Subsequently, VHH-specific primers (29) were used to amplify a VHH library from the bone marrow cDNA by nested polymerase chain reaction (PCR) (Figure S1, A to C). After gel purification, PCR products were directly cloned into the dephosphorylated prokaryotic expression vector pMES4, tagging the VHHs with six histidine amino acids at the C terminus (29). To obtain a high-diversity repertoire of VHHs, we reduced the number of amplification cycles. The ligated VHH plasmid library was transformed into E. coli strain WK6 and plated on ampicillin nutrient agar plates without preculturing the bacteria in nutrient medium. A total of 560 VHH clones (225 from camel 1 and 335 from camel 2) were obtained in a single transformation event, and grown individually in 96-deep-well plates. Periplasmic expression of recombinant VHHs was induced by isopropyl-β-d-thiogalactopyranoside (Figure 1). VHHs were purified from the periplasm as a crude extract (30), and expression was verified using SDS–polyacrylamide gel electrophoresis (PAGE) analysis (Figure S1D).

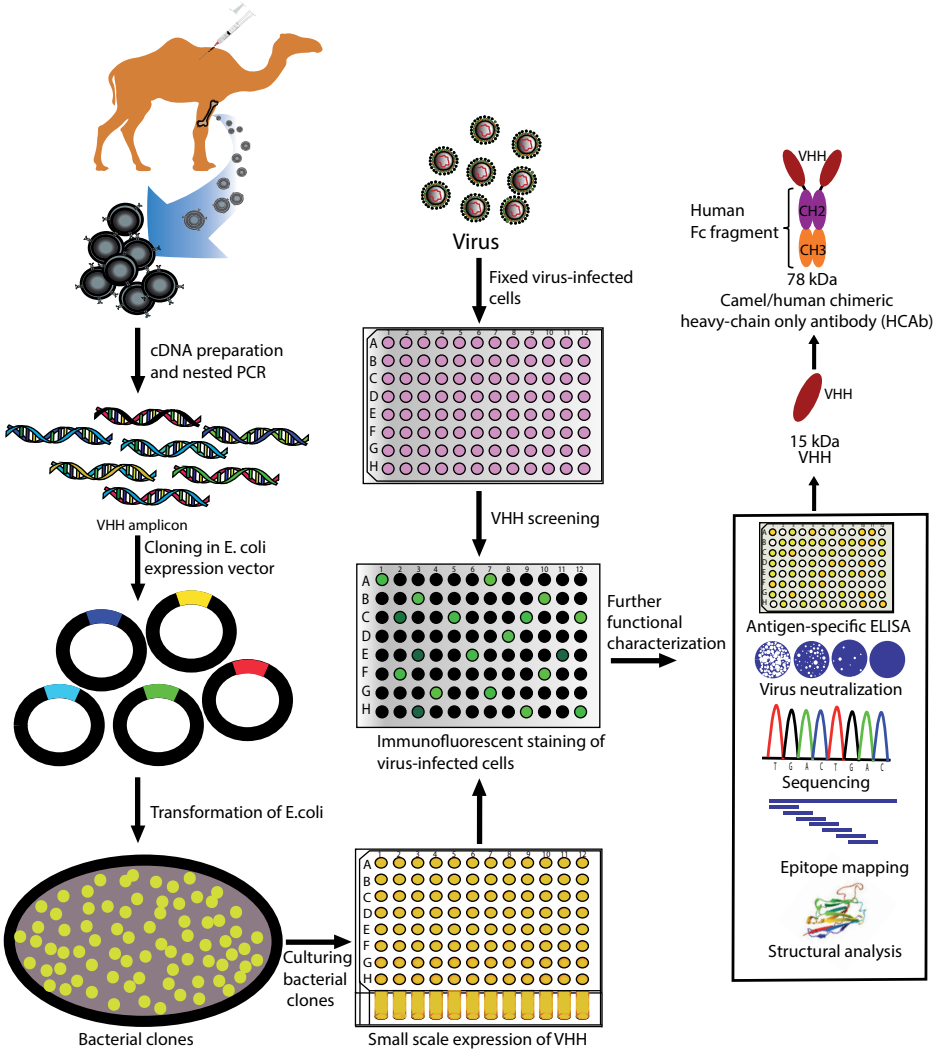

Figure 1. Schematic overview of VHH identification by direct cloning using bone marrow from immunized dromedary camels. Immunized dromedary camels were anesthetized, and bone marrow aspirations were performed. After total RNA isolation and first-strand cDNA synthesis, VHH genes were amplified and cloned into a prokaryotic expression vector (pMES4) and transformed into *E. coli* WK6. Individual clones were grown overnight in 96-deep-well plates, during which they expressed the VHHs in the periplasm. Next, crude VHHs were released from the periplasm by freeze-thawing the bacterial pellet. Crude VHHs were used for immunofluorescent staining on virus-infected cells. Immunofluorescent positive clones were further characterized for their genetic makeup, specificity, and potency by sequencing, antigen-specific enzyme-linked immunosorbent assay (ELISA), virus neutralization assay, epitope mapping, and structural analysis. Finally, potent VHHs were produced as camel/human chimeric single chain–only antibodies.

Next, we used formalin-fixed and permeabilized virus-infected cells [either MERS-CoV–infected or severe acute respiratory syndrome coronavirus (SARS-CoV)–infected] to select for MERS-CoV–specific VHHs using immunofluorescent staining. Crude periplasmic VHH extracts were incubated on the infected cells, and VHH cell binding was visualized with a fluorescently labeled anti-histidine antibody as a secondary antibody. All 560 VHH clones were screened by confocal microscopy (Figure 2B). We obtained 204 MERS-CoV–reactive VHHs (41.7% from camel 1 and 58.3% from camel 2), of which none reacted to SARS-CoV–infected cells. To confirm the specificity of the VHHs for MERS-CoV, we randomly selected several clones for double staining of MERS-CoV–infected cells using a rabbit anti–MERS-CoV serum, revealing that these VHHs exclusively targeted MERS-CoV–infected cells (Figure 2C).

Blocking of RBD binding to receptor DPP4 by MERS-CoV spike-specific VHHs in vitro

To test whether the VHHs identified in our study recognized the RBD or other parts of the S1, we performed MERS-CoV S1– and MERS-CoV RBD–specific ELISAs. Out of 204 MERS-CoV–reactive VHHs, 188 (92.15%) were directed against the MERS-CoV S1 subunit, of which 46 VHHs (22.5%) blocked the binding of recombinant S1 to the MERS-CoV receptor present on Huh-7 cells (Figure S2). All these in vitro blocking VHHs were directed against the RBD (Figure 2D).

Next, we selected all blocking VHHs for further characterization. The VHH clone p2E6 (negative for immunofluorescent staining and S1 ELISA) was used as the negative control. Using a MERS-CoV plaque reduction neutralization test (PRNT), we estimated the virus neutralization capacity for each VHH. Except for the control VHH-p2E6, all tested VHHs inhibited MERS-CoV entry at varying concentrations ranging from 100 to 900 pM ($PRNT_{90}$; table S1). VHHs with high neutralizing capacity (VHH-1, VHH-4, VHH-83, and VHH-101) were selected for further characterization.

We obtained sequences from all 46 blocking VHHs. Because CDR3 is known to be of most importance for the interaction with the antigen, the assumption was made that VHHs with the identical CDR3 would recognize the same epitope. Overall, 33 VHHs had different CDR3 sequences ranging in length from 16 to 20 amino acids (Figure S3). Phylogenetic analysis of these sequences revealed considerable diversity among the different VHH clones and showed that the selected VHHs formed 14 different clusters with different CDR3 sequences (Figure S4). All sequences contained the characteristic VHH tetrad, except clone 10 that, at amino acid positions 37, 45, and 47, shows VH characteristics (valine, leucine, and tryptophan). The best MERS-CoV–neutralizing VHHs (VHH-1, VHH-4, VHH-83, and VHH-101) had different CDR3 sequences (Figure S4).

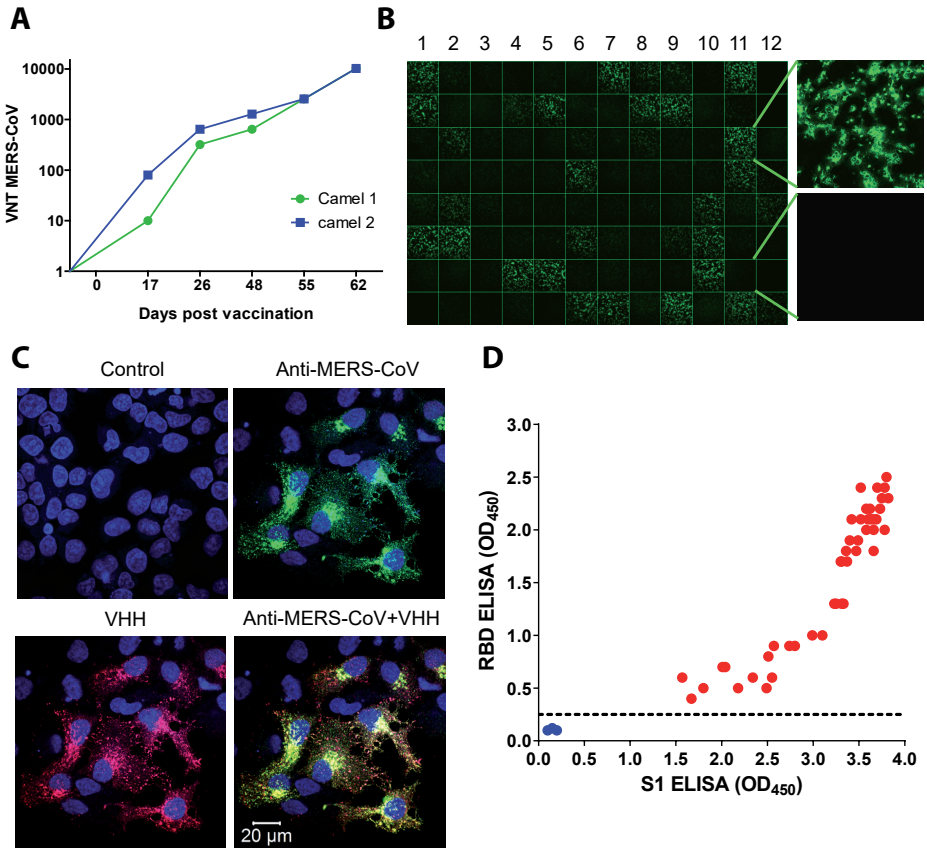

Figure 2. Identification of VHHs directed against the spike (S) protein of MERS-CoV. **(A)** Virus-neutralizing antibody titers (VNT) of sera from two dromedary camels immunized with MVA expressing the MERS-CoV-S (MVA-S) and challenged with MERS-CoV. **(B)** Immunofluorescent staining of MERS-CoV–infected Huh-7 cells with crude VHHs. Each square represents staining of an individual VHH. **(C)** Immunofluorescent staining of MERS-CoV–infected Huh-7 cells with rabbit serum (anti–MERS-CoV) or crude VHHs and overlay. **(D)** Correlation of the S1-specific ELISA and the RBD-specific ELISA for the 46 MERS-CoV–neutralizing VHHs (red dots) and control VHHs indicated as blue dots (Spearman correlation r = 0.9258; p < 0.0001; 95% confidence interval, 0.8677 to 0.9589). OD, optical density.

VHHs bind to MERS-CoV spike protein with high affinity

Subsequently, the best four neutralizing VHHs and the control VHH-p2E6 were selected for large-scale production and purification. We obtained high quantities (5 to 30 mg) of pure (>95%) His-tag affinity-purified VHHs from 1 liter of bacterial culture (Figure S5A). Mixing these VHHs with recombinant MERS-CoV spike S1 protein generated VHH-spike complexes, as observed by nonreducing PAGE analysis (Figure S5B). In addition, the equilibrium dissociation constant (K_d) between the VHH and spike protein of these four VHHs was relatively low, with K_d values ranging from 1 to 0.1 nM, indicating high-affinity binding (Figure S6, A and B).

Neutralization of MERS-CoV by VHHs and camel/human chimeric HCAbs

Next, we tested the neutralizing activities of these VHHs in vitro by PRNT. All four VHHs were confirmed to neutralize MERS-CoV with high efficiency, with PRNT50 values ranging from 0.0014 to 0.012 µg/ml (93 to 800 pM), while no inhibition was observed using the control VHH-p2E6 at high concentration (>1.0 µg/ml; 67 µM; Figure 3A). Because of their small size, VHHs are rapidly cleared from the circulation (30, 31). Therefore, we additionally produced the four VHHs as camel/human chimeric HCAbs by C-terminal tagging the VHHs with the Fc part of human immunoglobulin G2 (IgG2) (containing the hinge and CH2 and CH3 exons) (Figure 1, right). These HCAbs (HCAb-1, HCAb-4, HCAb-83, and HCAb-101) form homodimers of about 78 kDa in size and exhibit approximately the same neutralizing capacity as the monomeric VHHs in vitro (Figure 3B). Moreover, using an S1-specific ELISA, we could detect HCAb binding at even lower concentrations, down to 0.00019 µg/ml (2.5 pM; Figure 3C).

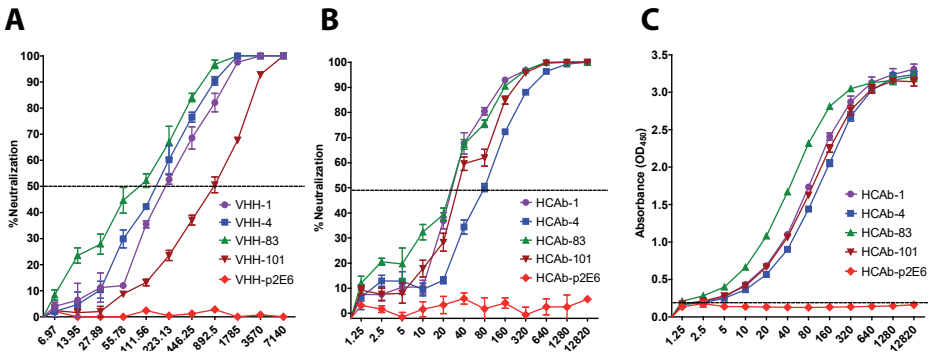

Figure 3. MERS-CoV–neutralizing efficacy of monomeric VHHs and chimeric antibodies on Huh-7 cells. MERS-CoV (EMC isolate) was incubated with either VHHs (monomer), chimeric antibodies, or controls at various concentrations for 1 hour and then the mix was transferred on Huh-7 cells. Cells were fixed 8 hours after infection and stained using rabbit polyclonal antibodies. The PRNT titer was calculated on the basis of a 50% or greater reduction of infected cells ($PRNT_{50}$). **(A)** PRNT assay for VHH monomer. **(B)** PRNT for camel/human chimeric heavy-chain antibodies. Experiments were performed at least two times in triplicate, data from an experiment were presented, and error bars show SEM. **(C)** MERS-CoV S1 ELISA using different HCAbs. The optical density at 450 nm was presented in triplicate, with error bars showing SEM.

Epitope mapping of four potent MERS-CoV–neutralizing VHHs

To map the VHH binding epitopes, we first tested the binding of the four different VHHs to recombinant S1 protein using ForteBio's Octet system. As shown in Figure S7, all four VHHs competed for a single epitope. Subsequently, we used a set of recombinant S1 proteins that contain single amino acid mutations present in spike proteins of MERS-CoV field isolates, located within the receptor binding subdomain (residues 483 to 566) of the RBD that engages DPP4. MERS-CoV polyclonal antibodies, an irrelevant VHH, and four VHHs were then tested for their ability to bind to these S1 variants. MERS-CoV polyclonal antibodies,

but not the control VHH-p2E6, bound to all variants (Figure 4, A and B), whereas the four MERS-CoV–specific VHHs did not bind to the D539N variant and differed in their binding to the other variants. VHH-1 also did not bind to variant E536K, whereas VHH-4 and VHH-101 showed partial binding to three additional variants (I529T, V534A, and E536K) (Figure 4, C to F). These data show that all four VHHs bind an epitope in the receptor binding subdomain that is partially overlapping, consistent with the binding competition analysis (Figure S7). The RBD residues D537, D539, Y540, and R542 are important for the virus to bind to its cellular receptor DPP4 (32, 33). Because all four VHHs did not bind to the D539N variant, this suggests that these VHHs neutralize MERS-CoV most likely by blocking its binding to its cellular receptor. Despite several attempts, we were not able to identify MERS-CoV escape variants in vitro. Because of the best neutralizing capacity and epitope recognition, we selected VHH-83 and HCAb-83 for further in vivo testing.

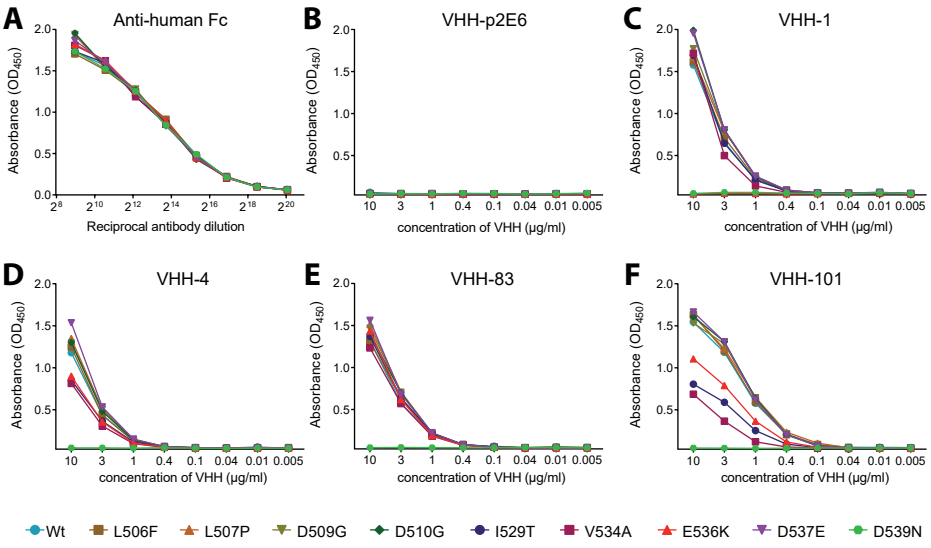

Figure 4. Effect of MERS-CoV RBD residue substitution on VHH binding. Binding efficiency of VHHs to the wild-type and mutant forms of viral spike glycoprotein was analyzed by ELISA. The binding efficiency was calculated on the basis of optical density (OD_{450}) of mutant protein versus that of the wild-type spike. **(A)** Anti-human IgG polyclonal antibodies were used to corroborate equivalent coating of the S1-hFc variants. **(B)** One irrelevant VHH (VHH-p2E6) lacked binding to wild-type and mutant proteins. **(C)** VHH-1. **(D)** VHH-4. **(E)** VHH-83. **(F)** VHH-101.

In vivo efficacy of VHH-83 and HCAb-83

To test the prophylactic efficacy of VHH-83 or HCAb-83 in vivo, we used the K18 transgenic mouse model (34). In our first experiment, mice were given VHH-83 or an irrelevant VHH control (p2E6) at 20 or 200 µg per mouse (nine mice per group) by intraperitoneal injection

6 hours before intranasal infection with a lethal dose of MERS-CoV (EMC isolate). Mice that received VHH-83 lost weight and died within 7 days post-inoculation (dpi), as well as those injected with the control VHH (Figure S8).

Next, we tested HCAb-83 or the control HCAb-p2E6 using a similar experimental setup. Mice treated with 200 µg of HCAb-83 gained weight (Figure 5A), and all mice survived (Figure 5B). In contrast, control HCAb-p2E6–treated groups lost weight and died within 7 dpi (Figure 5,

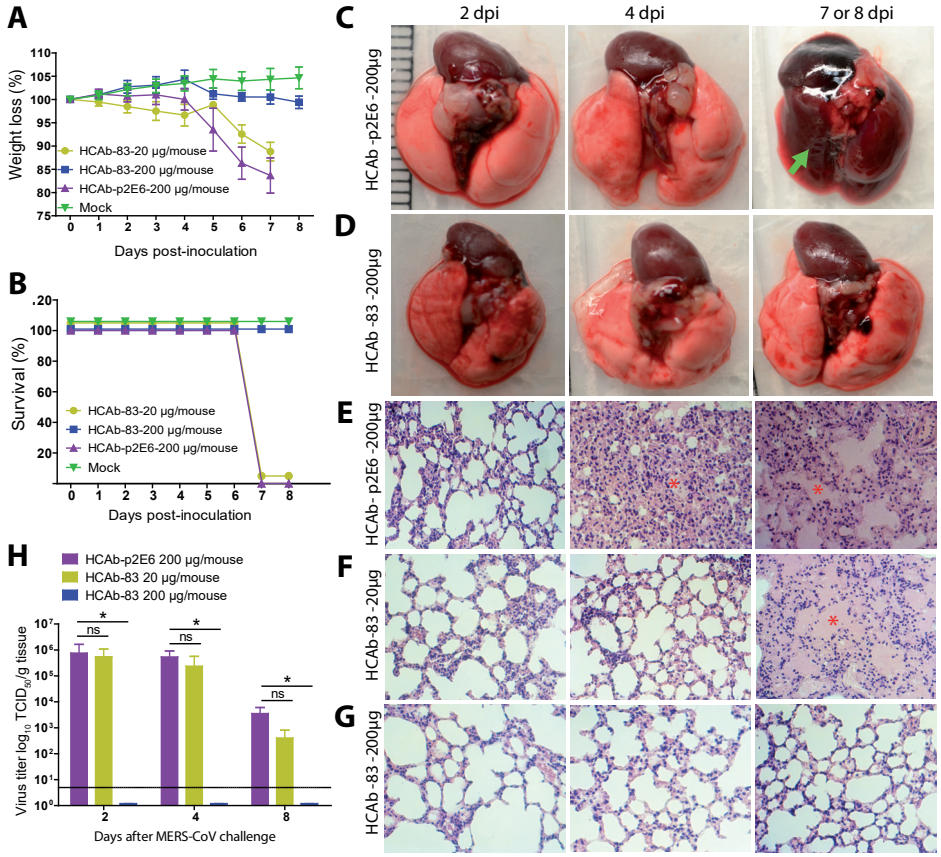

Figure 5. Prophylactic efficacy of HCAb-83 in K18 mice challenged with a lethal dose of MERS-CoV. K18 mice (n = 9 per group) were injected intraperitoneally with HCAb-83 (20 or 200 µg per mouse) 6 hours before challenge with 10^5 $TCID_{50}$ (median tissue culture infectious dose) of MERS-CoV (EMC isolate). HCAb-p2E6 was injected as a negative control (n = 9). Mice were monitored daily for **(A)** weight loss and **(B)** mortality. Weight loss is expressed as a percentage of the initial weight. Lungs were collected at days 2, 4, and 8 (n = 3 per time point) or from mice that died in between and were processed to asses gross pathology **(C** and **D)** and histopathological changes **(E** to **G)**. Gross pathology of one representative animal that died at day 7 when treated with HCAb-p2E6 is indicated by a green arrow (C, right). Lung sections were stained with hematoxylin and eosin. Asterisk indicates alveolar edema. **(H)** MERS-CoV viral titer quantitation of infected lungs at days 2, 4, and 8 (n = 3 per time point) after infection (n = 3 mice per time point); one-way ANOVA. * $p < 0.05$. ns, not significant.

A and B). Gross pathological changes (Figure 5C), mononuclear cell infiltration, and alveolar edema (Figure 5E) were observed in the lungs of control HCAb-p2E6–treated mice on day 4 after inoculation. Whereas low doses (20 μg) of HCAb-83–treated mice were only partially protected on the basis of the observed reduction of pathological abnormalities on 4 dpi (Figure 5F), the lungs of high-dose HCAb-83–treated mice showed no pathological changes at any time point tested (Figure 5G). In addition, no infectious virus could be isolated from the lungs of these mice, while high viral titers were observed in the low dose– and control HCAb–treated mice (Figure 5H).

Pharmacokinetics of HCAb-83

We also evaluated the pharmacokinetics of VHH and HCAb in the sera of mice treated with either VHH-83 or HCAb-83. First, we estimated the presence of MERS-CoV–neutralizing activity in sera obtained 2 days after treatment. No neutralization of the virus was observed in the sera of VHH-83– or control VHH-p2E6–treated mice (Figure 6A), consistent with the reported rapid clearance of small VHH domains from the circulation (31). Significant levels of neutralizing antibodies (mean titer, 1024) were observed in the sera of mice treated with 200 μg of HCAb-83 and, to a limited extent, in low dose–treated mice (mean titer, 64; Figure 6A). Second, we tested the presence of circulating HCAb-83 in the sera obtained at various time points after injection (0, 2, 4, and 8 days after treatment) by ELISA. As shown in Figure 6B, 200 μg of HCAb-83–treated mice still had high levels of HCAb-83 8 days after treatment, with an apparent serum half-life of approximately 4.5 days.

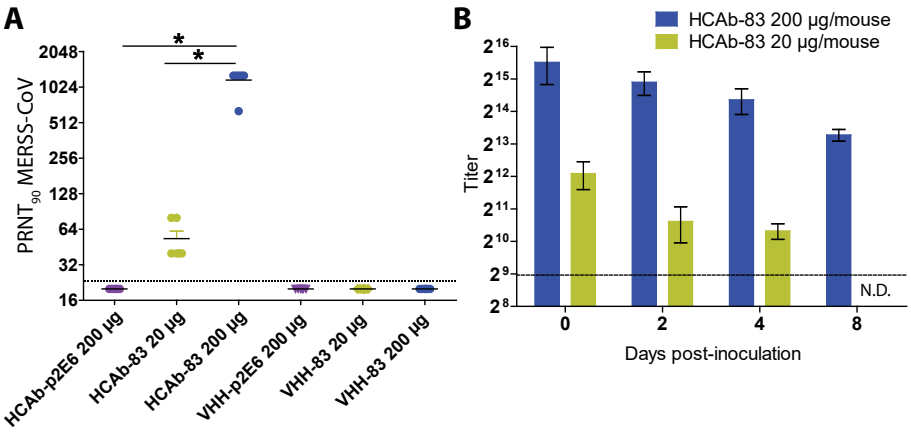

Figure 6. Pharmacokinetics of HCAb-83 in K18 transgenic mice. **(A)** MERS-CoV PRNT performed on sera of mice collected 2 days after treatment with VHH-83, HCAb-83, or controls. The PRNT titer was calculated on the basis of a 90% reduction in the infected cell counts. Statistically significant differences were observed between groups HCAb-p2E6 200 μg, HCAb-83 200 μg, and HCAb-83 20 μg (one-way ANOVA test, * $p < 0.05$). **(B)** Detection of HCAbs in the sera of HCAb-83–treated mice at various time points using ELISA. N.D., not determined.

Discussion

VHHs are small in size; have high stability, solubility, and affinity; and efficiently recognize antigens. They have many potential biomedical applications including the treatment of cancer, autoimmune diseases, and virus infections (18, 19, 22, 24, 31). Moreover, VHHs are gaining much attention in the field of diagnostics and therapeutics for viral diseases. They have been used for the detection of viruses, such as Marburg virus, human immunodeficiency virus (HIV), influenza virus, dengue virus, and norovirus (22, 24). VHHs also block virus attachment to the host cells in respiratory syncytial virus, influenza virus, hepatitis B virus, rotavirus, and HIV infections (22, 24). Some VHHs inhibit viral RNA transcription or nuclear import of viral ribonucleoproteins (35). Here, we have shown that MERS-CoV–neutralizing VHHs can be obtained from immunized dromedary camels that were challenged with MERS-CoV. The engineered camel/human chimeric HCAbs were highly stable in mice, and prophylactically treated mice were fully protected from MERS-CoV infection upon challenge with live virus.

Naturally infected dromedary camels have remarkably high levels of neutralizing antibodies against MERS-CoV (25, 36). We used dromedaries that showed high levels of neutralizing antibodies in their sera and identified MERS-CoV–neutralizing VHHs by direct cloning from a VHH cDNA library using bone marrow, a major source of highly enriched long-lived antibody-producing plasma cells. After immunization, antigen-stimulated B cells undergo affinity maturation in germinal centers of secondary lymphoid organs, where they differentiate into plasma cells that secrete antibodies. Significant portion of long-lived plasma cells migrate to the bone marrow. A small portion of plasma cells reside in the lymphoid organs, but these are often short-lived (37, 38). In mice, 8 days after boost immunization with ovalbumin, about 10 to 20% of the antigen-specific plasma cells migrate from secondary lymphoid organs to the bone marrow (39). In particular, bone marrow plasma cells are long-lived and are thus suitable for maintaining antibody levels in the serum for an extended period, which plays a significant role in pathogen neutralization and humoral immune responses (40). The number of S1-specific clones found in the VHH library generated from vaccinated and infected camels (188 of 560 clones; 33.5%) was much higher compared to nonvaccinated infected camels (12 of 496 clones; 2.4%), suggesting that the vaccination and challenge protocol used in this study had a major impact on the frequency of S1-specific B cells detected in the bone marrow.

Camelid species have naturally occurring HCAbs. These antibodies contain long CDR3 sequences (20), which allow them to interact with unique and even recessed epitopes that may not be recognized by conventional antibodies (20, 41). We identified 46 MERS-CoV–neutralizing VHHs, of which 4 bound to the RBD of the spike protein with high affinity

and neutralized MERS-CoV infection at picomolar concentrations. VHH-83 showed a neutralizing capacity down to a concentration of 30 pM ($PRNT_{50}$), making it more potent than the most potent mAbs described thus far (7, 42). However, direct comparisons between different antibodies would require determining the exact differences in vitro. Competition and spike protein binding assays showed that the four VHHs competed for binding to an overlapping epitope on the RBD, which partially overlaps with the RBD-DPP4 interface. Binding assays using variant recombinant spike proteins revealed that all four VHHs bound to wild-type spike protein but not to a D539N-mutant protein. Amino acids E536, D537, and D539 are negatively charged residues on the surface of the RBD, which interact with three positively charged residues on the outer surface of the DPP4 (32, 33).This indicates that the four VHHs can prevent virus attachment and entry. Given the critical role of these amino acids in the DPP4-virus interaction, viral escape mutants without loss of fitness are less likely to develop (32, 33). This could be the reason why we did not identify HCAb-83 escape variants in vitro. However, further (structural) studies are needed to pinpoint all RBD-VHH contact residues involved.

Next, we produced the four VHHs as HCAbs, which showed threefold enhanced MERS-CoV–neutralizing capacity in comparison to the monomeric VHHs in vitro ($PRNT_{50}$, 30 pM). In contrast to VHH-83, mice prophylactically treated with 200 µg of HCAb-83 were fully protected from weight loss and death upon challenge with live virus. No infectious virus was detected in the lungs of these mice, and protection correlated with the presence of sustained high levels of HCAbs-83 in the sera of mice. In addition, most in vivo studies testing mAbs to MERS-CoV showed only reduced MERS-CoV replication (two to four log reductions in lung virus titer) or complete protection only at higher doses used (1000 µg per mouse) (6, 7, 13). The high level of neutralizing activity of HCAb-83 ($PRNT_{50}$, 30 pM) could be due to the different antigen recognition pattern of camelid HCAbs. Recent studies also revealed the importance of long CDR3 sequences from bovine antibodies raised against HIV in cross-neutralization against different viral serotypes (43). The therapeutic efficacy of HCAb-83 still needs further evaluation, but given the limited therapeutic efficacy of other mAbs against acute respiratory infections such as respiratory syncytial virus in humans (44), prophylactic administration of antibodies may also be preferred to contain outbreaks of MERS-CoV.

Apart from direct neutralization, antibodies may also play a role in mediating effector functions such as complement-dependent cytotoxicity and antibody-dependent cell-mediated cytotoxicity (16). HCAb-83 has an Fc domain of human IgG2, which has limited effector function in vivo (17); suggesting that the observed protection in mice could be mainly due to the neutralizing activity. Therefore, additional studies need to evaluate whether the potency of HCAb-83 may be increased further by replacing the IgG2 Fc with the IgG1 Fc or by combination with other antibodies targeting different epitopes.

In summary, we identified and characterized potent HCAbs that neutralized MERS-CoV in vitro and in vivo. Because of their high affinity, in vivo stability, and efficacy, these HCAbs may be used as a prophylaxis for MERS-CoV.

Materials and methods

Immunization

One female (6-month-old) and one male (8-month-old) healthy dromedary camels (*Camelus dromedarius*), negative for antibodies against MERS-CoV and modified vaccinia virus Ankara (MVA), were obtained from the Canary Islands and housed in biosecurity level 3 (BSL-3) facilities [Centre de Recerca en Sanitat Animal (CReSA)], as described previously (28). Experimental procedures were approved by the local Ethics Committee of the Autonomous University of Barcelona (number 8003). Both animals were immunized twice with a 4-week interval with 10^8 plaque-forming units of MVA-S via both nostrils and intramuscularly in the neck of the animals. After the second immunization, both animals were anesthetized with midazolam (5 mg/ml) and inoculated with 10^7 $TCID_{50}$ MERS-CoV in 3 ml of phosphate-buffered saline (PBS) intranasally in both nostrils using a laryngo-tracheal mucosal atomization device (45). Blood samples were taken at different dpi. On day 14 after inoculation, both animals were anesthetized and femoral bone marrow samples (about 1 cm^3) were collected next to the epiphysis and placed, each, in tubes containing 3.6 ml of ice-cold fetal calf serum. Specimens were gently crushed with a 1-ml tip and homogenized by slow up and down pipetting. After 10-min incubation on ice, 400 µl of dimethyl sulfoxide was mixed into each tube, and the preparation was dispensed into 2-ml cryovials discarding debris and slurs and stored at −135°C.

Protein expression

The recombinant S1-Fc fusion proteins were produced as described previously (46). Briefly, plasmids encoding MERS-CoV S1-Fc or MERS-CoV RBD-Fc were generated by ligating a fragment encoding the S1 subunit (GenBank accession number;AFS88936; residues 1 to 747) or RBD (residues 358 to 588) 3′ terminally to a fragment encoding the Fc domain of human IgG1 into the pCAGGS expression vector. Plasmids encoding S1-Fc variants with single amino acid substitutions were generated by site-directed mutagenesis. S1-Fc fusion proteins were expressed by transfection of the expression plasmids into human embryonic kidney (HEK)–293T (CRL-11268, American Type Culture Collection) cells and affinity-purified from the culture supernatant using Protein A-Sepharose beads (GE Healthcare).

Estimation of antibody/VHH titers

MERS-CoV–specific antibody titers were measured by ELISA. First, 96-well plates were coated with MERS-CoV S1 or MERS-CoV RBD proteins at 1 μg/ml in PBS (pH 7.4) and incubated overnight at 4°C. Wells were then washed three times with PBS, blocked with 10% normal goat serum in PBS, and incubated at 37°C for 30 min. Dromedary camel sera or VHHs were serially diluted in PBS, 100 μl was added per well, and plates were incubated at 37°C for 1 hour. Next, plates were washed three times in PBS containing 0.05% Tween 20 (PBST), after which they were incubated with biotin-conjugated goat anti-llama antibodies (1:2000, Abcore) or mouse anti-histidine antibodies (1:2000, Thermo Fisher Scientific) at 37°C for 1 hour. After three washes with PBST, plates were incubated with streptavidin horseradish peroxidase (HRP; 1:10,000, Dako) or goat anti-mouse HRP (1:2000, Dako) at 37°C for 1 hour. After this incubation, plates were washed three times in PBST and incubated at room temperature for 10 min in the presence of 3,3′,5,5′-tetramethylbenzidine substrate (eBioscience). Reactions were stopped with 2N H_2SO_4 (Sigma). The absorbance of each sample was read at 450 nm with an ELISA reader (Tecan Infinite F200).

RNA isolation and cDNA synthesis

For RNA isolation, cryopreserved bone marrow cells were removed from the –135°C freezer and transferred to a 37°C water bath. The thawed cell suspension was quickly transferred to 40 ml of ice-cold RPMI 1640 (Lonza) medium. Cells were counted, and 10^7 cells were transferred to a new ribonuclease (RNase)–free falcon tube and centrifuged at room temperature at 300g for 10 min. The supernatant was completely removed, and cells were subsequently lysed with 1 ml of TRIzol reagent (Life Technologies) and 0.2 ml of RNase-free chloroform (Life Technologies). The mixture was vortexed for 15 s and incubated for 3 min at room temperature, followed by centrifugation at 13,000 rpm for 15 min at 4°C. The aqueous phase was transferred to a new tube. Subsequently, RNA was isolated using the RNeasy MinElute Cleanup Kit (Qiagen) according to the manufacturer's protocol. Total RNA was quantified at 260 nm using the NanoDrop 2000, and the quality of the isolated RNA sample was determined by measuring the A_{260}/A_{280} ratio. cDNA was synthesized from 1.5 μg of total RNA using a First-Strand cDNA Synthesis kit (Life Technologies). For a 20-μl reaction mix, 10 μl of RNA, 1 μl of deoxynucleoside triphosphate (dNTPs; 10 mM each), 1 μl of random hexamers (10 mM; Promega), and 1.5 μl of distilled water (dH_2O) were added to a microvial. The mixture was incubated at 65°C for 10 min and then at 4°C for 2 min. Next, 6.5 μl of reverse transcriptase mix containing 4 μl of 5× SuperScript III reaction buffer, 1 μl of dithiothreitol (100 mM), 0.5 μl of RNase inhibitor (20 U/μl), and 1 μl of SuperScript III reverse transcriptase (200 U/μl; Life Technologies) were added to the microvial and incubated at 25°C for 5 min, 50°C for 45 min, and 70°C for 20 min. cDNA was stored at 4°C until PCR amplification.

PCR amplification and cloning of VHH

The amplification of VHH was performed using a nested PCR approach (29) that was adapted for use with a high-fidelity DNA polymerase (PfuUltra II Fusion HS DNA Polymerase, Stratagene). The first PCR mix (50 µl of reaction volume) consisted of 5.0 µl of 10× PfuUltra II Fusion HS DNA polymerase buffer, 2.5 µl of dNTPs (10 mM each), 1.5 µl of gene-specific forward primer (CALL001, 5′-GTCCTGGCTGCTCTTCTACAAGG-3′; 10 mM), 1.5 µl of gene-specific reverse primer (CALL002, 5′-GGTACGTGCTGTTGAACTGTTCC-3′; 10 mM), 1.0 µl of PfuUltra II Fusion HS DNA polymerase, 36.5 µl of dH_2O, and 2.0 µl of cDNA. PCR amplification was performed in a thermocycler with the following protocol: initial denaturation at 94°C for 3 min, followed by 20 cycles at 94°C for 20 s, 50°C for 30 s, and 72°C for 2 min, and a final extension at 72°C for 10 min. The first PCR generated two amplified products: the heavy chain of conventional antibodies (~1000 bp) and the VHH heavy chain (~700 bp; Figure S1). The amplified VHH amplicon (~700 bp) was purified from the agarose gel using the QIAquick Gel Extraction Kit (Qiagen), according to the manufacturer's instructions. The product was then subjected to the second round of PCR amplification using VHH inner primers that contained restriction sites for cloning: forward, 5′-CTAGTGCGGCCGCTGGAGACGGTGACCTGGGT-3′ (Eco 91I); reverse, 5′-GATGTGCAGCTGCAGGAGTCTGGRGGAGG-3′ (Pst I). PCR amplification continued for 12 to 14 cycles, after which the amplicons were purified with the QIAquick PCR Purification Kit (Qiagen) and digested using Eco 91I and Pst I. The vector pMES4 (GenBank accession number GQ907248) was digested with the same enzymes and dephosphorylated using alkaline phosphatase (New England Biolabs). VHH amplicons were ligated into pMES4 using a ratio of 100 ng of vector to 46 ng of VHH (~1:3 molar ratio). Next, we used *E. coli* strain WK6, prepared using the Mix & Go! *E. coli* Transformation Kit and Buffer Set (Zymo Research), for transformation according to the manufacturer's instructions. After transformation, cells were directly plated onto an ampicillin (100 µg/ml) nutrient agar plates. The following day, the insertion of VHH into the vector was confirmed by randomly picking 25 clones, screening by PCR for the insert, and Sanger sequencing, as described below.

Sequencing

To sequence the inserts, colony PCR was performed using PfuUltra II Fusion HS DNA Polymerase (Agilent Technologies) and primers (29) 5′-TTATGCTTCCGGCTCGTATG-3′ (MP57) and 5′-CCACAGACAGCCCTCATAG-3′ (GIII) under the following conditions: initial denaturation at 95°C for 3 min, followed by 39 cycles of (95°C for 20 s, 55°C for 30 s, and 72°C for 40 s), and a final extension at 72°C for 5 min. The amplicons were gel-purified and sequenced in both directions using the BigDye Terminator v3.1 Cycle Sequencing Kit and an ABI PRISM 3100 genetic analyzer (Applied Biosystems). The obtained sequences were assembled and aligned using CLC Genomics Workbench (CLC Bio 4.9).

Acknowledgments

We thank C. Vincke (Vrije Universiteit Brussel, Belgium) for providing the pMES4 plasmid and *E. coli* strain WK6 used to produce VHHs. We thank G. van Cappellen (Erasmus MC Optical Imaging Centre) for obtaining 96-well confocal pictures. We also thank the technical assistance of D. Solanes, X. Abad, I. Cordón, and all the animal caretakers from the CReSA BSL-3 animal facilities during the dromedary experiment. Evaluation of the protection of K18 mice was performed in CISA-INIA (Centro de Investigacion en Sanidad Animal – Instituto de Tecnologia Agraria y Alimentaria, Madrid, Spain).

References

1. Zaki AM, van Boheemen S, Bestebroer TM, Osterhaus AD, Fouchier RA. Isolation of a novel coronavirus from a man with pneumonia in Saudi Arabia. The New England journal of medicine. 2012 Nov 8;367(19):1814-20.
2. Cauchemez S, Nouvellet P, Cori A, Jombart T, Garske T, Clapham H, et al. Unraveling the drivers of MERS-CoV transmission. Proceedings of the National Academy of Sciences of the United States of America. 2016 Aug 9;113(32):9081-6.
3. Raj VS, Farag EA, Reusken CB, Lamers MM, Pas SD, Voermans J, et al. Isolation of MERS coronavirus from a dromedary camel, Qatar, 2014. Emerg Infect Dis. 2014 Aug;20(8):1339-42.
4. Cotten M, Watson SJ, Kellam P, Al-Rabeeah AA, Makhdoom HQ, Assiri A, et al. Transmission and evolution of the Middle East respiratory syndrome coronavirus in Saudi Arabia: a descriptive genomic study. Lancet (London, England). 2013 Dec 14;382(9909):1993-2002.
5. Tang XC, Agnihothram SS, Jiao Y, Stanhope J, Graham RL, Peterson EC, et al. Identification of human neutralizing antibodies against MERS-CoV and their role in virus adaptive evolution. Proceedings of the National Academy of Sciences of the United States of America. 2014 May 13;111(19):E2018-26.
6. Corti D, Zhao J, Pedotti M, Simonelli L, Agnihothram S, Fett C, et al. Prophylactic and post-exposure efficacy of a potent human monoclonal antibody against MERS coronavirus. Proceedings of the National Academy of Sciences of the United States of America. 2015 Aug 18;112(33):10473-8.
7. Pascal KE, Coleman CM, Mujica AO, Kamat V, Badithe A, Fairhurst J, et al. Pre- and postexposure efficacy of fully human antibodies against Spike protein in a novel humanized mouse model of MERS-CoV infection. Proceedings of the National Academy of Sciences of the United States of America. 2015 Jul 14;112(28):8738-43.
8. Raj VS, Mou H, Smits SL, Dekkers DH, Muller MA, Dijkman R, et al. Dipeptidyl peptidase 4 is a functional receptor for the emerging human coronavirus-EMC. Nature. 2013 Mar 14;495(7440):251-4.
9. Mou H, Raj VS, van Kuppeveld FJ, Rottier PJ, Haagmans BL, Bosch BJ. The receptor binding domain of the new Middle East respiratory syndrome coronavirus maps to a 231-residue region in the spike protein that efficiently elicits neutralizing antibodies. Journal of Virology. 2013 Aug;87(16):9379-83.
10. Al-Amri SS, Abbas AT, Siddiq LA, Alghamdi A, Sanki MA, Al-Muhanna MK, et al. Immunogenicity of Candidate MERS-CoV DNA Vaccines Based on the Spike Protein. Scientific Reports. 2017 Mar 23;7:44875.

11. Li Y, Wan Y, Liu P, Zhao J, Lu G, Qi J, et al. A humanized neutralizing antibody against MERS-CoV targeting the receptor-binding domain of the spike protein. Cell Res. 2015 Nov;25(11):1237-49.
12. Jiang L, Wang N, Zuo T, Shi X, Poon KM, Wu Y, et al. Potent neutralization of MERS-CoV by human neutralizing monoclonal antibodies to the viral spike glycoprotein. Sci Transl Med. 2014 Apr 30;6(234):234ra59.
13. Agrawal AS, Ying T, Tao X, Garron T, Algaissi A, Wang Y, et al. Passive Transfer of A Germline-like Neutralizing Human Monoclonal Antibody Protects Transgenic Mice Against Lethal Middle East Respiratory Syndrome Coronavirus Infection. Scientific Reports. 2016 Aug 19;6:31629.
14. Yu X, Zhang S, Jiang L, Cui Y, Li D, Wang D, et al. Structural basis for the neutralization of MERS-CoV by a human monoclonal antibody MERS-27. Scientific Reports. 2015 Aug 18;5:13133.
15. Chames P, Van Regenmortel M, Weiss E, Baty D. Therapeutic antibodies: successes, limitations and hopes for the future. Br J Pharmacol. 2009 May;157(2):220-33.
16. Spadiut O, Capone S, Krainer F, Glieder A, Herwig C. Microbials for the production of monoclonal antibodies and antibody fragments. Trends in biotechnology. 2014 Jan; 32(1):54-60.
17. Irani V, Guy AJ, Andrew D, Beeson JG, Ramsland PA, Richards JS. Molecular properties of human IgG subclasses and their implications for designing therapeutic monoclonal antibodies against infectious diseases. Mol Immunol. 2015 Oct;67(2 Pt A):171-82.
18. Hamers-Casterman C, Atarhouch T, Muyldermans S, Robinson G, Hamers C, Songa EB, et al. Naturally occurring antibodies devoid of light chains. Nature. 1993 Jun 3;363(6428):446-8.
19. Muyldermans S. Nanobodies: natural single-domain antibodies. Annual review of biochemistry. 2013;82:775-97.
20. De Genst E, Silence K, Decanniere K, Conrath K, Loris R, Kinne J, et al. Molecular basis for the preferential cleft recognition by dromedary heavy-chain antibodies. Proceedings of the National Academy of Sciences of the United States of America. 2006 Mar 21;103(12):4586-91.
21. Rothbauer U, Zolghadr K, Tillib S, Nowak D, Schermelleh L, Gahl A, et al. Targeting and tracing antigens in live cells with fluorescent nanobodies. Nat Methods. 2006 Nov;3(11):887-9.
22. Hassanzadeh-Ghassabeh G, Devoogdt N, De Pauw P, Vincke C, Muyldermans S. Nanobodies and their potential applications. Nanomedicine (Lond). 2013 Jun;8(6):1013-26.
23. Peyvandi F, Scully M, Kremer Hovinga JA, Cataland S, Knobl P, Wu H, et al. Caplacizumab for Acquired Thrombotic Thrombocytopenic Purpura. The New England journal of medicine. 2016 Feb 11;374(6):511-22.
24. Vanlandschoot P, Stortelers C, Beirnaert E, Ibanez LI, Schepens B, Depla E, et al. Nanobodies(R): new ammunition to battle viruses. Antiviral Res. 2011 Dec;92(3):389-407.
25. Farag EA, Reusken CB, Haagmans BL, Mohran KA, Stalin Raj V, Pas SD, et al. High proportion of MERS-CoV shedding dromedaries at slaughterhouse with a potential epidemiological link to human cases, Qatar 2014. Infection ecology & epidemiology. 2015;5:28305.
26. Reusken CB, Haagmans BL, Muller MA, Gutierrez C, Godeke GJ, Meyer B, et al. Middle East respiratory syndrome coronavirus neutralising serum antibodies in dromedary camels: a comparative serological study. The Lancet Infectious diseases. 2013 Oct;13(10):859-66.
27. Muller MA, Corman VM, Jores J, Meyer B, Younan M, Liljander A, et al. MERS coronavirus neutralizing antibodies in camels, Eastern Africa, 1983-1997. Emerg Infect Dis. 2014 Dec;20(12):2093-5.
28. Haagmans BL, van den Brand JM, Raj VS, Volz A, Wohlsein P, Smits SL, et al. An orthopoxvirus-based vaccine reduces virus excretion after MERS-CoV infection in dromedary camels. Science. 2016 Jan 1;351(6268):77-81.

29. Pardon E, Laeremans T, Triest S, Rasmussen SG, Wohlkonig A, Ruf A, et al. A general protocol for the generation of Nanobodies for structural biology. Nat Protoc. 2014 Mar;9(3):674-93.
30. Hassanzadeh-Ghassabeh G, Saerens D, Muyldermans S. Generation of Anti-infectome/Anti-proteome Nanobodies. In: Toms SA, Weil RJ, editors. Nanoproteomics. Totowa, NJ: Humana Press; 2011. p. 239-59.
31. Chakravarty R, Goel S, Cai W. Nanobody: the "magic bullet" for molecular imaging? Theranostics. 2014 2014;4(4):386-98.
32. Wang N, Shi X, Jiang L, Zhang S, Wang D, Tong P, et al. Structure of MERS-CoV spike receptor-binding domain complexed with human receptor DPP4. Cell Res. 2013 Aug;23(8):986-93.
33. Lu G, Hu Y, Wang Q, Qi J, Gao F, Li Y, et al. Molecular basis of binding between novel human coronavirus MERS-CoV and its receptor CD26. Nature. 2013 Aug 8;500(7461):227-31.
34. Li K, Wohlford-Lenane C, Perlman S, Zhao J, Jewell AK, Reznikov LR, et al. Middle East Respiratory Syndrome Coronavirus Causes Multiple Organ Damage and Lethal Disease in Mice Transgenic for Human Dipeptidyl Peptidase 4. The Journal of Infectious Diseases. 2016 Mar 1;213(5):712-22.
35. Schmidt FI, Hanke L, Morin B, Brewer R, Brusic V, Whelan SP, et al. Phenotypic lentivirus screens to identify functional single domain antibodies. Nature microbiology. 2016 Jun 20;1(8):16080.
36. Haagmans BL, Al Dhahiry SH, Reusken CB, Raj VS, Galiano M, Myers R, et al. Middle East respiratory syndrome coronavirus in dromedary camels: an outbreak investigation. The Lancet Infectious diseases. 2014 Feb;14(2):140-5.
37. Radbruch A, Muehlinghaus G, Luger EO, Inamine A, Smith KG, Dorner T, et al. Competence and competition: the challenge of becoming a long-lived plasma cell. Nat Rev Immunol. 2006 Oct;6(10):741-50.
38. Ellyard JI, Avery DT, Phan TG, Hare NJ, Hodgkin PD, Tangye SG. Antigen-selected, immunoglobulin-secreting cells persist in human spleen and bone marrow. Blood. 2004 May 15;103(10):3805-12.
39. Paramithiotis E, Cooper MD. Memory B lymphocytes migrate to bone marrow in humans. Proceedings of the National Academy of Sciences of the United States of America. 1997 Jan 7;94(1):208-12.
40. Manz RA, Hauser AE, Hiepe F, Radbruch A. Maintenance of serum antibody levels. Annual review of immunology. 2005;23:367-86.
41. Nguyen VK, Hamers R, Wyns L, Muyldermans S. Camel heavy-chain antibodies: diverse germline V(H)H and specific mechanisms enlarge the antigen-binding repertoire. EMBO J. 2000 Mar 1;19(5):921-30.
42. Ying T, Du L, Ju TW, Prabakaran P, Lau CC, Lu L, et al. Exceptionally potent neutralization of Middle East respiratory syndrome coronavirus by human monoclonal antibodies. Journal of Virology. 2014 Jul;88(14):7796-805.
43. Sok D, Le KM, Vadnais M, Saye-Francisco KL, Jardine JG, Torres JL, et al. Rapid elicitation of broadly neutralizing antibodies to HIV by immunization in cows. Nature. 2017 Aug 3;548(7665):108-11.
44. Simoes EA, DeVincenzo JP, Boeckh M, Bont L, Crowe JE, Jr., Griffiths P, et al. Challenges and opportunities in developing respiratory syncytial virus therapeutics. The Journal of Infectious Diseases. 2015 Mar 15;211 Suppl 1(suppl 1):S1-S20.
45. Song F, Fux R, Provacia LB, Volz A, Eickmann M, Becker S, et al. Middle East respiratory syndrome coronavirus spike protein delivered by modified vaccinia virus Ankara efficiently induces virus-neutralizing antibodies. Journal of Virology. 2013 Nov;87(21):11950-4.
46. Raj VS, Lamers MM, Smits SL, Demmers JAA, Mou H, Bosch B-J, et al. Identification of Protein Receptors for Coronaviruses by Mass Spectrometry. In: Maier HJ, Bickerton E, Britton P, editors. Coronaviruses. New York, NY: Springer New York; 2015. p. 165-82.

47. Nakabayashi H, Taketa K, Miyano K, Yamane T, Sato J. Growth of human hepatoma cells lines with differentiated functions in chemically defined medium. Cancer Res. 1982 Sep;42(9):3858-63.
48. van Boheemen S, de Graaf M, Lauber C, Bestebroer TM, Raj VS, Zaki AM, et al. Genomic characterization of a newly discovered coronavirus associated with acute respiratory distress syndrome in humans. mBio. 2012 Nov 20;3(6).
49. Smits SL, de Lang A, van den Brand JM, Leijten LM, van IWF, Eijkemans MJ, et al. Exacerbated innate host response to SARS-CoV in aged non-human primates. PLoS pathogens. 2010 Feb 5;6(2):e1000756.
50. van Kuppeveld FJ, van der Logt JT, Angulo AF, van Zoest MJ, Quint WG, Niesters HG, et al. Genus- and species-specific identification of mycoplasmas by 16S rRNA amplification. Appl Environ Microbiol. 1992 Aug;58(8):2606-15.
51. Haagmans BL, van den Brand JM, Provacia LB, Raj VS, Stittelaar KJ, Getu S, et al. Asymptomatic Middle East respiratory syndrome coronavirus infection in rabbits. Journal of Virology. 2015 Jun;89(11):6131-5.
52. Abdiche YN, Malashock DS, Pinkerton A, Pons J. Exploring blocking assays using Octet, ProteOn, and Biacore biosensors. Anal Biochem. 2009 Mar 15;386(2):172-80.

SUPPLEMENTARY MATERIALS

Supplementary Materials and Methods

Small scale expression and crude extraction of VHHs

The crude VHH extraction was performed as previously described with slight modifications described below (30). All obtained bacterial clones were picked from the agar plate independently using a sterile tooth pick and grown in 96 deep-well format plates (as shown in Figure 1) at 37°C overnight in a shaking incubator (200 rpm). The following day, 50 µL of the culture was transferred to a 96-deepwell format plate containing 1 mL of 2× TY medium (for 100 mL: 1.6 g tryptone or peptone, 1 g yeast extract, 0.5 g NaCl), supplemented with 100 µg/mL ampicillin, and 0.1% (wt/vol) glucose per well. Plates were incubated at 37 °C using a shaking incubator (200 rpm.) until the wells reached an optical density (OD) of 0.6-0.8. Next, VHH expression was induced by adding 100 µL of 10 mM IPTG in 2× TY medium per well, and plates were incubated in a shaking incubator (200 rpm) for 4 h at 37°C. Subsequently, cells were pelleted at 3,500 rpm. for 10 min and the supernatant was discarded. Plates were frozen at -20°C for 1 h or overnight. Next, plates were removed from the freezer to thaw at room temperature for 15 min. To release the VHHs from the periplasm, 100 µL of PBS was added to each well and the plates were incubated for 30 min at room temperature on a vibrating platform (700 rpm). Next, crude VHH extracts were recovered by centrifuging for 10 min at 3,500 rpm at 4°C. These crude extracts were used for the primary characterization of the VHHs (antigen specific ELISAs, virus neutralization assays, in vitro blocking assays).

Purification of VHHs

Two mL of starter culture was transferred in 1 liter of 2x TY medium supplemented with 100 µg/mL ampicillin, and 0.1% (wt/vol) glucose. The flasks were then incubated at 37°C using a shaking incubator (200 rpm) until the cells growth reached an optical density (OD) of 0.6-0.8. Next, VHH expression was induced by adding 10 ml of 100 mM IPTG, and cells were induced overnight at 28°C, and then pelleted by centrifugation for 10 min at 5,000 rpm. The periplasmic VHH was then released by osmotic shock (29). This VHH was bound to His-select nickel affinity resin (Sigma), washed with His wash buffer (20 mM sodium phosphate, pH 8.0, 1 M NaCl, 20 mM imidazole), and eluted with His elution buffer (20 mM sodium phosphate, pH 8.0, 0.5 M NaCl, 0.3 M imidazole). The elute was then dialyzed against PBS. The concentrations of the purified VHHs were determined spectrophotometrically using NanoDrop (ThermoFisher Scientific) and confirmed using BCA protein assay kit (ThermoFisher Scientific).

Cells and viral stocks

Human hepatocellular carcinoma cells (Huh-7) (47) were grown in RPMI 1640 supplemented with 10% fetal bovine serum (FBS), 100 U penicillin, 100 mg/mL streptomycin and African green monkey kidney cells (Vero 118, ATCC CCL-81) were cultured in Dulbecco's modified Eagle medium (DMEM, BioWhittaker) supplemented with 10% FBS, 100 U penicillin, 100 mg/mL streptomycin, 20 mM HEPES buffer (Bio Whittaker), 0.2% (wt/vol) sodium bicarbonate and 2 mM glutamine (Bio Whittaker). Stocks of MERS-CoV and SARS-CoV were produced by preparing a seventh passage of the MERS-CoV EMC isolate and SARS-CoV HKU-39849 strain, respectively, on Vero cells. Cells were inoculated with MERS-CoV or SARS-CoV in DMEM supplemented with 1% serum, 100 U/mL penicillin, 100 mg/mL streptomycin, and 2 mM glutamine. After inoculation, the cultures were incubated at 37°C in a CO_2 incubator; after 3 days the supernatant was collected and stored at -80°C. All techniques using replication competent MERS-CoV and SARS-CoV were performed under BSL-3 containment. MERS-CoV and SARS-CoV titrations were performed on African green monkey kidney cells (Vero E6, ATCC CRL1586) cells as described previously (48, 49). All cell lines used in this study were tested (50) and were mycoplasma free.

Immunofluorescent staining and confocal microscopy

Human hepatocellular carcinoma cells (Huh-7 cells) or Vero cells were seeded in 96-well plate and confluent cells were infected with either MERS-CoV or SARS-CoV at 0.1 multiplicity of infection (moi) or mock infected and incubated for 1 h at 37°C. The viral suspension was then removed and replaced with maintenance medium containing 1% FBS, and cells were incubated at 37°C for 24 h. Subsequently, cells were washed once with PBS, fixed with 4% formalin, permeabilized with 70% ethanol and stored at 4°C in 70% ethanol until they were used for immunofluorescent staining. MERS-CoV or SARS-CoV infection was confirmed by detection of MERS-CoV or SARS-CoV antigens using the Rabbit anti-MERS-CoV polyclonal serum (1:400) (51), and anti-SARS-CoV nucleocapsid antibody (1:400, Imgenex). Briefly, cells were washed three times with PBS, blocked with 10% normal goat serum (MP Biomedicals) for 30 min at 37°C, and subsequently incubated with either rabbit-anti MERS-CoV, mouse anti-SARS-CoVnucleocapsid or VHHs, for 1 h at 37°C, followed by staining with goat anti-rabbit (1:250, Life technologies) or goat anti-mouse IgG conjugated with either Alexa Fluor 488 or Alexa Fluor 594 (1:250, Life Technologies) for 1 h at 37°C. Staining with VHHs was revealed using mouse anti-his antibody (1:400, Thermo scientific) followed by goat-anti mouse IgG conjugated with Alexa Fluor 488. After washing with PBS, cells were counterstained with 4, 6-diamidino-2phenylindole (DAPI, Vector laboratories) and pictures were taken using a confocal microscope (ZEISS LSM700).

Blocking of the MERS-CoV spike-receptor interaction by VHHs

VHHs (5 µg/mL) were pre-incubated with 5 µg/mL of MERS-CoV S1-Fc protein at 4°C for 30 min. Subsequently, 100 µl of this mixture was transferred onto Huh-7 cells (105 /well) and incubated at 4°C for 30 min, after which cells were stained for S1 with FITC or DyLight-488-labelled goat-anti-human IgG (1:50, Dako or 1:500, Life technologies, respectively) and analyzed by flow cytometry (FACS). The FACS data were analyzed using Flowjo v10.

Virus neutralization assay

Plaque reduction neutralization test (PRNT), is the most common assay used to measure neutralizing antibodies. VHH dilutions were prepared in two-fold serial dilutions in 96 well plates with a starting concentration of 1000 ng/mL. MERS-CoV was diluted in RPMI 1640 supplemented with penicillin, streptomycin, and 1% fetal bovine serum, to a dilution of 2000 $TCID_{50}$ per mL. We then added 50 µL of virus suspension to the plates and the plates were incubated at 37°C for 1 hour. Next, we incubated virus-serum mixtures on 96 well plates containing Huh-7 cells for 1 hour, and then washed them with PBS and incubated them with RPMI 1640 and 1% fetal bovine serum for 8 hours. Subsequently, cells were washed with PBS and fixed with 4% formaldehyde, permeabilized with 70% ethanol and stored at 4°C until they were subjected to immunofluorescent staining as described above. The PRNT titer was calculated based on a 50% or greater reduction in infected cells counts ($PRNT_{50}$).

Antigen biotinylation

MERS-CoV S1 protein and VHHs were biotinylated with EZ-Link Sulfo–NHS–Biotin sulfosuccinimidobiotin (Thermo Fischer Scientific) dissolved in dimethyl sulfoxide (1.0 g/L) according to the manufacturer instruction. The antigen was incubated with NHS–LC–Biotin (10:1 molar) in PBS on ice for 2 h. After incubation biotinylated proteins were recovered and concentrated using Amicon Ultra-4 (Merk Millipore) centrifugal filter units.

Affinity measurement

Affinity measurements were done on the Octet system (ForteBio QK) instrument. VHHs were biotinylated as indicated above. Samples were desalted to remove excess of unincorporated biotin using Amicon Ultra-0.5 centrifuge filters (Millipore). Streptavidin biosensors (forteBIO, A division of Pall Life Sciences) were used for loading. The concentration of ligand necessary for optimal binding for each VHH was estimated with a titration experiment. Binding assays were performed at 30°C with agitation at 900 rpm in PBS buffer (200 µl per well) in black 96 well plates (Costar). After equilibration of sensors for 5 min in PBS, the ligand was loaded (5 min), followed by baseline (2 min), association step with analyte (5 min) and dissociation

step (10 min). MERS-CoV S1-Fc dimeric protein was used as an analyte in concentration ranging from 100 nM down to 3 nM in 2X dilution steps. Data analyses and curve fitting was done using the Octet software 7.1.

Immunoprecipitation

Biotinylated VHHs and non-biotinylated MERS-CoV S1-Fc (1:1 ratio) were prepared in TNE (20 mM Tris HCl pH 7.5, 300 mM NaCl, and 1 mM EDTA) binding buffer. Mixtures were incubated at 4°C under rotation for 1 h. After incubation S1-Fc protein was pulled down from the mixtures using Goat anti-human IgG Fc magnetic beads (MEDNA BIO), following three PBS washes. Proteins were eluted from the beads using 1X protein loading buffer and run on Any kD Mini-PROTEAN TGX Precast Protein Gels (BioRad) under non-reducing conditions. The S1-Fc protein was detected by western blotting using IRDye 800CW goat anti-human IgG (LI-COR Biosciences) and VHHs were detected using IRDye 680RD Streptavidin (LI-COR Biosciences).

Phylogenetic analysis of VHH sequences

Sequence alignment was performed using the ClustalW algorithm incorporated in MEGA5.0 (www.megasoftware.net), and phylogenetic trees were constructed using the neighbor-joining method with the p-distance model (gap/missing data treatment; complete deletion) and 1,000 bootstrap replicates in MEGA5.0.

Epitope mapping

Single amino acid substitutions in the receptor binding subdomain (residues 483 to 566) of the spike proteins found in natural isolates (L506F [Genbank accession no (GB): K9N5Q8.1], L507P [GB: ALJ54518.1], D509G [GB: AGV08379.1], D510G [GB: ALK80291.1], I529T [GB: ALK80251.1], V534A [GB: AGV08584.1], E536K [GB: ALX27228.1], D537E [GB: ALJ76277.1], D539N [GB: ALJ54517.1]), D556V [GB: ALJ54486.1], T560I [GB: ALJ76278.1]) were generated in plasmids encoding S1-Fc variants by Q5 site-directed mutagenesis (NEB Biolabs) and expressed as described previously (43). To check the reactivity of nanobodies with different S1 mutants, Nunc Maxisorp 96-well plates were coated with 100 ng/well of (mutant) MERS-CoV S1-Fc in PBS and incubated overnight at 4°C. Plates were washed thrice with washing buffer (PBS containing 0.05% Tween-20) and subsequently blocked with 3% Bovine Serum Albumin (BSA) in PBS containing 0.1% Tween-20 for 2 hours at room temperature. Plates were washed thrice with washing buffer and incubated with serial dilution of nanobodies at room temperature for 1 hour. The plates were washed and incubated with mouse anti-His antibody (1:2,000, Thermo Scientific) at room temperature for 1 hour. After washing,

the plates were incubated with rabbit anti-mouse conjugated to HRP (1:2,000, DAKO) and incubated at room temperature for 1 hour. After washing, the plates were detected with 3,3',5,5'Tetramethylbenzidine (TMB) substrate (BioConnect). Reactions were stopped with 2N H2SO4 (Sigma). The absorbance of each sample was read at 450 nm with an ELISA reader (ELx808 BioTek).

Competitive binding assay

Competitive binding assay was performed through biolayer-interferometry using the Octet QK System (ForteBio) that measures changes in the interferometry wave pattern of light produced by the binding of molecules to a biosensor layer according to a previously described method (52) . Briefly, streptavidin sensors (ForteBio, USA) were coated with biotinylated MERS-CoV S1-Fc protein until saturation. S1-Fc loaded sensor was exposed to a first VHH, followed by a brief wash and subsequently exposed to a second VHH while recording the interferometry signal.

In vivo infections and antibody inoculations

Transgenic K18 mice were kindly provided by Paul B. McCray (University of Iowa, U.S.). Animal experimental protocols were approved by the Environmental Council of Madrid (permit number: PROEX 112/14) and the Ethical Committee of the Center for Animal Health Research (CISA-INIA) (permit numbers: CBS 2014/005 and CEEA 2014/004) in strict accordance with Spanish National Royal Decree (RD 53/2013) and international EU guidelines 2010/63/UE about protection of animals used for experimentation and other scientific purposes and Spanish national law 32/2007 about animal welfare. All work with infected animals was performed in a BSL3 laboratory of the Center for Animal Health Research (CISA-INIA, Madrid, Spain). Sixteen to twenty four week-old female K-18 mice (34) were intranasally inoculated with 105 PFU of MERS-CoV wild type (recombinant MERS-CoV reproducing the EMC strain engineered in CNB-CSIC laboratory) . For the VHH or HCAb inhibition experiment, 6 hours prior to infection mice were intraperitoneally inoculated with 200 µL containing 20 or 200 µg of the VHH-83 or HCAb-83 or 200 µg of an isotype matched non-specific antibody (VHH-p2E6 or HCAb-p2E6). For intranasal inoculations, mice were anesthetized with isoflurane and then 50 µl of solution containing the virus were laid on the nostrils of the mouse using a pipette tip. The small droplet was naturally inhaled by the mouse about 2-3 seconds later. Since this procedure is non-invasive it did not cause any injury and consequent inflammation in the mice.

Lung and blood samples from MERS-CoV infected mice

To analyze MERS-CoV titers, one-quarter of the right lung was homogenized in 2 mL of Phosphate Buffered Saline (PBS) containing 100 UI/mL penicillin, 100 µg/mL streptomycin, 50 µg/mL gentamicin and 0.5 µg/mL fungizone using a MACS homogenizer (Miltenyi Biotec) according to manufacturer's protocols. Virus titrations were performed on Huh-7 cells following standard procedures and using closed flasks or plates sealed in plastic bags. Briefly, cells were overlaid with DMEM containing 0.6% low-melting agarose and 2% FBS, and at 72 hours post infection, cells were fixed with 10% formaldehyde and stained with 0.1% crystal violet. All work with MERS-CoV infectious viruses was performed in biosafety level 3 facilities at CNB-CSIC. To examine lung histopathology, the left lung of infected mice was fixed in 10% zinc formalin for 24 hours at 4°C and paraffin embedded. Serial longitudinal 5 µm-sections were stained with hematoxylin and eosin (H&E) by the Histology Service in the National Center of Biotechnology (CNB, Spain) and subjected to histopathological examination with a ZEISS Axiophot fluorescence microscope. Samples were obtained using a systematic uniform random procedure, consisting in serial parallel slices made at a constant thickness interval of 50 µm. Histopathology analysis was conducted in a blind manner by acquiring images of 50 random microscopy fields from around 40 non-adjacent sections for each of the three independent mice analyzed per treatment group. Blood samples were collected at the indicated days from the submandibular vein. In order to facilitate the coagulation and the separation of the serum, blood samples were incubated at 37°C for 1 hour in a water bath and then placed O/N at 4°C. The serum was clarified by centrifugation and maintained frozen at -80°C until titer evaluation was performed.

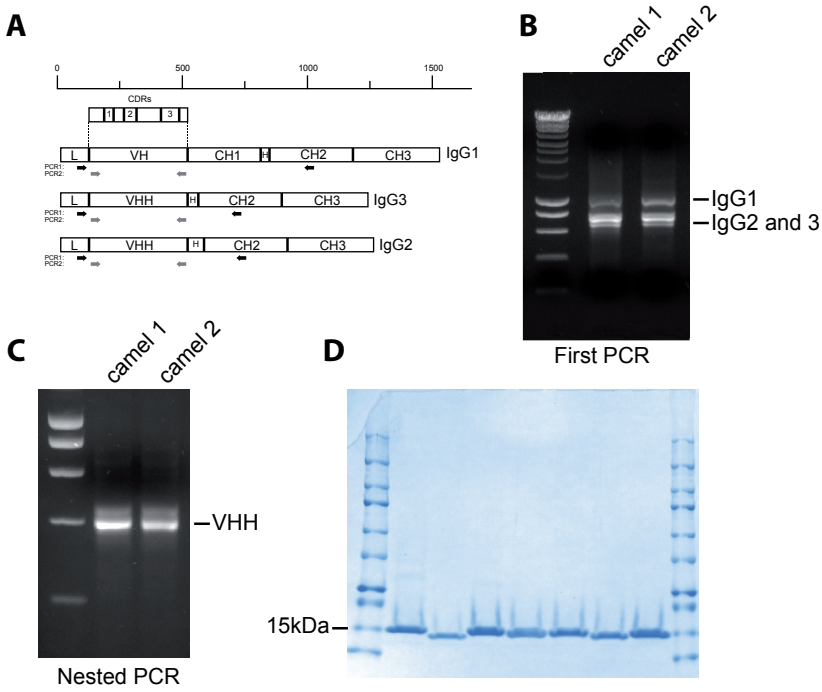

Figure S1. Direct cloning and expression of VHHs. **(A)** Organization of dromedary camel IgG genes and nested PCR primer design targeting the VH and VHH regions. **(B)** The first PCR, 1st lane is smart DNA ladder; 2nd, is first PCR product (~ 1000 bp IgG1, ~ 800bp IgG2 and IgG3) and **(C)** second PCR using the inner primers amplifying the VHH region, 1st lane is smart DNA ladder; 2nd, 3rd, lanes are VHH (~ 400 bp). **(D)** VHH expression was confirmed by SDS-PAGE analysis from 7 randomly selected clones. VHHs were expressed in E. coli strain WK6 and purified from crude periplasmic extract using Ni-NTA agarose column. The expression was confirmed by coomassie blue stained SDS-PAGE gel. Outer lanes are protein markers; inner lanes are purified VHHs.

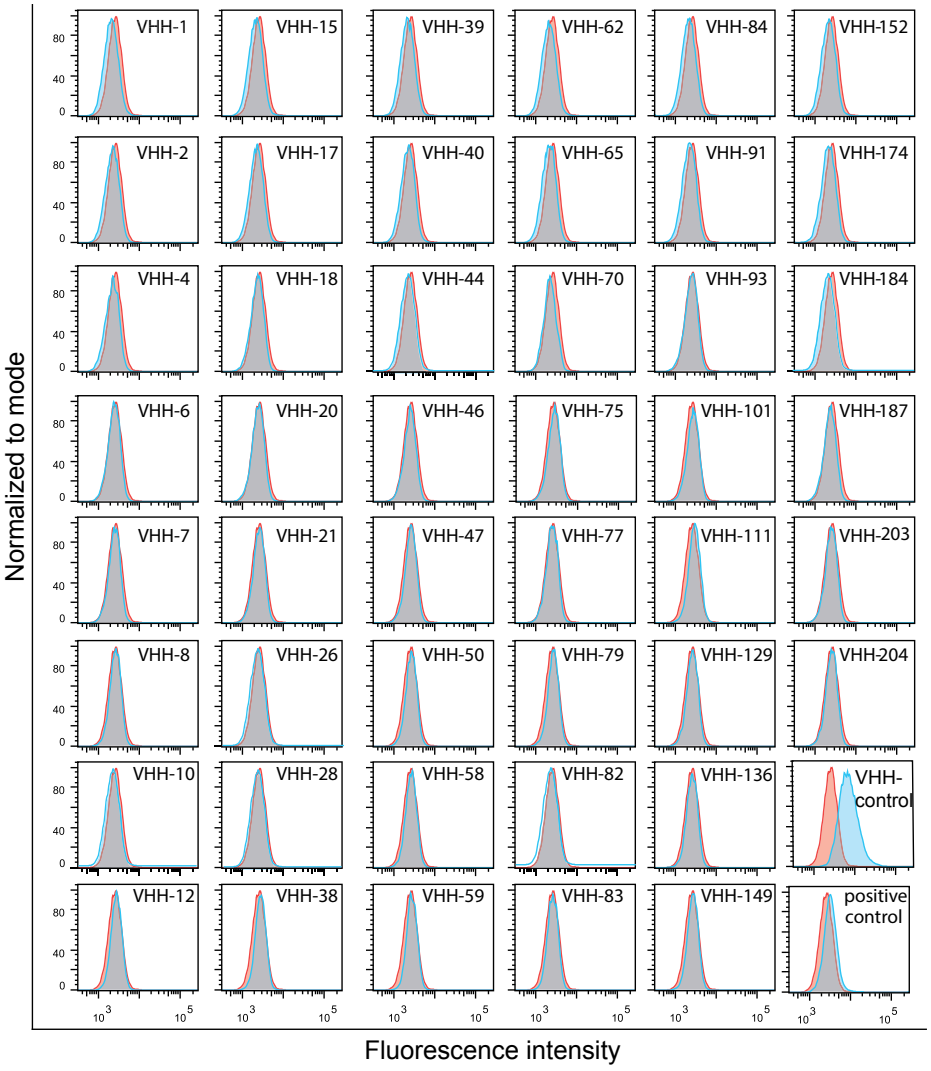

Figure S2. VHHs block the interaction between the S1 protein and the MERS-CoV entry receptor DPP4. Forty-six VHHs were incubated with human Fc-tagged MERS-CoV S1, after which the S1 protein was incubated on DPP4-expressing Huh-7 cells. S1-Fc binding was detected by FACS analysis after staining with FITC-labeled goat-anti human IgG. Control VHHp2E6 and rabbit serum (MERS-CoV) were used as a negative and positive controls, respectively. Shown in the panels are the FACS analyses of MERS-CoV S1 binding (blue shading), and mock incubated (red shading) Huh-7 cells. VHH-, Variable heavy chain.

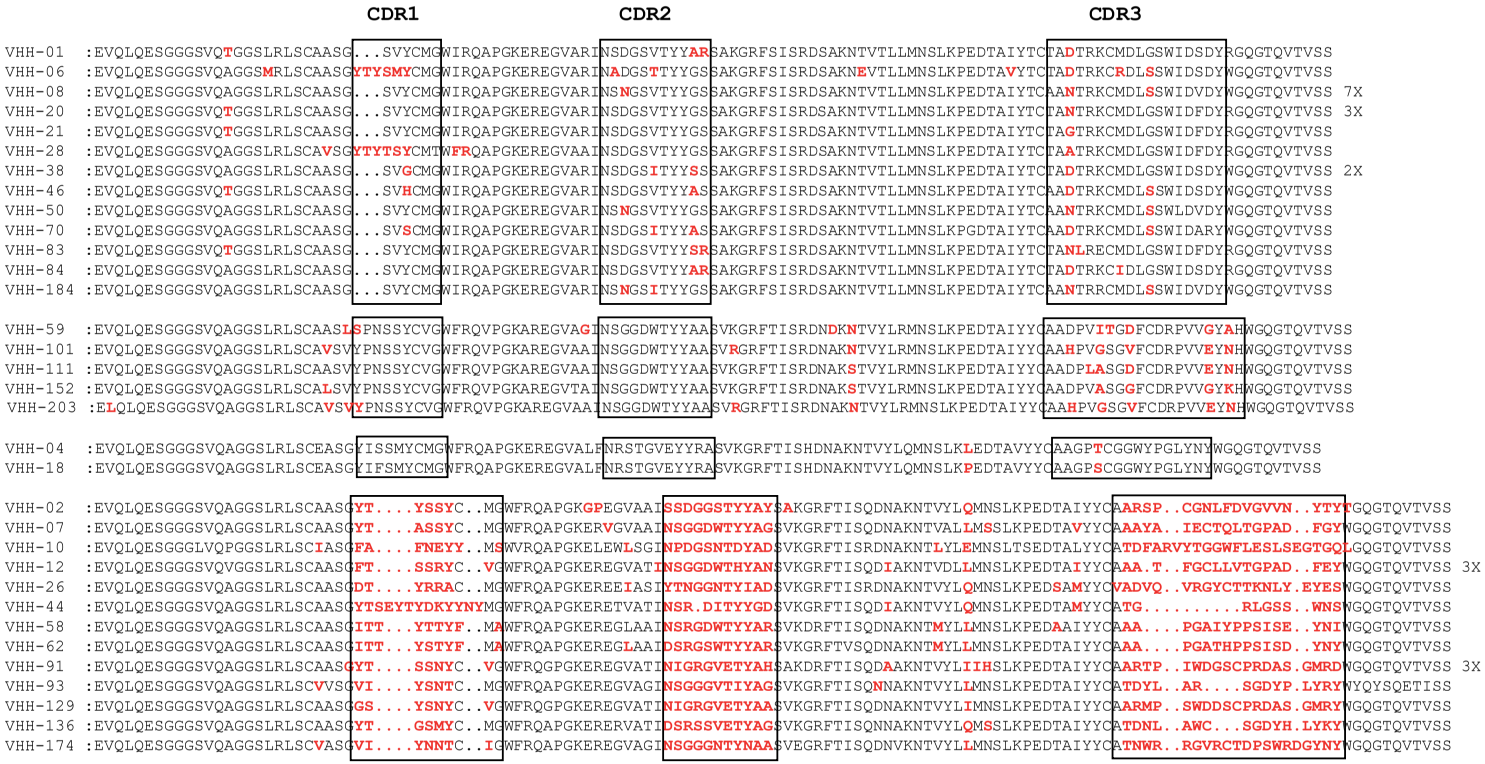

Figure S3. Amino acid sequences of VHH regions of anti–MERS-CoV spike VHHs. Alignment of the sequences of 46 selected VHHs. The alignment was performed using the ClustalW algorithm. The sequences were grouped based on the identity and length. The CDR1, 2 and 3 regions are indicated in boxes, the amino acid residues that are different from the consensus are indicated in red. VHH, Variable heavy chain

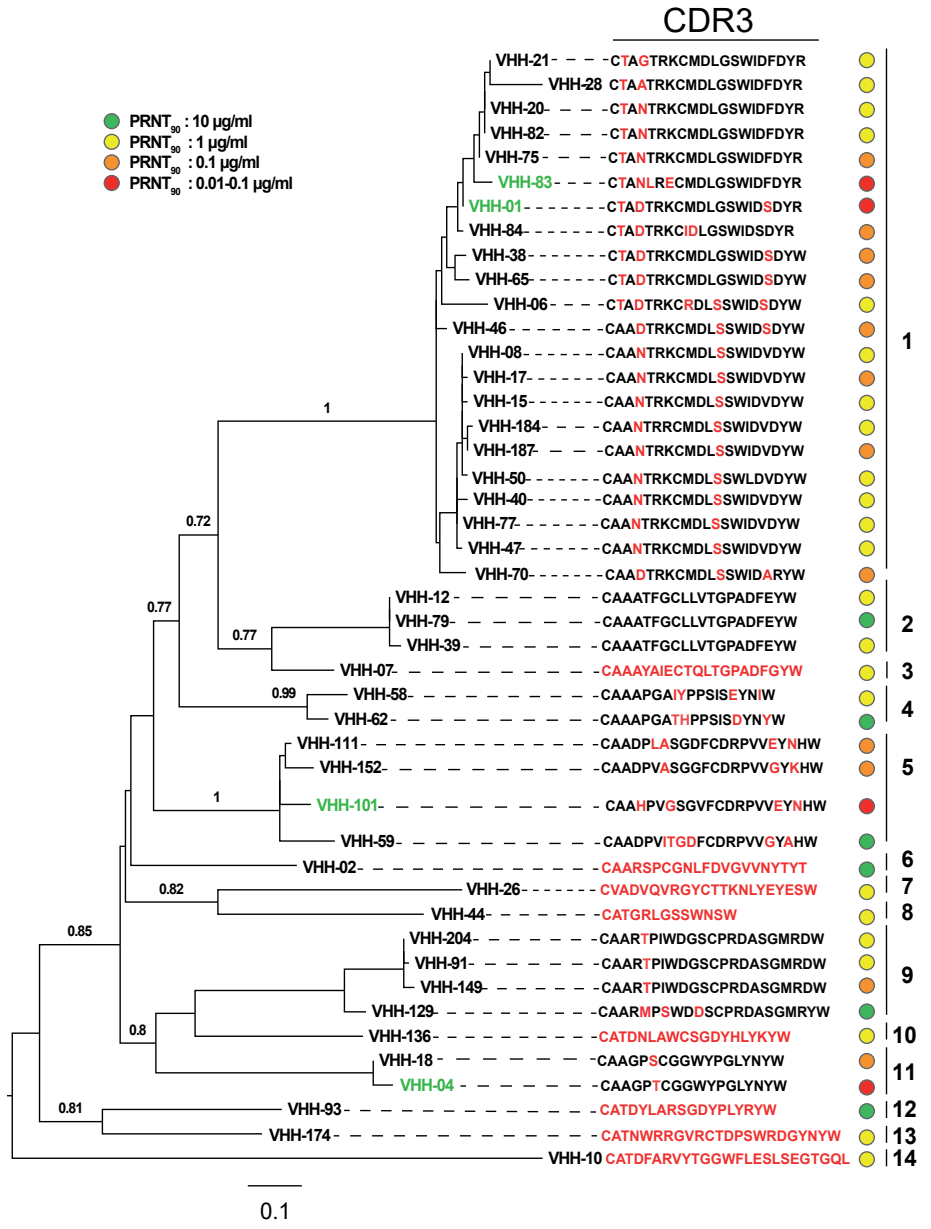

Figure S4. Phylogenetic tree of the amino acid sequences of the 46 MERS-CoV–neutralizing VHHs showing the corresponding neutralizing capacity of each VHH. Sequence alignment was performed using the ClustalW algorithm incorporated in MEGA5.0 (www.megasoftware.net), and phylogenetic trees were constructed using the neighbor-joining method with the p-distance model (gap/missing data treatment; complete deletion) and 1,000 bootstrap replicates in MEGA5.0. Scale bars indicate nucleotide substitutions per site; boostrap values (>0.7) are indicated at nodes. CDR3 sequences are placed on branch tips and variable amino acids that differed from the consensus within a given cluster are indicated in red. The four most potent MERS-CoV neutralizing VHHs are labeled in green. The neutralizing capacities ($PRNT_{90}$) in µg/ml is indicated by the colored circles to the right of each VHH.

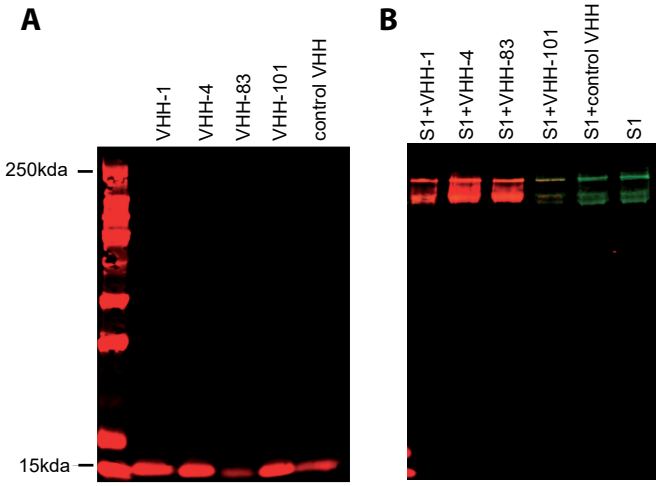

Figure S5. Interaction of selected VHHs with recombinant MERS-CoV spike protein. **(A)** Histagged VHHs (VHH-1, -4, -83, -101 and control p2E6) were purified from the bacteria using NiNTA agarose after which they were biotinylated. Western blot analysis was performed with IRDye 680RD Streptavidin. **(B)** Co-immunoprecipitation of VHHs with human Fc-tagged MERS-CoV S1. VHH-p2E6 was used as a negative control. Western blot analysis was performed with IRDye 680RD Streptavidin for biotinylated VHHs and with IRDye 800CW Goat anti-Human IgG for Fc-tagged MERS-CoV S1.

A

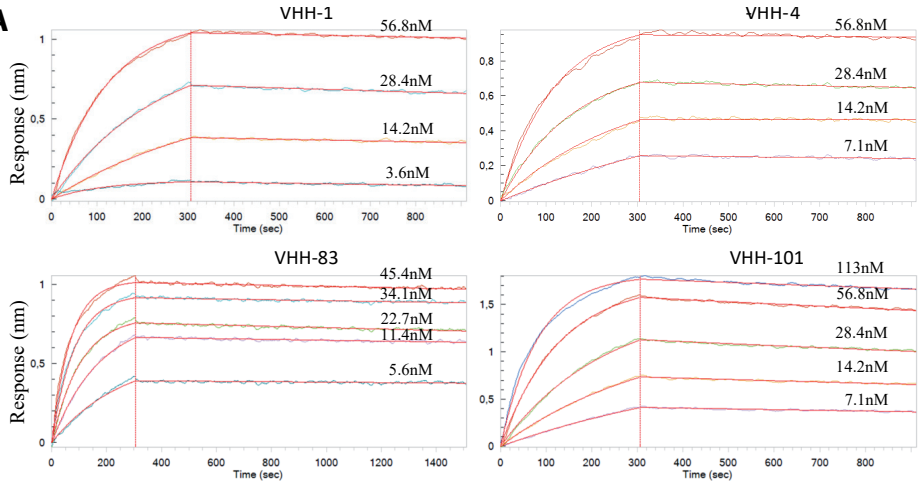

B

VHH	kon(1/Ms)	kdis(1/s)	KD (M)
VHH-1	$7.23x10^{5} \pm 5.66x10^{5}$	$1.66x10^{-4} \pm 8.62x10^{-5}$	$4.23x10^{-10} \pm 1.35x10^{-10}$
VHH-4	$1.91x10^{5} \pm 2.08x10^{4}$	$6.91x10^{-5} \pm 2.53x10^{-5}$	$2.93x10^{-10} \pm 1.13x10^{-10}$
VHH-83	$4.00x10^{5} \pm 4.09x10^{4}$	$4.07x10^{-5} \pm 6.31x10^{-6}$	$1.03x10^{-10} \pm 1.41x10^{-11}$
VHH-101	$1.66x10^{5} \pm 2.08x10^{4}$	$1.65x10^{-4} \pm 1.79x10^{-5}$	$9.99x10^{-10} \pm 1.41x10^{-11}$

Figure S6. Kinetics of VHH-1, VHH-4, VHH-83, and VHH-101 binding to MERS-CoV spike protein. **(A)** Sensograms showing the MERS-CoV spike protein association and disassociation with VHH-1, 4, 83, and 101. The MERS-CoV spike protein immobilized on the streptavidin biosensors surface, followed by injection of VHHs at the concentration indicated in the figure. The line fitted to the experimental data and used to calculate the binding affinities is drawn in orange. **(B)** The KD values of each VHH are indicated in the table. VHH, Variable heavy chain.

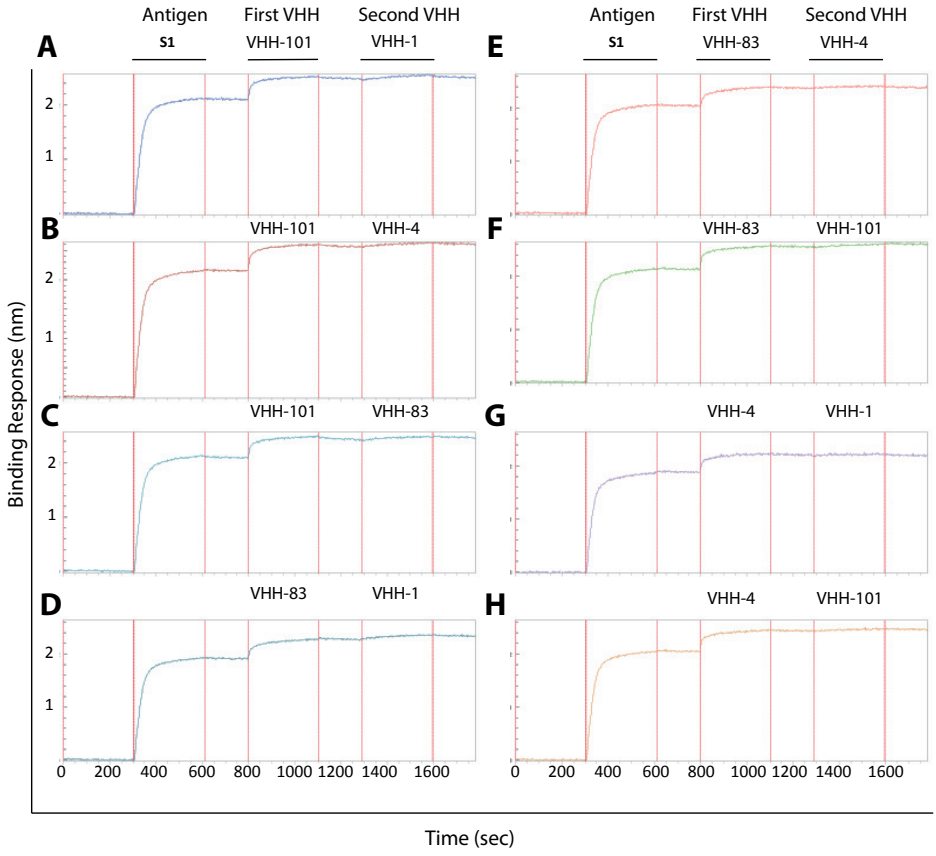

Figure S7. Cross-competitive behavior of four different VHH-1, VHH-4, VHH-83, and VHH101 determined using an Octet biosensor (ForteBio QK). Biotinylated MERS-CoV S1 protein was first captured on Streptavidin biosensors (step1), followed by a washing step (step 2), after which the first VHH was allowed to bind to the captured spike protein (step 3). After a washing step (step 4), a second VHH was allowed to bind to the spike protein using different combinations as indicated (A-H). The association and disassociation kinetics of first and second VHH binding to MERS-CoV spike at 30°C were measured using Octet. Data analyses and curve fitting was done using the Octet software 7.1.

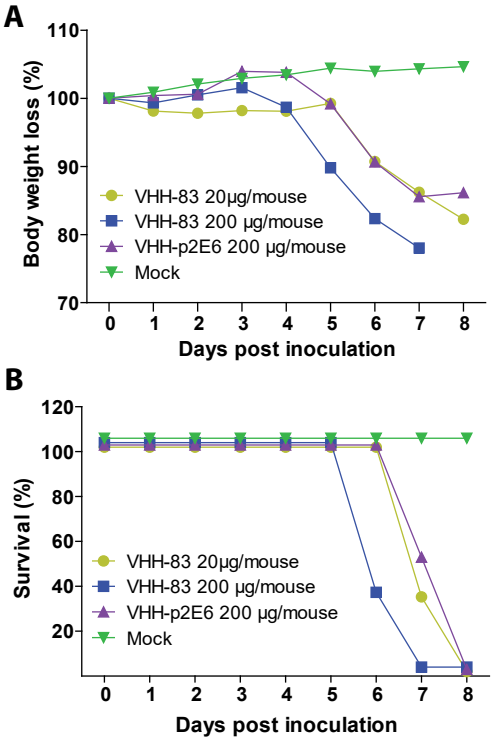

Figure S8. Protective efficacy of MERS-CoV–specific VHHs in transgenic mice. Mice were intraperitoneally injected with either 20 µg or 200 µg of VHH-83 or a VHH-p2E6 control 6 hours prior to challenge with MERS-CoV. **(A)** Weight loss and **(B)** Survival rate. Table S1. Characteristics of MERS-CoV–specific VHHs.

Table S1. Characteristics of MERS-CoV–specific VHHs

VHH-clone number	Animal number	MW (kDa)	IFS	MERS-CoV S1 ELISA	MERS-CoV RBD ELISA	$PRNT_{90}$ (μg/mL)
VHH-1	camel 1	13.87	+	+	+	0.1-0.01*
VHH-2	camel 1	14.08	+	+	+	10
VHH-4	camel 1	14.23	+	+	+	0.01*
VHH-6	camel 1	14.32	+	+	+	1
VHH-7	camel 1	13.99	+	+	+	1
VHH-8	camel 1	13.79	+	+	+	1
VHH-10	camel 1	14.94	+	+	+	1
VHH-12	camel 1	14.11	+	+	+	1
VHH-15	camel 1	13.82	+	+	+	1
VHH-17	camel 1	13.86	+	+	+	0.1
VHH-18	camel 1	14.26	+	+	+	0.1
VHH-20	camel 1	13.84	+	+	+	1
VHH-21	camel 1	13.79	+	+	+	1
VHH-26	camel 1	14.76	+	+	+	1
VHH-28	camel 1	14.22	+	+	+	1
VHH-38	camel 1	13.72	+	+	+	0.1
VHH-39	camel 1	14.15	+	+	+	1
VHH-40	camel 1	13.88	+	+	+	1
VHH-44	camel 1	14.42	+	+	+	1
VHH-46	camel 1	13.80	+	+	+	0.1
VHH-47	camel 1	13.82	+	+	+	1
VHH-50	camel 1	13.79	+	+	+	1
VHH-58	camel 1	14.42	+	+	+	1
VHH-59	camel 1	14.36	+	+	+	10
VHH-62	camel 1	14.34	+	+	+	10
VHH-65	camel 1	13.73	+	+	+	0.1
VHH-70	camel 1	13.69	+	+	+	0.1
VHH-75	camel 1	13.86	+	+	+	0.1
VHH-77	camel 1	13.80	+	+	+	1
VHH-79	camel 1	14.11	+	+	+	10
VHH-82	camel 1	13.84	+	+	+	1
VHH-83	camel 1	13.96	+	+	+	0.01*
VHH-84	camel 1	13.82	+	+	+	0.1
VHH-91	camel 2	14.39	+	+	+	1
VHH-93	camel 2	14.20	+	+	+	10
VHH-101	camel 2	14.50	+	+	+	0.1-0.01*
VHH-111	camel 2	14.44	+	+	+	1
VHH-129	camel 2	14.40	+	+	+	10
VHH-136	camel 2	14.33	+	+	+	1
VHH-149	camel 2	14.41	+	+	+	0.1
VHH-152	camel 2	14.38	+	+	+	1
VHH-174	camel 2	14.65	+	+	+	1
VHH-184	camel 2	13.84	+	+	+	1
VHH-187	camel 2	13.81	+	+	+	0.1
VHH-203	camel 2	14.51	+	+	+	0.1
VHH-204	camel 2	14.44	+	+	+	1
VHH-p2E6 control	camel 1	14.95	-	-	-	>10

Molecular weight (MW) of each VHH was determined using the online software http://www.bioinformatics.org/sms2/protein_mw.html. Reactivity against MERS-CoV spike S1 subunit (S1) and receptor binding domain (RBD) were analyzed by ELISA; MERS-CoV neutralization capacity of 47 VHHs were analyzed by plaque reduction neutralization assay (PRNT) on Huh-7 cells, The PRNT titer was calculated based on a 90% or greater reduction in infected cells counts ($PRNT_{90}$). * VHHs with high neutralizing capacity. IFS, immunofluorescence staining; VHH, Variable heavy chain.

Table S2. List of antibodies used in this study

Antibody name	Company	Catalog number
Goat-anti-Llama antibodies Biotin	Abcore	AC15-0352
Mouse anti-histidine antibodies	Thermo Scientific	MA1-21315
Rabbit anti-MERS-CoV polyclonal serum [52]		
Mouse-anti-SARS-CoV-nucleocapsid	Imgenex	IMG-5029
Goat anti-Rabbit Alexa Fluor 488	Life Technologies	A11070
Goat anti-Rabbit Alexa Fluor 594	Life Technologies	A11012
Goat anti-mouse IgG Alexa Fluor 488	Life Technologies	A11029
Goat-anti-human IgG Alexa Fluor 488	Life technologies	A11013
Rabbit-anti-human IgG FITC	DAKO	F0315
IRDye 680RD Streptavidin	LI-COR Biosciences	926-68079
IRDye 800CW goat anti-human IgG	LI-COR Biosciences	925-32232
Goat anti-mouse HRP	DAKO	P0447
Streptavidin HRP	DAKO	P0397
Normal goat serum	MP Biomedicals	642921
Rabbit anti-mouse HRP	DAKO	P0260

Chapter 3.2

Species-specific colocalization of Middle East respiratory syndrome coronavirus attachment and entry receptors

W. Widagdo* | Nisreen M.A. Okba* | Wentao Li | Alwin de Jong | Rik L. de Swart | Lineke Begeman | Judith M.A. van den Brand | Berend-Jan Bosch | Bart L. Haagmans

*Authors contributed equally

J Virol. 2019;93:e00107-19

Abstract

Middle East respiratory syndrome coronavirus (MERS-CoV) uses the $S1^B$ domain of its spike protein to bind to dipeptidyl peptidase 4 (DPP4), its functional receptor, and its $S1^A$ domain to bind to sialic acids. The tissue localization of DPP4 in humans, bats, camelids, pigs, and rabbits generally correlates with MERS-CoV tropism, highlighting the role of DPP4 in virus pathogenesis and transmission. However, MERS-CoV $S1^A$ does not indiscriminately bind to all α2,3-sialic acids, and the species-specific binding and tissue distribution of these sialic acids in different MERS-CoV-susceptible species have not been investigated. We established a novel method to detect these sialic acids on tissue sections of various organs of different susceptible species by using nanoparticles displaying multivalent MERS-CoV $S1^A$. We found that the nanoparticles specifically bound to the nasal epithelial cells of dromedary camels, type II pneumocytes in human lungs, and the intestinal epithelial cells of common pipistrelle bats. Desialylation by neuraminidase abolished nanoparticle binding and significantly reduced MERS-CoV infection in primary susceptible cells. In contrast, $S1^A$ nanoparticles did not bind to the intestinal epithelium of serotine bats and frugivorous bat species, nor did they bind to the nasal epithelium of pigs and rabbits. Both pigs and rabbits have been shown to shed less infectious virus than dromedary camels and do not transmit the virus via either contact or airborne routes. Our results depict species-specific colocalization of MERS-CoV entry and attachment receptors, which may be relevant in the transmission and pathogenesis of MERS-CoV.

IMPORTANCE MERS-CoV uses the $S1^B$ domain of its spike protein to attach to its host receptor, dipeptidyl peptidase 4 (DPP4). The tissue localization of DPP4 has been mapped in different susceptible species. On the other hand, the $S1^A$ domain, the N-terminal domain of this spike protein, preferentially binds to several glycotopes of α2,3-sialic acids, the attachment factor of MERS-CoV. Here we show, using a novel method, that the $S1^A$ domain specifically binds to the nasal epithelium of dromedary camels, alveolar epithelium of humans, and intestinal epithelium of common pipistrelle bats. In contrast, it does not bind to the nasal epithelium of pigs or rabbits, nor does it bind to the intestinal epithelium of serotine bats and frugivorous bat species. This finding supports the importance of the $S1^A$ domain in MERS-CoV infection and tropism, suggests its role in transmission, and highlights its potential use as a component of novel vaccine candidates.

Introduction

Coronaviruses use their spike (S) protein to attach to host cell surface molecules and enter target cells. The N-terminal part of this S protein, known as S1, is responsible for attachment to host cells, while the C-terminal part mediates virus fusion to host cells.postattachment (1). For Middle East respiratory syndrome coronavirus (MERS-CoV), the S1 protein comprises four individually folded domains, designated S1^{A} through S1^{D} (2, 3). Two of these domains, S1^{A} and S1^{B}, are involved in binding to host cell surface molecules during the attachment phase. The S1^{A} domain preferentially binds to several glycotopes of α2,3-sialic acids, while the S1^{B} domain recognizes a host exopeptidase named dipeptidyl peptidase 4 (DPP4), the viral receptor (4, 5). The absence of DPP4 renders cells insusceptible to MERS-CoV (4). Meanwhile, elimination of sialic acids in susceptible cell lines significantly reduces MERS-CoV infection (5). These findings indicated that besides DPP4, the functional entry receptor of MERS-CoV, α2,3-sialic acids act as attachment receptors (4, 5).

DPP4 expression has been mapped in tissues of different susceptible species. It is expressed in the nasal epithelium of camelids, pigs, and rabbits, in which MERS-CoV causes upper respiratory tract infection (6-12). In the human respiratory tract, it is mainly expressed in type II pneumocytes in the lungs (8, 13), in line with clinical data showing that in humans, MERS-CoV mainly replicates in the lower respiratory tract (14-16). In common pipistrelle bats, a potential reservoir for MERS-CoV-like viruses, DPP4 is scarcely detected in the respiratory tract but abundantly present in the intestinal tract (17). Accordingly, MERS-CoV-like viruses are detected mostly in fecal samples of this species as well as in other insectivorous bat species (18-20). Sheep, on the other hand, do not seem to express DPP4 in their respiratory tract and thus hardly shed infectious virus and did not seroconvert upon experimental intranasal MERS-CoV inoculation (7, 21). Epidemiological studies did not reveal MERS-CoV-seropositive sheep in the field, except for one study using sheep sera obtained from Senegal (22-25). Altogether, these data support the role of DPP4 in determining the host range and tissue tropism of MERS-CoV.

The localization of α2,3-sialic acids in the respiratory tract of both humans and dromedary camels has been mapped using lectin histochemistry (5). These molecules are mainly present in the lower respiratory tract epithelium of humans and the upper respiratory tract epithelium of dromedary camels, in line with the localization of DPP4 (5, 26). However, it is important to note that MERS-CoV S1^{A} does not indiscriminately bind to all α2,3-sialic acids. It does not recognize those with 5-*N*-glycosylation or 9-*O*-acetylation but preferentially binds 5-*N*-acetyl-modified sialic acids (5). Among these α2,3-linked, *N*-acetyl-modified sialic acids, MERS-CoV S1^{A} predominantly binds to short, sulfated, α2,3-linked monosialosaccharides and to long, branched, di- and triantennary α2,3-linked sialic acids, with a minimum

extension of 3 *N*-acetyl-d-lactosamine tandem repeats (5). These glycotopes were previously identified by glycan array analysis using nanoparticles displaying multivalent MERS-CoV $S1^A$ (5). Here, using these nanoparticles, we developed a histochemistry-based technique to map the MERS-CoV-recognized glycotopes in the tissues of different susceptible species. The results of our study offer further insight into the importance of these glycotopes in MERS-CoV host range, tropism, and transmission.

Results

MERS-CoV $S1^A$ binds specifically to the nasal epithelium of dromedary camels

The nasal epithelia of dromedary camels express DPP4 and are susceptible to MERS-CoV upon experimental inoculation (8, 27). Recent studies revealed that these tissues also express α2,3-sialic acids based on *Maackia amurensis* lectin II binding (5). However, this lectin binds to a broad range of modified α2,3-sialic acids and thus may not represent a specific marker for glycotopes recognized by MERS-CoV $S1^A$ (28).

In order to map these glycotopes, we displayed MERS-CoV $S1^A$ in a multivalent manner using 60-meric self-assembled nanoparticles generated from the lumazine synthase protein of the bacterium *Aquifex aeolicus* (np-$S1^A$) (5) and subsequently used these nanoparticles to set up a histochemistry assay. We previously showed that both np-$S1^A$ and MERS-CoV virions can agglutinate human erythrocytes, while dimeric MERS-CoV $S1^A$ cannot, indicating that multivalent presentation is necessary for the hemagglutination phenotype of MERS-CoV $S1^A$. Similarly, np-$S1^A$, but not dimeric MERS-CoV $S1^A$, can bind to tissues in our assay. As shown in Figure 1, np-$S1^A$ binds specifically to the nasal epithelium of dromedary camels. We found that these glycotopes are expressed in clusters of ciliated and goblet cells in the nasal epithelium in a random multifocal pattern (Figure 1A). We determined the binding specificity of np-$S1^A$ by using blank nanoparticles and tissues pretreated with neuraminidase as negative controls (Figure 1A). Goblet cells, however, are DPP4 negative and thus are not susceptible to MERS-CoV despite expressing these glycotopes (Figure 1B). The nasal tissues used for the np-$S1^A$ binding experiment, DPP4 detection, and periodic acid-Schiff staining were obtained from noninfected dromedary camels, while those used to visualize both np-$S1^A$ binding and MERS-CoV nucleoprotein were obtained from MERS-CoV-infected dromedary camels. The tissues of these animals were collected during a previous study (27).

In a previous study, we generated a nanobody library from the bone marrow of dromedary camels vaccinated with modified vaccinia virus Ankara (MVA) expressing the MERS-CoV spike protein and identified $S1^B$-reactive nanobodies (29). We rescreened this library using the $S1^A$ domain and identified an $S1^A$-reactive nanobody. We confirmed its specific binding

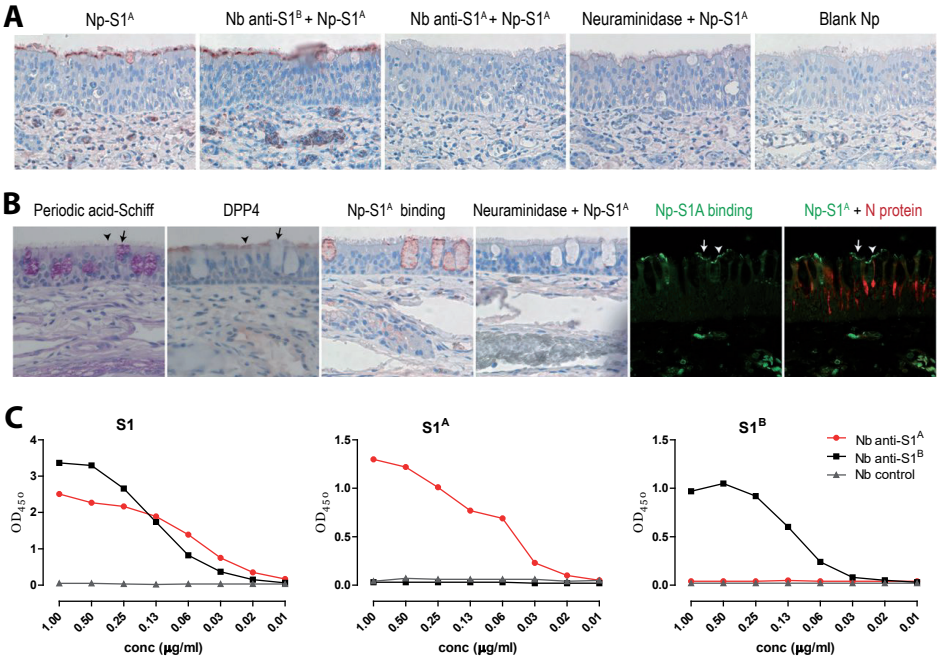

Figure 1. MERS-CoV S1^A binds specifically to the nasal epithelium of dromedary camels. **(A)** Nanoparticles displaying a multivalent MERS-CoV S1^A domain (np-S1^A) bind to the apical surface of camel nasal ciliated epithelial cells, as revealed by red staining. np-S1^A binding is inhibited by prior neuraminidase treatment of these nasal tissues. Blank nanoparticles also do not bind to these tissues. **(B)** Goblet cells (arrows), visualized in purple by periodic acid-Schiff stain, are DPP4 negative, unlike nasal ciliated columnar epithelial cells (arrowheads). DPP4 expression is indicated in red. MERS-CoV S1^A binding to these goblet cells (red) can be abrogated by neuraminidase treatment. In MERS-CoV-infected camels, MERS-CoV S1^A (green) binds to both nasal ciliated columnar epithelial cells and goblet cells, while MERS-CoV N protein (red) is detected only in nasal ciliated columnar epithelial cells. np-S1^A binding is abrogated by a nanobody against the S1^A domain (Nb anti-S1^A) but not by one against the S1^B domain (Nb anti-S1^B). The tissues used in these experiments were sequentially cut. All pictures were taken at a ×400 magnification. **(C)** Nb anti-S1^A and Nb anti-S1^B bind specifically to S1^A and S1^B domains, respectively, and both bind to S1 protein, as revealed by an ELISA. The control nanobody does not bind to S1, S1^A, and S1^B. Nanobody binding is expressed as optical density at 450 nm (OD_{450}) values determined by an ELISA.

to the S1^A domain through S1, S1^B, and S1^A enzyme-linked immunosorbent assays (ELISAs). While the control nanobody (29) was negative in all three ELISAs, each of the anti-S1^A and anti-S1^B nanobodies reacted specifically to its corresponding domain and to S1 in a dose-dependent manner (Figure 1B). The identified S1^A nanobody inhibited np-S1^A binding to nasal epithelial cells, whereas the S1^B-reactive nanobody did not, further confirming the np-S1^A binding specificity and the potential role of S1^A-specific antibodies in blocking MERS-CoV attachment (Figure 1A).

MERS-CoV $S1^A$ does not bind to the nasal epithelium of pigs and rabbits

Similar to dromedary camels, pigs and rabbits also develop upper respiratory tract infection upon MERS-CoV inoculation. However, both pigs and rabbits shed less infectious virus (mainly between 10^2 and 10^3 50% tissue culture infectious doses [$TCID_{50}$]/ml) than do dromedary camels (between 10^4 and 10^5 $TCID_{50}$/ml) postinoculation (6, 7, 9-11, 27, 30). In line with these findings, we found smaller numbers of infected nasal epithelial cells in the nasal tissues of these MERS-CoV-infected pigs and rabbits than in dromedary camels (Figure 2). Using the nasal tissues obtained from mock-infected dromedary camels, pigs, and rabbits, we show that DPP4 is highly expressed in the nasal epithelium of these three species (Figure 2), indicating that the differences in infectious virus shedding observed in these three species are not likely due to differences in DPP4 expression. Subsequent screening for the presence of α2,3-sialic acids in these tissues using lectin histochemistry revealed that the nasal epithelium of pigs does not express these sialic acids, in accordance with the results of previous studies (31, 32). In contrast, these sialic acids were detected in the nasal epithelium of dromedary camels and rabbits (Figure 2). We then used np-$S1^A$ to test for the presence of MERS-CoV-recognized glycotopes in the nasal epithelium of pigs and rabbits and found that unlike dromedary camels, both species do not express these glycotopes (Figure 2). The absence of these glycotopes in the nasal epithelium of rabbits, despite the abundant presence of α2,3-sialic acids, further supports the fine specificity of A domain binding.

MERS-CoV $S1^A$ binds specifically to the intestinal epithelium of pipistrelle bats

DPP4 has been reported to mediate MERS-CoV infection in various bat cell lines derived from different bat species (33, 34). It has also been shown to mediate entry of pseudotyped viruses expressing spike proteins of two MERS-CoV-like viruses, i.e., HKU4 and *Hypsugo pulveratus* BatCoV HKU25, in target cells (19, 35, 36). DPP4, detected using a previously described immunohistochemistry method (8, 17), has also been shown to be abundantly expressed in the intestinal epithelium of both insectivorous and frugivorous bats (17). Altogether, these studies suggest the susceptibility of various bat species to MERS-CoV-like viruses. However, not all susceptible bat species may act as hosts for these viruses, as they were preferentially detected in insectivorous bats (18-20). One study conducted a large screening of over 5,000 insectivorous bats, from Ghana, Ukraine, Romania, Germany, and The Netherlands, showing that these viruses were mainly detected in *Nycteris* bats and pipistrelle bats (20). Using np-$S1^A$, we investigated whether MERS-CoV-recognized glycotopes were differentially expressed in the intestinal epithelium of insectivorous bats, i.e., common pipistrelle (*Pipistrellus pipistrellus*) and serotine (*Eptesicus serotinus*) bats, and frugivorous bats, i.e., Gambian epauletted (*Epomophorus gambianus*) and Egyptian fruit

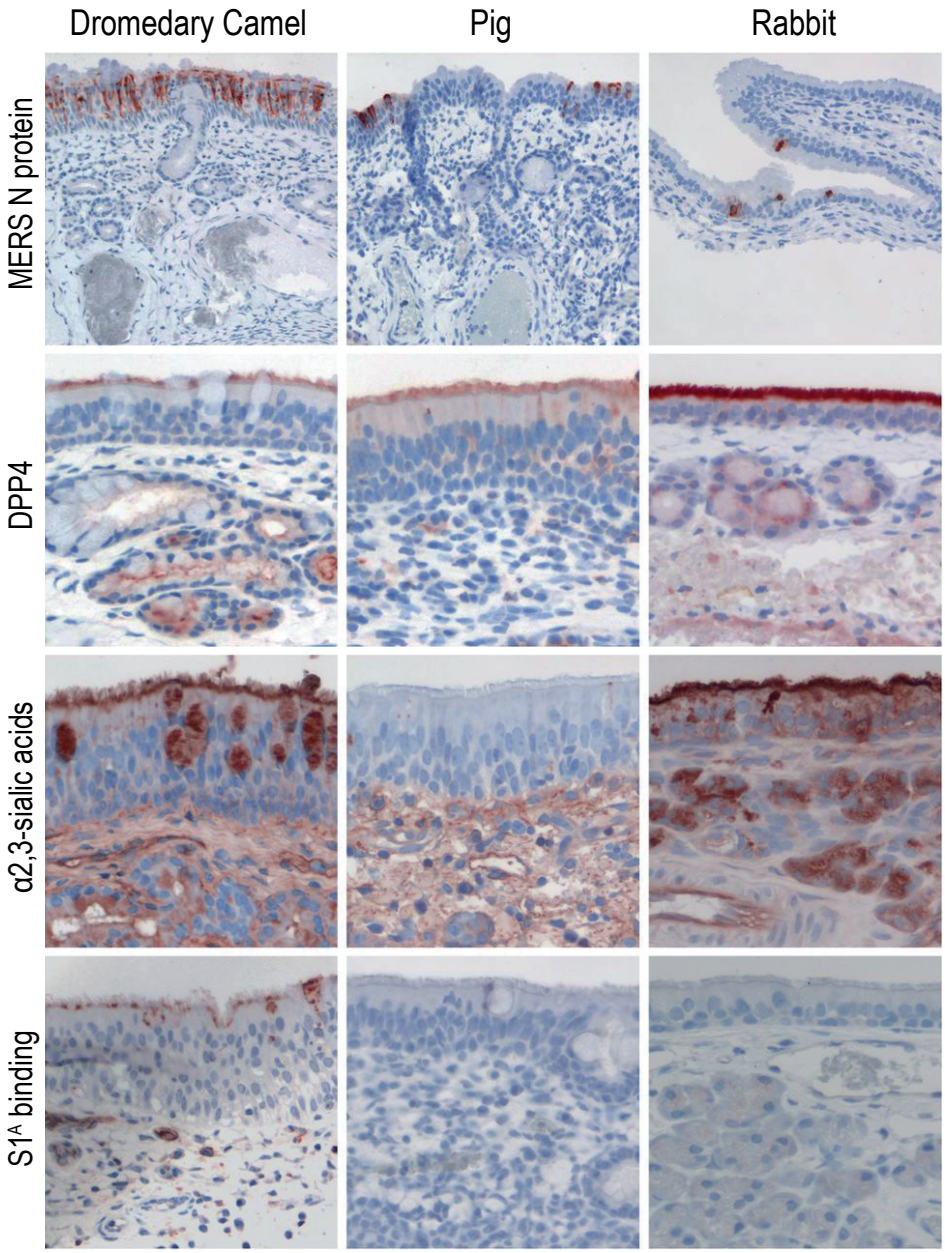

Figure 2. Detection of MERS-CoV N protein, DPP4, α2,3-sialic acids, and MERS-CoV S1^{A} binding in the nasal epithelium of dromedary camels, pigs, and rabbits. MERS-CoV N protein, DPP4, α2,3-sialic acid, and MERS-CoV S1^{A} binding are all indicated in red. MERS-CoV N protein is detected in the nasal epithelium tissues of MERS-CoV-infected dromedary camels, pigs, and rabbits. DPP4, α2,3-sialic acid, and MERS-CoV S1^{A} binding were evaluated on the tissues of noninfected animals. MERS-CoV N protein and DPP4 are detected in the nasal epithelium of dromedary camel, pig, and rabbit. α2,3-Sialic acids are detected in the nasal epithelium of dromedary camel and rabbit but not in that of pig. Meanwhile, MERS-CoV S1^{A} binds merely to the nasal epithelium of dromedary camel. Magnification, ×400.

(*Rousettus aegyptiacus*) bats. We observed that np-S1^{A} binds to the apical surface of the intestinal epithelium of common pipistrelle bats in both villi and crypts, while in others, np-S1^{A} binds only to the intestinal crypts (Figure 3).

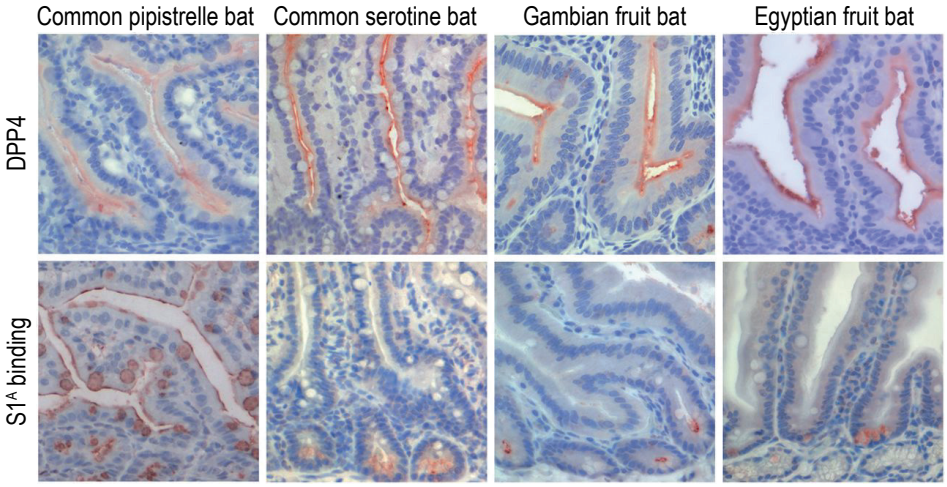

Figure 3. DPP4 expression and MERS-CoV S1^{A} binding in intestinal tissues of common pipistrelle bat, serotine bat, Gambian epauletted fruit bat, and Egyptian fruit bat. DPP4 expression and MERS-CoV S1^{A} binding are indicated in red. DPP4 is expressed at the apical surface of the intestinal epithelial cells of these four bat species. MERS-CoV S1^{A} binds to the apical surface of the intestinal epithelial cells of common pipistrelle bats in both villi and crypts, while in other bat species, it mostly binds to intestinal epithelial cells within the crypts. Magnification, ×400.

MERS-CoV S1^{A} binds specifically to cells in the human lower respiratory tract

Since lower respiratory tract samples from MERS human cases have higher levels of virus and the virus was detected by immunohistochemistry in the lungs of two cases, it has been concluded that MERS-CoV mainly replicates in the human lower respiratory tract (14-16, 37). In line with these observations, DPP4 is expressed in the lower airway epithelium but not in the upper airway epithelium. It was detected in bronchiolar and alveolar epithelial cells but primarily in type II pneumocytes (Figure 4A), consistent with previous studies (8, 13). Our lectin histochemistry staining showed that both bronchiolar epithelial cells and type II pneumocytes express α2,3-sialic acids (26). Both cell types also express MERS-CoV-recognized glycotopes, as indicated by the binding of np-S1^{A} (Figure 4B). Using immunofluorescence, we show that DPP4 expression and np-S1^{A} binding colocalize in the same alveolar epithelial cells in the human lung (Figure 4C).

The function of MERS-CoV-recognized glycotopes as an attachment factor thus far has been observed only in Calu3 cells, which is a cell line originating from a human lung

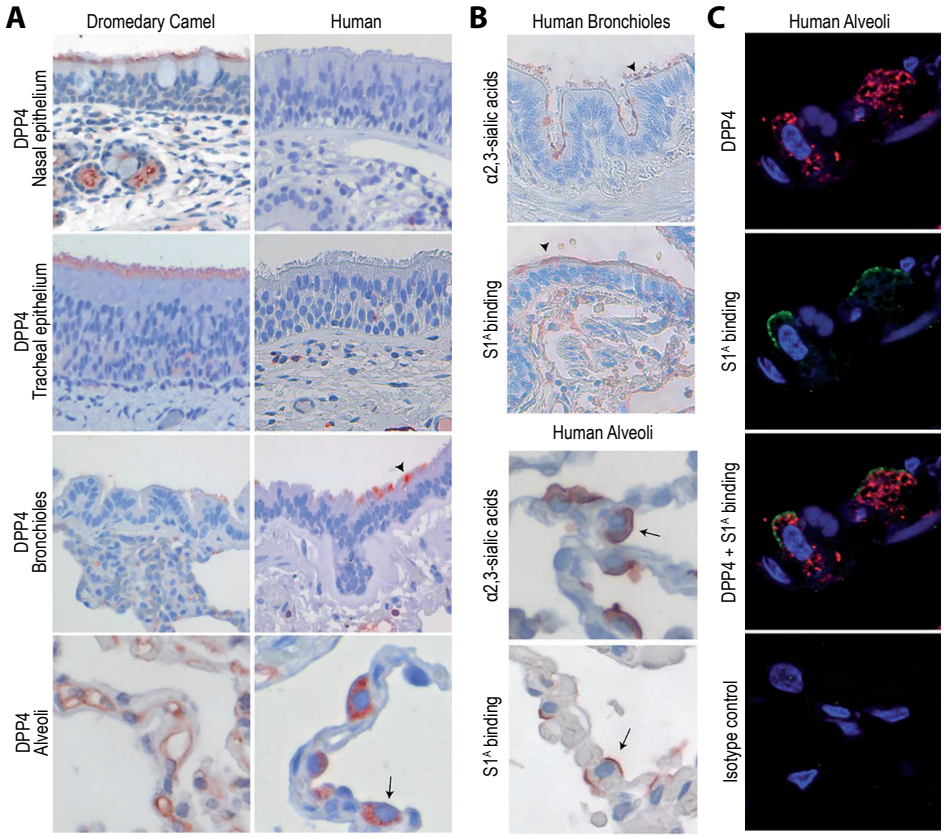

Figure 4. MERS-CoV receptor and attachment factor in the human lower respiratory tract epithelium. **(A)** The MERS-CoV receptor, DPP4, is expressed in the nasal epithelium of dromedary camels, while in the lungs, it is mainly expressed in endothelial cells. In the human respiratory tract, DPP4 is expressed in bronchiolar epithelial cells (arrowhead) and type II pneumocytes (arrow) in the lungs but not in the nasal epithelium. **(B)** α2,3-Sialic acid expression and MERS-CoV S1^{A} binding are also detected in human bronchiolar epithelial cells (arrowheads) and type II pneumocytes (arrows). DPP4 expression, α2,3-sialic acids, and MERS-CoV S1^{A} binding are indicated in red. **(C)** In human alveoli, DPP4 expression (red) colocalizes in the same cells where MERS-CoV S1^{A} binds (green). Pictures of the nasal epithelium were taken at a ×400 magnification, and those of the alveoli were taken at a ×1,000 magnification.

adenocarcinoma. These cells express both DPP4 and the glycotopes of α2,3-sialic acids recognized by MERS-CoV. Removal of sialic acids on these cells using neuraminidase prior to MERS-CoV infection significantly reduced the number of infected cells (5). In contrast, neuraminidase treatment of Vero cells, which do not express MERS-CoV-recognized glycotopes, had no effect on the number of infected cells (5). Primary well-differentiated normal human bronchiolar epithelial (wd-NHBE) cells also express DPP4 and MERS-CoV-recognized glycotopes (Figure 5A). These wd-NHBE cells were obtained from healthy human bronchial epithelial cells and cultured at the air-liquid interface to mimic the human airway

environment. Previous studies have reported that these cells are susceptible to MERS-CoV in a DPP4-dependent manner (38-40). Here we show that neuraminidase treatment of paraffin-embedded wd-NHBE cells reduces np-S1^{A} binding but not DPP4 expression (Figure 5A). Neuraminidase treatment prior to MERS-CoV infection of these cells also significantly reduced the number of infected cells (Figure 5B), similar to our previous findings in Calu3 cells (5). Thus, our results further support the importance of MERS-CoV-recognized glycotopes as an attachment factor during infection of human airway epithelial cells.

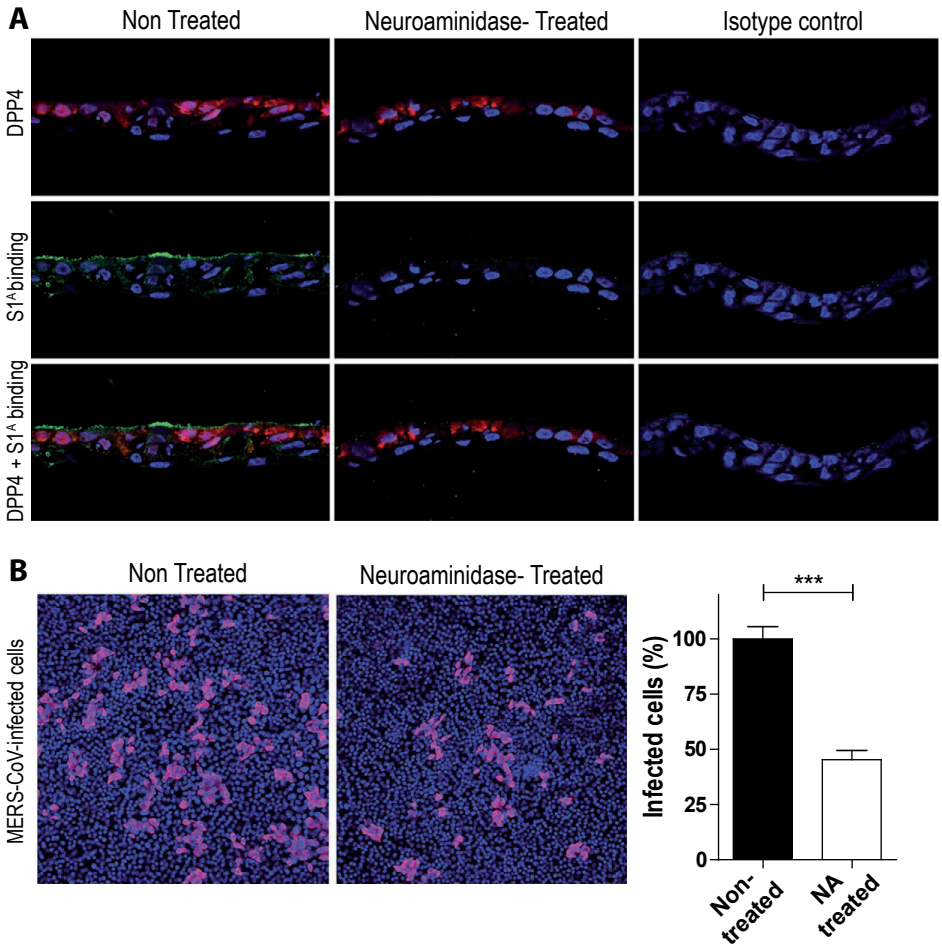

Figure 5. Binding of the MERS-CoV S1^{A} domain and MERS-CoV infection in primary normal human bronchial epithelial cells are inhibited upon prior neuraminidase treatment. **(A)** Removal of sialic acids using neuraminidase (NA) treatment diminishes MERS-CoV S1^{A} binding to primary normal human bronchial epithelial cells but not DPP4 expression in these cells. **(B)** The same treatment also significantly inhibits MERS-CoV infection in these cells up to 50%. Immunofluorescence images in panel A were taken at a ×400 magnification, and those in panel B were taken at a ×100 magnification. ***, p-value of <0.0001 by a *t* test.

Discussion

The S1 protein is an important determinant for the host range and tissue tropism of coronaviruses. This domain initiates infection by binding to host cell surface molecules, either proteinaceous, sialoglycan based, or both (41). The S1 proteins of feline coronavirus, transmissible gastroenterovirus, and MERS-CoV have been demonstrated to have dual-binding specificity, allowing them to engage both sialoglycans and proteinaceous molecules (5, 38, 41-45). We have previously reported that for MERS-CoV, this dual binding is facilitated by distinct domains of its S1 protein, i.e., $S1^A$ and $S1^B$ (4, 5). The $S1^B$ domain binds DPP4, the functional receptor of MERS-CoV (38). DPP4 has been demonstrated to have a major influence on viral host range and tropism since its tissue localization varies between species (7, 8, 13, 17, 33, 38, 46-48). It is detected in the nasal epithelium of camelids, pigs, and rabbits (7, 8). In bats, it is mainly expressed in the small intestinal epithelium of common pipistrelle and serotine bats and in both the respiratory and intestinal epithelia of Gambian epauletted and Egyptian fruit bats (17). Meanwhile, in the human airways, it is present merely in the lower respiratory tract epithelium, particularly in type II pneumocytes (8, 13). Besides DPP4, MERS-CoV preferentially binds α2,3-linked sialic acids via its $S1^A$ domain and uses these sialic acids as an attachment factor (5). Using nanoparticles displaying a multivalent $S1^A$ domain, we show that the tissue localization of these glycotopes varies between various tissues in susceptible species. The $S1^A$ domain bound to the nasal epithelium of dromedary camels and type II pneumocytes in human lungs but not the nasal epithelium of pigs and rabbits. Binding of particles to other molecules besides sialic acids such as mucus and extracellular factors that are removed during the preparation of tissue sections as a result of the boiling procedure, however, cannot be excluded.

Previous studies have shown that MERS-CoV-inoculated pigs and rabbits shed less infectious virus than did dromedary camels (6, 7, 10, 11, 27). In addition, these animals did not transmit the virus via either contact or airborne routes (30, 49). In contrast, MERS-CoV is easily transmitted among dromedary camels (12, 50-53). The absence of MERS-CoV-recognized glycotopes in the nasal epithelium of pigs and rabbits might render them less permissive to MERS-CoV, thus shedding less infectious virus, which subsequently limited virus transmission. This is supported by our finding that the loss of these glycotopes, e.g., through desialylation, could significantly reduce MERS-CoV infection (5). However, it is important to note that the expression of other factors, such as proteases and interferons, may also influence MERS-CoV replication and transmission. MERS-CoV has been reported to use host cell proteases, such as TMPRSS2, furin, and cathepsins, to mediate fusion to host cells (54-56). The virus has been shown to be sensitive to type I interferon, an essential host innate immune cytokine (5, 54-58). Thus, the absence of these proteases and the presence

of an inhibiting host innate immune response could effectively limit MERS-CoV replication and transmission, in combination with the absence of MERS-CoV-recognized glycotopes (5, 54-58). The importance of glycotopes in MERS-CoV transmission, either solely or in combination with other factors, remains to be further elucidated. These studies would likely require experimental infection of camelids, particularly dromedary camels (50, 51, 59, 60).

Our data also show that besides their presence in the respiratory tract of dromedary camels and humans, MERS-CoV-recognized glycotopes are expressed at the apical surface of the villi and crypts of the intestinal epithelium of common pipistrelle bats. Interestingly, in serotine bats and both Gambian epauleted and Egyptian fruit bats, these glycotopes are detected merely in the intestinal crypts. This finding further supports the belief that insectivorous bats are one of the natural hosts of MERS-CoV-like viruses (18-20) and also suggests that not all insectivorous bats express the α2,3-sialic acid glycotopes recognized by MERS-CoV in their intestines. However, how sialic acid abundance and distribution in the intestine relate to infection by MERS-CoV-like viruses in various bat species remains to be investigated. Such studies would likely rely on the availability of primary bat intestinal cell culture or bat intestinal organoids, since experiments in insectivorous bats are difficult to perform, partly due to legal restrictions.

In general, our results showed that the tissue localization of α2,3-sialic acid glycotopes recognized by MERS-CoV $S1^A$ varies between susceptible species. These glycotopes and DPP4 are both expressed in the nasal ciliated epithelial cells of dromedary camels, type II pneumocytes of humans, and intestinal epithelial cells of common pipistrelle bats, providing further evidence that these tissues are the main replication sites of MERS-CoV in the respective species. This study corroborates α2,3-sialic acid glycotopes as an important attachment factor for MERS-CoV (5), and highlights the necessity to further understand their role in MERS-CoV pathogenesis and transmission. Importantly, our results also imply that the MERS-CoV $S1^A$ domain should be considered a target for vaccines (61, 62).

Materials and Methods

Tissue samples

Human formalin-fixed paraffin-embedded (FFPE) lung tissues were obtained from the Erasmus MC Tissue Bank and had been used in a previous study (8). These tissue samples were residual human biomaterials taken either from healthy donors or from patients with nonmalignant lung tumors, which were collected, stored, and issued by the Erasmus MC Tissue Bank under ISO 15189:2007 standard operating procedures. Use of these materials for research purposes is regulated according to human tissue and medical research under

the code of conduct for responsible use (63). Dromedary camel, pig, and rabbit FFPE nasal tissues, both MERS-CoV infected and mock infected, were obtained from previous studies. The dromedary camels and pigs were inoculated via the intranasal route with 10^7 tissue culture infectious doses ($TCID_{50}$), while the rabbits were inoculated with 10^6 $TCID_{50}$ via the intranasal route and 4×10^6 $TCID_{50}$ via the intratracheal route. Mock-infected animals were inoculated with cell culture medium. Infected animals were all sacrificed at day 4 postinoculation (6, 7, 27). Bat FFPE intestinal tissues were also obtained from a previous study (17). Tissues of common pipistrelle and serotine bats were obtained from bats that were stranded or severely wounded and admitted to an official local bat shelter in The Netherlands. The Gambian and Egyptian fruit bats used in this study originated from free-ranging populations in Ghana. The animals were euthanized and necropsied by licensed veterinarians. The bat tissues included in this study were histologically normal as determined by using hematoxylin-eosin staining prior to our experiment.

Histochemistry and immunofluorescence analysis

MERS-CoV nucleoprotein was detected with 5 µg/ml mouse anti-MERS nucleoprotein (Sino-Biological, Beijing, China), while DPP4 expression was detected with either 5 µg/ml goat anti-human DPP4 (R&D, Minneapolis, MN, USA) or 10 µg/ml mouse anti-human DPP4 (clone 11D7; Origene, Rockville, MD, USA). Briefly, the paraffin-embedded tissues were deparaffinized using xylene, hydrated using graded concentrations of alcohol, boiled in 10 mM citric acid buffer (pH 6) for 15 min, and subsequently incubated in 3% H_2O_2 for 10 min and in 5% normal goat serum for 30 min before staining with antibodies. This protocol has been more thoroughly described in previous studies (7, 8, 13, 17). Periodic acid-Schiff staining was performed by deparaffinizing and hydrating the tissue slides, subsequently incubating them in a periodic acid solution for 5 min and Schiff's reagent for 15 min, and counterstaining them with Gill's hematoxylin for 1 min, with water rinsing between steps. This protocol has also been used in our previous study (7). Expression of α2,3-sialic acids was detected using biotinylated *Maackia amurensis* lectin II (Vector Labs, Burlingame, CA, USA) at a 1:800 dilution and streptavidin-horseradish peroxidase (HRP) at a 1:300 dilution, both diluted in 1× Tris-buffered saline containing 0.1 M $MnCl_2$, 1 M $MgCl_2$, and 0.1 M $CaCl_2$, and then subsequently visualized using 3-amino-9-ethylcarbazole and counterstained with hematoxylin. Detection of S1^A binding on the tissues was performed using nanoparticles displaying a multivalent S1^A domain (np-S1^A) and a Strep-tag generated in a previous study (5). The tissues were boiled in 10 mM citric acid buffer (pH 6) for 15 min and blocked with 5% normal goat serum (Dako, Glostrup, Denmark) before staining with 3 µg/ml np-S1^A overnight at 4°C. Tissues that were stained with an equal concentration (3 µg/ml) of blank nanoparticles and those that were pretreated with 800 mU/ml neuraminidase from

Vibrio cholerae (Sigma-Aldrich, St. Louis, MO, USA) for 4 h at 37°C were used as negative controls. Additional controls were performed by staining tissues with np-S1^{A} previously incubated for 1 h at 37°C with either anti-S1^{A}, anti-S1^{B}, or control nanobodies at a 15-µg/ml concentration. These nanobodies were obtained from a nanobody library generated in a previous study (29). These tissues were subsequently stained with rabbit anti-Strep-tag sera generated in-house and goat anti-rabbit IgG-HRP (Dako, Glostrup, Denmark), each at a 1:100 dilution, for 1 h at room temperature and then visualized with 3-amino-9-ethylcarbazole and counterstained with hematoxylin. For immunofluorescence staining, fluorescence-conjugated secondary antibody was applied in the experiment, i.e., goat anti-rabbit IgG conjugated with Alexa Fluor 488 and goat anti-mouse IgG conjugated with Alexa Fluor 594 (Life Technologies, Carlsbad, CA, USA), both at a 1:250 dilution, with a 1-h incubation at room temperature.

MERS-CoV S1, S1^{B}, and S1^{A} ELISAs

The specificity of anti-S1^{A}, anti-S1^{B}, and control nanobodies for MERS-CoV S1, S1^{A}, and S1^{B} proteins was determined using ELISAs as previously described (29). In brief, 96-well ELISA plates were coated with 1 µg/ml MERS-CoV S1 (amino acids 1 to 751), S1^{A} (amino acids 1 to 357), or S1^{B} (amino acids 358 to 588) protein in phosphate-buffered saline (PBS) (pH 7.4) and incubated overnight at 4°C. Wells were then washed with PBS and blocked with 1% bovine serum albumin in PBS–0.5% Tween 20 for 1 h at 37°C. Nanobodies were 2-fold serially diluted in blocking buffer starting at a 1-µg/ml concentration, 100 µl of each dilution was added per well, and plates were incubated at 37°C for 1 h. Next, plates were washed three times in PBS–0.05% Tween 20 (PBST), after which they were incubated with mouse anti-His tag antibodies (1:2,000; Thermo Fisher Scientific) at 37°C for 1 h. Following incubation, the plates were washed and further incubated with goat anti-mouse HRP (1:2,000; Dako) at 37°C for 1 h. After this incubation, plates were washed three times in PBST, a 3,3′,5,5′-tetramethylbenzidine substrate (eBioscience) was added, and the plates were incubated for 10 min. The reaction was stopped with 0.5 N H2SO4 (Sigma). The absorbance of each sample was read at 450 nm with an ELISA reader (Tecan Infinite F200).

MERS-CoV infection in well-differentiated primary normal human bronchial epithelial cells

Primary NHBE cells (Lonza, Basel, Switzerland) were cultured on Transwell permeable support (Costar) according to the protocol suggested by the manufacturer (Clonetics airway epithelial cell systems; Lonza, Basel, Switzerland). The cells were differentiated at the air-liquid interface for 6 weeks to promote mucociliary differentiation, resulting in the

presence of a multilayered epithelium, ciliated cells, and goblet cells (64). These cells were subsequently either mock treated or pretreated with a mixture of 40 mU of *Arthrobacter ureafaciens* neuraminidase (Sigma-Aldrich, St. Louis, MO, USA) and 50 U of *Clostridium perfringens* neuraminidase (NEB, Ipswich, MA, USA) for 1 h before infection. Each well was inoculated with the MERS-CoV EMC/2012 strain (6, 7) at 10^6 $TCID_{50}$/ml (multiplicity of infection [MOI] of 5), incubated for 36 h, and fixed in 10% formalin. MERS-CoV-infected cells were visualized with 5 μg/ml mouse anti-MERS nucleoprotein (Sino-Biological, Beijing, China) and a 1:250 dilution of goat anti-mouse IgG conjugated with Alexa Fluor 594 (Life Technologies, Carlsbad, CA, USA). MERS-CoV infection experiments in NHBE cells were performed in triplicate per individual donor. The number of infected cells was counted for each well, and the percentage of infected cells was determined as described in our previous study (5). Statistical analysis was performed using Student's *t* test, and results are presented as means ± standard deviations for each group.

Acknowledgments

The *E. gambianus* and *R. aegyptiacus* tissues used in this study originated from Ghana in collaboration with Richard Suu-Ire, Forestry Commission, Accra, Ghana; Andrew A. Cunningham, Institute of Zoology, Zoological Society of London (ZSL), United Kingdom; and James Wood, University of Cambridge, United Kingdom. We thank Louise Gibson, ZSL, for assistance with sampling the African fruit bats. We thank Stichting Vleermuisopvang Oss for providing the tissues of common pipistrelle and serotine bats and Laurine Rijsbergen for technical assistance.

References

1. Fehr AR, Perlman S. Coronaviruses: an overview of their replication and pathogenesis. Methods in molecular biology (Clifton, NJ). 2015;1282:1-23.
2. Kirchdoerfer RN, Cottrell CA, Wang N, Pallesen J, Yassine HM, Turner HL, et al. Pre-fusion structure of a human coronavirus spike protein. Nature. 2016 Mar 3;531(7592):118-21.
3. Walls AC, Tortorici MA, Bosch BJ, Frenz B, Rottier PJM, DiMaio F, et al. Cryo-electron microscopy structure of a coronavirus spike glycoprotein trimer. Nature. 2016 Mar 3; 531(7592):114-7.
4. Mou H, Raj VS, van Kuppeveld FJ, Rottier PJ, Haagmans BL, Bosch BJ. The receptor binding domain of the new Middle East respiratory syndrome coronavirus maps to a 231-residue region in the spike protein that efficiently elicits neutralizing antibodies. Journal of Virology. 2013 Aug;87(16):9379-83.
5. Li W, Hulswit RJG, Widjaja I, Raj VS, McBride R, Peng W, et al. Identification of sialic acid-binding function for the Middle East respiratory syndrome coronavirus spike glycoprotein. Proceedings of the National Academy of Sciences of the United States of America. 2017 Oct 3;114(40):E8508-E17.
6. Haagmans BL, van den Brand JM, Provacia LB, Raj VS, Stittelaar KJ, Getu S, et al. Asymptomatic Middle East respiratory syndrome coronavirus infection in rabbits. Journal of Virology. 2015 Jun;89(11):6131-5.
7. Vergara-Alert J, van den Brand JM, Widagdo W, Munoz Mt, Raj S, Schipper D, et al. Livestock Susceptibility to Infection with Middle East Respiratory Syndrome Coronavirus. Emerg Infect Dis. 2017 Feb;23(2):232-40.
8. Widagdo W, Raj VS, Schipper D, Kolijn K, van Leenders G, Bosch BJ, et al. Differential Expression of the Middle East Respiratory Syndrome Coronavirus Receptor in the Upper Respiratory Tracts of Humans and Dromedary Camels. Journal of Virology. 2016 May;90(9):4838-42.
9. Houser KV, Broadbent AJ, Gretebeck L, Vogel L, Lamirande EW, Sutton T, et al. Enhanced inflammation in New Zealand white rabbits when MERS-CoV reinfection occurs in the absence of neutralizing antibody. PLoS pathogens. 2017 Aug;13(8):e1006565.
10. de Wit E, Feldmann F, Horne E, Martellaro C, Haddock E, Bushmaker T, et al. Domestic Pig Unlikely Reservoir for MERS-CoV. Emerg Infect Dis. 2017 Jun;23(6):985-8.
11. Adney DR, van Doremalen N, Brown VR, Bushmaker T, Scott D, de Wit E, et al. Replication and shedding of MERS-CoV in upper respiratory tract of inoculated dromedary camels. Emerg Infect Dis. 2014 Dec;20(12):1999-2005.
12. Adney DR, Bielefeldt-Ohmann H, Hartwig AE, Bowen RA. Infection, Replication, and Transmission of Middle East Respiratory Syndrome Coronavirus in Alpacas. Emerg Infect Dis. 2016 Jun;22(6):1031-7.
13. Meyerholz DK, Lambertz AM, McCray PB, Jr. Dipeptidyl Peptidase 4 Distribution in the Human Respiratory Tract: Implications for the Middle East Respiratory Syndrome. The American journal of pathology. 2016 Jan;186(1):78-86.
14. Bermingham A, Chand MA, Brown CS, Aarons E, Tong C, Langrish C, et al. Severe respiratory illness caused by a novel coronavirus, in a patient transferred to the United Kingdom from the Middle East, September 2012. Euro surveillance : bulletin Europeen sur les maladies transmissibles = European communicable disease bulletin. 2012 Oct 4;17(40):20290.
15. Drosten C, Seilmaier M, Corman VM, Hartmann W, Scheible G, Sack S, et al. Clinical features and virological analysis of a case of Middle East respiratory syndrome coronavirus infection. The Lancet Infectious diseases. 2013 Sep;13(9):745-51.
16. Ng DL, Al Hosani F, Keating MK, Gerber SI, Jones TL, Metcalfe MG, et al. Clinicopathologic, Immunohistochemical, and Ultrastructural Findings of a Fatal Case of Middle East Respiratory Syndrome Coronavirus Infection in the United Arab Emirates, April 2014. The American journal of pathology. 2016 Mar;186(3):652-8.

17. Widagdo W, Begeman L, Schipper D, Run PRV, Cunningham AA, Kley N, et al. Tissue Distribution of the MERS-Coronavirus Receptor in Bats. Scientific Reports. 2017 Apr 26; 7(1):1193.
18. Anthony SJ, Gilardi K, Menachery VD, Goldstein T, Ssebide B, Mbabazi R, et al. Further Evidence for Bats as the Evolutionary Source of Middle East Respiratory Syndrome Coronavirus. mBio. 2017 Apr 4;8(2).
19. Lau SKP, Zhang L, Luk HKH, Xiong L, Peng X, Li KSM, et al. Receptor Usage of a Novel Bat Lineage C Betacoronavirus Reveals Evolution of Middle East Respiratory Syndrome-Related Coronavirus Spike Proteins for Human Dipeptidyl Peptidase 4 Binding. The Journal of Infectious Diseases. 2018 Jun 20;218(2):197-207.
20. Annan A, Baldwin HJ, Corman VM, Klose SM, Owusu M, Nkrumah EE, et al. Human betacoronavirus 2c EMC/2012-related viruses in bats, Ghana and Europe. Emerg Infect Dis. 2013 Mar;19(3):456-9.
21. Adney DR, Brown VR, Porter SM, Bielefeldt-Ohmann H, Hartwig AE, Bowen RA. Inoculation of Goats, Sheep, and Horses with MERS-CoV Does Not Result in Productive Viral Shedding. Viruses. 2016 Aug 19;8(8).
22. Hemida MG, Perera RA, Wang P, Alhammadi MA, Siu LY, Li M, et al. Middle East Respiratory Syndrome (MERS) coronavirus seroprevalence in domestic livestock in Saudi Arabia, 2010 to 2013. Euro surveillance : bulletin Europeen sur les maladies transmissibles = European communicable disease bulletin. 2013 Dec 12;18(50):20659.
23. Reusken CB, Ababneh M, Raj VS, Meyer B, Eljarah A, Abutarbush S, et al. Middle East Respiratory Syndrome coronavirus (MERS-CoV) serology in major livestock species in an affected region in Jordan, June to September 2013. Euro surveillance : bulletin Europeen sur les maladies transmissibles = European communicable disease bulletin. 2013 Dec 12; 18(50):20662.
24. Ali M, El-Shesheny R, Kandeil A, Shehata M, Elsokary B, Gomaa M, et al. Cross-sectional surveillance of Middle East respiratory syndrome coronavirus (MERS-CoV) in dromedary camels and other mammals in Egypt, August 2015 to January 2016. Euro surveillance: bulletin Europeen sur les maladies transmissibles = European communicable disease bulletin. 2017 Mar 16;22(11).
25. Kandeil A, Gomaa M, Shehata M, El-Taweel A, Kayed AE, Abiadh A, et al. Middle East respiratory syndrome coronavirus infection in non-camelid domestic mammals. Emerging Microbes & Infections. 2019;8(1):103-8.
26. Shinya K, Ebina M, Yamada S, Ono M, Kasai N, Kawaoka Y. Avian flu: influenza virus receptors in the human airway. Nature. 2006 Mar 23;440(7083):435-6.
27. Haagmans BL, van den Brand JM, Raj VS, Volz A, Wohlsein P, Smits SL, et al. An orthopoxvirus-based vaccine reduces virus excretion after MERS-CoV infection in dromedary camels. Science. 2016 Jan 1;351(6268):77-81.
28. Geisler C, Jarvis DL. Effective glycoanalysis with Maackia amurensis lectins requires a clear understanding of their binding specificities. Glycobiology. 2011 Aug;21(8):988-93.
29. Stalin Raj V, Okba NMA, Gutierrez-Alvarez J, Drabek D, van Dieren B, Widagdo W, et al. Chimeric camel/human heavy-chain antibodies protect against MERS-CoV infection. Science Advances. 2018 Aug;4(8):eaas9667.
30. Widagdo W, Okba NMA, Richard M, de Meulder D, Bestebroer TM, Lexmond P, et al. Lack of Middle East Respiratory Syndrome Coronavirus Transmission in Rabbits. Viruses. 2019 Apr 24;11(4):381.
31. Van Poucke SG, Nicholls JM, Nauwynck HJ, Van Reeth K. Replication of avian, human and swine influenza viruses in porcine respiratory explants and association with sialic acid distribution. Virol J. 2010 Feb 16;7:38.

32. Trebbien R, Larsen LE, Viuff BM. Distribution of sialic acid receptors and influenza A virus of avian and swine origin in experimentally infected pigs. Virol J. 2011 Sep 8;8:434.
33. Cai Y, Yu SQ, Postnikova EN, Mazur S, Bernbaum JG, Burk R, et al. CD26/DPP4 cell-surface expression in bat cells correlates with bat cell susceptibility to Middle East respiratory syndrome coronavirus (MERS-CoV) infection and evolution of persistent infection. PloS one. 2014;9(11):e112060.
34. Munster VJ, Adney DR, van Doremalen N, Brown VR, Miazgowicz KL, Milne-Price S, et al. Replication and shedding of MERS-CoV in Jamaican fruit bats (Artibeus jamaicensis). Scientific Reports. 2016 Feb 22;6:21878.
35. Wang Q, Qi J, Yuan Y, Xuan Y, Han P, Wan Y, et al. Bat origins of MERS-CoV supported by bat coronavirus HKU4 usage of human receptor CD26. Cell host & microbe. 2014 Sep 10;16(3):328-37.
36. Yang Y, Du L, Liu C, Wang L, Ma C, Tang J, et al. Receptor usage and cell entry of bat coronavirus HKU4 provide insight into bat-to-human transmission of MERS coronavirus. Proceedings of the National Academy of Sciences of the United States of America. 2014 Aug 26;111(34):12516-21.
37. Alsaad KO, Hajeer AH, Al Balwi M, Al Moaiqel M, Al Oudah N, Al Ajlan A, et al. Histopathology of Middle East respiratory syndrome coronovirus (MERS-CoV) infection - clinicopathological and ultrastructural study. Histopathology. 2018 Feb;72(3):516-24.
38. Raj VS, Mou H, Smits SL, Dekkers DH, Muller MA, Dijkman R, et al. Dipeptidyl peptidase 4 is a functional receptor for the emerging human coronavirus-EMC. Nature. 2013 Mar 14; 495(7440):251-4.
39. Tao X, Hill TE, Morimoto C, Peters CJ, Ksiazek TG, Tseng CT. Bilateral entry and release of Middle East respiratory syndrome coronavirus induces profound apoptosis of human bronchial epithelial cells. Journal of Virology. 2013 Sep;87(17):9953-8.
40. Kindler E, Jonsdottir HR, Muth D, Hamming OJ, Hartmann R, Rodriguez R, et al. Efficient replication of the novel human betacoronavirus EMC on primary human epithelium highlights its zoonotic potential. mBio. 2013 Feb 19;4(1):e00611-12.
41. Hulswit RJ, de Haan CA, Bosch BJ. Coronavirus Spike Protein and Tropism Changes. Advances in virus research. 2016;96:29-57.
42. Delmas B, Gelfi J, L'Haridon R, Vogel LK, Sjostrom H, Noren O, et al. Aminopeptidase N is a major receptor for the entero-pathogenic coronavirus TGEV. Nature. 1992 Jun 4;357(6377):417-20.
43. Tresnan DB, Levis R, Holmes KV. Feline aminopeptidase N serves as a receptor for feline, canine, porcine, and human coronaviruses in serogroup I. Journal of Virology. 1996 Dec;70(12):8669-74.
44. Schwegmann-Wessels C, Zimmer G, Laude H, Enjuanes L, Herrler G. Binding of transmissible gastroenteritis coronavirus to cell surface sialoglycoproteins. Journal of Virology. 2002 Jun;76(12):6037-43.
45. Desmarets LM, Theuns S, Roukaerts ID, Acar DD, Nauwynck HJ. Role of sialic acids in feline enteric coronavirus infections. J Gen Virol. 2014 Sep;95(Pt 9):1911-8.
46. Eckerle I, Corman VM, Muller MA, Lenk M, Ulrich RG, Drosten C. Replicative Capacity of MERS Coronavirus in Livestock Cell Lines. Emerg Infect Dis. 2014 Feb;20(2):276-9.
47. Raj VS, Smits SL, Provacia LB, van den Brand JM, Wiersma L, Ouwendijk WJ, et al. Adenosine deaminase acts as a natural antagonist for dipeptidyl peptidase 4-mediated entry of the Middle East respiratory syndrome coronavirus. Journal of Virology. 2014 Feb;88(3):1834-8.
48. van Doremalen N, Miazgowicz KL, Milne-Price S, Bushmaker T, Robertson S, Scott D, et al. Host species restriction of Middle East respiratory syndrome coronavirus through its receptor, dipeptidyl peptidase 4. Journal of Virology. 2014 Aug;88(16):9220-32.

49. Vergara-Alert J, Raj VS, Munoz M, Abad FX, Cordon I, Haagmans BL, et al. Middle East respiratory syndrome coronavirus experimental transmission using a pig model. Transboundary and emerging diseases. 2017 Oct;64(5):1342-5.
50. Muller MA, Corman VM, Jores J, Meyer B, Younan M, Liljander A, et al. MERS coronavirus neutralizing antibodies in camels, Eastern Africa, 1983-1997. Emerg Infect Dis. 2014 Dec;20(12):2093-5.
51. Reusken CB, Messadi L, Feyisa A, Ularamu H, Godeke GJ, Danmarwa A, et al. Geographic distribution of MERS coronavirus among dromedary camels, Africa. Emerg Infect Dis. 2014 Aug;20(8):1370-4.
52. Meyer B, Muller MA, Corman VM, Reusken CB, Ritz D, Godeke GJ, et al. Antibodies against MERS coronavirus in dromedary camels, United Arab Emirates, 2003 and 2013. Emerg Infect Dis. 2014 Apr;20(4):552-9.
53. Reusken CB, Schilp C, Raj VS, De Bruin E, Kohl RH, Farag EA, et al. MERS-CoV Infection of Alpaca in a Region Where MERS-CoV is Endemic. Emerg Infect Dis. 2016 Jun;22(6):1129-31.
54. Shirato K, Kawase M, Matsuyama S. Middle East respiratory syndrome coronavirus infection mediated by the transmembrane serine protease TMPRSS2. Journal of Virology. 2013 Dec;87(23):12552-61.
55. Zheng Y, Shang J, Yang Y, Liu C, Wan Y, Geng Q, et al. Lysosomal Proteases Are a Determinant of Coronavirus Tropism. Journal of Virology. 2018 Dec 15;92(24).
56. Millet JK, Whittaker GR. Host cell entry of Middle East respiratory syndrome coronavirus after two-step, furin-mediated activation of the spike protein. Proceedings of the National Academy of Sciences of the United States of America. 2014 Oct 21;111(42):15214-9.
57. de Wilde AH, Raj VS, Oudshoorn D, Bestebroer TM, van Nieuwkoop S, Limpens RW, et al. MERS-coronavirus replication induces severe in vitro cytopathology and is strongly inhibited by cyclosporin A or interferon-alpha treatment. J Gen Virol. 2013 Aug;94(Pt 8): 1749-60.
58. Falzarano D, de Wit E, Martellaro C, Callison J, Munster VJ, Feldmann H. Inhibition of novel beta coronavirus replication by a combination of interferon-alpha2b and ribavirin. Scientific Reports. 2013;3:1686.
59. Alagaili AN, Briese T, Mishra N, Kapoor V, Sameroff SC, Burbelo PD, et al. Middle East respiratory syndrome coronavirus infection in dromedary camels in Saudi Arabia. mBio. 2014 Feb 25;5(2):e00884-14.
60. Chu DKW, Hui KPY, Perera R, Miguel E, Niemeyer D, Zhao J, et al. MERS coronaviruses from camels in Africa exhibit region-dependent genetic diversity. Proceedings of the National Academy of Sciences of the United States of America. 2018 Mar 20;115(12):3144-9.
61. Chen Y, Lu S, Jia H, Deng Y, Zhou J, Huang B, et al. A novel neutralizing monoclonal antibody targeting the N-terminal domain of the MERS-CoV spike protein. Emerging Microbes & Infections. 2017 May 24;6(5):e37.
62. Wang L, Shi W, Chappell JD, Joyce MG, Zhang Y, Kanekiyo M, et al. Importance of Neutralizing Monoclonal Antibodies Targeting Multiple Antigenic Sites on the Middle East Respiratory Syndrome Coronavirus Spike Glycoprotein To Avoid Neutralization Escape. Journal of Virology. 2018 May 15;92(10).
63. Anonymous. Human tissue and medical research: code of conduct for responsible use (2011). Federa, Rotterdam, The Netherlands: https://www.federa.org/sites/default/files/digital_version_first_part_code_of_conduct_in_uk_2011_12092012.pdf. 2011.
64. Verkaik NJ, Nguyen DT, de Vogel CP, Moll HA, Verbrugh HA, Jaddoe VW, et al. Streptococcus pneumoniae exposure is associated with human metapneumovirus seroconversion and increased susceptibility to in vitro HMPV infection. Clin Microbiol Infect. 2011 Dec;17(12):1840-4.

Chapter 4.1

Blocking transmission of Middle East respiratory syndrome coronavirus (MERS-CoV) in llamas by vaccination with a recombinant spike protein

Jordi Rodon* | Nisreen M.A. Okba* | Te Nigeer | Brenda van Dieren | Berend-Jan Bosch | Albert Bensaid | Joaquim Segalés | Bart L. Haagmans | Júlia Vergara-Alert

*Authors contributed equally

Emerging microbes & infections. 2019;8(1):1593-603

Abstract

The ongoing Middle East respiratory syndrome coronavirus (MERS-CoV) outbreaks pose a worldwide public health threat. Blocking MERS-CoV zoonotic transmission from dromedary camels, the animal reservoir, could potentially reduce the number of primary human cases. Here we report MERS-CoV transmission from experimentally infected llamas to naïve animals. Directly inoculated llamas shed virus for at least 6 days and could infect all in-contact naïve animals 4–5 days after exposure. With the aim to block virus transmission, we examined the efficacy of a recombinant spike S1-protein vaccine. In contrast to naïve animals, in-contact vaccinated llamas did not shed infectious virus upon exposure to directly inoculated llamas, consistent with the induction of strong virus neutralizing antibody responses. Our data provide further evidence that vaccination of the reservoir host may impede MERS-CoV zoonotic transmission to humans.

Introduction

The Middle East respiratory syndrome coronavirus (MERS-CoV) was first identified in September 2012 (1). This emerging zoonotic pathogen is associated with severe pneumonia, acute respiratory distress syndrome, and multi-organ failure in humans resulting in fatal outcomes. As of September of 2019, the World Health Organization (WHO) has been notified of 2,458 laboratory-confirmed cases in humans with at least 848 deaths (2). MERS-CoV cases have been reported in 27 countries, mainly in the Middle East. In addition, a major outbreak occurred in South Korea in 2015 with 186 cases and 39 fatalities (3). Therefore, MERS-CoV appears to be a current worldwide public health threat.

The dromedary camel is the main reservoir for MERS-CoV and plays a key role in the infection of primary human cases (4,5). In New World camelid species, MERS-CoV infection was evidenced by the presence of MERS-CoV neutralizing antibodies (NAbs) (6,7). Furthermore, MERS-CoV experimental infections in alpacas and llamas confirmed that both could serve as potential reservoirs (8-10).

Due to the high human lethality rates and the absence of MERS-CoV-licensed vaccines or treatments, MERS-CoV has been prioritized for research and product development in the WHO R&D Blueprint for Action to Prevent Epidemics (11,12). The WHO has suggested animal vaccination as the best strategy to control MERS-CoV infections, since reduction of virus shedding can potentially prevent both animal-to-animal and zoonotic transmissions, and might have a faster development and licensing pathway compared to human vaccination (11).

The current MERS-CoV vaccine candidates mainly use the entire or sub regions of the spike (S) protein or its coding gene. This virus surface structural glycoprotein binds to the host receptor, dipeptidyl peptidase 4 (DPP4) (13), through its S1 subunit and is therefore the target of choice to raise Nabs (14,15). The S1 subunit protein is immunogenic and can induce both T-cell mediated and NAb responses mainly directed towards the receptor binding domain (RBD, also named as $S1^B$ domain) (14,16). Recently, we reported that although most NAbs target the $S1^B$ domain, antibodies targeting the S1 sialic acid binding domain ($S1^A$ domain) can also provide protection against lethal MERS-CoV challenge in a mouse model (17).

Several vaccine prototypes to control MERS-CoV have been tested using a wide variety of delivery systems, including DNA vaccines, protein-based vaccines, vector-based vaccines and live attenuated vaccines (15,18). Vector-based-vaccines have been developed using the orthopox modified virus Ankara (MVA) (19), different host-origin adenovirus (AdV) (20-23), measles virus (MeV) (24), rabies virus (RABV) (25), and Venezuelan equine encephalitis

replicons (VRP) (22,26), all expressing different lengths of the S protein. These vector-based candidates were tested in human DPP4 (hDPP4) transgenic or transduced mice, except the orthopox-based recombinant vaccine, which expresses the full-length MERS-CoV spike protein and induced efficient protective immunity in dromedaries (19). Due to reticence in applying live genetically modified organisms, protein recombinant subunit or DNA vaccines mainly based on the S1 protein or gene, respectively, are also under study. A DNA-based vaccine expressing the full-length S protein was shown to induce MERS-CoV specific NAbs and confer protection in rhesus macaques (27). In addition, MERS-CoV protein-based vaccines using the full-length or fragments of the S protein were produced in the form of virus-like particles, nanoparticles, peptides, or recombinant protein. Partial protection efficacy for some candidates has been demonstrated in non-human primates (NHP) (28,29) and hDPP4 transgenic mice (30-36). A more recent study demonstrated that an S protein subunit vaccine conferred protection to MERS-CoV (EMC/2012 strain) in an alpaca model, although in dromedary camels the vaccine was only able to reduce and delay viral shedding (37). However, there is no evidence that any of the MERS-CoV vaccine candidates developed so far are able to block MERS-CoV transmission in camelids when tested in a direct-contact virus transmission setting, mimicking natural transmission in the field. Vaccinating the MERS-CoV animal reservoirs can potentially reduce transmission to humans and provide a simple and economical solution to avoid expansion of this threatening disease.

In the present study, we show efficient MERS-CoV transmission among llamas. Furthermore, we have successfully used this direct-contact transmission model to demonstrate the efficacy of a recombinant S1-protein vaccine, using a registered adjuvant, to block MERS-CoV transmission.

Materials and methods

Animal welfare and ethics

Experiments with MERS-CoV were performed at the Biosafety Level-3 (BSL-3) facilities of the Biocontainment Unit of IRTA-CReSA (Barcelona, Spain). The present study was approved by the Ethical and Animal Welfare Committee of IRTA (CEEA-IRTA) and by the Ethical Commission of Animal Experimentation of the Autonomous Government of Catalonia (file No. FUE-2017-00561265).

Cell culture and MERS-CoV

Vero cells were cultured in Dulbecco's modified Eagle medium, DMEM (Lonza) supplemented with 2% fetal calf serum (FCS; EuroClone), 100 U/ml penicillin (ThermoFisher Scientific, Life

Technologies), 100 µg/ml streptomycin (ThermoFisher Scientific, Life Technologies), and 2 mM glutamine (ThermoFisher Scientific, Life Technologies). A passage 2 MERS-CoV stock (Qatar15/2015 strain) was propagated in Vero cells at 37°C in a CO_2 incubator for 3 days. The infectious virus titer was determined in Vero cells and calculated by determining the dilution that caused cytopathic effect (CPE) in 50% of the inoculated cell cultures (50% tissue culture infectious dose endpoint, $TCID_{50}$).

Vaccine

Full-length MERS-CoV S1 recombinant protein, including A and B domains, was produced in house using baculovirus and HEK 293T cells production systems as previously described (17,38). In brief, to produce soluble MERS-CoV S1 using the baculovirus expression system, the gene fragment encoding the MERS-CoV S1 subunit (amino acid 19–748; EMC/2012 isolate; GenBank Accession YP_009047204.1) was codon-optimized for insect cell expression and cloned in-frame between honeybee melittin (HBM) secretion signal peptide and a triple StrepTag purification tag in the pFastbac transfer vector. Generation of bacmid DNA and recombinant baculovirus was performed according to protocols from Bac-to-Bac system (Invitrogen), and expression of MERS-CoV S1 was performed by infection of recombinant baculovirus of Sf-9 cells. Recombinant proteins were harvested from cell culture supernatants 3 days post infection and purified using StrepTactin sepharose affinity chromatography (IBA).

Production of recombinant MERS-S1 in HEK 293T cells was described previously (17,38). In brief, the MERS-S1 (amino acid 1–747; EMC/2012 isolate; GenBank Accession YP_009047204.1) encoding sequence was C-terminally fused to a gene fragment encoding the Fc region of human IgG and cloned into the pCAGGS mammalian expression vector, expressed by plasmid transfection in HEK-293T cells, and affinity purified from the culture supernatant using Protein-A affinity chromatography. The Fc part of S1-Fc fusion protein was proteolytically removed by thrombin following Protein-A affinity purification using the thrombin cleavage site present at the S1-Fc junction.

Animals, vaccination and experimental design

Sixteen healthy llamas were purchased and housed at IRTA farm facilities at Alcarràs (Catalonia, Spain) during the immunization period and transferred for challenge at the BSL-3 animal facilities of the Biocontainment Unit of IRTA-CReSA, in Barcelona (Spain).

Five llamas were prime vaccinated each with 35 µg of a recombinant S1 protein produced in a baculovirus system, emulsified (1:1 volume) with Montanide™ ISA 206 VG (Seppic) adjuvant and intramuscularly administered (2 ml per animal and dose) in the right side of the neck. A boosting immunization was conducted 3 weeks later as above (left side of the

neck) but with 50 µg of recombinant S1 protein produced in HEK 293T cells, emulsified (1:1 volume) with Montanide™ ISA 206 VG (Seppic) adjuvant. The correct structure of the S1 antigens was previously confirmed by reactivity of conformational antibodies, DPP4 solid phase and sialic acid binding assays (17). Two weeks later, MERS-CoV challenge was performed. The experiments on virus transmission and vaccine efficacy were conducted in two separate boxes. In box 1, a group of llamas ($n = 3$) were intranasally inoculated with a 10^7 $TCID_{50}$ dose of MERS-CoV Qatar15/2015 strain (GenBank Accesion MK280984) in 3 ml saline solution (1.5 ml in each nostril) using a nebulization device (LMA® MADgic®, Teleflex Inc.). At 2 days post-inoculation (dpi) naïve llamas ($n = 5$) were put in contact with infected llamas (Figure 1a, Supplementary Figure S1). In box 2, the same protocol as in box 1 was followed but using vaccinated llamas ($n = 5$) as a contact group (Figure 1b). Each box was set up as in a previous transmission study performed in pigs (39).

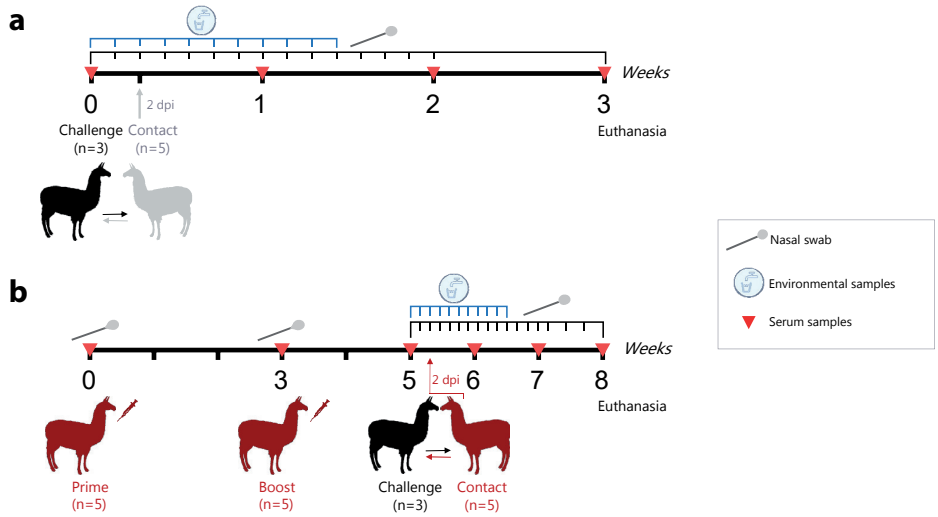

Figure 1. Schematic diagram of the llama transmission **(a)** and vaccination **(b)** experiments. **(a)** Three llamas (black, LL1-3) were intranasally inoculated with MERS-CoV (Qatar15/2015) and two days later were brought in contact with five naïve llamas (grey, LL7-11). **(b)** Vaccination, challenge and sampling scheme showing vaccinated llamas (red, $n = 5$, LL12-16) and directly inoculated llamas (black, $n = 3$; LL4-6) used as a transmission challenge model for MERS-CoV. Dpi, days post-inoculation.

Regarding to the nomenclature used in this study, animals 1–3 and 4–6 corresponded to intranasally inoculated llamas in boxes 1 and 2, respectively. Llamas 7–11 were naïve contact animals and llamas 12–16 were immunized contact animals.

Animals were monitored daily for clinical signs (sneezing, coughing, nasal discharge or dyspnea). Rectal temperatures were recorded with a fast display digital thermometer

(AccuVet®) until day 13 or 15 post-inoculation (pi) for animals in boxes 1 and 2, respectively. For llamas housed in box 1, nasal swabs (NS) were obtained daily until day 14 pi, while in box 2 NS were collected daily until day 15 pi and two extra collections were performed on 17 and 19 dpi. Serum samples were obtained before the first and the second immunizations, prior to challenge, and weekly after the MERS-CoV challenge. Animals were euthanized 3-weeks after challenge, with an overdose of pentobarbital. An extra sampling of NS was performed prior to necropsy procedures.

Environmental samples

Three different types of environmental samples (ES) were collected to determine viral loads in the boxes throughout the study (see Supplementary Figure S1), as previously described (39). An air filtering device (Sartorius MD8, Sartorius Stedim) was used for testing one thousand liters of air during 20 min (50 L/min air volume) through a gelatin membrane filter (ES1). One wall was scrubbed with two swabs (ES2 and ES3) and a water sample from the drinking point (ES4) was also obtained. ES were collected daily until 10 dpi.

Viral RNA detection by RT-qPCR

Viral RNA in collected samples was detected by RT-qPCR as previously described (10,39}. Briefly, NS and ES, except water samples, were transferred into cryotubes containing either 500 µL DMEM (Lonza) or PBS (Lonza) supplemented with 100 U/ml penicillin (ThermoFisher Scientific, Life Technologies) and 100 µg/ml streptomycin (ThermoFisher Scientific, Life Technologies), vortexed and stored at −80°C until use. Water samples were directly frozen at −80°C instead. Viral RNA from NS and ES was extracted with a NucleoSpin® RNA virus kit (Macherey-Nagel) following the manufacturer's instructions. The RNA extracts were tested by using the UpE PCR (40). RT-qPCR was carried out using AgPath-IDTM One-Step RT–PCR Reagents (Applied Biosystems, Life Technologies), and amplification was done by using a 7500 Fast Real-Time PCR System (Applied Biosystems, Life Technologies) programmed as follows: 10 min at 50°C, 10 sec at 95°C, and 45 cycles of 15 s at 95°C and 30 sec at 58°C. Samples with a quantification cycle (Cq) value ≤ 40 were considered positive for MERS-CoV RNA. To test for viral replication, viral RNA extracted form NS was tested for the presence of M mRNA according to the previously published protocol by Coleman et al. (41).

Viral RNA sequencing

Viral RNA was extracted from llama NS using the QIAamp viral RNA mini kit (Qiagen) according to the manufacturer's instructions. cDNA was produced from RNA using Superscript III first strand synthesis system (Invitrogen Corp) using random hexamers.

The cDNA was then used as a template to PCR amplify the MERS-CoV spike S1 encoding region (nucleotides positions 21,304–25,660, GenBank Accession JX869059) using the PfuUltra II Fusion HS DNA polymerase (Aligent Technologies). The PCR was carried out as follows: 95°C for 5 min, 39 cycles of 20 sec at 95°C, 20 sec at 48°C, and 45 sec at 72°C, and a final extension at 72°C for 1 min. The amplicons were sequenced bidirectionally using the BigDye Terminator v3.1 cycle sequencing kit on an ABI PRISM 3130XL Genetic analyzer (Applied Biosystems).

Virus titration

NS and ES collected at different times pi were evaluated for the presence of infectious virus by titration in Vero cells, as previously reported (10,19). Ten-fold dilutions were done, starting with a dilution of 1:10, and dilutions were transferred to Vero cells. Plates were daily monitored under the light microscope and wells were evaluated for the presence of CPE at 5 dpi. The amount of infectious virus in swabs was calculated by determining the $TCID_{50}$.

MERS-CoV S1-ELISA

Specific S1-antibodies in serum samples from all collected time-points and from all animals were determined by a MERS-CoV S1-ELISA as previously described (10,19). Briefly, 96-well high-binding plates (Sigma-Aldrich) were coated with 100 µl of S1 protein (42) at 1 µg/ml in PBS o/n at 4°C. After blocking with 1% bovine serum albumin/PBS/0.5% Tween20 for 1 h at 37°C, serum samples were tested at a 1:100 dilution, followed by 1 h incubation at 37°C. Plates were washed 4 times with PBS, and wells were incubated with a goat anti-llama biotin conjugate (Abcore, 1:1,000 diluted in blocking buffer), followed by incubation with streptavidin peroxidase (Sigma-Aldrich). After 1 h of incubation at 37°C, wells were washed 4 times with PBS, and a TMB substrate solution (Sigma-Aldrich) was added and allowed to develop for 8–10 min at room temperature, protected from light. Optical density was measured at 450 nm.

MERS-CoV N-LIPS

We tested llama sera for MERS-CoV nucleocapsid (N) specific antibody responses using a luciferase immunoprecipitation (LIPS) assay (43). The N protein was expressed as an N-terminal *Renilla* luciferase (Ruc)-tagged protein (Ruc-N) using pREN2 expression vector. The cells were lysed, and the luminescence units (LU)/µl was measured in cell lysates. LIPS assay was done according to a previous protocol with minor modifications (44). Briefly, serum samples were diluted 1:100 and mixed with 1×10^7 LU of Ruc-N in a total volume of 100 µl in buffer A (20 mM Tris, pH 7.5, 150 mM NaCl, 5 mM $MgCl_2$, 1% Triton X-100). The

mixture was incubated on a rotary shaker for 1 h at room temperature. Then, the mixture was transferred into MultiScreenHTS BV Filter Plate (Merk Millipore) containing 5 µl of a 30% suspension of UltraLink protein A/G beads and further incubated for one hour. The wells were then washed and luminescence was measured for each well after adding 100 µl of 0.1 µM coelenterazine (Nanolight Technology) in assay buffer (50 mM potassium phosphate, pH 7.4, 500 mM NaCl, 1 mM EDTA). The sera were tested in duplicates in at least two independent assays and the data was averaged to determine the LU value for each sample.

Hemagglutination inhibition (HI) assay

To test llama sera from the vaccine efficacy study for functional antibodies against the sialic acid binding S1 N-terminal domain ($S1^A$), a nanoparticle-based HI assay was used. $S1^A$ lumazine synthase (LS) nanoparticles were produced as described previously (17,45). Two-fold diluted sera were mixed with 4 HA units of $S1^A$-LS and incubated for 30 min at 37°C. Following incubation, 0.5% washed turkey RBCs were added and further incubated for 1 h at 4°C. HI titers were determined as the reciprocal of highest serum dilution showing inhibition of hemagglutination.

Receptor binding inhibition (RBI) assay

We tested llama sera from the vaccine efficacy study for antibodies able to block MERS-CoV binding to its receptor (DPP4) using a competitive ELISA. ELISA plates were coated with 2 µg/ml recombinant soluble DPP4 protein (13) overnight at 4°C. The plates were washed with PBS and blocked with 1% BSA in PBS/0.1% Tween-20 at 37°C for 1 h. Serum samples were tested at a 1:20 dilution. Recombinant MERS-CoV S1-mFc was mixed with diluted sera, incubated for 1 hr at 37°C, added to the plate and further incubated for 1 h. The plates were then washed and HRP-labelled rabbit anti-mouse Igs was added to detect S1 bound to DPP4. Following 1 h of incubation, the plates were washed and the signal was detected using TMB as described above. Optical density was measured at 450 nm.

Plaque reduction neutralization assay

Serum samples and nasal swabs were further tested for neutralizing antibodies against MERS-CoV (Qatar15/2015 and EMC/2012 isolates) using a plaque reduction neutralization (PRNT) assay. PRNT assay was carried out using according to the previously published protocol (19) with some modification. Briefly, samples were first inactivated at 56°C for 30 min. Then, 50 µl of 2-fold serial dilutions of heat-inactivated serum were mixed 1:1 with virus (400 PFU) prior to over-layering onto Huh7 cells. After 8 h of infection, the cells were

fixed and stained using mouse anti-MERS-CoV nucleocapsid protein (SinoBiological) and HRP-conjugated goat anti-mouse IgG1 (SouthernBiotech). The number of infected cells were detected using a precipitate-forming TMB substrate (True Blue, KPL) and counted using an ImmunoSpot® Image analyzer (CTL Europe GmbH). The PRNT titer was calculated based on a 50% or greater reduction in infected cells counts.

Results

Clinical signs

Three out of the six directly-inoculated and one out of the five contact naïve llamas showed moderate nasal mucus secretion at 8–15 dpi (see Supplementary Figure S2). No clinical signs were noticed in any of the five vaccinated llamas throughout the study. Despite higher basal body temperatures, no animals housed in box 1 (inoculated and non-vaccinated in-contact llamas) showed a significant increase in body temperatures above 40°C upon MERS-CoV challenge. In box 2 (inoculated and vaccinated in-contact llamas), body temperatures in llamas remained constant all along the experiment and never exceeded 39.5°C.

MERS-CoV RNA and infectious virus

All MERS-CoV inoculated llamas shed viral RNA in the nasal cavity during a 2-week period (Figure 2a, b). The amount of viral RNA was still high (Cq values < 25) in all inoculated llamas at 6-7 dpi, but a decrease in RNA load was observed from 8 dpi onwards. In-contact naïve llamas from box 1 revealed evidence of infection (detectable viral RNA) 4–5 days after contact, with viral RNA loads and duration of shedding similar to those of the inoculated animals (Figure 2a). In box 2, only one out of the five vaccinated llamas (No. 15) had viral RNA in the nasal cavity to levels comparable to non-vaccinated in-contact animals, while the other four animals had very low levels of viral RNA (Figure 2b). Additionally, the viral RNA from this llama was sequenced at days 9–12 pi and used for comparative analysis of the S1 protein (see Supplementary Figure S3). A substitution of serine for phenylalanine was found at the amino acid position 465 (S465F) in comparison with the inoculum isolate S1 protein (see Supplementary Figure S3a). This mutation was also found in another vaccinated llama (No. 13) at 10 dpi. Interestingly, we identified the S465F mutation arising at 5–6 dpi in three directly inoculated llamas (No. 1, 4, 5). Furthermore, the naïve contact animals were also investigated and the same mutation was found in llama No. 9 at 10 dpi (see Supplementary Figure S3b). To ensure that this mutant is not a neutralization escape mutant, the mutant virus was plaque-purified form the nasal swab of llama No. 4 at 6 dpi. The virus was sequenced (Llama-passaged-Qatar15; GenBank Accession MN507638) to ensure no other mutations

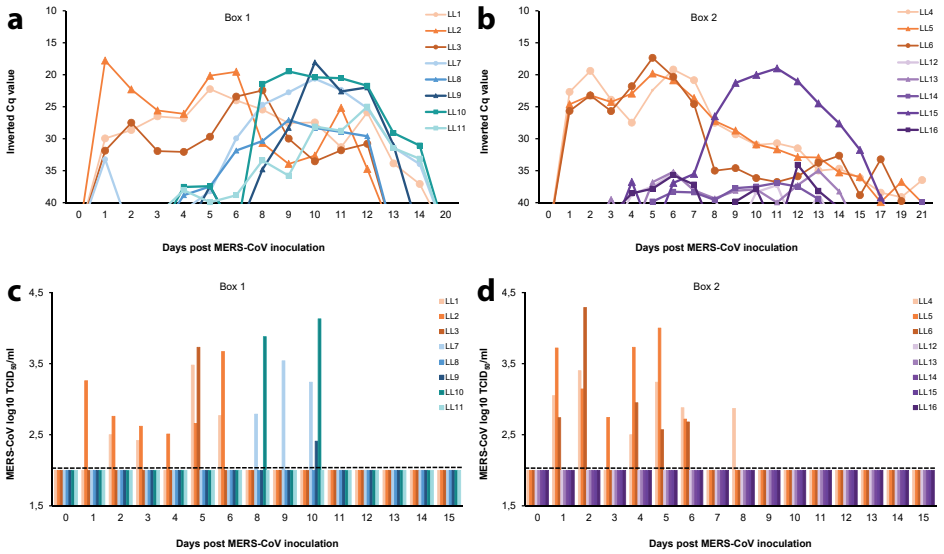

Figure 2. Viral shedding in llamas after experimental inoculation or contact with MERS-CoV-infected llamas. Viral RNA detected in nasal swab samples collected from naïve **(a)** and S1 vaccinated **(b)** llamas at different time points after contact with directly inoculated animals. Panels **c)** and **d)** display infectious MERS-CoV in nasal swab samples collected from naïve **(c)** and S1 vaccinated animals **(d)** at different time points after inoculation. Each line/bar represents an individual animal. Orange lines/bars indicate experimentally inoculated llamas. Blue and green lines/bars indicate in-contact naïve animals, while purple lines/bars indicate vaccinated llamas. Dashed lines depict the detection limit of the assays. Cq, quantification cycle; MERS-CoV, Middle East respiratory syndrome coronavirus; $TCID_{50}$, 50% tissue culture infective dose.

were present in the spike protein and then used to carry out neutralization assays. The virus was neutralized by serum of all five vaccinated animals (Supplementary Figure S4a).

RT-qPCR positive nasal swab samples were tested for the presence of infectious virus. All intranasally inoculated llamas excreted infectious MERS-CoV at some point until 8 dpi (Figure 2c, d). The duration of infectious virus shedding varied among individual animals ranging from 1 up to 6 consecutive days. In each box, at least one inoculated llama (animals No. 2 and 5) shed infectious virus continuously from days 1–6 pi (Figure 2c, d). Three out of the five direct contact naïve llamas from box 1 shed infectious virus at 8, 9 and 10 dpi (Figure 2c). These non-vaccinated in-contact animals (No. 7, 9 and 10) exhibited virus titers at least equal to those observed in inoculated llamas (Figure 2c, d). The peaks of viral RNA coincided with the highest levels of infectious virus shed. Although llama No. 15 had MERS-CoV mRNA indicative of replication in the nasal cavity to levels comparable to non-vaccinated in-contact animals (Supplementary Figure S5), as assessed by the specific RT-qPCR described by Coleman and collaborators (41), none of the vaccinated animals from box 2 (including llama No. 15) shed infectious virus at any point in the study (Figure 2d),

Llama No. 7 showed low levels of MERS-CoV RNA at 1 dpi before in-contact challenge (Figure 2a). However, this animal remained negative to RT-qPCR until 5 dpi, suggesting that a contamination occurred during the collection or the processing of this sample. Additionally, no infectious virus was detected in this animal at 1 dpi (Figure 2c).

Relatively low levels of viral RNA were detected in all types of environmental samples that were taken in the boxes during the experiment (≥ 30 Cq) (Table 1). The highest MERS-CoV RNA levels were found in drinking water samples. However, titration of infectious virus was not successful.

Table 1. MERS-CoV RNA detection in environmental samples expressed in Cq values at different times after inoculation. Swab 1 and 2 correspond to ES2 and ES3 of Supplementary Figure S1, respectively. Cq, quantification cycle; MERS-CoV, Middle East respiratory syndrome coronavirus; nc, non-collected samples.

Days post-inoculation	0	1	2	3	4	5	6	7	8	9	10
Box 1 – transmission study											
Sartorius	–	–	35.0	–	36.2	39.4	38.5	nc	38.2	38.7	31.9
Swab 1	–	–	–	–	36.6	–	39.5	nc	32.2	39.6	38.0
Swab 2	–	39.9	–	38.3	35.9	35.4	37.0	nc	34.3	38.1	36.6
Water	–	36.3	–	–	–	–	36.0	nc	38.7	33.4	33.2
Box 2 – vaccine trial											
Sartorius	–	–	–	–	–	–	–	36.8	38.5	–	–
Swab 1	–	–	–	–	36.4	–	39.1	37.9	37.3	30.9	34.0
Swab 2	–	–	–	36.8	–	37.2	–	37.6	–	31.4	35.9
Water	–	–	–	37.9	35.2	30.9	31.9	33.9	34.6	38.8	37.5

Humoral immune response

We evaluated the MERS-CoV specific antibody responses induced in llamas following infection and vaccination. Regarding the transmission study, all directly inoculated and in-contact naïve llamas seroconverted to MERS-CoV as detected by MERS-CoV S1 ELISA (Figure 3a) and virus neutralization (Figure 3b). In contrast, only three of those, two directly inoculated and one in-contact, also developed anti-N antibody responses (see Supplementary Figure S6a). Antibodies against the $S1^A$ sialic acid binding domain were detected in one of the directly inoculated and four in-contact naïve animals using a HI assay (Figure 3c). Receptor-binding blocking (mainly RBD-directed) antibodies were detected in the sera of all directly inoculated animals and in four out of the five in-contact naïve llama sera using a competitive RBI ELISA (Figure 3d).

Following MERS-CoV S1 vaccination, all vaccinated animals (Figure 4a-d, red) developed high titers of serum S1-reactive antibodies (Figure 4a) and virus neutralizing antibodies

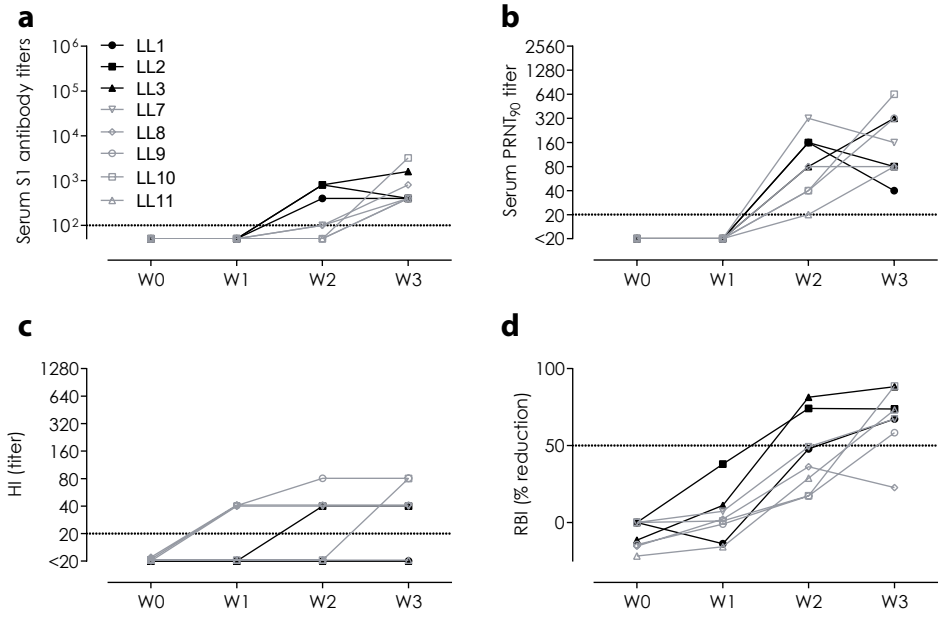

Figure 3. Serum antibodies elicited against MERS-CoV in inoculated and in-contact naïve llamas. **(a)** MERS-CoV spike S1, **(b)** MERS-CoV neutralizing (Qatar15/2015 strain), **(c)** hemagglutination inhibition (HI; anti-$S1^A$ N-terminal domain), and **(d)** receptor binding inhibition (RBI; anti-S1 receptor binding domain) antibodies. The horizontal dotted lines indicate the cutoff of each assay. HI, hemagglutination inhibition; LL, llama; PRNT, plaque reduction neutralization assay; RBI, receptor binding inhibition; W, week.

against both clade B Qatar15/2015 and a clade A EMC/2102 isolates as detected by PRNT (Figure 4b, Supplementary Figure S4b). In particular, the vaccination induced antibodies against the two functional domains of S1, the $S1^A$ binding N-terminal domain as detected by HI assay (Figure 4c) and the RBD as detected by a competitive RBI ELISA (Figure 4d). Additionally, only one directly inoculated but none of the vaccinated animals developed antibodies against the N protein (Supplementary Figure S6b). Aiming to assess mucosal immunity elicited upon vaccination, we evaluated the presence of antibodies in the nasal cavity. Remarkably, we detected low levels of both MERS-CoV S1-directed and neutralizing antibodies in the nasal swabs of three out of the five vaccinated animals (Figure 4e,f).

Discussion

In this study, experimental MERS-CoV transmission from infected llamas to naïve in-contact llamas has been demonstrated for the first time. Consistent with previous studies (10), all MERS-CoV inoculated llamas got infected, shed infectious virus and were able to transmit

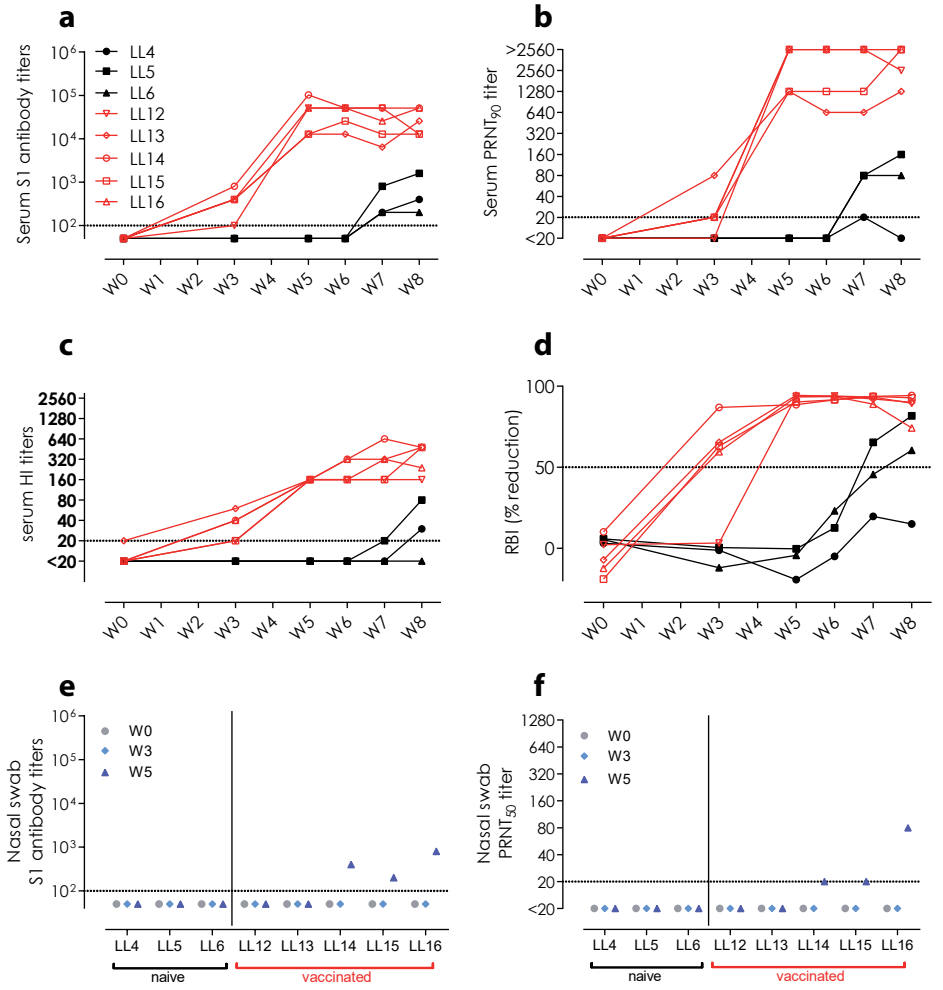

Figure 4. Antibody responses to MERS-CoV elicited in directly inoculated (LL4-6; black) and in-contact MERS-CoV S1 vaccinated (LL12-16; red) llamas in sera **(a-d)** and nasal swabs **(e,f)**. **(a,e)** MERS-CoV S1-reactive antibodies, **(b,f)** MERS-CoV neutralizing antibodies (Qatar15/2015 strain), **(c)** hemagglutination inhibition (HI; anti-S1^N terminal domain) antibodies, and **(d)** receptor binding inhibition (RBI; anti-S1 receptor binding domain) antibodies. The horizontal dotted lines indicate the cutoff of each assay. HI, hemagglutination inhibition; LL, llama; PRNT, plaque reduction neutralization assay; RBI, receptor binding inhibition; W, week.

the virus to all naive contact animals as assessed by MERS-CoV RNA and viral titration of the nasal swabs. We confirmed that 3 infected llamas were able to transmit MERS-CoV to at least 5 naïve animals; nonetheless, further studies are needed to determine the basic reproduction ratio of this virus transmission in camelids. Interestingly, the three contact llamas shedding infectious MERS-CoV showed the highest viral RNA loads, while the remaining two had higher Cq values and no infectious virus was isolated. Altogether, taking

into account that (i) viral genomic replication was observed in all in-contact naïve llamas for an extended period, (ii) 3 out of 5 in-contact animals shed detectable infectious virus and (iii) one of them exhibited nasal discharges, this in-contact model of virus transmission is valuable to test vaccine efficacy. However, before stating that llamas can be surrogates of dromedaries for vaccine testing in an in-contact model, it would be important to assess whether infectious viral pressure elicited by the experimental challenge are similar between these two animal species. In that respect, in a previous report, two dromedaries inoculated with the MERS-CoV EMC/2012 strain shed viral RNA and infectious virus for 13 and 6 days, respectively (19), similar to what we found in the present study in llamas infected intranasally with the MERS-CoV Qatar15/2015 strain.

Based on the *in vivo* protective capacity of monoclonal antibodies directed against different domains of the spike protein (17), a broader protective immune response can be achieved using multi-domain vaccines ($S1^A$ and $S1^B$ domains) compared to RBD-focused vaccines. Thus, the efficacy of an S1 recombinant protein emulsified with the adjuvant Montanide™ ISA 206 VG was evaluated as a potential vaccine candidate. We showed that immunized llamas were efficiently protected against MERS-CoV infection; no infectious virus was detected in the nose of any of the vaccinated animals and viral RNA shedding remained low (Cq ≥ 34), with the exception of one llama (No. 15). Viral mRNA was also detected in the nasal cavity of this llama, which might be from intracellular viral mRNA from cells harvested in the nasal swabs; nonetheless, we could not detect any infectious virus. Neutralization of the virus by antibodies at mucosal level may have inhibited infectious viral particle production. The lack of detectable infectious virus in the vaccinated llamas despite being infected, renders these animals unlikely to transmit the virus further to other animals and thus blocking the transmission chain. In addition, our studies revealed a mutation (S465F) in the spike protein encoded by this viral RNA, which may suggest a potential escape variant being produced. However, the emergence of the same mutation in another vaccinated llama, in one naïve in-contact animal and in other three directly inoculated llamas was revealed. In addition, the capacity of vaccinated animals to induce NAbs against this variant when isolated, indicate that it is unlikely an escape variant induced under antibody pressure. Mutation at this site (S465F) is not directly involved in receptor binding but has been previously reported to occur as a result of virus adaptation to its host receptor (46). Overall, this indicates a probable adaptive mutation rather than a vaccine escape mutation.

Immunization with the S1 protein induced antibodies against the RBD as confirmed by the RBI and virus neutralization assays as well as antibodies to the $S1^A$ domain as confirmed by HI assay. These latter antibodies may be important in blocking virus attachment to sialic acid present in camelids, as it has been demonstrated in the dromedary camel upper respiratory tract (45). Importantly, serum NAbs were generated in all vaccinated animals

after the boosting immunization and were maintained during challenge. Therefore, a correlation of NAb levels in serum upon vaccination and protection occurred, as previously described in another vaccination study in camelids (37). Notably, we detected mucosal NAb in the nasal cavity of 3 out of 5 vaccinated llamas, as also reported in dromedary camels immunized with an MVA-based candidate (19). In addition, we demonstrate that vaccination of llamas with a spike protein from a clade A MERS-CoV (EMC/2012 isolate) provides protection against a challenge with a clade B virus (Qatar15/2015 islolate). Since evidence of MERS-CoV reinfection has been reported in camels in the field (47), further studies to determine whether intramuscular administration of the subunit vaccine can boost mucosal immunity in the upper respiratory tract of animals that have been previously exposed to MERS-CoV are needed.

A critical component of a vaccine that influences the duration and the quality of immune responses is the adjuvant. Here we used the Montanide™ ISA 206 VG adjuvant, which was shown to induce long-term protective immunity in large animal species by stimulating both cell-mediated and humoral immune responses (48). Further studies should be conducted in target species in order to determine the optimal antigen dose and the persistence of NAb following S1 recombinant vaccination. In fact, here, two doses of 35 and 50 µg were enough to induce protection, as opposed to a recent study which used 3 doses of 400 µg of the S1 antigen with a combination of adjuvants (37). Unlike vector-based vaccines, protein-based vaccines do not require safety testing in high containment facilities and field studies could be directly conducted; thus, reducing the cost of the proposed vaccine. The registered adjuvant used in this study, Montanide™ ISA 206 VG, offers economical and practical use for field applications. Therefore, the S1 recombinant vaccine tested in this study appears as a good candidate to prevent animal-to-animal and, eventually, animal-to-human transmission.

Overall, this work revealed that the llama model can be a surrogate for dromedary camel in MERS-CoV transmission and vaccination studies. Moreover, immunization with the MERS-CoV S1 recombinant protein, in combination with a commercial adjuvant, efficiently limits infectious viral shedding from vaccinated llamas upon exposure to directly inoculated ones.

Acknowledgements

The authors want to thank Dr. Joan Pujols and Dr. Xavier Abad for scientific discussions. The pREN2 expression vector was kindly provided by Dr. Peter D Burbelo.

References

1. Zaki AM, van Boheemen S, Bestebroer TM, Osterhaus AD, Fouchier RA. Isolation of a novel coronavirus from a man with pneumonia in Saudi Arabia. The New England journal of medicine. 2012 Nov 8;367(19):1814-20.
2. World Health Organization. Middle East respiratory syndrome coronavirus (MERS-CoV) [cited 01-11-2019]; Available from: http://www.who.int/emergencies/mers-cov/en/
3. World Health Organization. WHO MERS Global Summary and Assessment of Risk. 2019.
4. Sabir JS, Lam TT, Ahmed MM, Li L, Shen Y, Abo-Aba SE, et al. Co-circulation of three camel coronavirus species and recombination of MERS-CoVs in Saudi Arabia. Science. 2016 Jan 1;351(6268):81-4.
5. Mohd HA, Al-Tawfiq JA, Memish ZA. Middle East Respiratory Syndrome Coronavirus (MERS-CoV) origin and animal reservoir. Virol J. 2016 Jun 3;13:87.
6. Reusken CB, Schilp C, Raj VS, De Bruin E, Kohl RH, Farag EA, et al. MERS-CoV Infection of Alpaca in a Region Where MERS-CoV is Endemic. Emerg Infect Dis. 2016 Jun;22(6):1129-31.
7. David D, Rotenberg D, Khinich E, Erster O, Bardenstein S, van Straten M, et al. Middle East respiratory syndrome coronavirus specific antibodies in naturally exposed Israeli llamas, alpacas and camels. One Health. 2018 Jun;5:65-8.
8. Crameri G, Durr PA, Klein R, Foord A, Yu M, Riddell S, et al. Experimental Infection and Response to Rechallenge of Alpacas with Middle East Respiratory Syndrome Coronavirus. Emerg Infect Dis. 2016 Jun;22(6):1071-4.
9. Adney DR, van Doremalen N, Brown VR, Bushmaker T, Scott D, de Wit E, et al. Replication and shedding of MERS-CoV in upper respiratory tract of inoculated dromedary camels. Emerg Infect Dis. 2014 Dec;20(12):1999-2005.
10. Vergara-Alert J, van den Brand JM, Widagdo W, Munoz Mt, Raj S, Schipper D, et al. Livestock Susceptibility to Infection with Middle East Respiratory Syndrome Coronavirus. Emerg Infect Dis. 2017 Feb;23(2):232-40.
11. World Health Organization. WHO Target Product Profiles for MERS-CoV Vaccines. 2017.
12. FAO-OIE-WHO MERS Technical Working Group. MERS: Progress on the global response, remaining challenges and the way forward. Antiviral Res. 2018 Nov;159:35-44.
13. Raj VS, Mou H, Smits SL, Dekkers DHW, Müller MA, Dijkman R, et al. Dipeptidyl peptidase 4 is a functional receptor for the emerging human coronavirus-EMC. Nature. 2013 03/13/online;495:251.
14. Okba NM, Raj VS, Haagmans BL. Middle East respiratory syndrome coronavirus vaccines: current status and novel approaches. Current opinion in virology. 2017 Apr;23:49-58.
15. Cho H, Excler JL, Kim JH, Yoon IK. Development of Middle East Respiratory Syndrome Coronavirus vaccines - advances and challenges. Hum Vaccin Immunother. 2018 Feb 1;14(2):304-13.
16. Stalin Raj V, Okba NMA, Gutierrez-Alvarez J, Drabek D, van Dieren B, Widagdo W, et al. Chimeric camel/human heavy-chain antibodies protect against MERS-CoV infection. Science Advances. 2018 Aug;4(8):eaas9667.
17. Widjaja I, Wang C, van Haperen R, Gutierrez-Alvarez J, van Dieren B, Okba NMA, et al. Towards a solution to MERS: protective human monoclonal antibodies targeting different domains and functions of the MERS-coronavirus spike glycoprotein. Emerging Microbes & Infections. 2019 2019/01/01;8(1):516-30.
18. Xu J, Jia W, Wang P, Zhang S, Shi X, Wang X, et al. Antibodies and vaccines against Middle East respiratory syndrome coronavirus. Emerging Microbes & Infections. 2019;8(1):841-56.
19. Haagmans BL, van den Brand JM, Raj VS, Volz A, Wohlsein P, Smits SL, et al. An orthopoxvirus-based vaccine reduces virus excretion after MERS-CoV infection in dromedary camels. Science. 2016 Jan 1;351(6268):77-81.

20. Guo X, Deng Y, Chen H, Lan J, Wang W, Zou X, et al. Systemic and mucosal immunity in mice elicited by a single immunization with human adenovirus type 5 or 41 vector-based vaccines carrying the spike protein of Middle East respiratory syndrome coronavirus. Immunology. 2015 Aug;145(4):476-84.
21. Kim E, Okada K, Kenniston T, Raj VS, AlHajri MM, Farag EA, et al. Immunogenicity of an adenoviral-based Middle East Respiratory Syndrome coronavirus vaccine in BALB/c mice. Vaccine. 2014 Oct 14;32(45):5975-82.
22. Cockrell AS, Yount BL, Scobey T, Jensen K, Douglas M, Beall A, et al. A mouse model for MERS coronavirus-induced acute respiratory distress syndrome. Nature microbiology. 2016 Nov 28;2:16226.
23. Hashem AM, Algaissi A, Agrawal AS, Al-Amri SS, Alhabbab RY, Sohrab SS, et al. A Highly Immunogenic, Protective, and Safe Adenovirus-Based Vaccine Expressing Middle East Respiratory Syndrome Coronavirus S1-CD40L Fusion Protein in a Transgenic Human Dipeptidyl Peptidase 4 Mouse Model. The Journal of Infectious Diseases. 2019 Oct 8;220(10):1558-67.
24. Malczyk AH, Kupke A, Prufer S, Scheuplein VA, Hutzler S, Kreuz D, et al. A Highly Immunogenic and Protective Middle East Respiratory Syndrome Coronavirus Vaccine Based on a Recombinant Measles Virus Vaccine Platform. Journal of Virology. 2015 Nov;89(22):11654-67.
25. Wirblich C, Coleman CM, Kurup D, Abraham TS, Bernbaum JG, Jahrling PB, et al. One-Health: a Safe, Efficient, Dual-Use Vaccine for Humans and Animals against Middle East Respiratory Syndrome Coronavirus and Rabies Virus. Journal of Virology. 2017 Jan 15;91(2).
26. Zhao J, Li K, Wohlford-Lenane C, Agnihothram SS, Fett C, Zhao J, et al. Rapid generation of a mouse model for Middle East respiratory syndrome. Proceedings of the National Academy of Sciences of the United States of America. 2014 Apr 1;111(13):4970-5.
27. Muthumani K, Falzarano D, Reuschel EL, Tingey C, Flingai S, Villarreal DO, et al. A synthetic consensus anti-spike protein DNA vaccine induces protective immunity against Middle East respiratory syndrome coronavirus in nonhuman primates. Sci Transl Med. 2015 Aug 19;7(301):301ra132.
28. Wang C, Zheng X, Gai W, Zhao Y, Wang H, Wang H, et al. MERS-CoV virus-like particles produced in insect cells induce specific humoural and cellular imminity in rhesus macaques. Oncotarget. 2017 Feb 21;8(8):12686-94.
29. Lan J, Yao Y, Deng Y, Chen H, Lu G, Wang W, et al. Recombinant Receptor Binding Domain Protein Induces Partial Protective Immunity in Rhesus Macaques Against Middle East Respiratory Syndrome Coronavirus Challenge. EBioMedicine. 2015 Oct;2(10):1438-46.
30. Zhang N, Channappanavar R, Ma C, Wang L, Tang J, Garron T, et al. Identification of an ideal adjuvant for receptor-binding domain-based subunit vaccines against Middle East respiratory syndrome coronavirus. Cellular & molecular immunology. 2016 Mar;13(2):180-90.
31. Lan J, Deng Y, Chen H, Lu G, Wang W, Guo X, et al. Tailoring subunit vaccine immunity with adjuvant combinations and delivery routes using the Middle East respiratory coronavirus (MERS-CoV) receptor-binding domain as an antigen. PloS one. 2014;9(11):e112602.
32. Tang J, Zhang N, Tao X, Zhao G, Guo Y, Tseng CT, et al. Optimization of antigen dose for a receptor-binding domain-based subunit vaccine against MERS coronavirus. Hum Vaccin Immunother. 2015;11(5):1244-50.
33. Tai W, Wang Y, Fett CA, Zhao G, Li F, Perlman S, et al. Recombinant Receptor-Binding Domains of Multiple Middle East Respiratory Syndrome Coronaviruses (MERS-CoVs) Induce Cross-Neutralizing Antibodies against Divergent Human and Camel MERS-CoVs and Antibody Escape Mutants. Journal of Virology. 2017 Jan 1;91(1):e01651-16.

34. Tao X, Garron T, Agrawal AS, Algaissi A, Peng BH, Wakamiya M, et al. Characterization and Demonstration of the Value of a Lethal Mouse Model of Middle East Respiratory Syndrome Coronavirus Infection and Disease. Journal of Virology. 2016 Jan 1;90(1):57-67.
35. Tai W, Zhao G, Sun S, Guo Y, Wang Y, Tao X, et al. A recombinant receptor-binding domain of MERS-CoV in trimeric form protects human dipeptidyl peptidase 4 (hDPP4) transgenic mice from MERS-CoV infection. Virology. 2016 Dec;499:375-82.
36. Jiaming L, Yanfeng Y, Yao D, Yawei H, Linlin B, Baoying H, et al. The recombinant N-terminal domain of spike proteins is a potential vaccine against Middle East respiratory syndrome coronavirus (MERS-CoV) infection. Vaccine. 2017 Jan 3;35(1):10-8.
37. Adney DR, Wang L, van Doremalen N, Shi W, Zhang Y, Kong WP, et al. Efficacy of an Adjuvanted Middle East Respiratory Syndrome Coronavirus Spike Protein Vaccine in Dromedary Camels and Alpacas. Viruses. 2019 Mar 2;11(3):212.
38. Mou H, Raj VS, van Kuppeveld FJ, Rottier PJ, Haagmans BL, Bosch BJ. The receptor binding domain of the new Middle East respiratory syndrome coronavirus maps to a 231-residue region in the spike protein that efficiently elicits neutralizing antibodies. Journal of Virology. 2013 Aug;87(16):9379-83.
39. Vergara-Alert J, Raj VS, Munoz M, Abad FX, Cordon I, Haagmans BL, et al. Middle East respiratory syndrome coronavirus experimental transmission using a pig model. Transboundary and emerging diseases. 2017 Oct;64(5):1342-5.
40. Corman VM, Eckerle I, Bleicker T, Zaki A, Landt O, Eschbach-Bludau M, et al. Detection of a novel human coronavirus by real-time reverse-transcription polymerase chain reaction. Euro surveillance : bulletin Europeen sur les maladies transmissibles = European communicable disease bulletin. 2012 Sep 27;17(39).
41. Coleman CM, Frieman MB. Growth and Quantification of MERS-CoV Infection. Current protocols in microbiology. 2015 May 1;37:15E 2 1-9.
42. Okba NMA, Raj VS, Widjaja I, GeurtsvanKessel CH, de Bruin E, Chandler FD, et al. Sensitive and Specific Detection of Low-Level Antibody Responses in Mild Middle East Respiratory Syndrome Coronavirus Infections. Emerg Infect Dis. 2019 Oct;25(10):1868-77.
43. Burbelo PD, Goldman R, Mattson TL. A simplified immunoprecipitation method for quantitatively measuring antibody responses in clinical sera samples by using mammalian-produced Renilla luciferase-antigen fusion proteins. BMC Biotechnol. 2005 Aug 18;5:22.
44. Burbelo PD, Ching KH, Klimavicz CM, Iadarola MJ. Antibody profiling by Luciferase Immunoprecipitation Systems (LIPS). Journal of visualized experiments : JoVE. 2009 Oct 7(32):e1549.
45. Li W, Hulswit RJG, Widjaja I, Raj VS, McBride R, Peng W, et al. Identification of sialic acid-binding function for the Middle East respiratory syndrome coronavirus spike glycoprotein. Proceedings of the National Academy of Sciences of the United States of America. 2017 Oct 3;114(40):E8508-E17.
46. Letko M, Miazgowicz K, McMinn R, Seifert SN, Sola I, Enjuanes L, et al. Adaptive Evolution of MERS-CoV to Species Variation in DPP4. Cell Rep. 2018 Aug 14;24(7):1730-7.
47. Hemida MG, Alnaeem A, Chu DK, Perera RA, Chan SM, Almathen F, et al. Longitudinal study of Middle East Respiratory Syndrome coronavirus infection in dromedary camel herds in Saudi Arabia, 2014-2015. Emerging Microbes & Infections. 2017 Jun 21;6(6):e56.
48. Ibrahim Eel S, Gamal WM, Hassan AI, Mahdy Sel D, Hegazy AZ, Abdel-Atty MM. Comparative study on the immunopotentiator effect of ISA 201, ISA 61, ISA 50, ISA 206 used in trivalent foot and mouth disease vaccine. Veterinary world. 2015 Oct;8(10):1189-98.

Supplementary Material

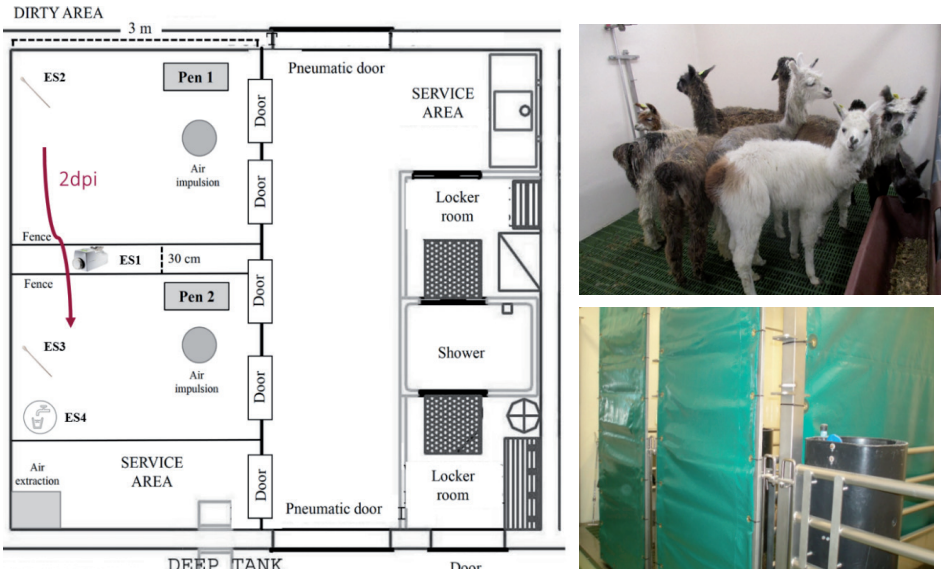

Supplementary Figure S1. Schematic representation of an experimental animal box. Contact and inoculated groups were placed in pens 1 and 2, respectively. Tarpaulin was used to prevent contact between groups during 2 days after inoculation.

Supplementary Figure S2. Clinical signs after MERS-CoV infection in contact llamas. Presence of mucus excretion in llama 7 at 13 days post-challenge.

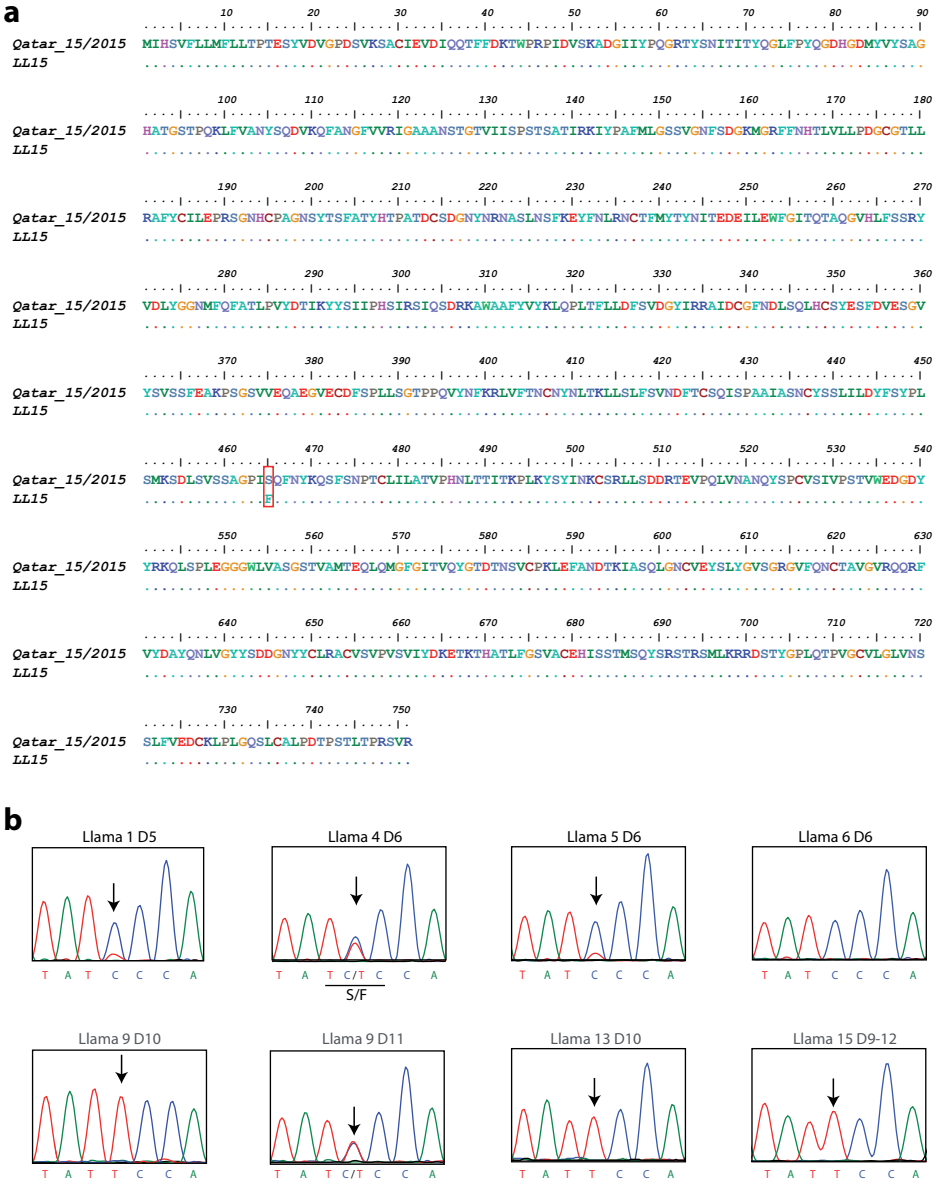

Supplementary Figure S3. (a) Sequence analysis of the spike S1 protein of MERS-CoV. The amino acid sequence of the S1 domain of MERS-CoV spike protein obtained by sequencing of the viral RNA isolated from an S1- vaccinated llama (LL15) at day 11 post-inoculation was compared to the sequence of the S1 of the virus used to directly inoculate the animals (Qatar_15/2015; GenBank Accession MK280984). **(b)** Sanger sequencing chromatograms of MERS-CoV spike S1 subunit from four directly inoculated llamas (No. 1 at day 5 pi and No. 4-6, day 6 pi), one in-contact naïve animal (No. 9 at days 10 and 11 pi) and two in-contact vaccinated llamas (No. 13 and 15, at 10 and 9-12 dpi, respectively). Arrows indicate emerging mutations.

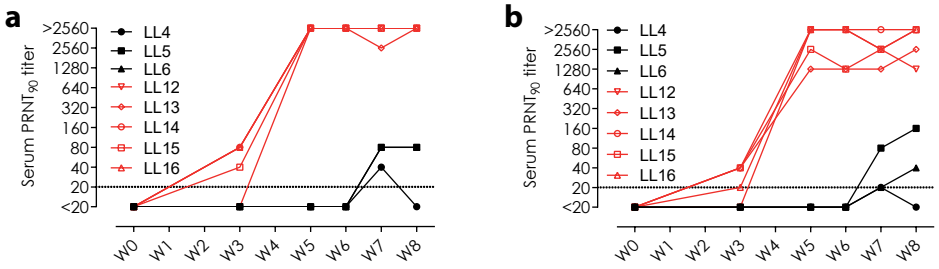

Supplementary Figure S4. Virus neutralizing antibodies against MERS-CoV **(a)** Llama-passaged-Qatar15 isolate and **(b)** EMC/2012 strain elicited in sera of directly inoculated (LL4-6; black) and in-contact MERS-CoV S1 vaccinated (LL12-16; red) llamas. The horizontal dotted lines indicate the cutoff of the assay. LL, llama; PRNT, plaque reduction neutralization assay; W, week.

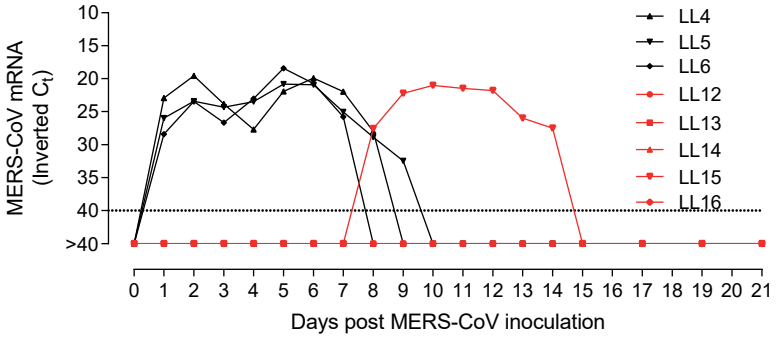

Supplementary Figure S5. Viral M mRNA detected in nasal swab samples collected from S1 vaccinated llamas at different time points after contact with directly inoculated animals.

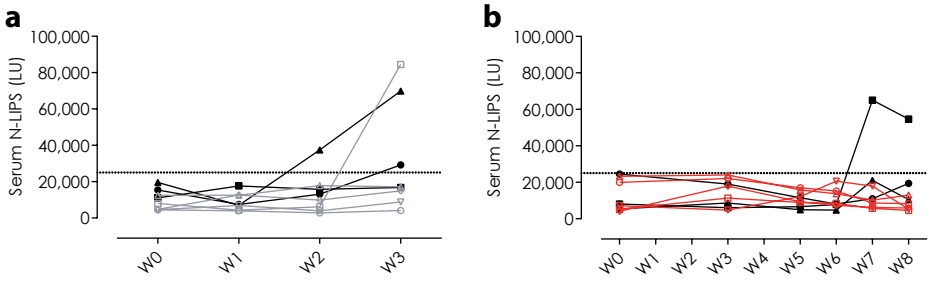

Supplementary Figure S6. Sera MERS-CoV nucleocapsid (N)-directed antibodies elicited in **(a)** inoculated (LL1-3; black) and in-contact naïve llamas (LL7-11; grey) and in **(b)** directly inoculated (LL4-6; black) and in-contact MERS-CoV S1 vaccinated (LL12-16; red) llamas. The horizontal dotted lines indicate the cutoff of the assay. LU, luminescence units; N-LIPS, nucleocapsid luciferase immunoprecipitation assay; W, week.

Chapter 4.2

Particulate multivalent presentation of the receptor binding domain induces protective immune responses against MERS-CoV

Nisreen M.A. Okba | Ivy Widjaja | Brenda van Dieren | Andrea Aebischer | Geert van Amerongen | Leon de Waal | Koert J. Stittelaar | Debby Schipper | Byron Martina | Judith M.A. van den Brand | Martin Beer | Berend-Jan Bosch | Bart L. Haagmans

Emerging Microbes & Infecttion, Accepted Manuscript

Abstract

Middle East respiratory syndrome coronavirus (MERS-CoV) is a WHO priority pathogen for which vaccines are urgently needed. Using an immune-focusing approach, we created self-assembling particles multivalently displaying critical regions of the MERS-CoV spike protein – fusion peptide, heptad repeat 2, and receptor binding domain (RBD) – and tested their immunogenicity and protective capacity in rabbits. Using a 'plug-and-display' SpyTag/SpyCatcher system, we coupled RBD to lumazine synthase (LS) particles producing multimeric RBD-presenting particles (RBD-LS). RBD-LS vaccination induced antibody responses of high magnitude and quality (avidity, MERS-CoV neutralizing capacity, and mucosal immunity) with cross-clade neutralization. The antibody responses were associated with blocking viral replication and upper and lower respiratory tract protection against MERS-CoV infection in rabbits. This arrayed multivalent presentation of the viral RBD using the antigen-SpyTag/LS-SpyCatcher is a promising MERS-CoV vaccine candidate and this platform may be applied for the rapid development of vaccines against other emerging viruses.

Introduction

Emerging zoonotic viruses, such as severe acute respiratory syndrome coronavirus (SARS-CoV) and Middle East respiratory syndrome coronavirus (MERS-CoV) have been able to cross the species barrier posing a threat to the human population. MERS-CoV causes severe respiratory disease and fatalities in humans (1, 2), and the virus is continuously introduced into the human population through infected dromedary camels, the viral reservoir with resulting outbreaks (3). The wide geographical distribution of this viral reservoir, the high case-fatality rate in humans (35%), and the lack of treatment and licensed vaccines, make the virus a threat to the human population. This has put MERS-CoV on the recent WHO list of diseases having an epidemic or even pandemic potential for which countermeasures are lacking and are urgently needed (4).

Vaccination is potentially one of the most effective ways to prevent the ongoing MERS-CoV outbreaks. Several MERS-CoV vaccine candidates have been developed using different platforms including inactivated, live-attenuated, and subunit vaccines (5). Compared to other vaccine production platforms, recombinant subunit proteins have a higher safety profile, are relatively faster and easier to produce, and can be scaled-up in a more cost-effective manner; nonetheless, they tend to induce lower levels of protective immunity (6). The use of self-assembling multimeric protein scaffold particles (MPSP) to present antigens in a multivalent virus-mimicking manner (size, repetitiveness, and geometry), has been shown to enhance vaccine-induced immune responses (7-11), and to offer advantages over other multimeric antigen presentation platforms (reviewed in (12)). Both lumazine synthase (LS) and I3-01 (I3) can self-assemble into 60-meric particles, which can be expressed in *E. coli* and have been used as scaffolds for development of multimeric vaccines with improved immune responses compared to monomeric forms (13-15). An LS-based HIV vaccine, (eOD-GT8), has recently advanced to a phase I human clinical trial (NCT03547245). Linking of antigens to these MPSP can be achieved through several mechanisms; as e.g. genetic fusion or the SypTag-SpyCatcher (ST/SC) system (16). While the former requires the antigen and scaffold to be produced in the same expression system, the latter allows each to be expressed in its suitable system harnessing a rapid post-translational 'plug-and-play' assembly. This is advantageous, allowing scaffold-SC to be produced at scalable levels in *E. coli* and SpyTagged glycosylated antigens such as viral surface proteins to be produced in its optimal system, such as mammalian or insect cells. The antigen-ST can then be multivalently displayed on the surface of the SC-scaffolds through the spontaneous formation of a stable isopeptide bond. This can be a platform for rapid vaccine manufacturing in case of epidemics or pandemics, to create optimized vaccines at reduced costs and also with reduced development times.

The MERS-CoV spike (S) protein is the main target for subunit vaccine development (5) It assembles as a homotrimer and consists of an N-terminal head (S1 subunit) and a C-terminal stalk (S2 subunit). The S1 subunit mediates virus attachment and entry through its N-terminal $S1^A$ domain and its C-terminal receptor binding domain (RBD), respectively (17, 18). The $S1^A$ domain binds sialic acids, a viral attachment factor, while the RBD binds to the viral receptor, dipeptidyl peptidase 4 (DPP4). Following attachment and entry, the S2 subunit mediates viral fusion to the host cell through its fusion machinery; comprised of the fusion peptide (FP) and the two heptad repeats - HR1 and HR2 (19). MERS-CoV neutralizing antibodies (Abs) mainly recognize epitopes in the RBD of the spike head S1 subunit; and to a lower extent, epitopes in the sialic acid binding domain and the fusion-mediating more conserved S stalk (S2). Nonetheless, antibodies directed against the sialic acid binding $S1^A$ domain or the more conserved S2 subunit, although subdominant, may protect against MERS-CoV (20, 21).

Immune focusing can enhance immune responses to subdominant regions (22). In the current study, using LS and I3 self-assembling particles, we evaluated whether immune focusing and multivalent presentation can induce immune responses to the more sequence-conserved S2 regions: FP and HR2. Furthermore, using a SypTag/SpyCatcher system and LS particles, we tested whether immune focusing with/without multivalent presentation of the viral RBD can lead to enhanced protection against a MERS-CoV challenge in rabbits.

Materials and Methods

Protein Design and Expression

Expression constructs were cloned using standard PCR methods. The gene encoding the 6,7-dimethyl-8-ribityllumazine synthase (LS; GenBank accession no. WP_010880027.1) of *A. aeolicus* was synthesized using human-preferred codons obtained from GenScript USA, Inc, as described previously (17). The cysteine at position 37 and asparagine at position 102 of LS were mutated to alanine and glutamine, respectively. The gene encoding I3-01 (I3; PDB 5KP9, amino acid residues 19-222) derived from *Thermotoga maritima* was synthesized using human-preferred codons obtained from GenScript USA. The gene fragments encoding the ΔN1SpyCatcher (SC; UniProt accession no. AFD50637.1; amino acid residues 48-139; (23)) and SpyTag (ST; UniProt accession no. WP_129284416.1 ; amino acid residues 981-994) based on the Cna B-type domain-containing protein of *Streptococcus pyogenes* were synthesized using human-preferred codons obtained from GenScript USA, Inc. The LS and I3 gene constructs were cloned into the pGEX-2T bacterial expression vector (Sigma Aldrich).

To generate the HR2-LS expression vector, the HR2 region (amino acid residues 1215-1287) encoding sequence of the MERS-CoV S gene (accession no. NC_019843) was ligated in-frame with an N-terminal sequence encoding a CD5 signal sequence and streptag tag purification tag, and with a C-terminal sequence encoding the LS via a linker, and subsequent cloned into the pCAGGS mammalian expression vector.

To generate the I3-HR2 expression vector, the heptad repeat 2 encoding region (HR2, amino acid residues 1215-1287) of the MERS-CoV S gene was ligated in-frame with an N-terminal sequence encoding the I3-01 and a C-terminal streptag purification tag interspaced with a linker, and subsequent cloned into the pGEX-2T bacterial expression vector (Sigma Aldrich).

To generate the FP-I3 and FP-LS expression vectors, the fusion peptide (FP; amino acid residues 884-898) encoding sequence of the MERS-CoV S gene was ligated in-frame with an N-terminal sequence encoding the I3-01 or LS, and a C-terminal Streptag purification tag and subsequently cloned into the pGEX-2T bacterial expression vector (Sigma Aldrich).

To generate the RBD-ST expression vector, the MERS-RBD (amino acid residues 358-588) encoding sequence of the MERS-CoV S gene was ligated in-frame with an N-terminal sequence encoding a CD5 signal sequence and with a C-terminal sequence encoding the ST followed by a double Streptag, and subsequently cloned into the pCAGGS mammalian expression vector.

To generate the LS-SC expression vector, the codon optimized SC sequence equipped with an N-terminal FLAG-tag (DYKDDDDK) was cloned to the N-terminus of the LS sequence in the pET15b bacterial expression vector (Novagen). All protein sequences are provided in Supplementary Figure S1 and S2.

Mammalian expression

Mammalian expression of the HR2-LS and RBD-ST constructs was done, as described previously (17). In short, expression plasmids were polyethylenimine (PEI)-transfected into 60% confluent HEK-293T cells for 6 h, after which transfections were removed and medium was replaced with 293 SFM II-based expression medium (Gibco Life Technologies) and incubated at 37°C in 5% CO_2. Tissue culture supernatants were harvested 5–6 d post transfection, and expressed proteins were purified using StrepTactin Sepharose beads (IBA) according to the manufacturer's instruction.

Bacterial protein expression

BL21 cells (Novagen) were transformed with pGEX-2T expression vectors and grown in 2× yeast-tryptone medium to log phase (OD_{600} ~1.0) and subsequently induced by adding

IPTG (isopropyl-β-d-thiogalactopyranoside) (GIBCO BRL) to a final concentration of 1 mM. Two hours later, the cells were pelleted, resuspended in 1/25 volume of 10 mM Tris (pH 8.0)-10 mM EDTA-1 mM phenylmethylsulfonyl fluoride, and sonicated on ice (five times, 2 min each). The cell homogenates were centrifuged at 20,000 × g for 60 min at 4°C. Proteins were purified from the cell lysate supernatant using StrepTactin Sepharose beads (IBA) according to the manufacturer's instruction.

All purified proteins were analyzed on a 12% SDS/PAGE gel under reducing conditions and stained with GelCodeBlue stain reagent (Thermo Scientific). Purified proteins were stored at 4°C until further use.

Expression of the FLAG-LS-SC was performed as described above with the following modifications: 1) Cells were treated with 1mg/ml lysozyme in lysis buffer (50 mM Tris-HCl, 150 mM NaCl, 1% Triton X-100) for 1h at room temperature prior to sonification on ice. 2) Purification was performed using ANTI-FLAG® M2 Affinity Gel (Sigma Aldrich) as recommended by the manufacturer. Purified proteins were dialyzed against 1x TBS buffer (50 mM Tris-HCl, 150 mM NaCl, pH 7.4) and stored at -80°C until further use.

Rabbit immunizations

Rabbit immunizations and challenge were carried out at Viroclinics Bioscience B.V. under permit no. AVD277002015283-WP03, using BSL-3 containment facilities. Female New Zealand White rabbits (Envigo, Venray, the Netherlands) of 11 weeks age were assigned to six groups (i-vi) of five animals each. Immunizations were performed intramuscularly with either i) HR2-LS, ii) FP-LS, iii) LS, at day 0 and boosted with either i) HR2-I3, ii) FP-I3, iii) I3 on day28 or iv) PBS, v) RBD+LS, vi) RBD-LS on days 0 and 28. Each animal received each time 15 µg of antigen adjuvanted with Adjuplex (5%; Sigma-Aldrich, Zwijndrecht, the Netherlands) in a total volume of 500 µL. Three weeks after the last vaccination (day 49 of the study), all animals were challenged intranasally under anesthesia with MERS-CoV (10^6 50% tissue culture infectious dose ($TCID_{50}$) MERS-CoV EMC strain (accession no. NC_019843) in a volume of 1 mL divided over both nostrils). The animals were euthanized on day 4 post-challenge (day 53 of the study). Serum samples were collected on days 0, 28, and 46. Nasal swabs were collected on day 46 (pre-challenge) and on days 1 through 4 post-challenge. Following euthanasia, lungs were examined for gross pathology and lung tissue samples were collected for virus detection, and in 10% formalin histopathology and immunohistochemistry.

Enzyme-linked immunosorbent assay (ELISA)

Antigen-binding and anti-LS (scaffold) antibodies produced after vaccination were tested in the sera collected at different time points as well as in pre-challenge nasal swabs using

ELISA. Costar high-binding 96-well ELISA plates were coated overnight at 4°C with 1 µg/ml of either recombinant LS, MERS-CoV S1 or S2 proteins in PBS. The plates were washed with PBS and blocked for 1 hr using 1%BSA/0.5%Tween-20/PBS. Following blocking, diluted samples (1:100 or serially diluted) were added and further incubated for 1 hr. The plates were then washed and and probed with an HRP-labeled goat anti-rabbit Ig (1:2000, Dako) secondary antibody. TMB was used for signal development and the absorbance of each sample was measured at 450 nm (OD_{450}).

Antibody Avidity ELISA

Antibody avidity was assessed using an ammonium thiocyanate (NH_4SCN)-displacement ELISA. This was carried out as described above using serum dilutions containing same level of S1 absorbance units added in triplicates. Following serum incubation and washing, NH4SCN (0-5 M) was added to the wells for 15 minutes. The plates were then washed and further developed as described above. The concentration of NH_4SCN resulting in a 50% reduction in signal was taken as the avidity index (IC_{50}).

ELISA analysis of immunogen binding by antibodies

To confirm the antigenicity of the RBD-LS particles, we tested its binding to well-characterized monoclonal antibodies binding conformational RBD epitopes (20). Human monoclonal antibodies 7.7G6, 1.6F9, 1.2G5, 1.8E5, 4.6E10 targeting the receptor binding domain of the MERS-CoV spike protein were produced and purified as described earlier (20). NUNC Maxisorp plates (Thermo Scientific) were coated with the RBD-LS antigen at 100 ng /well at 4°C overnight. Plates were washed three times with PBS containing 0.05% Tween-20 and blocked with PBS with 5% Protifar in PBS containing 0.1% Tween-20 at room temperature for 2 h. Four-folds serial dilutions of mAbs starting at 10 µg/ml (diluted in blocking buffer) were added and plates were incubated for 1 h at room temperature. Plates were washed three times and incubated with HRP-conjugated goat anti-human secondary antibody (ITK Southern Biotech) diluted 1:2000 in blocking buffer for one hour at room temperature. HRP activity was measured at 450 nm using tetramethylbenzidine substrate (BioFX) and an ELISA plate reader (EL-808, Biotek).

Plaque reduction neutralization assay

The presence of MERS-CoV neutralizing antibodies in the sera and nasal swabs of vaccinated animals was tested using a plaque reduction neutralization assay (PRNT). Heat –inactivated two-fold serially diluted samples (starting 1:10) were mixed 1:1 with 400 PFU of MERS-CoV (EMC/2012) and incubated for one hour. The mix was then overlaid on HuH-7 cells in 96-well

plates. Following one hour of incubation, the mix was removed and the cells were incubated for 8 hr. The cells were then fixed, permeabilized and stained using a mouse anti-MERS-CoV N protein monoclonal antibody (Sino Biological) followed by an HRP-labelled goat anti-mouse IgG1 (SouthernBiotech). The signal was developed using a precipitate forming peroxidase substrate (True Blue, KPL). The ImmunoSpot® Image analyzer (CTL Europe GmbH) was used to count the number of infected cells per well. The neutralization titer of each serum sample was determined as the reciprocal of the highest dilution resulting in a ≥50% (PRNT50) or ≥90% (PRNT90) reduction in the number of infected cells. A titer of ≥20 was considered to be positive.

Viral RNA detection

To evaluate the protective efficacy of vaccination against MERS-CoV challenge, nasal swabs, and homogenated lung tissues were tested for the presence of MERS-CoV RNA using RT-qPCR for and for the presence of infectious virus by virus titration.

The presence of viral RNA in nasal swabs and lung tissues was tested using UpE RT-qPCR as previously described (24). RNA was extracted from samples using Magnapure LC total nucleic acid isolation kit (Roche). RNA amplification and quantification were carried out using a 7500 Real-Time PCR System (Applied biosystems). Samples with a C_t value <40 were considered positive. RNA dilutions extracted from a MERS-CoV stock of known titer was used to generate a standard curve in order to calculate the $TCID_{50}$ equivalent of RNA detected in samples. Concentrations of viral RNA in lung tissue are expressed in as $TCID_{50}$ equivalents per gram tissue ($TCID_{50}$ eq/g), and in the nasal swabs as $TCID_{50}$ eq/mL.

Virus titration

The presence of MERS-CoV infectious viral particles in respiratory tract samples (nasal swabs and lung tissue homogenates) was detected by titration on Vero cells as described previously (24). Briefly, 10-fold serially diluted samples (starting undiluted) were overlaid on Vero cells and the plates were incubated for five days at 37°C and the cytopathic effect was recorded. Infectious virus titers in lung tissue are expressed as $TCID_{50}$ per gram tissue ($TCID_{50}$/g), and infectious virus titer in nose swabs are expressed as $TCID_{50}$/mL.

Histopathology and Immunohistochemistry

Lung tissue samples were collected in formalin and embedded in paraffin for pathological analysis. Hematoxylin-eosin staining was carried out for histopathological analysis. The presence of MERS-CoV nucleoprotein was detected by immunohistochemistry as previously published (24).

Statistical analysis

Statistical analyses were performed using Prism 7 (GraphPad Software Inc, USA). Data were compared using Mann-Whitney U test or Student's *t*-test. P-values <0.05 were considered significant.

Data availability

All data are available within the article and its supplementary information or available from the authors on request.

Results

Generation of MERS-CoV spike particles

Particulate multivalent antigen display can enhance immunogenicity through different mechanisms, allowing for induction of immune responses against otherwise weakly immunogenic antigens (7, 25). We sought to design antigens capable of inducing strong immune responses against critical parts of the viral entry and fusion machinery within the MERS-CoV spike protein through immune focusing and multivalent presentation on self-assembling particles (Figure 1). Within the S1 subunit, the RBD is the main target for the induction of neutralizing antibodies and has been used to develop several vaccine candidates for MERS-CoV (5, 26). Indeed, the immunogenicity of RBD can be enhanced by its presentation on ferritin nanoparticles (27). Likewise, the fusion peptide (FP) and the HR2, which show a high degree of sequence conservation among CoVs relative to the RBD, play crucial roles in the CoV spike-mediated fusion machinery, and can be targets for CoV protective antibodies (28-32). Genetic fusion was chosen for FP and HR2, due to their small size, whereas the ST/SC system was used for RBD display on particles to ensure correct folding of the protein.

Two 60-meric hyperstable self-assembling particles with icosahedral symmetry were used for multivalent display of MERS-CoV domains. The lumazine synthase (LS) particle, an icosahedron with a diameter of 15nm (PMID: 23539181) and the I3-01 (I3) particle, a dodecahedron with a diameter of 25nm (PMID: 27309817). The N- and C-termini of both scaffolds are surface exposed, providing a platform to multivalently present (antigenic) domains. Two functional segments of the S2 subunit of the MERS-CoV spike protein were genetically fused to these nanoparticles; the fusion peptide containing region (amino acid residues 884-898) and the HR2 containing region (amino acid residues 1215-1287) (Figure 1B, Supplementary Figure S1). Chimeric nanoparticles were purified after expression in eukaryotic (mammalian) or prokaryotic systems (Figure 1).

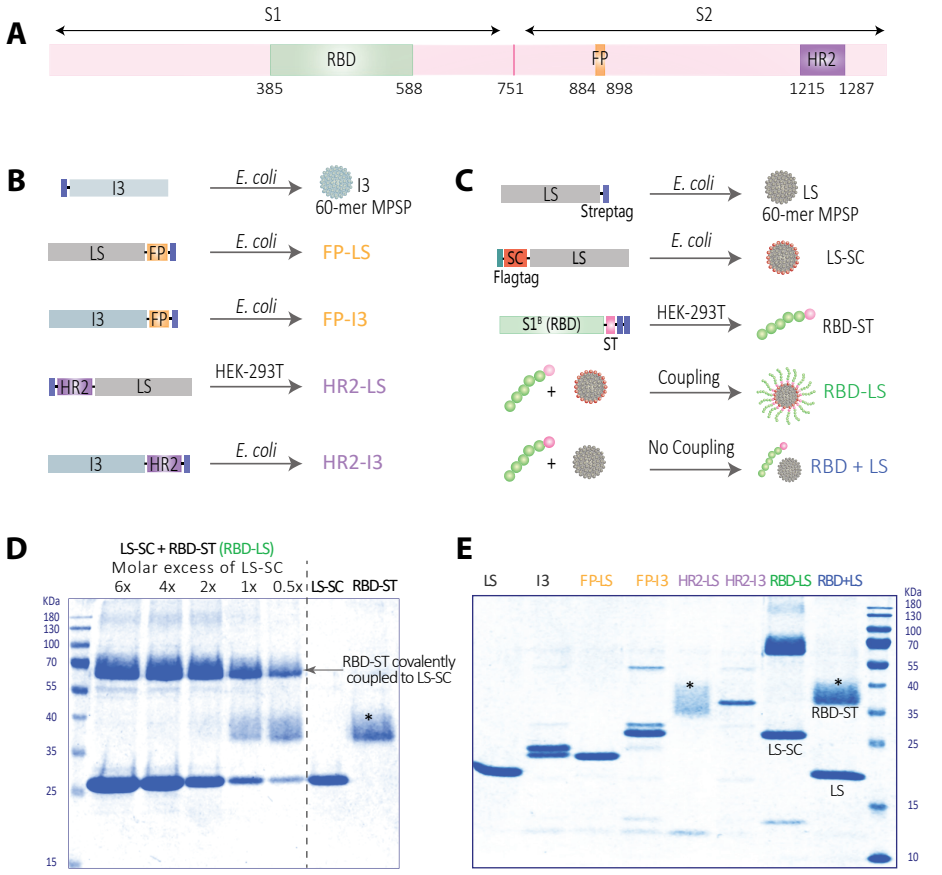

Figure 1. Generation of multimeric protein scaffold particles (MPSP)- based vaccines used in this study. **(A)** Schematic diagram of the MERS-CoV spike (S) protein mapping regions selected for vaccine generation; the receptor binding domain (RBD), the fusion peptide (FP) and heptad repeat 2 (HR2). **(B, C)** Schematic diagram illustrating the construct design and production of the lumazine synthase (LS) and I3-01 (I3)-based self-assembling MPSP vaccines. **(D)** Reducing SDS-PAGE showing generation of RBD-LS by covalent coupling of RBD-SpyTag (RBD-ST) and LS-SpyCatcher (LS-SC) at different molar ratios of LS-SC: RBD-ST with the last two lanes showing each in its free (uncoupled) form. **(E)** Reducing SDS-PAGE analysis of immunogens used in this study. The size of each protein (KDa) is given in Supplementary Table S1. * Fuzzy bands due to heterogeneous glycosylation of HR2 or RBD.

Generation of multimeric RBD-ST/LS-SC (RBD-LS)

In addition, we used the SpyTag/SpyCatcher system to multivalently display the MERS-CoV RBD on LS nanoparticle via covalent bonding (8). For this purpose, the SpyCatcher (SC) was genetically fused to LS and expressed and purified from *E. coli*. The SpyTag (ST) was genetically fused to the MERS-RBD (amino acid residues 358-588) and expressed and purified from HEK-293T cells (Figure 1C). RBD-ST was incubated with LS-SC in different

molar ratios to assess the optimal coupling of both components. A 1:2 molar ratio of RBD-ST and LS-SC allowed the optimal coupling of all of the provided RBD-ST antigens to the SC-LS particles (Figure 1D). The resulting conjugation products were used for immunization. In order to assess the effect of the particle-based multivalent antigen display on immunogenicity, a mixture of non-coupled RBD-ST and LS (without SC) was taken along for immunization in the same molar ratio. All particulate preparations displaying MERS-S antigenic domains (genetically fused or SC/ST coupled) were analyzed by SDS-PAGE (Figure 1E, Supplementary Table S1), confirming their molecular integrity. We further confirmed the antigenicity of the RBD-LS particles by testing their capacity to bind monoclonal antibodies directed against conformational epitopes on the RBD (20) using ELISA. All antibodies bound to RBD-LS in a dose dependant manner (Fig S3) indicating that the RBD is correctly folded confirming its antigenicity.

Immunogenicity of particulate MERS-CoV spike vaccines in rabbits

We then evaluated the immunogenicity of the multimeric spike antigens using six groups of rabbits (n = 5 per group), which were intramuscularly immunized twice at a 4-week interval (Figure 2A). The LS/I3 and PBS immunized groups served as controls. After the first immunization, we detected antibody responses against the corresponding S subunit (S1 or S2) in the vaccinated rabbits. while the control groups remained negative (Figure 2B-E). Endpoint antibody titers for the vaccinated groups are shown as geometric mean titers (GMT) in Supplementary Table S2. The antibody responses were further boosted after the second immunization in all groups, while no responses were detected in the control groups, confirming the immunogenicity of the tested antigens in rabbits.

Anti-S2 antibody responses were detected in the HR2 and FP vaccinated groups with weak to no MERS-CoV neutralizing capacity (Figure 2B,C). Only HR2 vaccination induced low levels of MERS-CoV neutralizing antibodies ($PRNT_{90}$ titers: 20 - 40) in 4/5 rabbits; all 5 had MERS-CoV neutralizing antibodies at a 50% cut-off (data not shown).

Likewise, both the monomeric RBD (RBD+LS) and the multimeric RBD-LS were immunogenic and elicited high S1-specific antibody titers which were further boosted after the second immunization. The RBD-LS-induced S1 antibody titers were significantly higher than those induced by the monomeric RBD following the prime- as well as booster-vaccination ($p = 0.0397$ and $p = 0.0317$, respectively by Mann-Whitney U test) (Figure 2D). Multimeric RBD-LS vaccination elicited higher MERS-CoV neutralizing antibodies, a main correlate of protection, than the monomeric RBD+LS when tested for live virus neutralization using PRNT90 assay ($p = 0.0109$, and $p = 0.0079$, post-prime and boost, respectively by Mann-Whitney U test) (Figure 2E). The vaccine induced antibodies were able to neutralize clade A

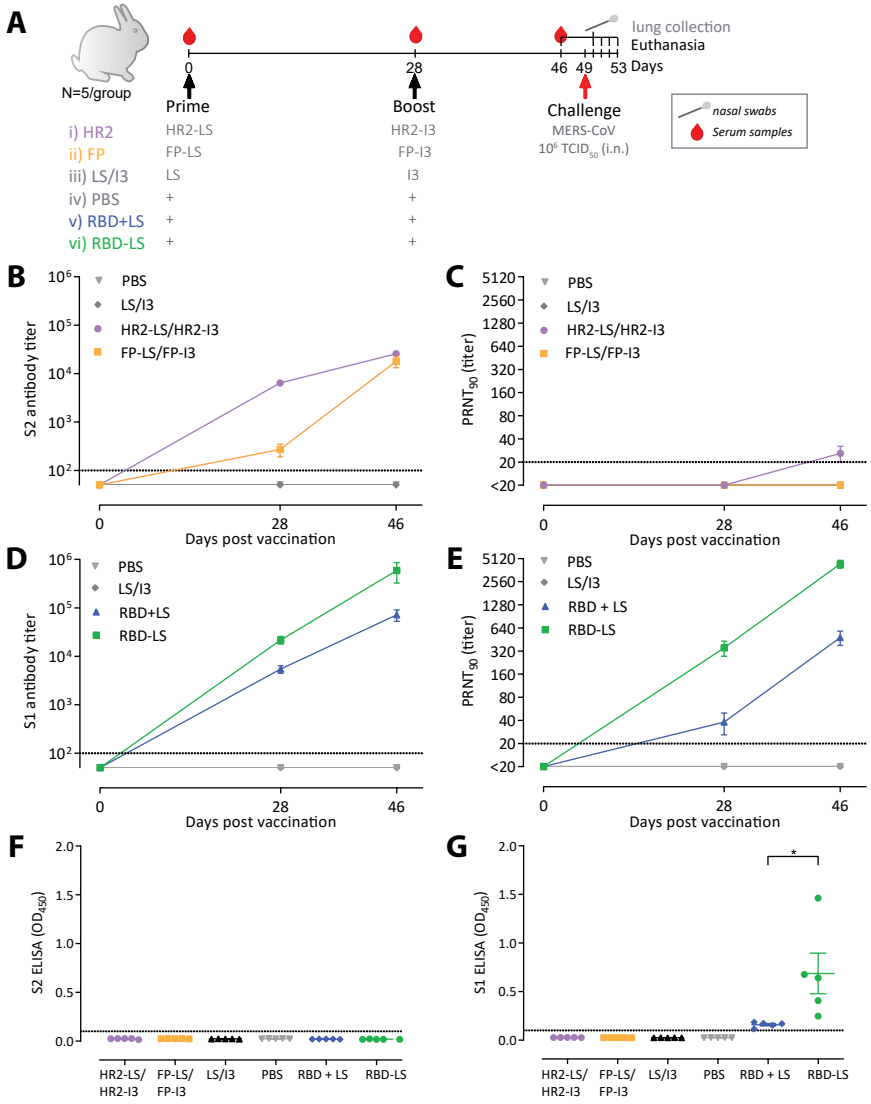

Figure 2. Immunogenicity of MERS-CoV spike MPSP vaccines. **(A)** Vaccination scheme for rabbit immunizations. Six groups of rabbits (5/group) were vaccinated in a prime/boost regimen with 15 µg of adjuvanted vaccine at 4-week interval and challenged with MERS-CoV (EMC strain; accession no. NC_019843) 3 weeks post-boost. Anti-MERS-CoV spike S2 **(B)** and S1 **(D)** IgG titers measured by ELISA in rabbits at different time points. Shown is the mean ± s.e.m. antibody titers from five rabbits per group. **(C,E)** MERS-CoV neutralizing antibody titers measured by a 90% reduction in a plaque reduction neutralization assay (PRNT90). **(B-E)** Shown is the mean ± s.e.m. of five rabbits per group. **(F,G)** Vaccine-induced antibodies in nasal swabs of vaccinated rabbits. Anti MERS-CoV S2 **(F)** and S1 **(G)** antibody responses in the nasal swabs (tested at a 1:50 dilution) of vaccinated rabbits pre-challenge (three weeks post-boost). The difference in antibody responses between monomeric (RBD+LS) and multimeric (RBD-LS) RBD was tested for statistical significance using a student's t-test, with asterisks indicating the level of significance. * $p \leq 0.05$. Error bars indicate mean ± s.e.m. The dotted lines represent the limits of detection. HR2, heptad repeat 2; FP, fusion peptide; LS, lumazine synthase 60-meric particles; I3, I3-01 60-meric particles; RBD, receptor binding domain; RBD + LS, monomeric uncoupled RBD; RBD-LS, multimeric RBD coupled to LS through covalent SpyTag/SpyCatcher.

(EMC/2012 strain; Figure 2E) as well as the more recently circulating clade B (Qatar15/2015 strain; Supplementary Figure S4) viruses. The spike protein of the former strain differs from the clade A EMC/2012 strain in two positions; T95S and Q1020R.

Following a single immunization, binding antibody titers were four-fold higher and neutralizing antibodies were eleven-fold higher in the coupled multimeric RBD-LS group than in the uncoupled monomeric RBD+LS (Supplementary Table S2). Three weeks after the boost, binding antibody responses were seven-fold higher ($p = 0.0079$, Mann-Whitney U test) and neutralizing antibodies were ten-fold higher ($p = 0.0079$, Mann-Whitney U test) in the coupled RBD-LS group than in the uncoupled RBD+LS (Figure 2D,E Supplementary Table S2). Additionally, we tested for vaccine induced mucosal immunity in the respiratory tract of vaccinated rabbits pre-challenge (Day 49) using ELISA. MERS-CoV specific antibodies were only detected in the nasal swabs of the groups vaccinated with conjugated or non-conjugated RBD (Figure 2 F,G). Antibody responses detected in the RBD-LS vaccinated group were higher than those in the RBD + LS vaccinated group ($p = 0.0357$, Student's *t*-test). This demonstrates that RBD-LS induces improved local mucosal immune responses compared to the monomeric RBD. Thus, vaccination with the newly produced RBD-LS MERS-CoV MPSP vaccines induce a robust immune response.

Avidity of RBD-LS induced antibodies

The avidity of MERS-CoV spike-specific antibodies in the monomeric versus the multimeric RBD vaccinated groups was analyzed at days 28 (4 weeks after prime) and 46 (3 weeks after boost) using an ammonium thiocyanate (NH4SCN)-displacement ELISA (33). The avidity index IC_{50} was determined for each vaccinated rabbit and compared between the two groups. The avidity of the S1-specific antibody responses was higher following RBD-LS vaccination compared to the monomeric RBD+LS vaccination ($p < 0.0001$, Student's *t*-test) (Figure 3), indicating that a multimeric RBD-LS vaccine can induce antibody responses of both higher quantity and quality (Figure 2D,E; Figure 3).

Antibody responses to lumazine synthase scaffolds

In addition to evaluating anti-S (antigen) responses, we also tested for the induction on LS-specific (scaffold) antibodies. Antibody responses were elicited against the LS-particle in all groups except the PBS group, indicating that the particle was accessible and not sterically hidden by antigens displayed on its surface; even when RBD was displayed on its surface using SpyTag:SpyCatcher linkage (Figure 4). Despite that, antigen-specific responses were not adversely affected by the presence of these anti-scaffold antibodies, as demonstrated by the booster effect after the second immunization (Figure 2D,E). Nonetheless, we

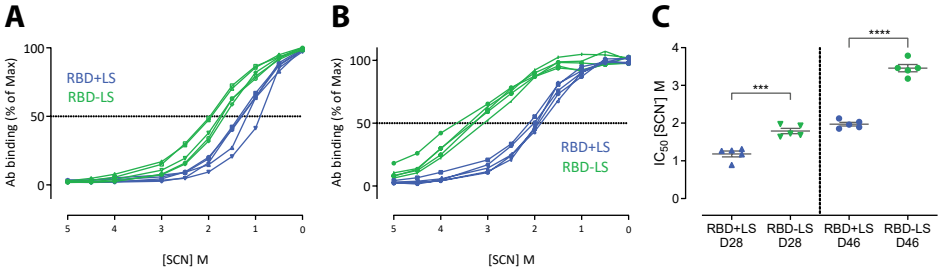

Figure 3. Avidity of vaccine-induced serum antibody responses. The avidity of serum IgG antibody responses after one (**A**, Day 28) and two immunizations (**B**, Day 46) with either monomeric RBD (RBD+LS, blue, *n* = 5) or multimeric RBD (RBD-LS, green, *n* = 5) was assessed using ammonium thiocyanate (SCN) avidity ELISA. **(A, B)** The percentage of serum antibodies bound following the addition of different concentration of SCN was used to determine **(C)** the avidity index (IC_{50}). The difference in serum avidity between both groups was tested for statistical significance using a student's *t*-test, with asterisks indicating the level of significance. *** $p \leq 0.001$, **** $p \leq 0.0001$. Error bars indicate mean ± s.e.m.

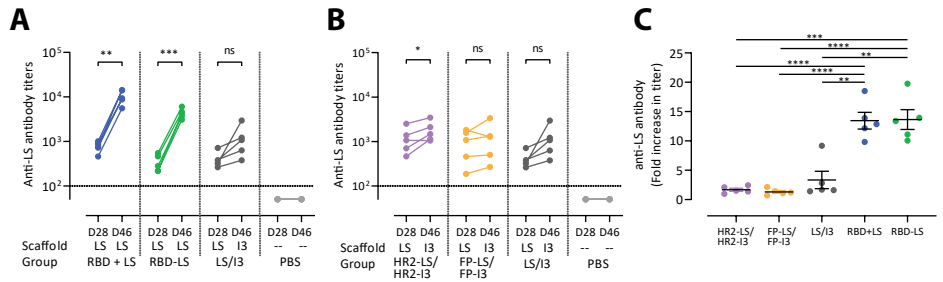

Figure 4. Anti-scaffold antibody responses in sera of vaccinated rabbits. Anti-lumazine synthase (LS) scaffold antibody titers following **(A)** homologous prime boost in monomeric RBD+LS and multimeric RBD-LS vs heterologous LS/I3 prime boost in control LS/I3 as well as **(B)** HR2-LS/I3 and FP-LS/I3. Shown are (average ± s.e.m. of *n* = 5 rabbit/group) antibody titers 4 weeks after prime (day 28, D28) and 3 weeks after boost (day 46, D46) as measured by ELISA. **(C)** Fold increase (from prime, day 28) in anti-LS antibody titers following boost vaccination (day 46). A paired t-test was performed to determine significant increases in antibody titers post-prime and post-boost within groups **(A, B)**, and an unpaired t-test was performed to determine significant changes in titers between groups **(C)**, with asterisks indicating the level of significance.* $p \leq 0.05$, ** $p \leq 0.01$, *** $p \leq 0.001$, **** $p \leq 0.0001$. The dotted lines represent the limits of detection. HR2, heptad repeat 2; FP, fusion peptide; LS, lumazine synthase 60-meric particles; I3, I3-01 60-meric particles; RBD, receptor binding domain; RBD + LS, monomeric uncoupled RBD; RBD-LS, multimeric RBD coupled to LS through covalent SpyTag/SpyCatcher.

tested whether a heterologous scaffold boost could help in minimizing such anti-scaffold responses using an LS/I3 prime-boost scheme. Using this approach, we found no significant increase in anti-scaffold antibody responses compared to the homologous prime-boost scheme (Figure 4C). This indicates that a heterologous scaffold prime-boost approach could be advantageous for limiting unnecessary anti-scaffold responses.

Efficacy of RBD-LS in preventing virus shedding and infection in rabbits

To evaluate the protective efficacy of the immune responses induced by the different MERS-CoV spike MPSP vaccines, rabbits were challenged intranasally with 10^6 $TCID_{50}$ of MERS-CoV (strain HCoV-EMC/2012) and nasal swabs were collected up to 4 days post inoculation (pi) (Figure 2A). On day 4 pi, the animals were euthanized, and lung tissue samples were collected. Consistent with earlier reports (34, 35), none of the rabbits in the control group developed any clinical signs of infection upon MERS-CoV inoculation, and titration of infectious virus from lung tissues and nasal swabs was variable. Thus, to evaluate protection, we tested for MERS-CoV RNA by qRT-PCR, for MERS-CoV infectious virus by virus titration, and for MERS-CoV antigen (N protein) in lung tissues by immunohistochemistry (IHC). Except for the RBD-LS vaccinated group, viral RNA was detected in all vaccinated groups from day 1 through day 4 post-challenge at levels similar to control groups (Figure 5, and 6). Viral RNA titers were significantly reduced in the nasal swabs of the RBD-LS vaccinated groups as early as day 1 post-challenge and were undetectable by day 4, in line with the absence of detectable infectious virus particles (Figure 5). Viral RNA was also reduced in the

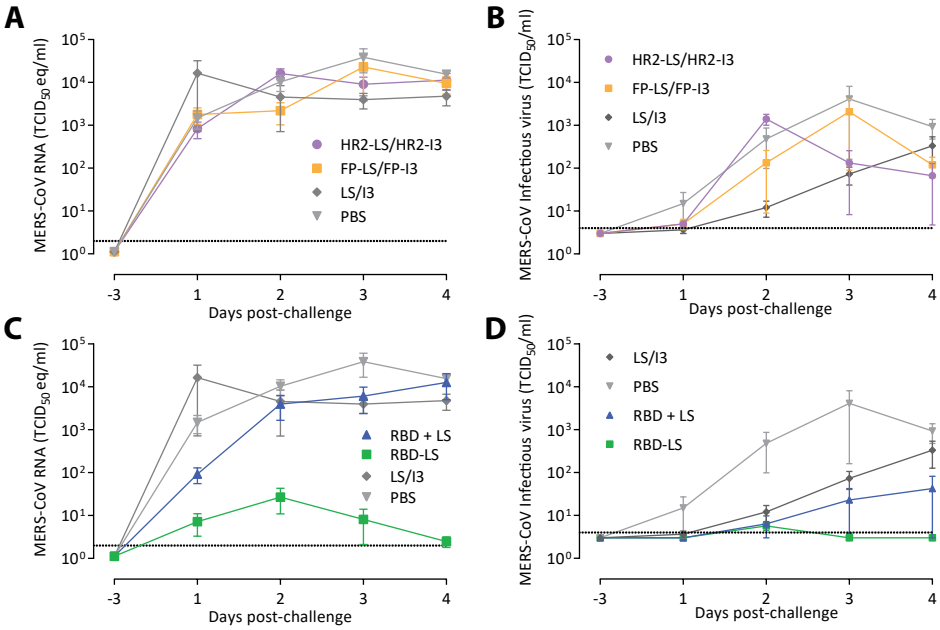

Figure 5. Protective capacity of MERS-CoV MPSP vaccines against upper respiratory tract infection in rabbits. Six groups of vaccinated and control rabbits (n = 5/group) were tested for the presence of viral RNA **(A, C)** and infectious virus particles **(B, D)** in the upper respiratory tract (nasal swabs) at days -3 and 1-4 post intranasal viral challenge (days 46 and 50-53 post first vaccination) with 10^6 $TCID_{50}$ MERS-CoV EMC strain. Shown is the average ± s.e.m. of five animals per group. The dotted lines represent the limits of detection. HR2, hepad repeat 2; FP, fusion peptide; LS, lumazine synthase 60-meric particles; I3, I3-01 60-meric particles; RBD, receptor binding domain; RBD + LS, monomeric uncoupled RBD; RBD-LS, multimeric RBD coupled to LS through covalent SpyTag/SpyCatcher.

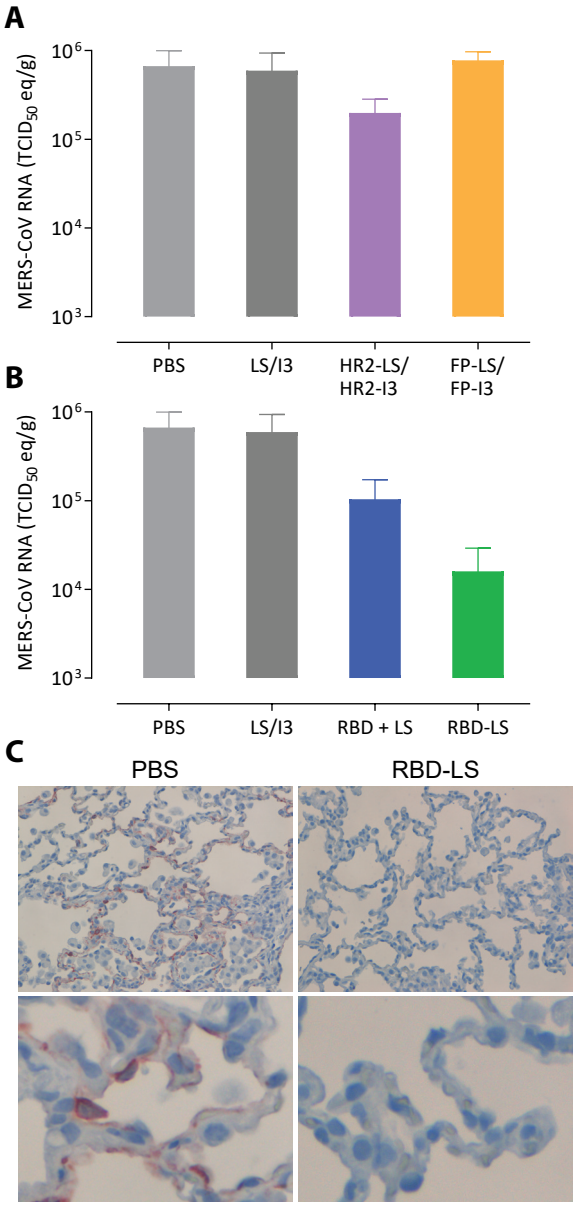

Figure 6. Protective capacity of MERS-CoV MPSP vaccines against lower respiratory tract infection in rabbits. Six groups of vaccinated and control rabbits (n = 5/group) were tested for the presence of viral RNA **(A, B)** in the lung tissue homogenates and viral nucleocapsid antigen in lung tissues **(C)** collected 4 days post intranasal viral challenge with 10^6 $TCID_{50}$ of MERS-CoV (EMC isolate). **(A, B)** Shown are the average and SEM equivalent virus titers/gram of tissue. **C)** Representative pictures of immunohistochemical detection of MERS-CoV nucleoprotein (shown in red) in the lungs of PBS (left) vs RBD-LS (right) immunized rabbits four days post-viral challenge; the upper and lower panels show a 200X and 1000X magnification, respectively. HR2, hepad repeat 2; FP, fusion peptide; LS, lumazine synthase 60-meric particles; I3, I3-01 60-meric particles; RBD, receptor binding domain; RBD + LS, monomeric uncoupled RBD; RBD-LS, multimeric RBD coupled to LS through covalent SpyTag/SpyCatcher.

lungs of RBD-LS-vaccinated rabbits (Figure 6). Consistently, IHC revealed no viral antigen in the lungs of the RBD-LS vaccinated rabbits (Figure 6C), and antigen was also not detected in the RBD+LS vaccinated rabbits. Overall, in contrast to the monomeric form, the antigen-focused multimeric RBD-LS vaccine was able to block MERS-CoV replication significantly in the nose and lungs of the infected rabbits.

The efficacy of RBD-LS immunization in protecting against a MERS-CoV challenge, makes it a potential vaccine candidate. However, for production at industrial scale, unnecessary sequences (e.g. tags) need to be removed, preparations have to be further structurally and biochemically characterized.

Discussion

Recombinant subunit proteins provide advantages regarding safety, costs, and speed of vaccine production, making them very attractive platforms for the development of vaccines for emerging viruses. Multivalent antigen display allows for virus-mimicking presentation of antigens and has been shown to induce antibodies of high avidity and magnitude (7, 10, 11, 27, 36); with non-viral self-assembling MPSP providing advantages over other multimeric antigen presentation platforms (8, 12). Among the MERS-CoV vaccine candidates developed so far, the latter approach has been used to design two candidates, both are based on the receptor-binding domain (27, 37), the main target for MERS-CoV protective antibodies (26). One used self-assembling ferritin nanoparticles (27) and the second used canine parvovirus (CPV) VP2 structural protein forming virus like particles (37) as scaffolds. Both vaccine candidates were able to induce humoral and cellular immune responses in mice, nonetheless none has been tested for its protective capacity in a viral-challenge animal model. In our study, using an immune-focusing approach to target protective epitopes and domains along with multivalent presentation on self-assembling LS particles using a spontaneous covalent linker (SpyTag/SpyCatcher). We report for the first time the *in-vivo* protective capacity of a multimeric MERS-CoV RBD particle vaccine.

We used self-assembling LS and I3 particles to generate chimeric multimeric protein scaffold particle displaying critical domains in the MERS-CoV spike protein and evaluated their immunogenicity and protective efficacy in rabbits. Multimeric FP and HR2 vaccinations induced high levels of anti-S2 antibodies, nonetheless, with low to undetectable virus neutralizing capacities and couldn't protect rabbits against virus challenge. Meanwhile, multimeric RBD-LS vaccination was highly immunogenic and induced robust antibody responses of high magnitude, avidity and neutralizing capacity. Following a live virus challenge, it protected upper and lower respiratory tract of rabbits as detected by decrease

in viral RNA titers, with an associated lack of MERS-CoV antigen (Figure 5, 6). Despite producing strong antibody responses, the monomeric RBD failed to protect rabbits against MERS-CoV following an intranasal challenge. The presence of LS did not seem to influence the outcome, as it was included in the formulation of the monomeric form (RBD+LS), indicating that the coupling and the multimeric presentation are responsible for the enhanced response seen with the multimeric RBD-LS vaccine. The "plug-and-display" SpyTag/SpyCatcher system (8) used to generate these multimeric RBD-LS particles allows for rapid and robust production of vaccines in a cost-effective manner. This enables the development of vaccines in a timely manner, which is crucial to prevent global public health consequences of evolving, emerging and re-emerging viruses.

The efficacy of RBD-LS immunization in protecting against a MERS-CoV challenge, makes it a potential vaccine candidate for further development. Nonetheless, in case of production at an industrial scale, unnecessary sequences (e.g. tags) need to be removed, preparations have to be further structurally and biochemically characterized.

When using scaffolds as antigen carriers, anti-scaffold antibody responses need to be considered to avoid their potential to compromise the targeted antigen-induced responses or to induce potential auto-antibodies against human antigens. Antibody responses were induced against the LS protein scaffold used in this study. However, antigen-specific responses were boosted following the second immunization and were not adversely affected by the presence of these anti-scaffold antibodies (Figure 4), similar to other reports (38). Since the sequence of the LS protein does not show any similarity to any human sequences, it is unlikely that they will induce unwanted auto- (antihuman) antibodies. An LS-based vaccine for HIV, in a current phase 1 clinical trial (NCT03547245), can provide further evidence for the safety of this platform. Nonetheless, we developed a heterologous scaffold prime-boost using LS and I3 which can help in reducing anti-scaffold responses.

A challenge facing MERS-CoV vaccine development is the limited number of appropriate animal models for testing protection against clinical virus isolates. Rabbits provide some advantages as an animal model for MERS-CoV. By having the MERS-CoV receptor DPP4 expressed in both the upper and lower respiratory tract epithelium (24), the rabbits can be naturally infected. This allows the evaluation of both upper and lower respiratory tract MERS-CoV infection and in turn protection using natural field virus isolates rather than adapted strains. However, the animals are not able to develop severe infection such as that seen in severe human cases (34). Nonetheless, severe infection, thus far, has not been established consistently in any of the other animal models without genetic modification and/or virus adaptation, except for marmosets (39). In addition to the aforementioned,

rabbits are readily available and easier to handle compared to other species that can be naturally infected such as non-human primates.

Following the addition of MERS-CoV as a priority pathogen in the WHO R&D Blueprint for action to prevent epidemics, a target product profile was developed which called for three types of MERS-CoV vaccines (40). These include one for camels to prevent virus shedding and transmission, and two for humans: a two-dose vaccine for long-term protection of those at continuous high risk such as camel handlers and health-care workers, and a single-dose vaccine for rapid onset of immune responses to protect those at acute risk in outbreak settings. The RBD-LS can be used to develop the two-dose vaccine required to protect the high-risk populations, and can be further optimized using the heterologous scaffold prime/boost scheme developed in this study. Nonetheless, evaluating the longevity of the induced immune responses is warranted. Following the prime, RBD-LS vaccination induced antibody responses of high avidity and MERS-CoV neutralizing capacity. Owing to the robust immune responses induced after one dose, the RBD-LS can be a candidate for developing a rapid single-dose vaccine for MERS-CoV, which is required for reactive use in outbreak situations (40). Additionally, this vaccine candidate was able to block MERS-CoV replication in the upper respiratory tract of infected rabbit, thus it could potentially be of use as a dromedary vaccine to block MERS-CoV transmission. However, both approaches need to be further validated.

Acknowledgments

We thank the technical staff of the preclinical department of Viroclinics Biosciences B.V. for their excellent technical support.

References

1. Zaki AM, van Boheemen S, Bestebroer TM, Osterhaus AD, Fouchier RA. Isolation of a novel coronavirus from a man with pneumonia in Saudi Arabia. The New England journal of medicine. 2012 Nov 8;367(19):1814-20.
2. World Health Organization. Middle East respiratory syndrome coronavirus (MERS-CoV) [cited 15-10-2019]; Available from: http://www.who.int/emergencies/mers-cov/en/
3. Haagmans BL, Al Dhahiry SH, Reusken CB, Raj VS, Galiano M, Myers R, et al. Middle East respiratory syndrome coronavirus in dromedary camels: an outbreak investigation. The Lancet Infectious diseases. 2014 Feb;14(2):140-5.
4. World Health Organization. R&D Blueprint: List of Blueprint priority diseases. [cited 20/05/2019]; Available from: https://www.who.int/blueprint/priority-diseases/en/
5. Okba NM, Raj VS, Haagmans BL. Middle East respiratory syndrome coronavirus vaccines: current status and novel approaches. Current opinion in virology. 2017 Apr;23:49-58.
6. Huber VC. Influenza vaccines: from whole virus preparations to recombinant protein technology. Expert review of vaccines. 2014 Jan;13(1):31-42.

7. Chattopadhyay S, Chen JY, Chen HW, Hu CJ. Nanoparticle Vaccines Adopting Virus-like Features for Enhanced Immune Potentiation. Nanotheranostics. 2017;1(3):244-60.
8. Brune KD, Leneghan DB, Brian IJ, Ishizuka AS, Bachmann MF, Draper SJ, et al. Plug-and-Display: decoration of Virus-Like Particles via isopeptide bonds for modular immunization. Scientific Reports. 2016 Jan 19;6:19234.
9. Wilson JT. A sweeter approach to vaccine design. Science. 2019 Feb 8;363(6427):584-5.
10. Tokatlian T, Read BJ, Jones CA, Kulp DW, Menis S, Chang JYH, et al. Innate immune recognition of glycans targets HIV nanoparticle immunogens to germinal centers. Science. 2019 Feb 8;363(6427):649-54.
11. Marcandalli J, Fiala B, Ols S, Perotti M, de van der Schueren W, Snijder J, et al. Induction of Potent Neutralizing Antibody Responses by a Designed Protein Nanoparticle Vaccine for Respiratory Syncytial Virus. Cell. 2019 Mar 7;176(6):1420-31 e17.
12. Lopez-Sagaseta J, Malito E, Rappuoli R, Bottomley MJ. Self-assembling protein nanoparticles in the design of vaccines. Comput Struct Biotechnol J. 2016;14:58-68.
13. Jardine J, Julien JP, Menis S, Ota T, Kalyuzhniy O, McGuire A, et al. Rational HIV immunogen design to target specific germline B cell receptors. Science. 2013 May 10;340(6133):711-6.
14. Hsia Y, Bale JB, Gonen S, Shi D, Sheffler W, Fong KK, et al. Design of a hyperstable 60-subunit protein dodecahedron. [corrected]. Nature. 2016 Jul 7;535(7610):136-9.
15. Bruun TUJ, Andersson AC, Draper SJ, Howarth M. Engineering a Rugged Nanoscaffold To Enhance Plug-and-Display Vaccination. ACS nano. 2018 Sep 25;12(9):8855-66.
16. Brune KD, Howarth M. New Routes and Opportunities for Modular Construction of Particulate Vaccines: Stick, Click, and Glue. Frontiers in Immunology. 2018;9:1432.
17. Li W, Hulswit RJG, Widjaja I, Raj VS, McBride R, Peng W, et al. Identification of sialic acid-binding function for the Middle East respiratory syndrome coronavirus spike glycoprotein. Proceedings of the National Academy of Sciences of the United States of America. 2017 Oct 3;114(40):E8508-E17.
18. Mou H, Raj VS, van Kuppeveld FJ, Rottier PJ, Haagmans BL, Bosch BJ. The receptor binding domain of the new Middle East respiratory syndrome coronavirus maps to a 231-residue region in the spike protein that efficiently elicits neutralizing antibodies. Journal of Virology. 2013 Aug;87(16):9379-83.
19. Lu L, Liu Q, Zhu Y, Chan KH, Qin L, Li Y, et al. Structure-based discovery of Middle East respiratory syndrome coronavirus fusion inhibitor. Nature communications. 2014;5:3067.
20. Widjaja I, Wang C, van Haperen R, Gutierrez-Alvarez J, van Dieren B, Okba NMA, et al. Towards a solution to MERS: protective human monoclonal antibodies targeting different domains and functions of the MERS-coronavirus spike glycoprotein. Emerging Microbes & Infections. 2019 2019/01/01;8(1):516-30.
21. Wang L, Shi W, Chappell JD, Joyce MG, Zhang Y, Kanekiyo M, et al. Importance of Neutralizing Monoclonal Antibodies Targeting Multiple Antigenic Sites on the Middle East Respiratory Syndrome Coronavirus Spike Glycoprotein To Avoid Neutralization Escape. Journal of Virology. 2018 May 15;92(10).
22. Lei Y, Zhao F, Shao J, Li Y, Li S, Chang H, et al. Application of built-in adjuvants for epitope-based vaccines. PeerJ. 2019;6:e6185.
23. Li L, Fierer JO, Rapoport TA, Howarth M. Structural analysis and optimization of the covalent association between SpyCatcher and a peptide Tag. Journal of molecular biology. 2014 Jan 23;426(2):309-17.
24. Widagdo W, Okba NMA, Richard M, de Meulder D, Bestebroer TM, Lexmond P, et al. Lack of Middle East Respiratory Syndrome Coronavirus Transmission in Rabbits. Viruses. 2019 Apr 24;11(4).
25. Bachmann MF, Jennings GT. Vaccine delivery: a matter of size, geometry, kinetics and molecular patterns. Nat Rev Immunol. 2010 Nov;10(11):787-96.

26. Zhou Y, Yang Y, Huang J, Jiang S, Du L. Advances in MERS-CoV Vaccines and Therapeutics Based on the Receptor-Binding Domain. Viruses. 2019 Jan 14;11(1).
27. Kim YS, Son A, Kim J, Kwon SB, Kim MH, Kim P, et al. Chaperna-Mediated Assembly of Ferritin-Based Middle East Respiratory Syndrome-Coronavirus Nanoparticles. Frontiers in Immunology. 2018;9:1093.
28. Daniel C, Anderson R, Buchmeier MJ, Fleming JO, Spaan WJ, Wege H, et al. Identification of an immunodominant linear neutralization domain on the S2 portion of the murine coronavirus spike glycoprotein and evidence that it forms part of complex tridimensional structure. Journal of Virology. 1993 Mar;67(3):1185-94.
29. Routledge E, Stauber R, Pfleiderer M, Siddell SG. Analysis of murine coronavirus surface glycoprotein functions by using monoclonal antibodies. Journal of Virology. 1991 Jan;65(1):254-62.
30. Elshabrawy HA, Coughlin MM, Baker SC, Prabhakar BS. Human monoclonal antibodies against highly conserved HR1 and HR2 domains of the SARS-CoV spike protein are more broadly neutralizing. PloS one. 2012;7(11):e50366.
31. Lai SC, Chong PC, Yeh CT, Liu LS, Jan JT, Chi HY, et al. Characterization of neutralizing monoclonal antibodies recognizing a 15-residues epitope on the spike protein HR2 region of severe acute respiratory syndrome coronavirus (SARS-CoV). Journal of biomedical science. 2005 Oct;12(5):711-27.
32. Lip KM, Shen S, Yang X, Keng CT, Zhang A, Oh HL, et al. Monoclonal antibodies targeting the HR2 domain and the region immediately upstream of the HR2 of the S protein neutralize in vitro infection of severe acute respiratory syndrome coronavirus. Journal of Virology. 2006 Jan;80(2):941-50.
33. Pullen GR, Fitzgerald MG, Hosking CS. Antibody avidity determination by ELISA using thiocyanate elution. Journal of immunological methods. 1986 Jan 22;86(1):83-7.
34. Haagmans BL, van den Brand JM, Provacia LB, Raj VS, Stittelaar KJ, Getu S, et al. Asymptomatic Middle East respiratory syndrome coronavirus infection in rabbits. Journal of Virology. 2015 Jun;89(11):6131-5.
35. Houser KV, Broadbent AJ, Gretebeck L, Vogel L, Lamirande EW, Sutton T, et al. Enhanced inflammation in New Zealand white rabbits when MERS-CoV reinfection occurs in the absence of neutralizing antibody. PLoS pathogens. 2017 Aug;13(8):e1006565.
36. Leneghan DB, Miura K, Taylor IJ, Li Y, Jin J, Brune KD, et al. Nanoassembly routes stimulate conflicting antibody quantity and quality for transmission-blocking malaria vaccines. Scientific Reports. 2017 Jun 19;7(1):3811.
37. Wang C, Zheng X, Gai W, Wong G, Wang H, Jin H, et al. Novel chimeric virus-like particles vaccine displaying MERS-CoV receptor-binding domain induce specific humoral and cellular immune response in mice. Antiviral Res. 2017 Apr;140:55-61.
38. Kanekiyo M, Wei CJ, Yassine HM, McTamney PM, Boyington JC, Whittle JR, et al. Self-assembling influenza nanoparticle vaccines elicit broadly neutralizing H1N1 antibodies. Nature. 2013 Jul 4;499(7456):102-6.
39. Falzarano D, de Wit E, Feldmann F, Rasmussen AL, Okumura A, Peng X, et al. Infection with MERS-CoV causes lethal pneumonia in the common marmoset. PLoS pathogens. 2014 Aug;10(8):e1004250.
40. Modjarrad K, Moorthy VS, Ben Embarek P, Van Kerkhove M, Kim J, Kieny MP. A roadmap for MERS-CoV research and product development: report from a World Health Organization consultation. Nat Med. 2016 Jul 7;22(7):701-5.

Supplementary Materials

Table S1. Immunogens used in this study

Protein	Number of amino acids	Size (KDa)
LS	194	20.47
I3	226	24.10
FP-LS	210	22.27
FP-I3	261	27.71
HR2-LS	257	27.46*
HR2-I3	319	34.07
RBD-ST	286	30.34*
LS-SC	270	28.80

* These proteins appear larger in SDS-PAGE analysis due to N-glycosylation of HR2/RBD domain.
FP, MERS-CoV fusion peptide; HR2, MERS-CoV heptad repeat 2; I3, I3-01; LS, Lumazine synthase; MERS-CoV, Middle East respiratory syndrome coronavirus, RBD, MERS-CoV receptor binding domain; SC, SpyCatcher, ST, SpyTag.

Table S2. Vaccine-induced antibody titers and fold changes following prime (4 weeks post-prime) and booster (3 weeks following booster) vaccinations

	S1/S2 antibody titers				Neutralizing antibody ($PRNT_{90}$) titers			
	Geometric mean titer GMT (95% CI)		Fold increase in titer (95% CI)		Geometric mean titer GMT (95% CI)		Fold increase in titer (95% CI)	
	Prime	Boost	Prime	Boost	Prime	Boost	Prime	Boost
HR2-LS/I3	6.4×10^3 ($6.4\text{-}6.4 \times 10^3$)	2.6×10^4 ($2.6 \times 10^4\text{-}2.6 \times 10^4$)	128 (128-128)	512 (512-512)	N/A	22.97 (11.2-47.2)	N/A	2.297 (1.1-4.72)
FP-LS/I3	200 (59.21-675.5)	1.5×10^4 ($5.7 \times 10^3\text{-}3.8 \times 10^4$)	4 (1.2-13.5)	294.1 (114.5-754.9)	N/A	N/A	N/A	N/A
LS/I3	neg	neg	neg	neg	N/A	N/A	N/A	N/A
PBS	neg	neg	neg	neg	N/A	N/A	N/A	N/A
RBD+LS	4.9×10^3 ($2.2 \times 10^3\text{-}1 \times 10^4$)	5.9×10^4 ($2.3 \times 10^4\text{-}1.5 \times 10^5$)	97.01 (44.9-209.5)	1176 (458.2-3020)	30.3 (11.4-80.9)	422.2 (195.5-911.8)	3.031 (1.1-8.1)	42.22 (19.6-91.2)
RBD-LS	1.9×10^4 ($9 \times 10^3\text{-}4.2 \times 10^4$)	4.1×10^5 ($1.2 \times 10^5\text{-}1.4 \times 10^6$)	388 (179.7-837.9)	8192 ($2.4 \times 10^3\text{-}2.8 \times 10^4$)	320 (174.1-588.1)	4208 (2883-6141)	32 (17.4-58.8)	420.8 (288.3-614.1)

Antibody titers and fold increase relative to baseline (Day 0) are expressed in GMT (95% CI) for $n = 5$ rabbits/group. CI, confidence interval; GMT, geometric mean titer FP, MERS-CoV fusion peptide; HR2, MERS-CoV heptad repeat 2; I3, I3-01; LS, Lumazine synthase; MERS-CoV, Middle East respiratory syndrome coronavirus, N/A, not applicable; neg, negative; $PRNT_{90}$, 90% reduction in plaque reduction neutralization test using MERS-CoV EMC strain; RBD, MERS-CoV receptor binding domain; S1, MERS-CoV Spike protein S1 subunit; S2, MERS-CoV spike protein S2 subunit; SC, SpyCatcher, ST, SpyTag.

>YP_009047204.1 spike glycoprotein [Human betacoronavirus 2c EMC/2012] RBD FP HR2

MIHSVFLLMFLLTPTESYVDVGPDSVKSACIEVDIQQTFFDKTWPRPIDVSKADGIIYPQGRTYSNITITYQGLFPYQGDHGDMYVYS
AGHATGTTPQKLFVANYSQDVKQFANGFVVRIGAAANSTGTVIISPSTSATIRKIYPAFMLGSSVGNFSDGKMGRFFNHTLVLLPDG
CGTLLRAFYCILEPRSGNHCPAGNSYTSFATYHTPATDCSDGNYNRNASLNSFKEYFNLRNCTFMYTYNITEDEILEWFGITQTAQGV
HLFSSRYVDLYGGNMFQFATLPVYDTIKYYSIIPHSIRSIQSDRKAWAAFYVYKLQPLTFLLDFSVDGYIRRAIDCGFNDLSQLHCSYESF
DVESGVYSVSSFEAKPSGSVVEQAEGVECDFSPLLSGTPPQVYNFKRLVFTNCNYNLTKLLSLFSVNDFTCSQISPAAIASNCYSSLILDY
FSYPLSMKSDLSVSSAGPISQFNYKQSFSNPTCLILATVPHNLTTITKPLKYSYINKCSRLLSDDRTEVPQLVNANQYSPCVSIVPSTVWE
DGDYYRKQLSPLEGGGWLVASGSTVAMTEQLQMGFGITVQYGTDTNSVCPKLEFANDTKIASQLGNCVEYSLYGVSGRGVFQNCT
AVGVRQQRFVYDAYQNLVGYYSDDGNYYCLRACVSVPVSVIYDKETKTHATLFGSVACEHISSTMSQYSRSTRSMLKRRDSTYGPLQ
TPVGCVLGLVNSSLFVEDCKLPLGQSLCALPDTPSTLTPRSVRSVPGEMRLASIAFNHPIQVDQLNSSYFKLSIPTNFSFGVTQEYIQTTI
QKVTVDCKQYVCNGFQKCEQLLREYGQFCSKINQALHGANLRQDDSVRNLFASVKSSQSSPIIPGFGGDFNLTLLEPVSISTGSRSAR
SAIEDLLFDKVTIADPGYMQGYDDCMQQGPASARDLICAQYVAGYKVLPPLMDVNMEAAYTSSLLGSIAGVGWTAGLSSFAAIPFA
QSIFYRLNGVGITQQVLSENQKLIANKFNQALGAMQTGFTTTNEAFQKVQDAVNNNAQALSKLASELSNTFGAISASIGDIIQRLDVL
EQDAQIDRLINGRLTTLNAFVAQQLVRSESAALSAQLAKDKVNECVKAQSKRSGFCGQGTHIVSFVVNAPNGLYFMHVGYYPSNHI
EVVSAYGLCDAANPTNCIAPVNGYFIKTNNTRIVDEWSYTGSSFYAPEPITSLNTKYVAPQVTYQNISTNLPPPLLGNSTGIDFQDELD
EFFKNVSTSIPNFGSLTQINTTLLDLTYEMLSLQQVVKALNESYIDLKELGNYTYYNKWPWYIWLGFIAGLVALALCVFFILCCTGCGTN
CMGKLKCNRCCDRYEEYDLEPHKVHVH

Figure S1. Domains of the MERS-CoV spike protein that are presented on multimeric protein scaffold particles. Domains are color-coded: receptor binding domain (RBD, green), fusion peptide (FP, orange), Heptad repeat 2 (HR2, lilac).

CD5 signal peptide
Lumazine synthase
I3-01
FP
HR2
Streptag
SpyTag
SpyCatcher
RBD
Linker
Flagtag

>LS
MQIYEGKLTAEGLRFGIVASRFNHALVDRLVEGAIDAIVRHGGREEDITLVRVPGSWEIPVAAGELARKE
DIDAVIAIGVLIRGATPHFDYIASEVSKGLANLSLELRKPITFGVITADTLEQAIERAGTKHGNKGWEAALS
AIEMANLFKSLRGGSGGSGGSGGSGGGASLINDYKDDDDKAGPGWSHPQFEK

>I3
MWSHPQFEKGGSGGSGGSGGSMKMEELFKKHKIVAVLRANSVEEAKKKALAVFLGGVHLIEITFTVP
DADTVIKELSFLKEMGAIIGAGTVTSVEQCRKAVESGAEFIVSPHLDEEISQFCKEKGVFYMPGVMTPT
ELVKAMKLGHTILKLFPGEVVGPQFVKAMKGPFPNVKFVPTGGVNLDNVCEWFKAGVLAVGVGSAL
VKGTPVEVAEKAKAFVEKIRGCTE

>FP-LS
MQIYEGKLTAEGLRFGIVASRFNHALVDRLVEGAIDAIVRHGGREEDITLVRVPGSWEIPVAAGELARK
EDIDAVIAIGVLIRGATPHFDYIASEVSKGLAQLSLELRKPITFGVITADTLEQAIERAGTKHGNKGWEAALSAIEMANLFKSLRGGSG
GSGGSGGSGGGGLARSARSAIEDLLFDKVLINDYKDDDDKAGPGWSHPQFEK

>FP-I3
MKMEELFKKHKIVAVLRANSVEEAKKKALAVFLGGVHLIEITFTVPDADTVIKELSFLKEMGAIIGAGTVTSVEQCRKAVESGAEFIV
SPHLDEEISQFCKEKGVFYMPGVMTPTELVKAMKLGHTILKLFPGEVVGPQFVKAMKGPFPNVKFVPTGGVNLDNVCEWFKAG
VLAVGVGSALVKGTPVEVAEKAKAFVEKIRGCTEGGSGGSGGSGGSGGGGLARSARSAIEDLLFDKVLINDYKDDDDKAGPGWS
HPQFEK

>HR2-LS
MPMGSLQPLATLYLLGMLVASVLAWSHPQFEKSALASTNLPPPLLGNSTGIDFQDELDEFFKNVSTSIPNFGSLTQINTTLLDLTYE
MLSLQQVVKALNESYIDLKELGLINGGSGGSGGSGGSGGGMQIYEGKLTAEGLRFGIVASRFNHALVDRLVEGAIDAIVRHGGREE
DITLVRVPGSWEIPVAAGELARKEDIDAVIAIGVLIRGATPHFDYIASEVSKGLAQLSLELRKPITFGVITADTLEQAIERAGTKHGNK
GWEAALSAIEMANLFKSLR

>HR2-I3
MKMEELFKKHKIVAVLRANSVEEAKKKALAVFLGGVHLIEITFTVPDADTVIKELSFLKEMGAIIGAGTVTSVEQCRKAVESGAEFIV
SPHLDEEISQFCKEKGVFYMPGVMTPTELVKAMKLGHTILKLFPGEVVGPQFVKAMKGPFPNVKFVPTGGVNLDNVCEWFKAG
VLAVGVGSALVKGTPVEVAEKAKAFVEKIRGCTEGGSGGSGGSGGSGGGGLASTNLPPPLLGNSTGIDFQDELDEFFKNVSTSIPN
FGSLTQINTTLLDLTYEMLSLQQVVKALNESYIDLKELGLINDYKDDDDKAGPGWSHPQFEK

>RBD-ST
MPMGSLQPLATLYLLGMLVASVLASGVYSVSSFEAKPSGSVVEQAEGVECDFSPLLSGTPPQVYNFKRLVFTNCNYNLTKLLSLFSV
NDFTCSQISPAAIASNCYSSLILDYFSYPLSMKSDLSVSSAGPISQFNYKQSFSNPTCLILATVPHNLTTITKPLKYSYINKCSRLLSDDRT
EVPQLVNANQYSPCVSIVPSTVWEDGDYYRKQLSPLEGGGWLVASGSTVAMTEQLQMGFGITVQYGTDTNSVCPKLLINGSGES
GAHIVMVDAYKPTKGGGGSWSHPQFEKGGGSGGGSGGGSWSHPQFEK

>LS-SC
MGSSDYKDDDDKGSGDSATHIKFSKRDEDGKELAGATMELRDSSGKTISTWISDGQVKDFYLYPGKYTFVETAAPDGYEVATAITF
TVNEQGQVTVNGKATKGDAHIGSGGSGGSGMQIYEGKLTAEGLRFGIVASRFNHALVDRLVEGAIDAIVRHGGREEDITLVRVPG
SWEIPVAAGELARKEDIDAVIAIGVLIRGATPHFDYIASEVSKGLANLSLELRKPITFGVITADTLEQAIERAGTKHGNKGWEAALSAI
EMANLFKSLR

Figure S2. Amino acid sequences of protein constructs used in this study for immunization of rabbits. Different domains are color-coded: signal sequence (grey), lumazine synthase (LS, orange), I3-01 (I3, pea green), Streptag (green), SpyTag (ST, light blue), SpyCatcher (SC, dark blue), MERS-FP (FP, lilac), MERS-HR2 (HR2, red), MERS-CoV RBD (RBD, purple).

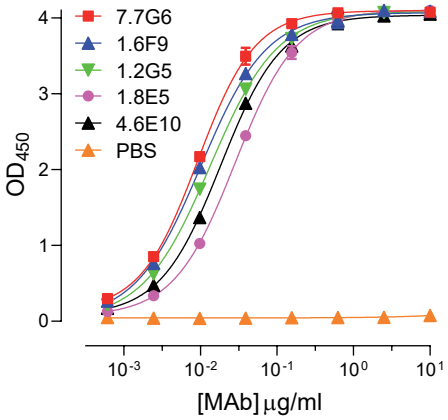

Figure S3. Binding of MERS-CoV RBD-LS particles by RBD-specific human monoclonal antibodies.

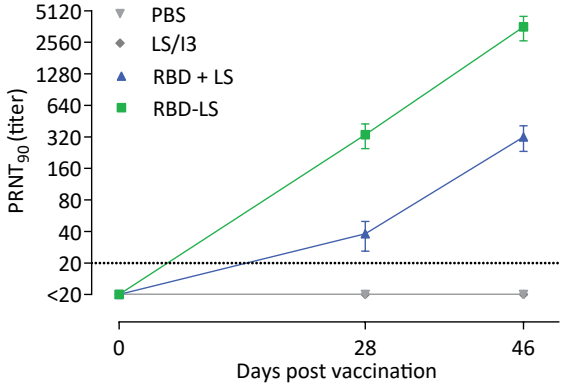

Figure S4. Vaccine-induced MERS-CoV neutralizing antibodies in sera of vaccinated rabbits against the clade B Qatar15 strain (GenBank accession no. MK280984.2) using plaque reduction neutralization assay (PRNT). The dotted line represents the lower limit of detection.

Chapter 5

Summarizing Discussion

Our approach to emerging infections has generally been a reactive post-emergence response, hampering the availability of intervention measures in due time to have substantial impact on outbreaks. Due to the time it takes to develop, test and license a vaccine candidate which can take years, we mostly miss the peak of an outbreak which can last for weeks to months (1-3). The presence of licensed platforms that can be deployed in outbreaks for the rapid generation of therapeutic antibodies and vaccines can reduce the time to develop these countermeasures. This will allow the timely supply of therapeutic and preventive products for emerging viruses, thereby limiting their spread and reducing the human and economic toll. In this thesis, the development of platforms for the rapid generation of countermeasures for an emerging zoonotic coronavirus, MERS-CoV, was addressed as part of a zoonotic preparedness approach (http://www.zapi-imi.eu/). The approach implemented for vaccine design is an immune-correlate-guided approach (Figure 1), whereby key viral immunogenic subunits are identified (Chapter 2) using validated assays. This is followed by further characterization of these immunogenic domains using specific single domain antibodies (VHHs) (Chapter 3). Following that, vaccine candidates are rationally designed and tested for their protective efficacy in animal models (Chapter 4). This process involves the development of platforms for rapid generation of serological assays, VHHs and HCAbs, as well as subunit protein immunogens. These platforms can be the basis for the rapid development of diagnostics, therapeutics and vaccines for future emerging viruses.

MERS-CoV Sero-diagnostics

Spike S1 is a target of protective antibodies and a sensitive predictor of previous MERS-CoV infections

Serologic assays for emerging viruses are crucial not only for identifying key viral immunogens, and evaluating vaccines and biotherapeutics, but also as diagnostics complementing molecular tools to confirm infections and perform serosurveillance which is necessary to develop evidence-based control strategies to contain outbreaks. In response to the emergence of MERS-CoV, various serological assays have been rapidly developed by different laboratories (4-10), most of which lacked proper validation and standardization. Sensitive, specific and easily administered serological assays are key to well-executed and interpreted MERS-CoV epidemiologic studies as well as vaccine efficacy studies (11) (12). Since HCoVs are highly prevalent in the human population and cross-reactivity among different CoVs has been reported (13), it is crucial to validate assays for specificity to avoid false positive results. Additionally, MERS-CoV can cause mild to asymptomatic infections, thus assay sensitivity is also crucial aspect, as MERS-CoV specific antibodies were found

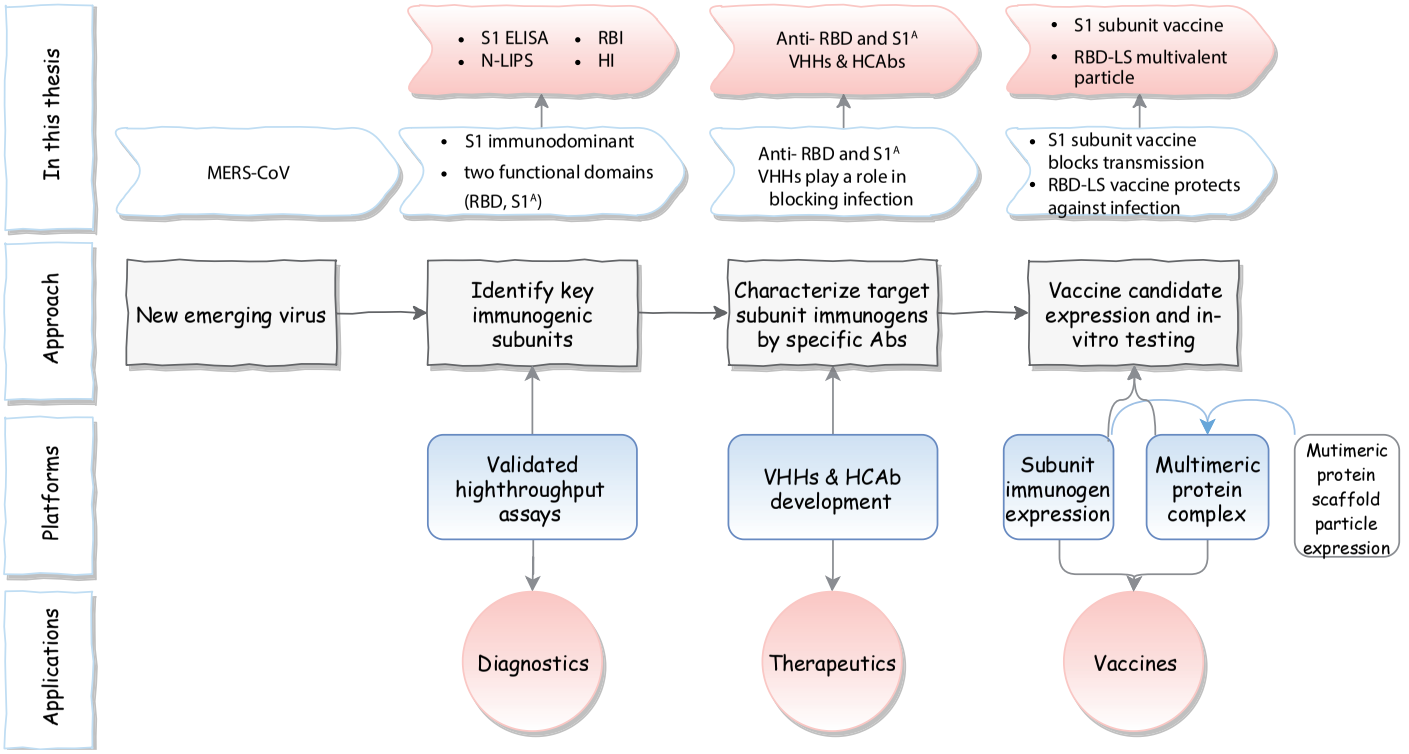

Figure 1. An immune-correlate-guided approach for rational vaccine design against emerging viruses, applied on MERS-CoV. Outcomes are diagnostic, therapeutic and vaccine platforms.

to be low among PCR-confirmed mild and asymptomatic infections (14, 15); which could severely impact serosurveillance studies aiming at estimating MERS-CoV prevalence, monitoring virus spread, evaluating the geographical extent of spillovers, the risk factors for human infection, and the routes of zoonotic transmission. By validating various MERS-CoV diagnostic platforms, we found that the HCoV spike S1 subunit is divergent and highly immunogenic following a MERS-CoV infection, compared to the S2 subunit and nucleocapsid (N) proteins, providing a sensitive and specific antigen for MERS-CoV serodiagnostics (Chapter 2.1). Using MERS-CoV S1 in optimized platforms (inhouse ELISA and protein microarray) showing high sensitivity and specificity, allowed us to detect MERS-CoV infections among mildly infected PCR-confirmed patients and asymptomatic camel contacts in Jordan (ongoing study) and in Kenya (Chapter 2.2). These were undetectable using a commercial ELISA routinely used in epidemiological studies and contact tracing indicating that MERS-CoV infections can go unnoticed. The commercial assay also may lead to false positive results due to HCoV-OC43 cross reactivity. This reduced sensitivity and specificity of the commercial platform has also been reported in several recent studies (5, 13-15). Failure in accurately detecting mild and asymptomatic infections means that these can go unnoticed, and indicates that the prevalence of MERS-CoV could be higher than our currently known estimates, since these were based on a less sensitive and specific platform. Since cellular responses were detected among seronegative camel contacts (16), T-cell assays have the potential to complement serological assays for a more complete picture of true MERS-CoV prevalence. However, these are technically and logistically-demanding assays which cannot be implemented in resource-limited settings. In addition, their outputs need to be further validated to rule out potential cross reactivity with other CoVs. Overall, using sensitive and specific assays can allow for more accurate estimates of MERS-CoV prevalence and geographical spread allowing us to evaluate and monitor its future epidemic potential and implement adequate control measures limiting the public health effect of future outbreaks.

Since assays have been developed and are carried out by different labs, calibration of assays is crucial to reduce interlaboratory variability and allow for more harmonized and reliable outcomes. As a part of a WHO collaborative study aiming at comparing different MERS-CoV serological assays, our inhouse S1 ELISA was further validated and compared to different MERS-CoV diagnostic assays, re-confirming its sensitivity and specificity (17). In the same study, evaluating results from various assays relative to a reference reduced interassay variability, emphasizing the role of reference reagent use in harmonizing the results obtained from various assays carried out in different labs. This is crucial for better comparison and interpretation of results of different studies as well as evaluation of vaccine trials, allowing for uniform assessment of immunogenicity, efficacy and better

understanding of correlates of immune protection (2). As they could facilitate validation of diagnostics, and development and evaluation of therapeutic monoclonals and vaccines for MERS-CoV and other emerging viruses, setting up reference panels is a vital element in our preparedness approaches to emerging viruses. This has been prioritized in the WHO R&D roadmap for MERS-CoV, and a working group on standards and assays has been established as a part of the Coalition for Epidemic Preparedness and Innovation (CEPI) aiming at accelerating vaccine development for high-threat pathogens (2, 11, 18).

MERS-CoV protein-based functional assays

Assessing antibody responses can be addressed through detection of binding to antigens (e.g. ELISAs, IFAs) or specific function (e.g. neutralization assays). Although assays based on binding can detect virus-specific antibodies, they provide limited information on antibody function. Assays for the detection of MERS-CoV-specific functional antibodies are crucial for the development MERS-CoV vaccines and biotherapeutics, and as confirmatory diagnostic assays. MERS-CoV functional antibodies are mainly detected through neutralization assays or a more recently developed image cytometry-based assay (19), both of which detect virus neutralizing antibodies. However, these require advanced equipment (e.g. flow cytometer for the cytometry-based assay), laboratory preparations (BSL3 for live virus neutralization assays) and technical expertise to carry out (19). Recombinant protein-based assays easy to standardize and operate, and don't require a BSL3 containment. The MERS-CoV spike S1 subunit is highly divergent among CoVs and thus can be used to detect MERS-CoV directed antibodies with high specificity (Chapter 2.1). Moreover, the S1 is highly immunogenic following natural infection (Chapter 2.1) and comprises two functional domains: the $S1^A$ mediating viral attachment to sialic acids (20), and the RBD mediating viral entry through its receptor DPP4 (21), making it a main target for MERS-CoV vaccine (Chapter 4) and therapeutic antibody development (Chapter 3). Thus, detecting antibodies that are specifically directed against those two functional domains is of value for MERS-CoV vaccine development as well as characterizing monoclonal antibodies. Using the fundamental knowledge on protein-protein interactions between the viral surface proteins and the cellular proteins in virus attachment and entry, we developed and validated two recombinant protein-based functional assays which can specifically detect antibodies capable of blocking virus binding to its receptor DPP4, and its attachment factor, sialic acid: a receptor binding inhibition assay (RBI) and a hemagglutination inhibition (HI) assay, respectively (Chapter 2.3). Both assays were able to detect MERS-CoV antibodies in virus infected dromedary camels (the viral reservoir) and humans. These species-independent assays are easy to operate and standardize. Both assays are protein-based and can be carried out in a 96-well plate format, therefore providing biosafety level 1 high-throughput

platforms. For serological diagnosis of MERS-CoV infection, the WHO recommends an initial screening using a binding assay such as an ELISA or IFA, followed by confirmation by a functional assay as neutralization assay (22). The latter requires technical expertise and laboratory preparations (BSL3 for live virus neutralization assays) to carry out, which are mainly present in central or reference laboratories and not in community and healthcare labs. Owing to their high specificity and easy administration, the RBI and HI assays can be useful confirmatory assays for both humans and dromedary MERS-CoV diagnostics which can be applied at community and hospital settings omitting the need to send samples to regional or central reference labs. Therefore, these species-independent assays can be useful for diagnostics (Chapter 2.3), monoclonal antibody characterization for development of therapeutics (Chapter 3) and vaccine evaluation studies (Chapter 4). Moreover, the principle used for the development and validation of these platforms can be applied for the development of protein-based functional assays for other viruses.

Therapeutics

Single-Domain antibodies for MERS-CoV therapeutics

Immunotherapeutics have revolutionized medicine, with an increasing number of monoclonal antibodies (mAbs)entering different phases of clinical trials and over 80 granted clinical approval over the past three decades (23, 24). Owing to their safety profile and relatively shorter licensure path compared to vaccines, mAbs can be promising alternatives for the rapid development of preventive and therapeutic agents for emerging viruses for which vaccines and antivirals are unavailable (25-28). Additionally, being a form of passive immunization, mAbs offer advantages over vaccines in case of emergencies; allowing for rapid onset of protective antibody responses, and for protection of immunosuppressed individuals (27). Antibodies have been the main focus of MERS-CoV therapeutic R&D, dominating over antiviral medications (11), with polyclonal and monoclonal antibodies entering clinical trials (29) (NCT03301090). Compared to polyclonal antibodies, monoclonals offer several advantages including standardization, safety and supply (27). Despite the aforementioned advantages, only a single mAb - palivizumab, an RSV-specific antibody - is approved for antiviral clinical use, while many are at different phases of clinical development (26, 27). Factors curtailing the use of mAbs as antivirals, are the high cost of production, the need for large volumes increasing the cost per dose, the difficulty of administration, bioavailability at infection sites, and the short window in which they can be administered to have a therapeutic effect (25).

Camelid-derived single domain antibodies (VHHs or nanobodies), derived by cloning the antigen-binding variable domain of camelid heavy chain-only antibodies (HCAbs)

are gaining interest for the development of antiviral biotherapeutics. Due to their small size, high affinity, stability, easy modularity, and the homology with their human-counterpart, VHHs can overcome some of the hurdles facing the therapeutic use of conventional antibodies (30-32). Being highly stable and soluble, they can be expressed in various microbial systems (yeast, fungi, bacteria) providing high yields at a reduced cost (33). Additionally, their high affinity and thus potency allowing for reducing the administered volume per dose have contributed to their low production cost. (27). These small, 15 KDa, domain antibodies with exceptional stability under extreme conditions (such as high temperature, pressure and pH) (30), can be easily administered through alternative needleless routes of administration, such as oral or inhalation routes, allowing targeted-delivery directly to infection sites (34, 35). Compared to systemic administration, targeted-delivery allows drugs to rapidly reach the infection site at high concentrations, thereby enhancing their therapeutic potential. Due to reduced off-target delivery, a lower amount of antibody is required per dose which in turn lowers the cost per dose providing an economical advantage for VHHs over conventional antibodies. Thus, VHHs present a promising class of antibody-based therapeutics for viruses, especially those causing lower respiratory tract infections where the systematically-administered conventional antibodies are known to have limited effect, due to limited transfer from blood to the lungs which lowers their bioavailability at target sites (36-38) The recent approval of the first therapeutic nanobody (Caplacizumab for the treatment of a clotting disorder) and several others in clinical trials most likely will boost the nanobody research (39).

Using bone marrow from MERS-CoV Spike vaccinated dromedary camels (40), we generated an affinity matured VHH library by direct cloning and expression in E.coli, bypassing the need for phage display. By screening this library, we found that the S1 subunit is immunodominant following MERS-CoV S vaccination, with S1-specific VHHs accounting for 92% of the generated MERS-CoV-specific VHHs, in line with our earlier finding that it is immune dominant following natural infection. From the generated library, we identified potent MERS-CoV neutralizing VHHs, all of which were directed against the RBD. We identified a nanobody that can bind and neutralize MERS-CoV at picomolar ranges. Exploiting the easily-engineered nature of these small molecules, the potency of this domain antibody (VHH83) and half-life were further enhanced by genetically fusing it to a human IgG Fc domain. The generated bivalent chimeric HCAb83, combining advantages of VHHs and human antibodies at half the size of a conventional antibody, had superior affinity and neutralizing capacity relative to other MERS-CoV Mabs (41), and it protected mice against a lethal MERS-CoV challenge when administered prophylactically. Moreover, we identified an $S1^A$-specific VHH capable of blocking the interaction of the spike $S1^A$ with sialic acids and -at high concentrations- blocking MERS-CoV infection. Further

characterization of this anti-$S1^A$ VHH and its protective potential against MERS-CoV is still ongoing. In addition to being potential immunoprophylactic/therapeutic candidates, the developed VHHs can have applications in MERS-CoV diagnostics, as well as standards for vaccine development and potency testing.

Despite the high potency of RBD directed antibodies and their ability to block MERS-CoV infection pre-and post-infection (41), a monospecific antibody for therapy has some limitations. There is a potential risk posed from escape mutants which could develop under selective pressure when an antibody targeting a single epitope, on either the RBD or the $S1^A$ domains, is used (42-49). Antigenic variability could also develop as the virus continues to be introduced from animals or adapts as it transmits among humans which could also result in antibody escape mutants (50-53). Although MERS-CoV escape mutations, so far, come at a cost of reduced viral fitness (44, 49, 52), the escape variants might adapt under pressure and become more transmissible. Therefore, antibody cocktails are crucial for therapy to avoid escape mutant development and provide higher resistance to antigenic viability. Combining antibodies targeting discrete epitopes and acting in different mechanisms could result in additive or synergistic effects potentiating their therapeutic outcome (45, 54, 55). Exploiting the ease of by which VHHs can be multimerized, multiple single domain antibodies targeting different epitopes can be combined into one multidomain molecule providing a cost advantage over mixtures of conventional antibodies (56).

Therefore, combining anti-$S1^A$ and anti-RBD VHHs generating a tetravalent bispecific HCAb could be of economic and efficacy benefit and might formulate a potential candidate for MERS-CoV therapeutics development. Moreover, identifying VHHs against the conserved epitopes on S2, could lead to the development of a broadly protective antibody against different CoVs. This approach has proven efficient for the development of a broadly protective multimeric antibody against both influenza A and B viruses with potency exceeding that of conventional antibodies (57).

Furthermore, exploiting their highly stable nature able to withstand high pressure, the therapeutic efficacy of these domain antibodies can be further enhanced by direct delivery into the lungs through nebulizers (34). This approach has been proven to be effective for the treatment of RSV (37), which could not be achieved by conventional antibodies most likely due to poor bioavailability in the respiratory tract following systemic administration and delayed onset of action (58). Longer-lasting bioavailability at a lower cost can be achieved through vectored or nucleic acid delivery providing long-term in-vivo expression (59-63). This class of biologics can cover an unmet need for the protection of the elderly and immunocompromised, at highest risk of developing severe disease and fatality (64), where active induction of antibody responses through vaccination is poor. Their outstanding

thermal stability, which can withstand high temperatures and provide for long shelf-lives, is advantageous for stockpiling to be readily deployed in emergency outbreak situations.

Antibodies to guide vaccine development

In addition to their preventive and therapeutic potential, monoclonal antibodies can be instrumental to accelerated vaccine development. They can be used to identify and characterize protective antigens and epitopes, their nature and conformation which can guide rational vaccine design, leading to novel or more effective vaccines (28, 65). Since the induction of protective antibody response is a main goal of successful vaccination, defining the nature of a protective antibody response is thus fundamental. In that sense, functional antibodies are the best correlate of vaccine protection. By mapping the immune responses induced following whole MERS-CoV Spike (S) vaccination, using the generated VHH library, we confirmed the immune dominance of S1 subunit following vaccination. Moreover, using the developed VHHs directed against the $S1^{A}$ and RBD domains, we identified those functional domains as targets for MERS-CoV protective antibodies (roles of antibodies against these two domains play in blocking or reducing MERS-CoV infections), making them potential targets for vaccine development. These findings have also been confirmed by several research groups using conventional mAbs (45, 46, 66, 67).

MERS-CoV Vaccines

S1 based vaccine candidates for MERS-CoV

To cope with the fast pace by which viruses emerge, we need to invest in developing and licensing platforms for the development of vaccines that can be easily and rapidly deployed when a new virus emerges. This can reduce the time required for vaccine development and licensure and thus can allow for the timely supply of vaccines, which is crucial to curb these outbreaks early in their infancy. Protein-based vaccines provide advantages over other vaccine platforms, overcoming the safety issues, low immunogenicity, and pre-existing vector immunity posed by other vaccine platforms such as attenuated/inactivated virus-, DNA-, or vector-based vaccines. Recombinant protein-based vaccines are safe and easy to produce, they are promising platforms for the development of vaccines for emerging viruses. In Chapter 4 of this study, we developed and tested the efficacy of two different recombinant protein platforms as candidates for MERS-CoV vaccine development which could be applied for the development of vaccines for other emerging viruses.

By mapping antibody responses, we identifying S1 as an immunodominant subunit following natural infection and vaccination. Along with its inclusion of two domains that are

targets for protective antibodies and to which antibodies are induced following natural infection and vaccination, the S1 subunit is an ideal target for vaccine development. Vaccinating llama with a recombinant S1 protein was able to limit viral replication and shedding following virus transmission from infected animals, providing evidence for its potential efficacy to block further virus transmission. This can be a potential candidate for the development of a dromedary camel vaccine. Vaccinating dromedaries, the animal reservoir, is set as a primary goal in the WHO target profile for MERS-CoV vaccine development aiming at preventing animal-to-human transmission, which could put an end to the ongoing outbreaks.

Within the S1 domain, the RBD is the main target for neutralizing antibodies and RBD-specific monoclonal HCAbs efficiently protected mice against a lethal MERS-CoV challenge (Chapter 3). Exploiting the current advanced protein engineering technology, we multivalently presented the RBD on self-assembling 60-meric lumazine synthase (LS) protein scaffold particles using an antigen-SpyTag/scaffold-SpyCatcher system (68), generating RBD-LS. This system allows for rapid 'plug-and-display' of antigens in an arrayed format through spontaneous isopeptide bond formation. Upon vaccination, the multimeric RBD-LS induced antibody responses of higher quality and quantity than the monomeric counterparts, and protected intranasally-challenged rabbits against both upper and lower respiratory tract infections which was associated with an extraordinary efficacy to block virus replication. Having shown higher efficacy in blocking and protecting against MERS-CoV infection in a direct challenge model, RBD-LS is likely to efficiently block MERS-CoV transmission, although experimental evidence is still warranted. Additionally, the longevity of the immune responses needs to be assessed. Other aspects that can be optimized to further enhance the vaccine-induced immune responses are the route of administration and adjuvants used (69-72). For example, by following the natural route of infections, intranasal delivery can induce local respiratory tract immune responses which enhances the protection against respiratory infections, in addition to providing a needless administration route (71, 73). Moreover, an optimal adjuvant can overcome immunesenescence (aging of the immune system) and thus provide promise for the development of vaccines for elderly, upon whom respiratory viruses have a disproportionate severe impact (70, 74). Overall, the developed RBD-LS can be a promising MERS-CoV vaccine candidate and the developed platform provides several advantages providing promise for the generation of vaccines for emerging viruses. However, since determining the next emerging pathogen is not something to guarantee, this promising potential to develop vaccines for emerging viruses needs to be complemented by our knowledge of immunogenic and protective target antigens within different classes or genera of viruses (e.g. S1 for coronaviruses) and having platforms to produce such antigens in correct conformations. This will allow

the rapid production of antigens form viral sequences once a new virus of a known class emerges. Whereas the particles can be pre-produced and stockpiled ready for on-demand plugging of the new antigens

A major aspect hindering the development of vaccines for emerging viruses is the lack of animal models for testing vaccine efficacy. While several animal models have been recently developed for MERS-CoV; except for common marmosets for which the outcome varied between research groups (75, 76), none was able to recapitulate severe human infections without genetic modification and sometimes virus adaptation (77-79). Despite resulting in lethal infections in genetically engineered mice, the virus adapted strains acquire strain-specific mutations and thus may not be able to recapitulate human pathogenesis. In this study we have established two animal models which can be naturally infected with MERS-CoV field isolates and used for testing vaccines, a rabbit direct challenge model and a llama transmission model. Despite showing asymptomatic infection (80), rabbits are readily available, can be easily infected with field isolates and can show both upper and lower respiratory tract infections. We have provided evidence for their usefulness as a vaccine testing model; however, we were unable to establish MERS-CoV transmission in this model (81). Meanwhile, llamas can be naturally infected (82), and we were able to establish transmission in llamas in a direct in-contact setting and test the efficacy of the recombinant S1-vaccine in blocking MERS-CoV transmission in this model. Thus, the llama transmission model is an attractive model for testing vaccine efficacy in a natural-mimicking transmission setting. Alpacas, another camelid species, are also susceptible to MERS-CoV infection and were recently shown to transmit the virus (83, 84).

Toward broader protection against CoVs

While the CoV spike S1 and the RBD are the main targets for therapeutic antibody and vaccine development, they are highly divergent among different CoVs providing virus specific protection. Thus far, the variability in the amino acid sequence of the spike protein observed among MERS-CoV strains is low (85), and circulating MERS-CoV strains did not show any significant variation in the serological reactivity (86, 87), implying that the development of a vaccine that is effective against one strain is likely to be protective against other circulating strains. However, this protection remains homotypic targeting only MERS-CoV. Future research needs to focus on identifying conserved protective epitopes aiming at the development of broadly-reactive CoV antibodies and vaccines which can protect against different CoVs and in preparation for potential future emerging ones. The spike S2 domain and the N protein are more conserved, and thus adaptive immune response directed against these proteins can potentially lay the basis for a more broadly-acting coronavirus

vaccine. However, evidence for cross reactive immune responses against different CoVs is still limited. Convalescent SARS-CoV patient sera weakly neutralized MERS-CoV (88) and SARS-S reactive antisera showed low level neutralization of MERS-CoV (89). Extra-RBD S1 or S2 epitopes could be responsible for this effect, as some neutralizing epitopes have been identified in these regions of the S protein (90, 91). Non-neutralizing conserved epitopes should also be sought, as non-neutralizing S2 epitopes were found to be protective against MERS-CoV (67). These may not be as immunodominant as the RBD epitopes but could provide a rationale for the development of a cross protective CoV epitope-focused vaccine. One study has also demonstrated the potential role of adaptive response against N protein in protection against MERS-CoV infection as this vaccine candidate produced a protective T-cell response against MERS-CoV challenge which was also partially protective against SARS-CoV (92). Moreover, infection of mice with SARS-CoV reduced MERS-CoV titers 5 days p.i. upon challenge suggesting the development of a cross reactive T-cell response (93). Thus, mapping and focusing the immune response towards these critical epitopes, which could be subdominant, may provide a way to induce immune responses with a broader activity against different CoVs. Developing broader active reagents such as antibodies and vaccines could potentially help in our preparedness efforts for potential future emerging CoVs.

Concluding remarks

Zoonotic CoVs pose a serious public health risk. SARS-CoV caused an epidemic in 2002-2003, and MERS-CoV with its ongoing outbreaks and continuous zoonotic introductions, could acquire mutations gaining the capacity for efficient transmission in humans and result in an epidemic with a devastating outcome sometime in the future. Additionallly, given the wide spread of CoVs in different animal species and propensity to cross species barriers, the emergence of a new zoonotic CoV in the future is not unlikely. Meanwhile there is no licensed CoV-specific vaccine or therapy. In this study we implemented an immune-correlate guided approach for MERS-CoV vaccine development, which resulted in the development not only of platforms for vaccine development but also for therapeutic antibodies and diagnostics.

As viruses continue to emerge, having a pandemic-free world is almost impossible, however preparedness and rapid responses at the earliest point in the outbreak can limit their further spread and prevent their devastating effects. Having rapidly implementable platforms for developing effective control measures (antibodies and vaccines) can allow swift responses to those emerging viruses. The development of such products, requires public-private partnerships involving research institutes, industry and funding agencies,

which is sometimes non-sustainable, hindering the development of even some promising candidates. In an initiative aiming at accelerating vaccine R&D process by providing sustained funding to be prepared for future epidemics, the Coalition for Epidemic Preparedness Innovations (CEPI) was launched (94). CEPI is an international non-profit association aiming at accelerating vaccine development for epidemic infections and getting ready for future epidemics, including MERS-CoV. Such coalitions can remove barriers facing vaccine development for emerging viruses, such as lack of incentive due to high cost and low market, and therefore provide promise for better preparedness against emerging diseases. Establishing standardized reagent panels and assays in advance of outbreaks is prerequisite for the rapid advancement efforts to develop these countermeasures, and this should be considered as well.

References

1. Graham BS, Mascola JR, Fauci AS. Novel Vaccine Technologies: Essential Components of an Adequate Response to Emerging Viral Diseases. Jama. 2018 Apr 10;319(14):1431-2.
2. Rampling T, Page M, Horby P. International Biological Reference Preparations for Epidemic Infectious Diseases. Emerg Infect Dis. 2019 Feb;25(2):205-11.
3. Bloom DE, Black S, Rappuoli R. Emerging infectious diseases: A proactive approach. Proceedings of the National Academy of Sciences of the United States of America. 2017 Apr 18;114(16):4055-9.
4. Corman VM, Muller MA, Costabel U, Timm J, Binger T, Meyer B, et al. Assays for laboratory confirmation of novel human coronavirus (hCoV-EMC) infections. Euro surveillance : bulletin Europeen sur les maladies transmissibles = European communicable disease bulletin. 2012 Dec 6;17(49).
5. Drosten C, Meyer B, Muller MA, Corman VM, Al-Masri M, Hossain R, et al. Transmission of MERS-coronavirus in household contacts. The New England journal of medicine. 2014 Aug 28;371(9):828-35.
6. Al-Abdallat MM, Payne DC, Alqasrawi S, Rha B, Tohme RA, Abedi GR, et al. Hospital-associated outbreak of Middle East respiratory syndrome coronavirus: a serologic, epidemiologic, and clinical description. Clin Infect Dis. 2014 Nov 1;59(9):1225-33.
7. Reusken C, Mou H, Godeke GJ, van der Hoek L, Meyer B, Muller MA, et al. Specific serology for emerging human coronaviruses by protein microarray. Euro surveillance : bulletin Europeen sur les maladies transmissibles = European communicable disease bulletin. 2013 Apr 4;18(14):20441.
8. Perera RA, Wang P, Gomaa MR, El-Shesheny R, Kandeil A, Bagato O, et al. Seroepidemiology for MERS coronavirus using microneutralisation and pseudoparticle virus neutralisation assays reveal a high prevalence of antibody in dromedary camels in Egypt, June 2013. Euro surveillance : bulletin Europeen sur les maladies transmissibles = European communicable disease bulletin. 2013 Sep 5;18(36):pii=20574.
9. Alagaili AN, Briese T, Mishra N, Kapoor V, Sameroff SC, Burbelo PD, et al. Middle East respiratory syndrome coronavirus infection in dromedary camels in Saudi Arabia. mBio. 2014 Feb 25;5(2):e00884-14.
10. Haagmans BL, Al Dhahiry SH, Reusken CB, Raj VS, Galiano M, Myers R, et al. Middle East respiratory syndrome coronavirus in dromedary camels: an outbreak investigation. The Lancet Infectious diseases. 2014 Feb;14(2):140-5.

11. Modjarrad K, Moorthy VS, Ben Embarek P, Van Kerkhove M, Kim J, Kieny MP. A roadmap for MERS-CoV research and product development: report from a World Health Organization consultation. Nat Med. 2016 Jul 7;22(7):701-5.
12. World Health Organization. WHO MERS Global Summary and Assessment of Risk. 2019.
13. Al Kahlout RA, Nasrallah GK, Farag EA, Wang L, Lattwein E, Muller MA, et al. Comparative Serological Study for the Prevalence of Anti-MERS Coronavirus Antibodies in High- and Low-Risk Groups in Qatar. J Immunol Res. 2019;2019:1386740.
14. Choe PG, Perera R, Park WB, Song KH, Bang JH, Kim ES, et al. MERS-CoV Antibody Responses 1 Year after Symptom Onset, South Korea, 2015. Emerg Infect Dis. 2017 Jul;23(7):1079-84.
15. Ko JH, Muller MA, Seok H, Park GE, Lee JY, Cho SY, et al. Serologic responses of 42 MERS-coronavirus-infected patients according to the disease severity. Diagnostic microbiology and infectious disease. 2017 Oct;89(2):106-11.
16. Alshukairi AN, Zheng J, Zhao J, Nehdi A, Baharoon SA, Layqah L, et al. High Prevalence of MERS-CoV Infection in Camel Workers in Saudi Arabia. mBio. 2018 Oct 30;9(5).
17. Harvey R, Mattiuzzo G, Hassall M, Sieberg A, Muller MA, Drosten C, et al. Comparison of Serologic Assays for Middle East Respiratory Syndrome Coronavirus. Emerg Infect Dis. 2019 Oct;25(10):1878-83.
18. Brende B, Farrar J, Gashumba D, Moedas C, Mundel T, Shiozaki Y, et al. CEPI-a new global R&D organisation for epidemic preparedness and response. Lancet (London, England). 2017 Jan 21;389(10066):233-5.
19. Rosen O, Chan LL, Abiona OM, Gough P, Wang L, Shi W, et al. A high-throughput inhibition assay to study MERS-CoV antibody interactions using image cytometry. J Virol Methods. 2019 Mar;265:77-83.
20. Li W, Hulswit RJG, Widjaja I, Raj VS, McBride R, Peng W, et al. Identification of sialic acid-binding function for the Middle East respiratory syndrome coronavirus spike glycoprotein. Proceedings of the National Academy of Sciences of the United States of America. 2017 Oct 3;114(40):E8508-E17.
21. Raj VS, Mou H, Smits SL, Dekkers DHW, Müller MA, Dijkman R, et al. Dipeptidyl peptidase 4 is a functional receptor for the emerging human coronavirus-EMC. Nature. 2013 03/13/online;495:251.
22. World Health Organization. Laboratory Testing for Middle East Respiratory Syndrome Coronavirus, Interim Guidance. (WHO/MERS/LAB/15.1/Rev1/2018). Licence: CC BY-NC-SA 3.0 IGO. Geneva, Switzerland; 2018.
23. Kaplon H, Reichert JM. Antibodies to watch in 2019. mAbs. 2019 Feb/Mar;11(2):219-38.
24. Buettner MJ, Shah SR, Saeui CT, Ariss R, Yarema KJ. Improving Immunotherapy Through Glycodesign. Frontiers in Immunology. 2018;9:2485.
25. Walker LM, Burton DR. Passive immunotherapy of viral infections: 'super-antibodies' enter the fray. Nat Rev Immunol. 2018 May;18(5):297-308.
26. Graham BS, Ambrosino DM. History of passive antibody administration for prevention and treatment of infectious diseases. Curr Opin HIV AIDS. 2015 May;10(3):129-34.
27. Sparrow E, Friede M, Sheikh M, Torvaldsen S. Therapeutic antibodies for infectious diseases. Bull World Health Organ. 2017 Mar 1;95(3):235-7.
28. Andreano E, Seubert A, Rappuoli R. Human monoclonal antibodies for discovery, therapy, and vaccine acceleration. Current opinion in immunology. 2019 Aug;59:130-4.
29. Beigel JH, Voell J, Kumar P, Raviprakash K, Wu H, Jiao JA, et al. Safety and tolerability of a novel, polyclonal human anti-MERS coronavirus antibody produced from transchromosomic cattle: a phase 1 randomised, double-blind, single-dose-escalation study. The Lancet Infectious diseases. 2018 Apr;18(4):410-8.
30. Vanlandschoot P, Stortelers C, Beirnaert E, Ibanez LI, Schepens B, Depla E, et al. Nanobodies(R): new ammunition to battle viruses. Antiviral Res. 2011 Dec;92(3):389-407.

31. De Vlieger D, Ballegeer M, Rossey I, Schepens B, Saelens X. Single-Domain Antibodies and Their Formatting to Combat Viral Infections. Antibodies (Basel, Switzerland). 2018 Dec 20;8(1).
32. Wu Y, Jiang S, Ying T. Single-Domain Antibodies As Therapeutics against Human Viral Diseases. Frontiers in Immunology. 2017;8:1802.
33. Liu Y, Huang H. Expression of single-domain antibody in different systems. Applied microbiology and biotechnology. 2018 Jan;102(2):539-51.
34. Van Heeke G, Allosery K, De Brabandere V, De Smedt T, Detalle L, de Fougerolles A. Nanobodies(R) as inhaled biotherapeutics for lung diseases. Pharmacology & therapeutics. 2017 Jan;169:47-56.
35. van der Vaart JM, Pant N, Wolvers D, Bezemer S, Hermans PW, Bellamy K, et al. Reduction in morbidity of rotavirus induced diarrhoea in mice by yeast produced monovalent llama-derived antibody fragments. Vaccine. 2006 May 8;24(19):4130-7.
36. Detalle L, Stohr T, Palomo C, Piedra PA, Gilbert BE, Mas V, et al. Generation and Characterization of ALX-0171, a Potent Novel Therapeutic Nanobody for the Treatment of Respiratory Syncytial Virus Infection. Antimicrobial agents and chemotherapy. 2016 Jan;60(1):6-13.
37. Larios Mora A, Detalle L, Gallup JM, Van Geelen A, Stohr T, Duprez L, et al. Delivery of ALX-0171 by inhalation greatly reduces respiratory syncytial virus disease in newborn lambs. mAbs. 2018 Jul;10(5):778-95.
38. Ibanez LI, De Filette M, Hultberg A, Verrips T, Temperton N, Weiss RA, et al. Nanobodies with in vitro neutralizing activity protect mice against H5N1 influenza virus infection. The Journal of Infectious Diseases. 2011 Apr 15;203(8):1063-72.
39. Morrison C. Nanobody approval gives domain antibodies a boost. Nature reviews Drug discovery. 2019 Jul;18(7):485-7.
40. Haagmans BL, van den Brand JM, Raj VS, Volz A, Wohlsein P, Smits SL, et al. An orthopoxvirus-based vaccine reduces virus excretion after MERS-CoV infection in dromedary camels. Science. 2016 Jan 1;351(6268):77-81.
41. Xu J, Jia W, Wang P, Zhang S, Shi X, Wang X, et al. Antibodies and vaccines against Middle East respiratory syndrome coronavirus. Emerging Microbes & Infections. 2019;8(1):841-56.
42. Ying T, Du L, Ju TW, Prabakaran P, Lau CC, Lu L, et al. Exceptionally potent neutralization of Middle East respiratory syndrome coronavirus by human monoclonal antibodies. Journal of Virology. 2014 Jul;88(14):7796-805.
43. Pascal KE, Coleman CM, Mujica AO, Kamat V, Badithe A, Fairhurst J, et al. Pre- and postexposure efficacy of fully human antibodies against Spike protein in a novel humanized mouse model of MERS-CoV infection. Proceedings of the National Academy of Sciences of the United States of America. 2015 Jul 14;112(28):8738-43.
44. Tang XC, Agnihothram SS, Jiao Y, Stanhope J, Graham RL, Peterson EC, et al. Identification of human neutralizing antibodies against MERS-CoV and their role in virus adaptive evolution. Proceedings of the National Academy of Sciences of the United States of America. 2014 May 13;111(19):E2018-26.
45. Zhou H, Chen Y, Zhang S, Niu P, Qin K, Jia W, et al. Structural definition of a neutralization epitope on the N-terminal domain of MERS-CoV spike glycoprotein. Nature communications. 2019 Jul 11;10(1):3068.
46. Wang N, Rosen O, Wang L, Turner HL, Stevens LJ, Corbett KS, et al. Structural Definition of a Neutralization-Sensitive Epitope on the MERS-CoV S1-NTD. Cell Rep. 2019 Sep 24;28(13):3395-405 e6.

47. Wang L, Shi W, Chappell JD, Joyce MG, Zhang Y, Kanekiyo M, et al. Importance of Neutralizing Monoclonal Antibodies Targeting Multiple Antigenic Sites on the Middle East Respiratory Syndrome Coronavirus Spike Glycoprotein To Avoid Neutralization Escape. Journal of Virology. 2018 May 15;92(10).
48. Yu X, Zhang S, Jiang L, Cui Y, Li D, Wang D, et al. Structural basis for the neutralization of MERS-CoV by a human monoclonal antibody MERS-27. Scientific Reports. 2015 Aug 18;5:13133.
49. Tai W, Wang Y, Fett CA, Zhao G, Li F, Perlman S, et al. Recombinant Receptor-Binding Domains of Multiple Middle East Respiratory Syndrome Coronaviruses (MERS-CoVs) Induce Cross-Neutralizing Antibodies against Divergent Human and Camel MERS-CoVs and Antibody Escape Mutants. Journal of Virology. 2017 Jan 1;91(1):e01651-16.
50. Shirato K, Melaku SK, Kawachi K, Nao N, Iwata-Yoshikawa N, Kawase M, et al. Middle East Respiratory Syndrome Coronavirus in Dromedaries in Ethiopia Is Antigenically Different From the Middle East Isolate EMC. Frontiers in Microbiology. 2019;10:1326.
51. Kiambi S, Corman VM, Sitawa R, Githinji J, Ngoci J, Ozomata AS, et al. Detection of distinct MERS-Coronavirus strains in dromedary camels from Kenya, 2017. Emerging Microbes & Infections. 2018 Nov 28;7(1):195.
52. Kleine-Weber H, Elzayat MT, Wang L, Graham BS, Muller MA, Drosten C, et al. Mutations in the Spike Protein of Middle East Respiratory Syndrome Coronavirus Transmitted in Korea Increase Resistance to Antibody-Mediated Neutralization. Journal of Virology. 2019 Jan 15;93(2).
53. Kim YS, Aigerim A, Park U, Kim Y, Rhee JY, Choi JP, et al. Sequential Emergence and Wide Spread of Neutralization Escape Middle East Respiratory Syndrome Coronavirus Mutants, South Korea, 2015. Emerg Infect Dis. 2019 Jun;25(6):1161-8.
54. Zhang S, Zhou P, Wang P, Li Y, Jiang L, Jia W, et al. Structural Definition of a Unique Neutralization Epitope on the Receptor-Binding Domain of MERS-CoV Spike Glycoprotein. Cell Rep. 2018 Jul 10;24(2):441-52.
55. Sui J, Deming M, Rockx B, Liddington RC, Zhu QK, Baric RS, et al. Effects of human anti-spike protein receptor binding domain antibodies on severe acute respiratory syndrome coronavirus neutralization escape and fitness. Journal of Virology. 2014 Dec;88(23):13769-80.
56. Hultberg A, Temperton NJ, Rosseels V, Koenders M, Gonzalez-Pajuelo M, Schepens B, et al. Llama-derived single domain antibodies to build multivalent, superpotent and broadened neutralizing anti-viral molecules. PloS one. 2011 Apr 1;6(4):e17665.
57. Laursen NS, Friesen RHE, Zhu X, Jongeneelen M, Blokland S, Vermond J, et al. Universal protection against influenza infection by a multidomain antibody to influenza hemagglutinin. Science. 2018 Nov 2;362(6414):598-602.
58. Ramilo O, Lagos R, Saez-Llorens X, Suzich J, Wang CK, Jensen KM, et al. Motavizumab treatment of infants hospitalized with respiratory syncytial virus infection does not decrease viral load or severity of illness. The Pediatric infectious disease journal. 2014 Jul;33(7):703-9.
59. Schlake T, Thran M, Fiedler K, Heidenreich R, Petsch B, Fotin-Mleczek M. mRNA: A Novel Avenue to Antibody Therapy? Molecular therapy : the journal of the American Society of Gene Therapy. 2019 Apr 10;27(4):773-84.
60. Yamazaki T, Chiba J, Akashi-Takamura S. Neutralizing Anti-Hemagglutinin Monoclonal Antibodies Induced by Gene-Based Transfer Have Prophylactic and Therapeutic Effects on Influenza Virus Infection. Vaccines. 2018 Jun 26;6(3).
61. Tiwari PM, Vanover D, Lindsay KE, Bawage SS, Kirschman JL, Bhosle S, et al. Engineered mRNA-expressed antibodies prevent respiratory syncytial virus infection. Nature communications. 2018 Oct 1;9(1):3999.

62. Sanders JW, Ponzio TA. Vectored immunoprophylaxis: an emerging adjunct to traditional vaccination. Tropical diseases, travel medicine and vaccines. 2017;3:3.
63. Adam VS, Crosariol M, Kumar S, Ge MQ, Czack SE, Roy S, et al. Adeno-associated virus 9-mediated airway expression of antibody protects old and immunodeficient mice against influenza virus. Clinical and vaccine immunology : CVI. 2014 Nov;21(11):1528-33.
64. Bernard-Stoecklin S, Nikolay B, Assiri A, Bin Saeed AA, Ben Embarek PK, El Bushra H, et al. Comparative Analysis of Eleven Healthcare-Associated Outbreaks of Middle East Respiratory Syndrome Coronavirus (Mers-Cov) from 2015 to 2017. Scientific Reports. 2019 May 14;9(1):7385.
65. Rappuoli R, Bottomley MJ, D'Oro U, Finco O, De Gregorio E. Reverse vaccinology 2.0: Human immunology instructs vaccine antigen design. The Journal of experimental medicine. 2016 Apr 4;213(4):469-81.
66. Zhou Y, Yang Y, Huang J, Jiang S, Du L. Advances in MERS-CoV Vaccines and Therapeutics Based on the Receptor-Binding Domain. Viruses. 2019 Jan 14;11(1).
67. Widjaja I, Wang C, van Haperen R, Gutierrez-Alvarez J, van Dieren B, Okba NMA, et al. Towards a solution to MERS: protective human monoclonal antibodies targeting different domains and functions of the MERS-coronavirus spike glycoprotein. Emerging Microbes & Infections. 2019 2019/01/01;8(1):516-30.
68. Brune KD, Howarth M. New Routes and Opportunities for Modular Construction of Particulate Vaccines: Stick, Click, and Glue. Frontiers in Immunology. 2018;9:1432.
69. Zhang L, Wang W, Wang S. Effect of vaccine administration modality on immunogenicity and efficacy. Expert review of vaccines. 2015;14(11):1509-23.
70. Weinberger B. Adjuvant strategies to improve vaccination of the elderly population. Current opinion in pharmacology. 2018 Aug;41:34-41.
71. Bhide Y, Dong W, Gribonika I, Voshart D, Meijerhof T, de Vries-Idema J, et al. Cross-Protective Potential and Protection-Relevant Immune Mechanisms of Whole Inactivated Influenza Virus Vaccines Are Determined by Adjuvants and Route of Immunization. Frontiers in Immunology. 2019;10:646.
72. Cirelli KM, Carnathan DG, Nogal B, Martin JT, Rodriguez OL, Upadhyay AA, et al. Slow Delivery Immunization Enhances HIV Neutralizing Antibody and Germinal Center Responses via Modulation of Immunodominance. Cell. 2019 May 16;177(5):1153-71 e28.
73. Kim MH, Kim HJ, Chang J. Superior immune responses induced by intranasal immunization with recombinant adenovirus-based vaccine expressing full-length Spike protein of Middle East respiratory syndrome coronavirus. PloS one. 2019;14(7):e0220196.
74. Crooke SN, Ovsyannikova IG, Poland GA, Kennedy RB. Immunosenescence and human vaccine immune responses. Immun Ageing. 2019;16:25.
75. Johnson RF, Via LE, Kumar MR, Cornish JP, Yellayi S, Huzella L, et al. Intratracheal exposure of common marmosets to MERS-CoV Jordan-n3/2012 or MERS-CoV EMC/2012 isolates does not result in lethal disease. Virology. 2015 Nov;485:422-30.
76. Falzarano D, de Wit E, Feldmann F, Rasmussen AL, Okumura A, Peng X, et al. Infection with MERS-CoV causes lethal pneumonia in the common marmoset. PLoS pathogens. 2014 Aug;10(8):e1004250.
77. Li K, Wohlford-Lenane CL, Channappanavar R, Park JE, Earnest JT, Bair TB, et al. Mouse-adapted MERS coronavirus causes lethal lung disease in human DPP4 knockin mice. Proceedings of the National Academy of Sciences of the United States of America. 2017 Apr 11;114(15):E3119-E28.
78. Cockrell AS, Yount BL, Scobey T, Jensen K, Douglas M, Beall A, et al. A mouse model for MERS coronavirus-induced acute respiratory distress syndrome. Nature microbiology. 2016 Nov 28;2:16226.

79. Li K, Wohlford-Lenane C, Perlman S, Zhao J, Jewell AK, Reznikov LR, et al. Middle East Respiratory Syndrome Coronavirus Causes Multiple Organ Damage and Lethal Disease in Mice Transgenic for Human Dipeptidyl Peptidase 4. The Journal of Infectious Diseases. 2016 Mar 1;213(5):712-22.
80. Haagmans BL, van den Brand JM, Provacia LB, Raj VS, Stittelaar KJ, Getu S, et al. Asymptomatic Middle East respiratory syndrome coronavirus infection in rabbits. Journal of Virology. 2015 Jun;89(11):6131-5.
81. Widagdo W, Okba NMA, Richard M, de Meulder D, Bestebroer TM, Lexmond P, et al. Lack of Middle East Respiratory Syndrome Coronavirus Transmission in Rabbits. Viruses. 2019 Apr 24;11(4):381.
82. Vergara-Alert J, van den Brand JM, Widagdo W, Munoz Mt, Raj S, Schipper D, et al. Livestock Susceptibility to Infection with Middle East Respiratory Syndrome Coronavirus. Emerg Infect Dis. 2017 Feb;23(2):232-40.
83. Adney DR, Bielefeldt-Ohmann H, Hartwig AE, Bowen RA. Infection, Replication, and Transmission of Middle East Respiratory Syndrome Coronavirus in Alpacas. Emerg Infect Dis. 2016 Jun;22(6):1031-7.
84. Crameri G, Durr PA, Klein R, Foord A, Yu M, Riddell S, et al. Experimental Infection and Response to Rechallenge of Alpacas with Middle East Respiratory Syndrome Coronavirus. Emerg Infect Dis. 2016 Jun;22(6):1071-4.
85. Drosten C, Muth D, Corman VM, Hussain R, Al Masri M, HajOmar W, et al. An observational, laboratory-based study of outbreaks of middle East respiratory syndrome coronavirus in Jeddah and Riyadh, kingdom of Saudi Arabia, 2014. Clin Infect Dis. 2015 Feb 1;60(3):369-77.
86. Muthumani K, Falzarano D, Reuschel EL, Tingey C, Flingai S, Villarreal DO, et al. A synthetic consensus anti-spike protein DNA vaccine induces protective immunity against Middle East respiratory syndrome coronavirus in nonhuman primates. Sci Transl Med. 2015 Aug 19;7(301):301ra132.
87. Muth D, Corman VM, Meyer B, Assiri A, Al-Masri M, Farah M, et al. Infectious Middle East Respiratory Syndrome Coronavirus Excretion and Serotype Variability Based on Live Virus Isolates from Patients in Saudi Arabia. J Clin Microbiol. 2015 Sep;53(9):2951-5.
88. Chan KH, Chan JF, Tse H, Chen H, Lau CC, Cai JP, et al. Cross-reactive antibodies in convalescent SARS patients' sera against the emerging novel human coronavirus EMC (2012) by both immunofluorescent and neutralizing antibody tests. The Journal of infection. 2013 Aug;67(2):130-40.
89. Coleman CM, Liu YV, Mu H, Taylor JK, Massare M, Flyer DC, et al. Purified coronavirus spike protein nanoparticles induce coronavirus neutralizing antibodies in mice. Vaccine. 2014 May 30;32(26):3169-74.
90. Yang Y, Deng Y, Wen B, Wang H, Meng X, Lan J, et al. The amino acids 736-761 of the MERS-CoV spike protein induce neutralizing antibodies: implications for the development of vaccines and antiviral agents. Viral immunology. 2014 Dec;27(10):543-50.
91. Wang L, Shi W, Joyce MG, Modjarrad K, Zhang Y, Leung K, et al. Evaluation of candidate vaccine approaches for MERS-CoV. Nature communications. 2015 Jul 28;6(1):7712.
92. Zhao J, Zhao J, Mangalam AK, Channappanavar R, Fett C, Meyerholz DK, et al. Airway Memory CD4(+) T Cells Mediate Protective Immunity against Emerging Respiratory Coronaviruses. Immunity. 2016 Jun 21;44(6):1379-91.
93. Zhao J, Li K, Wohlford-Lenane C, Agnihothram SS, Fett C, Zhao J, et al. Rapid generation of a mouse model for Middle East respiratory syndrome. Proceedings of the National Academy of Sciences of the United States of America. 2014 Apr 1;111(13):4970-5.
94. Hatchett R, Lurie N. Outbreak response as an essential component of vaccine development. The Lancet Infectious diseases. 2019 Nov;19(11):e399-e403.

Chapter 6

English Summary
Arabic Summary
Nederlandse samenvatting

6.1 English Summary

Our approach to emerging infections has generally been a reactive post-emergence response, hampering the availability of intervention measures in due time to have substantial impact on outbreaks. Due to the time it takes to develop, test and license a vaccine candidate which can take years, we mostly miss the peak of an outbreak which can last for weeks to months. The presence of licensed platforms that can be deployed in outbreaks for the rapid generation of therapeutic antibodies and vaccines can reduce the time to develop these countermeasures. This will allow the timely supply of therapeutic and preventive products for emerging viruses, thereby limiting their spread and reducing the human and economic toll. In this thesis, the development of platforms for the rapid generation of countermeasures for an emerging zoonotic coronavirus, Middle East respiratory syndrome coronavirus (MERS-CoV), was addressed as part of a zoonotic preparedness approach. The approach implemented for vaccine design was an immune-correlate-guided approach, whereby we developed and validated assays to identify key viral immunogenic subunits (Chapter 2). This was followed by further characterization of these immunogenic domains using specific single domain antibodies (VHHs) (Chapter 3). Following that, vaccine candidates were rationally designed and tested for their protective efficacy in animal models (Chapter 4). This process involved the development of platforms for rapid generation of serological assays, VHHs and HCAbs, as well as subunit protein immunogens. These platforms can be the basis for the rapid development of diagnostics, therapeutics and vaccines for future emerging viruses.

6.2 Arabic Summary

الملخص العربي

لقد كان نهجنا كبشر تجاه العدوى الناشئة بشكل عام هو الاستجابة التفاعلية بعد ظهور المرض، مما أعاق توافر تدابير التدخل السريع للحد من تفشي المرض. ونظراً للوقت الذي يستغرقه تطوير مرشح لقاح واختباره وترخيصه والذي قد يصل إلى سنوات، فإننا غالباً ما نفوت ذروة تفشي المرض والتي قد تمتد من أسابيع إلى شهور. ولذلك فإن وجود منصات مرخصة قابلة للتفعيل من أجل توليد سريع للقاحات والأجسام المضادة العلاجية في حالة تفشي الامراض، يمكن أن يقلل من الوقت اللازم لتطوير هذه الإجراءات المضادة. وسيتيح وجود تلك المنصات توفير المنتجات العلاجية والوقائية للفيروسات الناشئة في الوقت المناسب، مما سيحد من انتشارها و بالتالي يقلل الخسائر البشرية والاقتصادية.

في هذه الأطروحة، تم تناول تطوير منصات توليد سريع للتدابير المضادة لفيروس تاجي حيواني ناشئ، والمعروف بفيروس كورونا المسبب لمتلازمة الشرق الأوسط التنفسية (MERS-CoV) ، كجزء من نهج التأهب للعدوى حيوانيه المصدر. وقد كان النهج الذي اتبعناه لتصميم اللقاح هو نهج موجه مرتبط بالمناعة، حيث قمنا بتطوير وتصديق اختبارات للتعرف على الوحدات الفيروسية الرئيسية المستثيرة للمناعة المعروفة بالمستمنعات (فصل ٢). وأعقب ذلك مزيد من توصيف هذه المستمنعات باستخدام الأجسام المضادة أحاديه المجال (الأجسام النانونية) وهي عبارة عن المنطقة المتغيرة للسلسلة الثقيلة (VHHs) من الأجسام المضادة أحادية السلسلة والمأخوذة من الإبل عن طريق البيولوجيا الجزيئية (فصل ٣). بعد ذلك، تم تصميم اللقاحات المقترحة وإختبار فاعليتها الوقائية على النماذج الحيوانية مثل حيوانات اللاما والأرانب (فصل ٤). تضمنت هذه العملية تطوير منصات توليد سريع للآتي: (١) الاختبارات المصلية للكشف عن الأجسام المضادة، (٢) الأجسام النانونية والأجسام المضادة أحادية السلسلة (HCAbs) كمرشحات علاجية، (٣) مستمنعات كمرشحات للقاحات. وعليه فإن المنصات الناتجة عن هذه الأطروحة يمكن أن تشكل الأساس للتطوير السريع لتشخيص وعلاج و إنتاج اللقاحات للفيروسات الناشئة في المستقبل.

6.3 Nederlandse samenvatting

Tot voor kort was de respons op nieuwe opkomende infecties over het algemeen reactief, waardoor de tijdige beschikbaarheid van interventiemaatregelen werd belemmerd met als gevolg dat het veel moeite kan kosten uitbraken onder controle te krijgen. Vanwege de tijd die nodig is om een kandidaat-vaccin te ontwikkelen, te testen en in licentie te nemen (enkele jaren) missen we meestal de piek van een uitbraak die vaak slechts weken tot maanden kan duren. Door het ontwikkelen van platformtechnologieën, die kunnen worden ingezet bij uitbraken, kunnen antilichamen en vaccins mogelijk sneller gegenereerd worden. Dit zal de tijdige levering van therapeutische en preventieve producten voor opkomende virussen potentieel mogelijk maken, waardoor de verspreiding van pathogenen wordt beperkt en de menselijke en economische tol wordt verminderd. In dit proefschrift werd de ontwikkeling van platforms voor de snelle generatie van tegenmaatregelen voor een opkomend coronavirus, het Middle East respiratoir syndroom coronavirus (MERS-CoV), behandeld als onderdeel van een zoönotische paraatheidsbenadering. De aanpak die is geïmplementeerd voor het ontwerpen van vaccins was een immuun-gecorreleerde benadering, waarbij we testen ontwikkelden en valideren om belangrijke virale immunogene antigenen te identificeren (hoofdstuk 2). Dit werd gevolgd door verdere karakterisering van deze immunogene domeinen met behulp van specifieke antilichamen, nanobodies (hoofdstuk 3). Daarna werden kandidaat-vaccins rationeel ontworpen en getest op hun beschermende werkzaamheid in diermodellen (hoofdstuk 4). Dit hele proces omvatte de ontwikkeling van platforms voor snelle generatie van serologische assays, nanobodies en zware keten antilichamen, evenals subunit vaccins. Deze platforms kunnen de basis vormen voor de snelle ontwikkeling van diagnostiek, therapeutica en vaccins voor toekomstige opkomende virussen.

Chapter 7

About the author

7.1 Curriculum Vitae

Nisreen Mamdouh Ahmed Okba was born on the 3rd July 1983 in Cairo, Egypt; and grew up in between Egypt, USA and the Kingdom of Saudi Arabia. In 2005, she obtained her Bachelor in Pharmacy from Tanta University, after which she started working as a pharmacist for the Egyptian Ministry of Health and took a part-time Master program in Microbiology and Immunology. In 2009, she moved to Al-Azhar University to work as a teaching assistant for five years and, in the meantime, obtained her Master degree. Through her meeting with Dr Ali Zaki – the first to discover MERS-CoV – she became interested in the field of virology and moved to the Netherlands in 2014 as a visiting researcher, and later as a PhD candidate, at the Department of Viroscience, Erasmus MC, Rotterdam, the Netherlands. She was involved in an international collaboration that aims to develop platforms for the rapid responses to emerging zoonotic viruses viruses. The project culminates in the development of such platforms for MERS-CoV and is explained in great details in this thesis.

7.2 PhD portofolio

Name: Nisreen Mamdouh Ahmed Okba
Department: Viroscience, Erasmus MC
Graduate School: Molecular Medicine (Molmed) Post Graduate School
PhD period: 2015-2020
Promotor: Prof. dr. M.P.G. Koopmans
Co-promotor: Dr. B. L. Haagmans

Education

2020	PhD	*Erasmus MC*
2012	Master of Science (Microbiology & Immunology)	*Tanta University, Egypt*
2005	Bachelor of Pharmaceutical Sciences	*Tanta University, Egypt*

Courses & Workshops

2019	Personal Leadership & Communication	*Erasmus MC*
2018	Bayesians Statistics and JASP	*Erasmus MC*
2018	Advanced course on Applications in Flow Cytometry	*Erasmus MC*
2018	One Health Approach to Infectious Diseases Master Class	*Amsterdam*
2017	Flow Cytomety Advanced	*Nijmegen*
2017	Biomedical English Writing and Communication	*Erasmus MC*
2017	Research Integrity	*Erasmus MC*
2017	Advanced Immunology Course	*Erasmus MC*
2017	Microscopic Image Analysis: From Theory to Practice	*Erasmus MC*
2016	Preparedness, prediction and prevention of emerging zoonotic viruses with panedmic potential	*Paris, France*
2016	Course on Laboratory Animal Science	*Erasmus MC*
2015	Introduction in GraphPad Prism	*Erasmus MC*

Attended Conferences/ Seminars/ Meetings

2019	MiniSymposium: Zoonotic disease emergence: lessons learned and future directions	*Rotterdam*
2019	Protein and Antibody Engineering Summit	*Lisbon, Portugal*
2019	Vaccine Symposium 2019: Structural Vaccinology	*Utrecht*
2019	European Congress of Virology	*Rotterdam*
2019	Dutch Annual Virology Symposium	*Amsterdam*
2019	Keystone Symposia: Molecular Approaches to vaccines and immune monitoring	*Colorado, USA*
2018	7th international Conference of the Egyptian Society of Virology	*Hurgada, Egypt*
2018	Vaccine Symposium 2018: Novel Vaccine Platforms	*Utrecht*
2018	IMI 10th Anniversary Scientific Symposium	*Brussels, Belgium*
2018	ZAPI's Consortium General Assembly (Gena 6)	*Paris, France*
2018	Dutch Annual Virology Symposium	*Amsterdam*
2018	22nd Molmed Day 2018	*Rotterdam*
2018	Keystone Symposia: Antibodies as Drugs	*Wistler, Canada*
2017	Vaccine Symposium 2017: The Powerful Contributions of Vectors to Vaccine-Induced Immunity	*Utrecht*
2017	Emerging Viruses 2017	*Oxford, UK*
2017	XIVth International Nidovirus Symposium (Nido2017)	*Kansas City, USA*
2017	Dutch Annual Virology Symposium	*Amsterdam*
2017	21st Molmed Day 2017	*Rotterdam*

Poster Presentations

2019	Protein and Antibody Engineering Summit	*Lisbon, Portugal*
2019	European Congress of Virology	*Rotterdam*
2019	Keystone Symposia: Molecular Approaches to vaccines and immune monitoring	*Colorado, USA*
2018	22nd Molmed Day 2018	*Rotterdam*
2018	Keystone Symposia: Antibodies as Drugs	*Wistler, Canada*
2017	XIVth International Nidovirus Symposium (Nido2017)	*Kansas City, USA*
2017	21st Molmed Day 2017	*Rotterdam*

Oral Presentations

2019	Mini Symposium: Zoonotic disease emergence: lessons learned and future directions	*Rotterdam*
2019	Keystone Symposia: Molecular Approaches to vaccines and immune monitoring	*Colorado, USA*
2018	7th international Conference of the Egyptian Society of Virology Vaccine Symposium 2018: Novel Vaccine Platforms	*Hurgada, Egypt*
2018	IMI 10th Anniversary Scientific Symposium	*Utrecht*
2018	ZAPI's Consortium General Assembly (Gena 6)	*Brussels, Belgium*
2018	22nd Molmed Day 2018	*Rotterdam*
2017	Emerging Viruses 2017	*Oxford, UK*

Teaching

2019	Supervision of Bachelor student
2018	Supervision of Master student

Awards

2018	Best presentation award: 7th int. conference of the ESV	*Hurgada, Egypt*
2019	Egypt Best poster award: 22nd Molmed Day March 2018	*Rotterdam*

7.3 Publication List

1. **Okba NMA***, Muller MA*, Li W*, Wang C, GeurtsvanKessel CH, Corman VM, Lamers MM, Sikkema RS, de Bruin E, Chandler FD, Yazdanpanah Y, Le Hingrat Q, Descamps D, Houhou-Fidouh N, Reusken C, Bosch BJ, Drosten C, Koopmans MPG, Haagmans BL. Severe Acute Respiratory Syndrome Coronavirus 2-Specific Antibody Responses in Coronavirus Disease 2019 Patients. Emerging infectious diseases. 2020;26(7).
2. Wang C*, Li W*, Drabek D, **Okba NMA**, van Haperen R, Osterhaus ADME, van Kuppeveld FJM, Haagmans BL, Grosveld F, Bosch B-J. A human monoclonal antibody blocking SARS-CoV-2 infection. Nature Communications. Accepted Manuscript.
3. **Okba NMA**, Widjaja I, van Dieren B, Aebischer A, van Amerongen G, de Waal L, Stittelaar KJ, Martina B, van den Brand JMA , Beer M, Bosch BJ, Haagmans BL. Particulate multivalent presentation of the MERS-CoV receptor binding domain induces protective antiviral antibody responses in rabbits. Emerging microbes & infections. Accepted Manuscript.
4. Koch T, Dahlke C, Fathi A, Kupke A, Krähling V, **Okba NMA**, Halwe S, Rohde C, Eickmann M, Volz A, Hesterkamp T, Jambrecina A, Borregaard S, Ly ML, Zinser ME, Bartels E, Poetsch JSH, Neumann R, Fux R, Schmiedel S, Lohse AW, Haagmans BL, Sutter G, Becker S, Addo MM. Safety and immunogenicity of a modified vaccinia virus Ankara vector vaccine candidate for Middle East respiratory syndrome: an open-label, phase 1 trial. The Lancet Infectious Diseases. 2020.
5. **Okba NMA**, Widjaja I, Li W, GeurtsvanKessel CH, Farag E, Al-Hajri M, Park WB, Oh MD, Reusken C, Koopmans MPG, Bosch BJ, Haagmans BL. Serologic Detection of Middle East Respiratory Syndrome Coronavirus Functional Antibodies. Emerging infectious diseases. 2020;26(5).
6. Widjaja I, Wang C, van Haperen R, Gutierrez-Alvarez J, van Dieren B, **Okba NMA**, Raj VS, Li W, Fernandez-Delgado R, Grosveld F, van Kuppeveld FJM, Haagmans BL, Enjuanes L, Drabek D, Bosch BJ. Towards a solution to MERS: protective human monoclonal antibodies targeting different domains and functions of the MERS-coronavirus spike glycoprotein. Emerging microbes & infections. 2019;8(1):516-30.
7. Widagdo W*, **Okba NMA***, Richard M, de Meulder D, Bestebroer TM, Lexmond P, Farag E, Al-Hajri M, Stittelaar KJ, de Waal L, van Amerongen G, van den Brand JMA, Haagmans BL, Herfst S. Lack of Middle East Respiratory Syndrome Coronavirus Transmission in Rabbits. Viruses. 2019;11(4).
8. Widagdo W*, **Okba NMA***, Li W, de Jong A, de Swart RL, Begeman L, van den Brand JMA, Bosch BJ, Haagmans BL. Species-Specific Colocalization of Middle East Respiratory Syndrome Coronavirus Attachment and Entry Receptors. Journal of virology. 2019;93(16).

9. Rodon J*, **Okba NMA***, Te N, van Dieren B, Bosch BJ, Bensaid A, Segales J, Haagmans BL, Vergara-Alert J. Blocking transmission of Middle East respiratory syndrome coronavirus (MERS-CoV) in llamas by vaccination with a recombinant spike protein. Emerging microbes & infections. 2019;8(1):1593-603.
10. **Okba NMA**, Raj VS, Widjaja I, GeurtsvanKessel CH, de Bruin E, Chandler FD, Park WB, Kim NJ, Farag E, Al-Hajri M, Bosch BJ, Oh MD, Koopmans MPG, Reusken C, Haagmans BL. Sensitive and Specific Detection of Low-Level Antibody Responses in Mild Middle East Respiratory Syndrome Coronavirus Infections. Emerging infectious diseases. 2019;25(10):1868-77.
11. Harvey R, Mattiuzzo G, Hassall M, Sieberg A, Muller MA, Drosten C, Rigsby P, Oxenford CJ, **study p**. Comparison of Serologic Assays for Middle East Respiratory Syndrome Coronavirus. Emerging infectious diseases. 2019;25(10):1878-83.
12. Farag E, Sikkema RS, Mohamedani AA, de Bruin E, Munnink BBO, Chandler F, Kohl R, van der Linden A, **Okba NMA**, Haagmans BL, van den Brand JMA, Elhaj AM, Abakar AD, Nour BYM, Mohamed AM, Alwaseela BE, Ahmed H, Alhajri MM, Koopmans M, Reusken C, Elrahman SHA. MERS-CoV in Camels but Not Camel Handlers, Sudan, 2015 and 2017. Emerging infectious diseases. 2019;25(12):2333-5.
13. Anfasa F, Goeijenbier M, Widagdo W, Siegers JY, Mumtaz N, **Okba N**, van Riel D, Rockx B, Koopmans MPG, Meijers JCM, Martina BEE. Zika Virus Infection Induces Elevation of Tissue Factor Production and Apoptosis on Human Umbilical Vein Endothelial Cells. Front Microbiol. 2019;10:817.
14. Stalin Raj V*, **Okba NMA***, Gutierrez-Alvarez J, Drabek D, van Dieren B, Widagdo W, Lamers MM, Widjaja I, Fernandez-Delgado R, Sola I, Bensaid A, Koopmans MP, Segales J, Osterhaus A, Bosch BJ, Enjuanes L, Haagmans BL. Chimeric camel/human heavy-chain antibodies protect against MERS-CoV infection. Sci Adv. 2018;4(8):eaas9667.
15. David D, Rotenberg D, Khinich E, Erster O, Bardenstein S, van Straten M, **Okba NMA**, Raj SV, Haagmans BL, Miculitzki M, Davidson I. Middle East respiratory syndrome coronavirus specific antibodies in naturally exposed Israeli llamas, alpacas and camels. One Health. 2018;5:65-8.
16. Widagdo W, **Okba NMA**, Stalin Raj V, Haagmans BL. MERS-coronavirus: From discovery to intervention. One Health. 2017;3:11-6.
17. **Okba NM**, Raj VS, Haagmans BL. Middle East respiratory syndrome coronavirus vaccines: current status and novel approaches. Current opinion in virology. 2017;23: 49-58.
18. Haagmans BL, van den Brand JM, Raj VS, Volz A, Wohlsein P, Smits SL, Schipper D, Bestebroer TM, **Okba N**, Fux R, Bensaid A, Solanes Foz D, Kuiken T, Baumgartner W, Segales J, Sutter G, Osterhaus AD. An orthopoxvirus-based vaccine reduces virus excretion after MERS-CoV infection in dromedary camels. Science. 2016;351(6268):77-81.

*Authors contributed equally

7.4 Acknowledgements

As this journey is ending, and a new one starting, I would like to express my gratitude for this chance I've been given, to learn, grow and get to know a lot of amazing people. I would like to thank everyone who has helped me throughout the way… Thank you all for making this possible!

First, I would like to thank Dr. Ali Zaki for getting me first interested in virology and being a main reason for me being here at this moment, and my thanks extends to Ron Fouchier, who got me in first contact with Bart and started my journey in the Netherlands.

I would like to thank my promotor Marion Koopmans and co-promotor Bart Haagmans for all the guidance, learning opportunities, and challenges I've been given throughout the process and for all the brainstorming sessions. Thank you for everything!

My collaborators and colleagues, without whom this work wouldn't have been done. With special thanks to Berend-Jan Bosch, Ivy Widjaja, and Wentao Li at Utrecht University; Jordi Rodon, Julia Vergara-Alert and Joaquim Segales at Barcelona; Leon de Waal and Koert Stittelaar at the Viroclinics; Corine Geurts van Kessel, Chantal Reusken, Stalin Victor, Widagdo, Byron Martina, Erwin de Bruin, Felicity Chandler at the Viroscience department.

To all the people at the Viroscience department, I enjoyed being among you all. I would like to thank all my team members, specially Stalin, Gadissa, and Do for all their support, Katie and Tija for their help and the nice time I enjoyed working with both. Thanks to my office mates, Bri, Diana, Anouskha, Tamana, Katie, and Laurine for the unforgettable moments I spent among you all. I would also like to thank Theo, Pascal, Stefan, Oanh and Monique S. for helping whenever needed. Debby van Riel and Rik for being such great mentors. Loubna, Simone and Maria for all their help in all the administrative work.

A lot of wonderful new friends I've made who were my support system being away from home: Thank you all for everything you've provided and for making things easier, without you I couldn't go through. Bri, Do, Gadissa, Noureen, Shazad, Fatiha, Cynthia and Syriam; I am grateful for the chance I got to know you all. Those outside the Viroscience dept. who how have been my Family abroad: Asmaa, Soad, Lamees, Ghada, Sara, Mai, Marium, and Nouran thanks for helping me strive through and being there when the tides were high. T. Nagat and U. Yehia, I can't thank you enough for everything you've given me, you were my parents here. And my friends & Cousins back home, Manar, Sarah, Ola, Mai, Samar and Esraa who despite being far away in distance, were never far away whenever needed.

Last but most important is my family, My parents Soad and Mamdouh, My siblings Doaa and Ahmed, my in-laws Doaa and Mohamed and my beloved nephews Malik and Yassin…

Without you I wouldn't have been here, being the reason for my existence, success and joy. I am grateful for the endless support I've received in all kinds of ways throughout my life. Words cannot express my gratitude… If there was only one reason I've reached here, it would be you. From the deepest of my heart: THANK YOU! May you be rewarded all the best.

Nisreen Okba

Rotterdam, April 2020